INFORMATION TO USERS

This was produced from a copy of a document sent to us for microfilming. While the most advanced technological means to photograph and reproduce this document have been used, the quality is heavily dependent upon the quality of the material submitted.

The following explanation of techniques is provided to help you understand markings or notations which may appear on this reproduction.

1. The sign or "target" for pages apparently lacking from the document photographed is "Missing Page(s)". If it was possible to obtain the missing page(s) or section, they are spliced into the film along with adjacent pages. This may have necessitated cutting through an image and duplicating adjacent pages to assure you of complete continuity.

2. When an image on the film is obliterated with a round black mark it is an indication that the film inspector noticed either blurred copy because of movement during exposure, or duplicate copy. Unless we meant to delete copyrighted materials that should not have been filmed, you will find a good image of the page in the adjacent frame.

3. When a map, drawing or chart, etc., is part of the material being photographed the photographer has followed a definite method in "sectioning" the material. It is customary to begin filming at the upper left hand corner of a large sheet and to continue from left to right in equal sections with small overlaps. If necessary, sectioning is continued again—beginning below the first row and continuing on until complete.

4. For any illustrations that cannot be reproduced satisfactorily by xerography, photographic prints can be purchased at additional cost and tipped into your xerographic copy. Requests can be made to our Dissertations Customer Services Department.

5. Some pages in any document may have indistinct print. In all cases we have filmed the best available copy.

University
Microfilms
International

300 N. ZEEB ROAD, ANN ARBOR, MI 48106
18 BEDFORD ROW, LONDON WC1R 4EJ, ENGLAND

Downloaded from SHAREOK. Persistent Handle URL: https://hdl.handle.net/11244/4644

8004390

IQBAL, KHAN ZAFAR

ANALYSIS OF THE GEOTHERMAL BINARY CYCLE USING PARAFFIN HYDROCARBONS AS WORKING FLUIDS

The University of Oklahoma PH.D. 1979

University Microfilms International 300 N. Zeeb Road, Ann Arbor, MI 48106 18 Bedford Row, London WC1R 4EJ, England

PLEASE NOTE:

In all cases this material has been filmed in the best possible way from the available copy. Problems encountered with this document have been identified here with a check mark ✓.

1. Glossy photographs _____
2. Colored illustrations _____
3. Photographs with dark background _____
4. Illustrations are poor copy _____
5. Print shows through as there is text on both sides of page _____
6. Indistinct, broken or small print on several pages ✓ throughout _____
7. Tightly bound copy with print lost in spine _____
8. Computer printout pages with indistinct print ✓
9. Page(s) _____ lacking when material received, and not available from school or author _____
10. Page(s) _____ seem to be missing in numbering only as text follows _____
11. Poor carbon copy _____
12. Not original copy, several pages with blurred type _____
13. Appendix pages are poor copy _____
14. Original copy with light type _____
15. Curling and wrinkled pages _____
16. Other _____

University Microfilms International

300 N. ZEEB RD., ANN ARBOR, MI 48106 (313) 761-4700

THE UNIVERSITY OF OKLAHOMA

GRADUATE COLLEGE

ANALYSIS OF THE GEOTHERMAL BINARY CYCLE USING PARAFFIN HYDROCARBONS AS WORKING FLUIDS

A DISSERTATION

SUBMITTED TO THE GRADUATE FACULTY

in partial fulfillment of the requirements for the

degree of

DOCTOR OF PHILOSOPHY

BY

KHAN ZAFAR IQBAL

Norman, Oklahoma

1979

ANALYSIS OF THE GEOTHERMAL BINARY CYCLE USING

PARAFFIN HYDROCARBONS AS WORKING FLUIDS

APPROVED BY

K E Starling

C. M. Sliepcevich

Lloyd L. Lee

F M Townsend

DISSERTATION COMMITTEE

ACKNOWLEDGEMENTS

I would like to express my sincere gratitude and appreciation to the following persons and organizations:

Dr. K.E. Starling, George Lynn Cross Research Professor of Chemical Engineering, for his guidance, inspiration and encouragement throughout this research.

Professors C.M. Sliepcevich, F.M. Townsend, S.S. Sofer and L.L. Lee for serving on my advisory committee.

Dr. H.H. West for his support, encouragement and new ideas.

Yolanda Valdez and Laura Barbour for preparation of this manuscript.

F. Ali and C.T. Chu for their help in making all the diagrams in ink for this work.

U.S. Department of Energy, Idaho National Engineering Laboratory, School of Chemical Engineering and Materials Science and the University of Oklahoma for the financial support for this research and my research assistantship.

I would especially like to express my appreciation to my father, M. Azam Khan, for his continuous encouragement and my gratitude and respect to my mother for her love and devotion.

I would finally like to acknowledge my wife Carol and son Usman, for their love, devotion and sacrifice.

Khan Zafar Iqbal

TABLE OF CONTENTS

	Page
LIST OF TABLES	viii
LIST OF ILLUSTRATIONS	x
Chapter	
I. INTRODUCTION	1
Statement of Objectives	1
Scope of Investigation	2
Literature Review	5
Geothermal Binary Cycle Simulation	8
Cascade Binary Cycle	10
Thermodynamic Behavior of Paraffin Hydrocarbons in the Geothermal Binary Cycle	12
II. SENSITIVITY ANALYSIS OF THERMODYNAMIC AND PROCESS UNIT OPERATIONAL PARAMETERS	24
Cycle State Points	24
Turbine Inlet Temperature	25
Turbine Inlet Pressure	42
Condenser Dew Point Temperature	48
Process Equipment and Unit Operational Characteristics	54
Brine Heat Exchanger and Condenser Duties	55
Working Fluid Heat Transfer Coefficient in Brine Heat Exchanger	57
Working Fluid Heat Transfer Coefficient in Condenser	63
Turbine and Cycle Pump Efficiencies	66
III. SENSITIVITY ANALYSIS OF THE TOTAL SYSTEM COMPONENT COSTS	74
Total System Cost	74
Power Plant Cost	75
Brine System Cost	82
Power Plant Component Cost	87

Chapter Page

IV. INTERRELATIONSHIP OF THERMODYNAMIC AND OPERATIONAL AND COST PARAMETERS 96

Resource Utilization Optimum and Cost Optimum and Thermodynamic Optimum 97

Resource Utilization Optimum 98
Economic Optimum 106
Thermodynamic Optimum 109

Turbine Inlet Temperature and Pressure 115

Condenser Duty 118
Brine Heat Exchanger and Condenser Overall Heat Transfer Coefficients 122
Brine Heat Exchanger and Condenser Log Mean Temperature Differences 124
Brine Heat Exchanger and Condenser Costs 126
Turbine-Generator Cost 128
Cooling Tower Cost 130
Brine System Cost 131
Total System Cost 133

Brine Heat Exchanger Log Mean Temperature Difference 135
Condenser Log Mean Temperature Difference 148
Cooling Water Temperature Range in Condenser ... 156
Brine Flow Rate 160

V. ADVANTAGES AND DISADVANTAGES OF THE USE OF MIXTURES IN GEOTHERMAL BINARY CYCLES 174

Major Differences Between Pure and Mixture Fluid Cycle Parameters 175

Advantages and Disadvantages of Mixtures 178

Basis of Comparison 179
Single Boiler Conventional Binary Cycle 180
Cascade Binary Cycle 185

Effects of the Georesource Temperature Decline on Pure Fluid and Mixture Conventional Binary Cycle Performance 207
Equipment Needs Peculiar to Geothermal Binary Cycles Using Mixture Working Fluids 224

Brine Heat Exchanger 226
Condenser 230

Chapter Page

VI. CONCLUSIONS AND RECOMMENDATIONS 233

Conclusions 233
Recommendations 234

BIBLIOGRAPHY 235

APPENDIX

A. DESIGN BASIS ENGINEERING PARAMETERS 238

B. FIXED PLANT SIMULATION MODIFICATION TO GEO4 SIMULATOR 247

C. PROCEDURE USED FOR CASCADE BINARY CYCLE CALCULATION 259

D. SAMPLE COMPUTER OUTPUT 274

LIST OF TABLES

Table		page
1.	Rankine Cycle Working Fluid Thermodynamic Property Characterization Parameters	14
2.	Effects of Turbine Inlet Temperature on the Ideal Binary Cycle Performance	33
3.	Summary of the Effects of Turbine Inlet Temperature on the Ideal Binary Cycle Performance	35
4.	Effect of Condenser Dew Point Temperature on the Performance of the Binary Cycle	53
5.	Effect of Temperature and Pressure on the Working Fluid Heat Transfer Coefficient in the Brine Heat Exchanger	62
6.	Effect of Working Fluid Heat Transfer Coefficient in Condenser	65
7.	Effect of Turbine Efficiency on the Performance of the Binary Cycle	70
8.	Effect of Cycle Pump Efficiency on the Performance of the Binary Cycle	71
9.	Sensitivity of Total System Cost to Power Plant Cost	78
10.	Sensitivity of Total System Cost to Brine System Cost	86
11.	Effect of Turbine Inlet Temperature and Pressure on the Isobutane Cycle Parameters for the Georesource Temperature of 300°F	134
12.	Effect of Brine Heat Exchanger Log Mean Temperature Difference on Cycle and Cost Parameters	141
13.	Effect of Condenser Log Mean Temperature Difference on Cycle and Cost Parameters	154
14.	Effect of Cooling Water Temperature Range on Cycle and Cost Parameters	161
15.	Effect of Brine Flow Rate on the Cycle Parameters and Cost	169

Table page

16. Comparison of Pure Fluid and Mixture Fluid Cycle Parameters for the Georesource Temperature of 300°F 184

17. Summary of the Dual Boiler Binary Cycle Preliminary Calculations 195

18. Comparison of Pure and Mixture Fluid Dual Boiler Binary Cycle Preliminary Calculations 196

19. Net Plant Work Per Pound of Brine 201

20. Net Thermodynamic Cycle Efficiency, Percent 201

21. Effect of Georesource Temperature Decline on the Performance of Isobutane Binary Cycle 214

22. Effect of Georesource Temperature Decline on the Performance of Mixture Binary Cycle 215

23. Near Optimal Working Fluid Parameters for Georesource Temperature Range 300°F-500°F 220

Appendix

A-1 Design Basis Engineering Parameters 239

A-2 Design Basis Cost Parameters 242

C-1 Thermodynamic Cycle State Points 269

C-2 Thermodynamic Cycle State Points 272

LIST OF ILLUSTRATIONS

Figure		Page
1.0	Various Levels of the Geothermal Binary Cycle Analysis Task	3
2.0	Conventional Geothermal Binary Cycle	7
3.0	Geothermal Binary Cycle Streams and Nodes	9
4.0	Dual Boiler Binary Cycle State Points	11
5.0	Commonly Encountered Working Fluid Thermodynamic Behavior	16
6.0	Basic Variations of Rankine Cycle	18
7.0	T-s Diagram of Isobutane Reversible Cycle (Base Case)	26
8.0	P-h Diagram for Isobutane Ideal Cycles	29
9.0	Pressure-Temperature Plot of Base Case, Case 1 and Case 2 Isobutane Cycles	30
10.0	Temperature-entropy Diagram for Isobutane Ideal Binary Cycles	37
11.0	Temperature-enthalpy Diagram of the Isobutane Ideal Binary Cycle	40
12.0	Temperature-enthalpy Diagram of the Isobutane Ideal Binary Cycles	43
13.0	Temperature-entropy Diagram of the Isobutane Ideal Binary Cycles	46
14.0	Effect of Condenser Dew Point Temperature on Turbine Enthalpy Change	49
15.0	Effect of Condenser Dew Point Temperature on the Net Thermodynamic Cycle Work	51
16.0	Sensitivity of Total System Capital Cost to Power Plant Capital Cost	79
17.0	Effect of Power Plant Capital Cost on the Optimum Molecular Weight of the Working Fluid	80
18.0	Sensitivity of Total System Capital Cost to Brine System Cost	85

Figure		Page
19.0	Effect of Brine System Capital Cost on the Optimum Molecular Weight of the Working Fluid ...	88
20.0	Power Plant Component Costs as Percentages of Total System Cost	89
21.0	Sensitivity of Total System Cost to Power Plant Component Cost	91
22.0	Sensitivity of Total System Cost to Power Plant Component Cost	92
23.0	Sensitivity of Total System Cost to Power Plant Component Cost	93
24.0	Ideal Cycles Using Finite Resources	100
25.0	Isobutane Binary Cycles for Various Turbine Inlet Pressures for 300°F Georesource	105
26.0	Ideal Rankine Cycle with Infinite Source and Infinite Sink	108
27.0	Ideal Rankine Cycle With Infinite Source and Infinite Sink	112
28.0	Resource Utilization Optimum and Cost Optimum Turbine Inlet Pressure Versus Net Plant Work and Total System Cost of Isobutane Binary Cycles	116
29.0	Temperature-Enthalpy Diagram of Isobutane Cycle (Base Case)	119
30.0	Temperature-Enthalpy Diagrams of Isobutane Cycles (Base Case and Case 1)	120
31.0	Effects of Increasing Turbine Inlet T and P (fixed $\dot{M}_H$ and $\dot{Q}_H$) on Isobutane Cycle for 300°F Georesource	136
32.0	Effects of Increasing Turbine Inlet T and P (fixed $\dot{W}_N$) on Isobutane Cycle for 300°F Georesource	137
33.0	Effect of Increasing Brine Heat Exchanger LMTD on Isobutane Cycles (Base Case and Case 1)	139
34.0	Brine Heat Exchanger LMTD as a Function of Georesource Temperature	143

Figure		Page
35.0	Brine Heat Exchanger Brine Flow Rate Versus Georesource Temperature	144
36.0	Brine Heat Exchanger Surface Area as a Function of Georesource Temperature	145
37.0	Effects of Brine Heat Exchanger LMTD (Fixed $\dot{W}_N$)	147
38.0	Effect of Increasing Condenser LMTD on Isobutane Cycles (Base Case and Case 1)	150
39.0	Effects of Increasing Condenser LMTD (fixed $\dot{W}_N$) on Isobutane Cycle for 300°F Georesource	155
40.0	Effect of Increasing Cooling Water Temperature Range on Isobutane Cycles (Base Case and Case 1).	158
41.0	Effects of Cooling Water Temperature Range (for fixed $\dot{W}_N$) on Isobutane Cycle for 300°F Georesource	162
42.0	Effect of Increasing Brine Flow Rate on Isobutane Cycles (Revised Base Case and Case 1)	170
43.0	Effects of Increasing Brine Flow Rate (for Fixed A_H and A_C) on Isobutane Cycle for 300°F Georesource	173
44.0	Supercritical Cycles	176
45.0	Subcritical Cycles	177
46.0	Superimposed Temperature-Enthalpy Diagram of Isobutane and Mixture (50% isobutane - 50% isopentane) Cycle	181
47.0	Dual Boiler Binary Cycle State Points	186
48.0	Temperature-Entropy Diagram of Single Boiler Binary Cycles	188
49.0	T-$\dot{Q}$ Diagram of Cis-2-Butene	191
50.0	T-$\dot{Q}$ Diagram of Pure and Mixed Fluid	198
51.0	Net Plant Work Versus Number of Boilers for Multiple Boiler Binary Cycles	203
52.0	Net Thermodynamic Cycle Efficiency versus Number of Boilers for Multiple Boiler Binary Cycle	204

Figure Page

53.0 Molecular Weight as a Function of Georesource Temperature 217

54.0 Critical Temperature, Critical Density and Accentric Factor as a Function of Georesource Temperature 218

55.0 Near Optimal Turbine Inlet Pressure Versus Molecular Weight and Georesource Temperature 221

56.0 Near Optimal Turbine Inlet Pressure as a Function of Georesource Temperature and Molecular Weight 222

57.0 Effect of Georesource Temperature Decline (for Fixed A_H, A_C, $\dot{M}_H$) on Pure and Mixture Binary Cycles 225

Appendix

C-1 Steps 3 and 4 Shown for a Pure Fluid, Cis-2-Butene, Cycle 265

C-2 Steps 5 and 6 Shown for a Pure Fluid Cycle 267

C-3 Steps 3, 4, and 5 Shown for a Mixture Fluid Cycle 270

ABSTRACT

It has been demonstrated in this research that the analysis of geothermal binary cycles can be simplified through the use of basic thermodynamic relations. The complex interrelationships of thermodynamic, unit operational and cost parameters were developed and are presented in a simple form for the benefit of the reader. At lower georesource temperatures, the resource utilization optimum and cost optimum nearly coincide. Mixture working fluids provide a significantly greater amount of net plant work per unit mass of brine at lower georesource temperatures, when the design objective is the maximization of net plant work per unit mass of brine.

ANALYSIS OF THE GEOTHERMAL BINARY CYCLE USING PARAFFIN HYDROCARBONS AS WORKING FLUIDS

CHAPTER I

INTRODUCTION

Statement of Objectives

The analysis of the geothermal binary cycle using paraffin hydrocarbons as working fluids has been presented in this work in a relatively simple way. The paraffin hydrocarbons considered for this analysis include isobutane, isopentane and their binary mixtures. The complex interrelationships of thermodynamic, operational and cost parameters were explored. The understanding and discussion of these interrelationships has also been provided. The advantages and disadvantages of the use of hydrocarbon mixtures compared to pure fluids in the conventional binary and cascade binary cycles are discussed. The hydrocarbon fluids considered in this separate study include isobutane, cis-2-butene, and binary mixtures of cis-2-butene, propane and cyclopentane.

A fixed plant simulator[1], developed at the University of Oklahoma, was used in the study of the effects of the georesource temperature decline on the performance of the pure and mixture conventional binary cycles.

This research was part of an overall geothermal research project at the University of Oklahoma under contract from the Idaho National Engineering Laboratory and the U.S. Department of Energy.

Scope of Investigation

Basically, the analysis of the so-called binary cycle involves three fluids, the source, sink and working fluid, and their roles in the binary cycle operation. However, in order to clearly understand the scope of this investigation, the geothermal binary cycle analysis work was divided into three main levels: brine, working fluid selection and operating conditions selection, as shown in Figure 1.0. Figure 1.0 also represents a logical way for a design engineer to carry out the design engineering studies; or for an analyst to persue the analyses of the geothermal binary cycles.

Brine represents the starting point for the geothermal power cycle research. Once the brine is successfully produced from a geothermal well and analyzed, its temperature, pressure, quality (whether a mixture of saturated liquid and vapor, etc.), and the impurities (mainly brine content and non-condensable gases) if any, are thus known at the wellhead and can be assumed as fixed parameters for the analysis purposes. Thus at level I, the brine characteristics will determine the type of process most suitable for the process conditions. For example, it was assumed for this study that brine would be

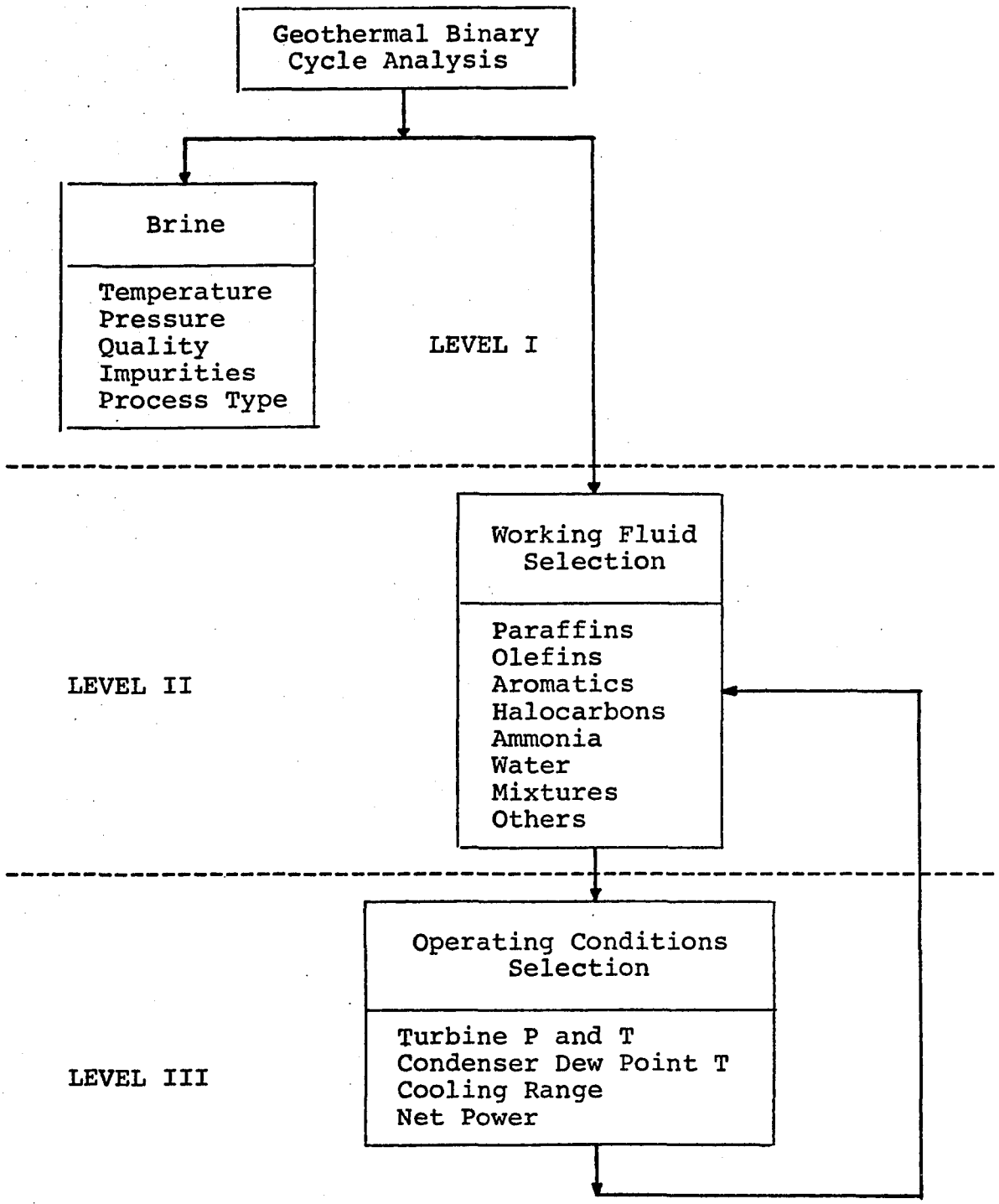

Figure 1.0 Various Levels of the Geothermal Binary Cycle Analysis Task

a saturated liquid, at a moderate (300-500 °F) temperature with no impurities, and that it may or may not contain non-condensable gases (e.g., carbon dioxide, nitrogen, etc.). Under these assumptions and when the design objective is the total system capital cost expressed in dollars per kilowatt, a conventional binary cycle is assumed as the most suitable energy conversion process out of the other competing binary cycles including staged flash, direct contact, preheat and cascade cycles, etc.[2,3,4]

The working fluid selection is the next level of research. Because of the large number and variety of fluids mentioned in the literature as potential candidates for the conventional geothermal binary cycle operation[5,6,7,8,9], it seems quite illogical to carry out a detailed analysis of each of these fluids in order to select the most suitable binary cycle fluid. This suggests a preliminary fluid screening procedure which could point out the low potential fluids without the use of a large simulator and with minimal amount of data. Reference (7) presents a three phase fluid screening procedure. The first and second phases of the three phase screening procedure permit a relatively quick evaluation, with potential working fluids identified for more detailed analysis. The final phase requires evaluation with the aid of a power cycle simulation program complete with rigorous thermodynamics, process and economic estimation subroutines. It can therefore be assumed here that by utilizing such a

procedure, the list of potential working fluids could be reduced to a few (possibly two or three) fluids for detailed analyses.

After the working fluid selection, the next important task is the selection of optimum operating conditions for a given fluid and a given georesource temperature. The parameters (objective functions) commonly chosen for optimization are: (1) maximization of net plant work per unit mass of brine, (2) maximization of the net thermodynamic cycle work, (3) minimization of the total plant capital cost in dollars per kilowatt for a specified net electrical output. The first two objective functions represent thermodynamic optima whereas the last one represents an economic optimum. The objective function chosen for this research was the capital cost in dollars per kilowatt for a power generation plant producing 25 MW_e net electrical output, unless otherwise stated.

The main objectives of this research fall into the last category of Figure 1.0, the selection of optimum operating conditions. However, this study also sheds light on the interrelationships of process and cost parameters, and shows to how a change in a given process or cost parameter can shift the optimum operating conditions to some other location.

Literature Review

When the geothermal resource is liquid dominated, i.e., available either as a saturated or compressed liquid, and is

at a low to moderate temperature (250-400°F), various arguments have been presented for the selection of a suitable energy conversion process for generating electric power.[4,14,15] A closed Rankine type cycle concept referred to as the binary cycle by Anderson[16] has been the subject of intense studies. A dual binary cycle power plant with a gross capacity of 10.5 MW_e is near completion in East Mesa, California.[17] Two additional binary cycle power plants are in the final planning and design phase.[17] Because of the growing interest in the binary cycle, a large number of working fluids have been studied by various investigators with emphasis on therodynamics and/or economics.[5,6,7,8,9,13,19]

In the conventional geothermal binary cycle, Figure 2.0, the geothermal fluid from the production wells is used in a heat exchanger to increase the temperature of a high pressure liquid phase working fluid, thereby converting the working fluid to a high temperature gas phase. The gas phase working fluid is then expanded through a turbine for power production. The working fluid at the turbine exhaust, which is usually a low pressure vapor, is then cooled and condensed in the condenser by heat exchange with cooling water. The slightly subcooled liquid phase working fluid at the condenser exit is then pumped to a high pressure thus completing the power cycle.

A few binary cycle studies have been carried out for the selection of optimum cycle operating conditions of a

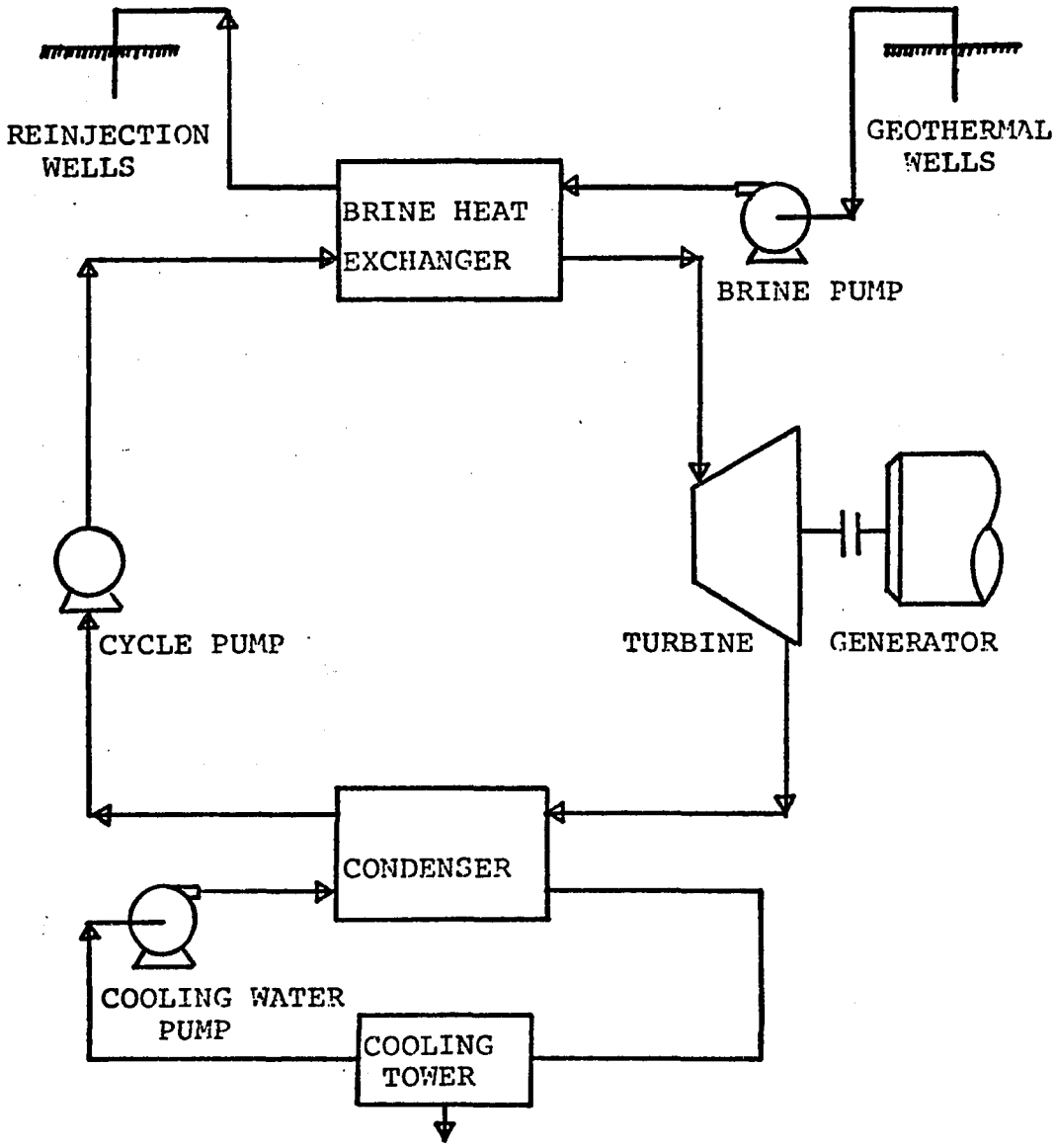

Figure 2.0 Conventional Geothermal Binary Cycle

given working fluid.[7,9,13,18] The objective function in these studies was either capital cost of the power plant expressed in dollars per kilowatt or net plant work per unit mass of brine. The capital cost (or net energy cost) is the logical objective function for private industry. However, studies utilizing the capital cost of the total power plant as the objective function are restricted to the specific cost models used to arrive at a local optimum condition. Thus, a change in any of the costs associated with major power plant components may shift the optimum to some other location. This shifting of the local cost optimum cannot be explained from cost analysis alone. However, if the interrelationships between thermodynamic, process and cost parameters were known or could be determined, then the shifting of the cost optimum would be easier to explain and predict. At present, the literature is minimal on the subject of the interrelationships between the thermodynamic, process and cost parameters of the geothermal binary cycle; the present work is an attempt to develop this type of information.

Geothermal Binary Cycle Simulation

A computer simulation of the conventional geothermal binary cycle, referred to as GEO4 has been developed at the University of Oklahoma.[10,11,12] The nodal points indicated in Figure 3.0 correspond to the cycle state points calculated in the GEO4 simulation program. The computer simulation is

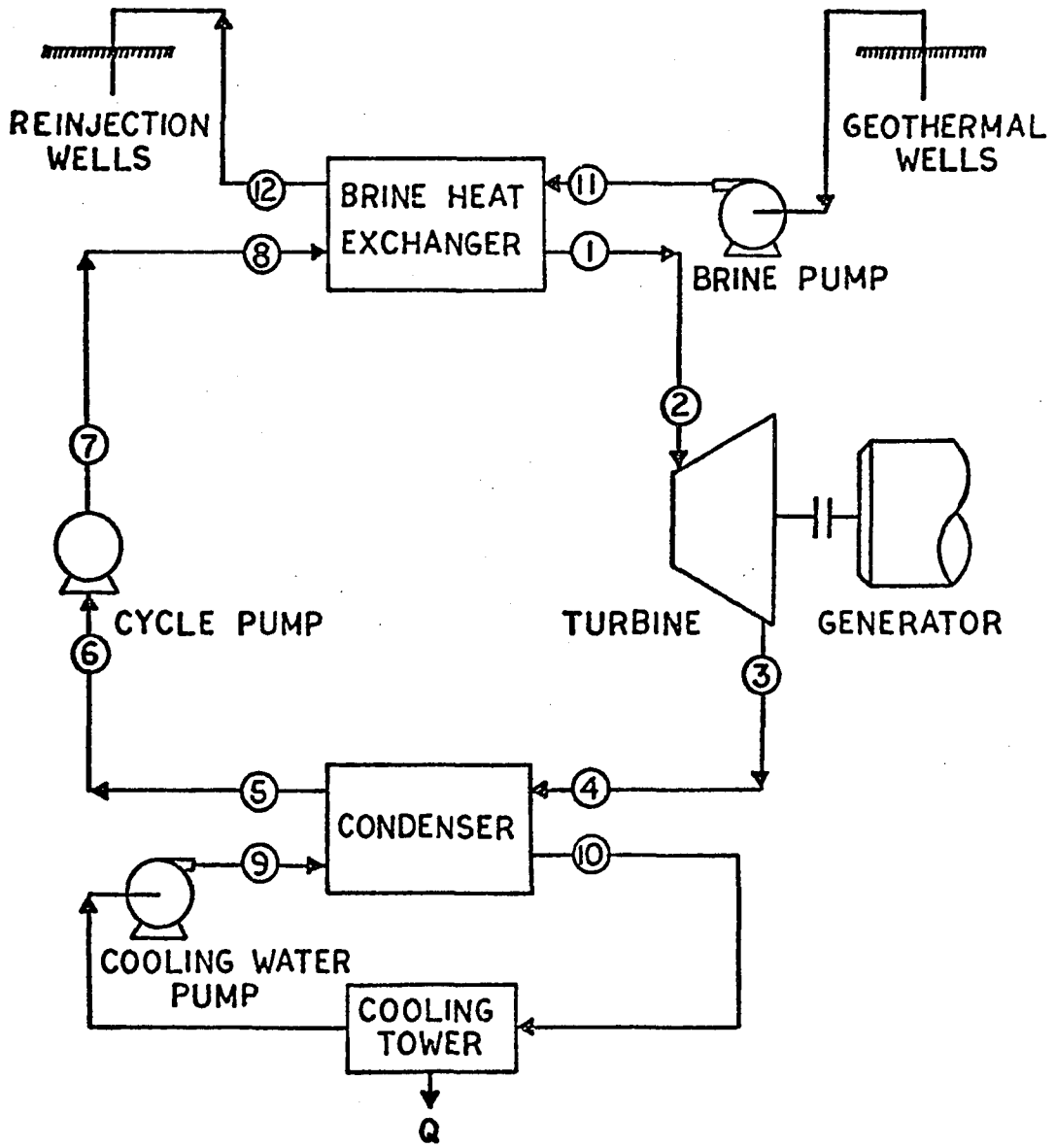

Figure 3.0 Geothermal Binary Cycle Streams and Nodes

an ordered set of calculations which describe the changes in the physical state of the working fluid as it moves through the power cycle, determines flow rates, sizes process units and calculates costs. The design basis parameters used with the conventional geothermal binary cycle simulator, GEO4, are detailed in Appendix A. A sample output of the cycle simulator is presented in Appendix D.

Cascade Binary Cycle

The major elements of the cascade binary cycle power plant, as considered in this work, are shown in Figure 4.0. The process consists of the following major units:

1. High Pressure Boiler 1
2. Low Pressure Boiler 2
3. High Pressure Turbine 1
4. Low Pressure Turbine 2
5. Condensers 1 and 2
6. Separator Vessel
7. Cycle Pumps 1, 2, and 3

Other process units not shown in Figure 4.0 include brine wells and gathering system and auxiliary plant equipment. The nodal points indicated in Figure 4.0 correspond to the process state points used in the calculation.

The process analysis starts at the working fluid inlet of low pressure boiler 2, in which the working fluid is partially vaporized by heat exchange with the brine coming from high pressure boiler 1. The working fluid vapor and liquid mixture

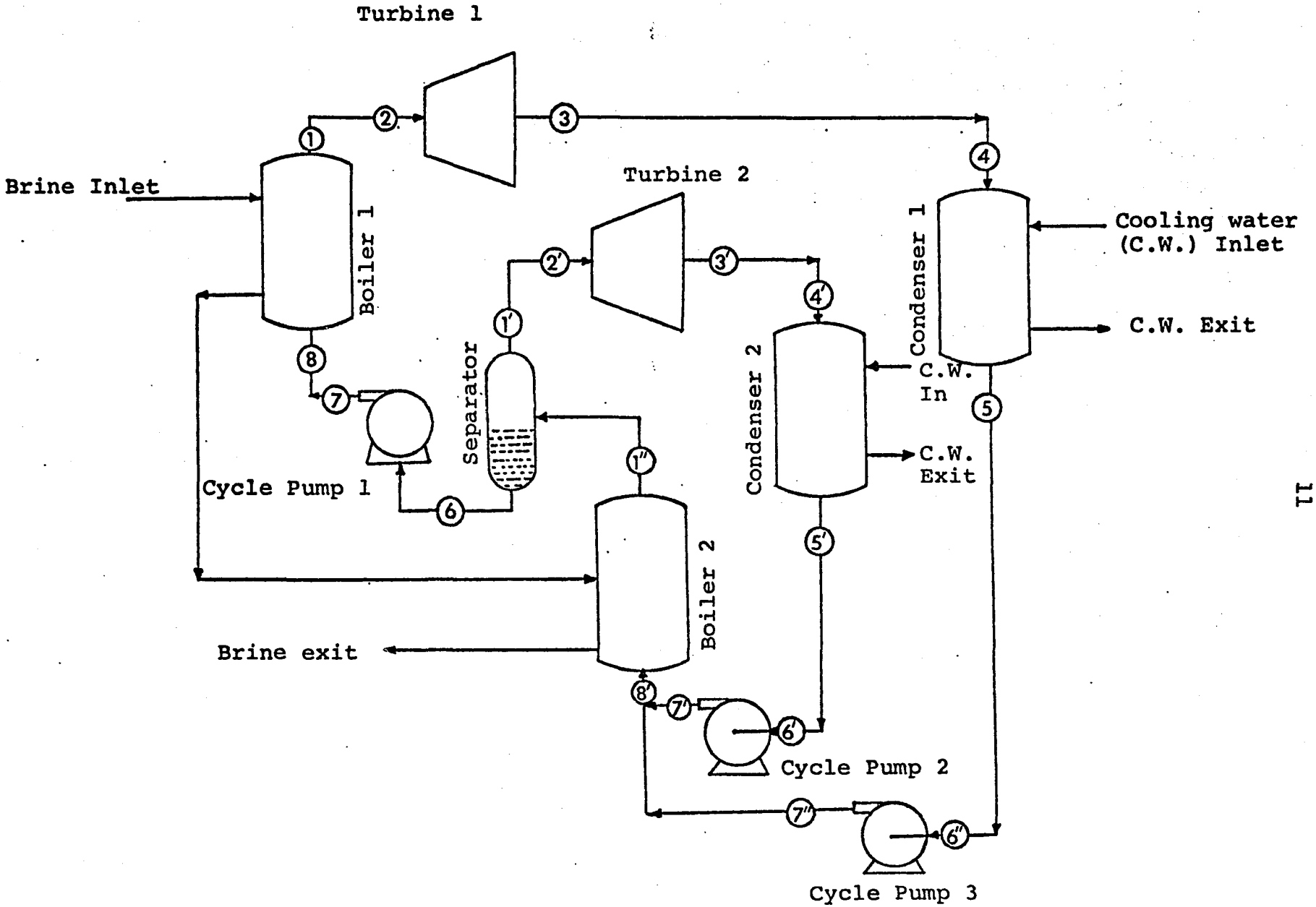

FIGURE 4.0 Dual Boiler Binary Cycle State Points

is transferred to a separator vessel where the low pressure gas leaves from the top of the separator and is expanded in low pressure turbine 2. The liquid working fluid leaving the separator bottom is pumped to the highest pressure in the cycle and is then passed through boiler 2 where it is converted to saturated vapor or superheated gas by heat transfer with the incoming brine from the production wells. The high pressure gas phase working fluid is then expanded through turbine 1 for power generation. The exhausts from turbines 1 and 2 are passed through two separate condensers and are cooled to a saturated or subcooled liquid state by the circulation of cooling water through the condensers. Thus, the working fluid streams at the exits of condensers 1 and 2 are at the lowest pressures and temperatures in the cycle. These subcooled liquid working fluid streams are then pumped to a higher pressure by cycle pumps 2 and 3 in order to complete the thermodynamic cycle. It has been considered here that the cycle pumps 2 and 3 exit streams 7' and 7" would be mixed together to give the working fluid temperature and pressure in process stream 8'.

Thermodynamic Behavior of Paraffin Hydrocarbons in the Geothermal Binary Cycle

The thermodynamic behavior of the working fluid as it is utilized in the binary, or more precisely a Rankine, cycle to produce power is the major criterion used in the selection of a suitable working fluid.

Since the thermodynamic behavior of the fluid in the binary cycle is very much influenced by its thermodynamic properties changes as it moves through the cycle, a brief mention of these properties is needed. Table 1 presents some of the important thermodynamic characterization parameters for the Rankine cycle working fluid. In Table 1, the I-factor is a modification of the following quantity defined by Kihara and Fukunaga.[5]

$$I = 1 - \left(\frac{ds}{dT}\frac{T_s}{C_p}\right)_{sat.vap.} = 1 - T_s \left(\frac{ds}{dh}\right)_{sat.\ vap.} \quad (1A)$$

where T_s is the saturation temperature corresponding to the condensing pressure, C_p is the specific heat at constant pressure, s and h are the specific entropy and enthalpy of the fluid.

For a fluid with a vertical saturated vapor locus on a temperature-enthalpy diagram, the I-factor is unity. If $I<1$, the turbine exhaust will be superheated, while for $I>1$, the turbine exhaust may be wet (depending on the turbine inlet conditions).

However, the I-factor, as defined by Kihara, is limited by the slope of the saturated vapor locus, dT/ds, which changes sign in the region of interest. A more convenient form of this dimensionless parameter is defined here as

$$I = 1 - T_{avg}\left(\frac{\Delta S}{\Delta h}\right)_{sat.vap.} \quad (1B)$$

Table 1

RANKINE CYCLE WORKING FLUID THERMODYNAMIC
PROPERTY CHARACTERIZATION PARAMETERS

Fluid	Formula	Molecular Weight	Critical			Vapor Pressure at 100°F, psia	Specific Volume Sat. Vapor at 100°F, cu ft/lb.	Temperature Range, Sat. Vapor for $\Delta S/\Delta T$, °F	$\Delta S/\Delta T$ Sat. Vapor Btu/lb- R^2	I-factor
			Temperature, °F	Pressure, psia	Density, lb mole/ cu ft.					
Methane	CH_4	16.04	-116.0	673.08	0.6274	S.C.	S.C.	-250—-150	-0.002323	5.14
Ethane	C_2H_6	30.07	90.03	708.35	0.4218	S.C.	S.C.	-150— -50	-0.000904	2.37
Propane	C_3H_8	44.09	208.0	615.9	0.3121	188.3	0.559	80— 180	-0.000155	1.75
i-Butane	C_4H_{10}	58.12	274.98	529.1	0.2373	72.0	1.26	100— 220	+0.000140	0.70
n-Butane	C_4H_{10}	58.12	305.6	551.7	0.2248	51.36	1.8102	100— 250	+0.000137	0.705
i-Pentane	C_5H_{12}	72.15	369.1	490.9	0.2027	20.44	3.8475	100— 250	+0.000263	0.55
n-Pentane	C_5H_{12}	72.15	385.7	489.6	0.2007	15.57	5.105	100— 250	+0.000265	0.56
n-Hexane	C_6H_{14}	86.17	437.7	436.9	0.1696	4.956	13.733	100— 300	+0.000201	0.68
n-Heptane	C_7H_{16}	100.2	513.0	358.0	0.1465	1.60	37.758	100— 350	+0.000273	0.564
cis-2-Butene	C_4H_8	56.11	324.4	610.0	0.2660	46.1	2.125	100— 250	+0.0000127	0.967
Cyclopentane	C_5H_{10}	70.135	460.0	654.1	0.240	10.04	8.28	100— 250	+0.000068	0.855

where T_{avg} is the arithmetic average temperature of the temperature ranges shown in Table 1. The second temperature, T_2, of the temperature range can be estimated from

$$T_2 = T_s + n\, T_c \qquad (1C)$$

where T_c is the critical temperature of the fluid and n is a fraction of T_c which may vary from 0.4 to 0.5 depending upon the choice of a suitable temperature.

The temperature-entropy diagrams of Figure 5.0 show these working fluid thermodynamic behavior types, and the resultant situations whith respect to the I-factor and the locus of the fluid states within the turbine (shown by a dashed line in each diagram). As can be seen from Table 1, the I-factor varies from fluid to fluid. Within the homologous series of normal paraffin hydrocarbons, the behavior for $I>1$, in diagram (a) in Figure 5.0 is exhibited by methane, ethane and propane, the behavior for $I<1$, in diagram (c) in Figure 5.0 is exhibited by the butanes and higher molecular weight normal paraffin hydrocarbons. The behavior for $I\approx1$, in diagram (b) in Figure 5.0, is exhibited by cis-2-butene (and other fluids not shown in Table 1). Other characterization parameters are discussed elsewhere.[7]

The analysis of the thermodynamic behavior of the fluid can be simplified if an ideal Rankine cycle type calculation is used for comparison purposes. By an ideal Rankine cycle it is implied here that the processes of the turbine

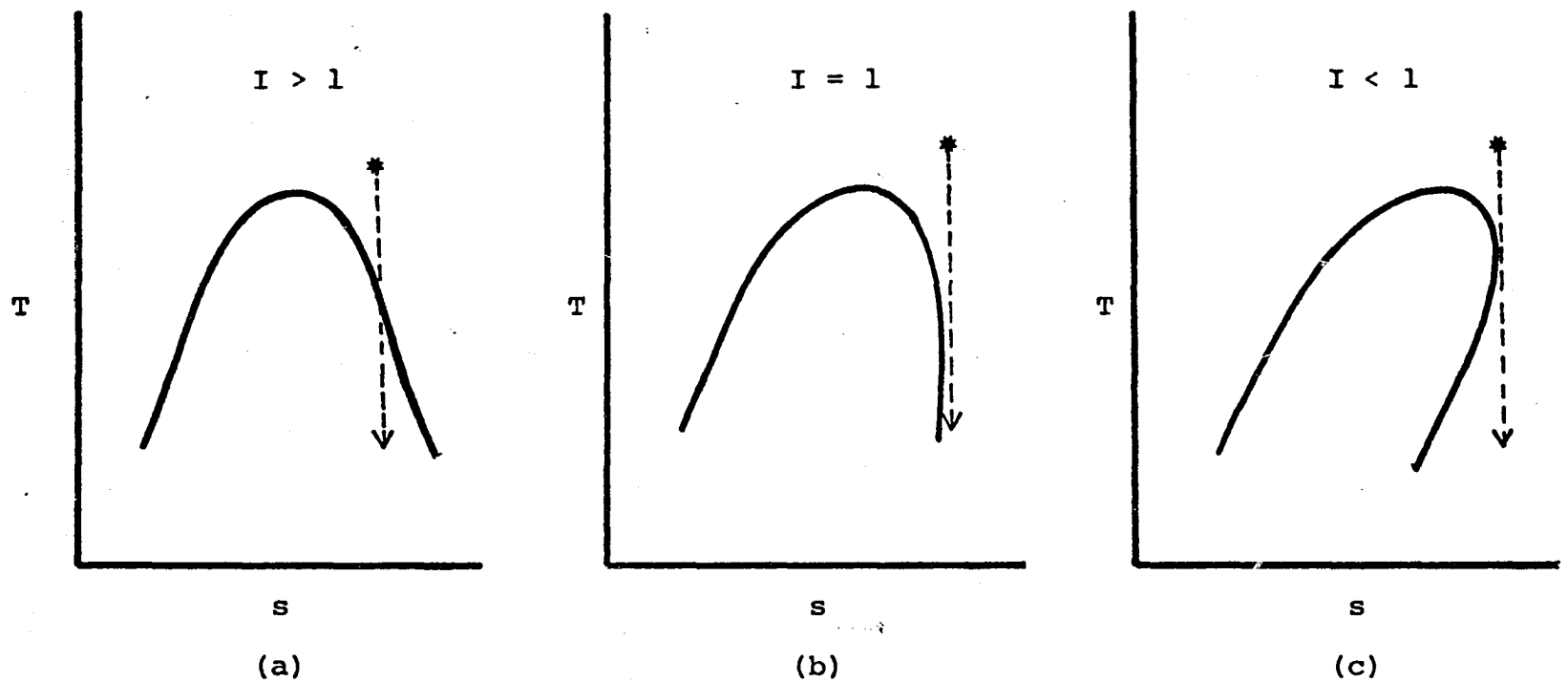

Figure 5.0 Commonly Encountered Working Fluid Thermodynamic Behavior

expansion and pump compression are reversible (isentropic) and adiabatic, and the heat transfer processes in the heat exchanger and condenser are isobaric (no frictional pressure drops). When the geothermal fluid exit condition is not taken into account, the parameters used as indicators of cycle behavior are the net cycle work and the net cycle efficiency. The net cycle specific work, $\underline{W}_N$, is the turbine specific work plus the cycle pump specific work. Net cycle efficiency, η_c, is defined as the ratio of the net cycle specific work ($\underline{W}_N$) to the specific heat input ($\underline{Q}_H$) required to produce that work, i.e.,

$$\eta_c = \frac{\underline{W}_N}{\underline{Q}_H} = \frac{\underline{W}_T + \underline{W}_P}{\underline{Q}_H} \qquad (2)$$

where $\underline{W}_T$ is the turbine specific work and $\underline{W}_P$ is the pump specific work.

Before discussing the Rankine cycle, it is desirable to exibit the cycle on a T-s (temperature-entropy) diagram. There are two basic variations of the Rankine cycle: (1) the subcritical cycle, where the turbine inlet pressure is less than the critical pressure of the fluid, and (2) the supercritical cycle, where the turbine inlet pressure is greater than the critical pressure of the fluid. The two variations of the Rankine cycle are shown on T-s diagrams in Figure 6.0.

If the assumption of a steady-state steady-flow process is made, and changes of kinetic and potential energy are neglected, then heat transfer and work may be represented by various areas on the T-s diagram. The specific heat transferred to the working fluid ($\underline{Q}_H$) is represented by the area

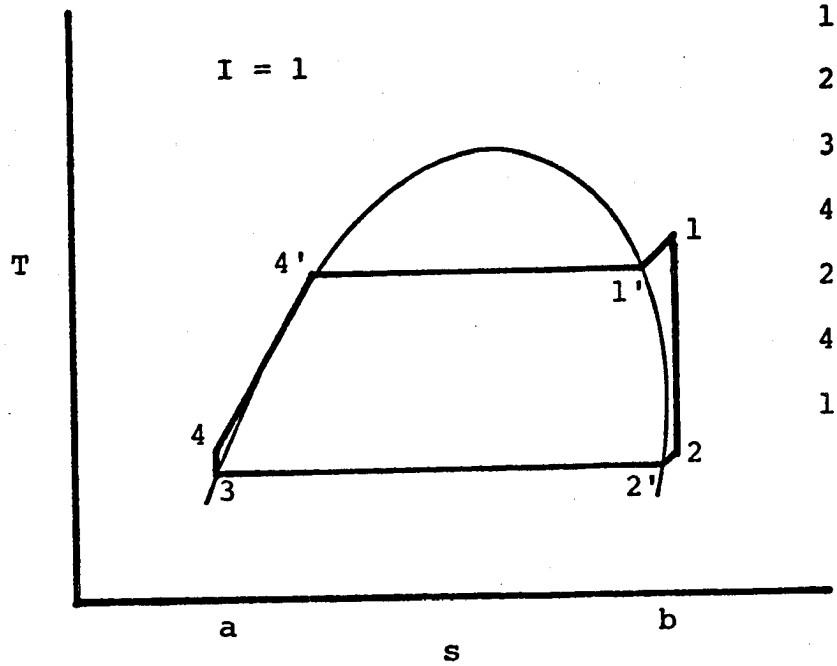

Legend:

1 = Turbine Inlet, Heat Exchanger Outlet
2 = Turbine Outlet, Condenser Inlet
3 = Condenser Outlet, Cycle Pump Inlet
4 = Cycle Pump Outlet, Heat Exchanger Inlet
2' = Dew Point in Condenser
4' = Bubble Point in Heat Exchanger
1' = Dew Point in Heat Exchanger

(a) Subcritical Rankine Cycle

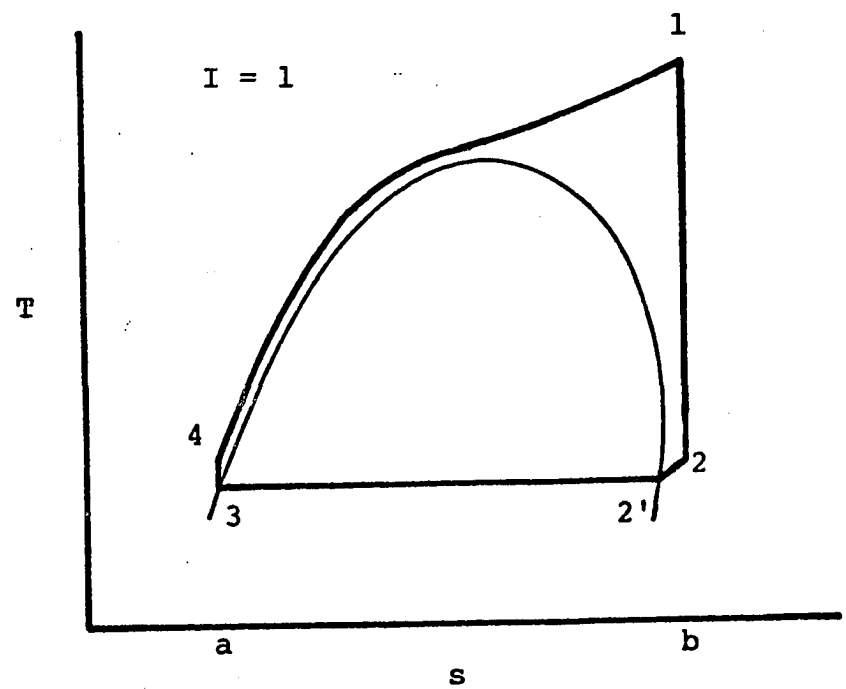

(b) Supercritical Rankine Cycle

Figure 6.0 Basic Variations of Rankine Cycle

a-4-4'-1'-1-b-a, and the magnitude (but not sign) of the specific heat transferred from the working fluid ($-\underline{Q}_C$) is represented by the area a-3-2'-2-b-a. From the first law of thermodynamics, we know that for a steady state process

$$\oint \delta\underline{Q} = \oint \delta\underline{W} \tag{3}$$

Therefore, we can conclude that the net cycle specific work, $\underline{W}_N$, will be represented by the area 3-4-4'-1'-1-2-2'-3. In terms of $\underline{Q}_H$ and $-\underline{Q}_C$, $\underline{W}_N$ can be written as

$$\underline{W}_N = \underline{Q}_H + \underline{Q}_C \tag{4}$$

$$\eta_C = \frac{\underline{Q}_H + \underline{Q}_C}{\underline{Q}_H} = 1 + \frac{\underline{Q}_C}{\underline{Q}_H} \tag{5}$$

From (5) it is evident that the net cycle efficiency, η_C, can be increased in two fundamental ways: (1) by increasing $\underline{Q}_H$ or (2) by decreasing $\underline{Q}_C$. These changes are achieved by increasing the temperature at which heat is transferred to the working fluid and decreasing the temperature at which heat is transferred from the working fluid.

In discussing the efficiency of the Rankine cycle it is useful to think in terms of the average temperatures at which heat is received or rejected by the working fluid. Any changes that increase the average temperature at which heat is supplied or decrease the average temperature at which heat is rejected will increase the Rankine cycle efficiency.

If the objective is to increase the net cycle specific work, $\underline{W}_N$, the focus should be on the turbine work, which changes more quantitatively than the pump work. The turbine work can be increased in two ways: (1) by increasing turbine inlet temperature or pressure or both (and therefore increasing enthalpy h_1), or (2) by decreasing the turbine outlet temperature (and therefore decreasing enthalpy h_2). It may be added here that turbine outlet temperature can be decreased indirectly by decreasing the turbine outlet pressure. It has been shown elsewhere that for optimum cost cycles the turbine work usually increases as the superheat at both ends of the turbine is decreased.[22] Thus, fluids with I-factor of unity would have minimal or no superheat (depending on the operating conditions) at both ends of the turbine are favored. Fluids in the homologous series of normal paraffin hydrocarbons have I-factor considerably different from unity. Thus, depending on operating conditions, normal paraffin hydrocarbons with $I>1$ generally will have some superheat at the turbine inlet, whereas the fluids with $I<1$ generally will have some superheat at the turbine exhaust. From Table 1, it can be noted that cis-2-butene (an alkene isomer) has $I\simeq1$. It has been shown that when the objective is the minimization of the total system capital cost in dollars per kilowatt, cis-2-butene gives greater turbine work than the normal paraffin hydrocarbons and certain halocarbons as well.[7]

Among paraffin hydrocarbons, methane has a very low (-116.4°F) critical temperature and cannot be considered a

candidate fluid for the geothermal binary cycle. Ethane has a critical temperature of 90°F, which is too low for condenser operation at normal cooling water temperatures. Propane and other higher molecular weight normal paraffin hydrocarbons can be compared with respect to their critical temperatures and pressures. Generally, fluids with a low critical temperature require a relatively high brine heat exchanger (and turbine inlet) operating pressure at the desired operating temperature. The vapor pressure at the condensing temperature will also tend to be higher, as can be seen in Table 1 for a condensing temperature of 100°F.

An important consideration for supercritical operation is, whether there is an adequate margin between operating temperatures and the critical temperature. A small margin would result in a very sensitive system (eg., to changes in the source temperature). An equally important consideration should be given to the lowest pressure of operation because fluid systems operating below atmospheric pressure are likely to develop continual maintenance problems.[23] The basic reason is simple: any large system will eventually leak, and leakage of air and oxygen into a system is almost invariably a serious cause of corrosion and maintenance problem. In addition to this, the partial pressure of air in a boiling and condensing fluid system can seriously impair the operating performance. It therefore is advisable to avoid fluids (like n-hexane and higher

molecular weight normal paraffins) which have vapor pressures below one atmosphere pressure at 100°F for the geothermal binary cycle. Thus, only propane, butane and pentane among the normal paraffins can be considered as potential working fluid candidates for the geothermal binary cycle operation when the geothermal resource fluid (brine) is available as a saturated liquid in the 300-500°F temperature range.

The discussion of the thermodynamic behavior of paraffin hydrocarbons and the effect on geothermal binary cycle efficiency would not be complete without considering the resource utilization efficiency. The resource utilization efficiency, η_{RU}, is defined here by the relation

$$\eta_{RU} = \frac{\underline{W}_{NP}}{b} \tag{5A}$$

where

$\underline{W}_{NP}$ = Net plant specific work obtained from the entire geothermal plant ($=\underline{W}_N + \underline{W}_{parasitic}$)

b = Maximum useful work which could be obtained in a reversible process between the brine and an infinite sink at the ambient or dump conditions; b is also referred to as the availability

The availability provides a convenient measure of the maximum extent to which the geothermal resource can be utilized in a geothermal energy conversion process. The mathematical expression for the availability can be determined by combining the first law energy balance and second law entropy balance

equations. For the steady-state processes encountered in geothermal energy conversion, the availability is the following function of brine properties[10] (neglecting the changes in the kinetic and potential energy of the brine).

$$B = [(h - h_D) - T_D (s - s_D)] M_H \qquad (5B)$$

where M_H is the mass of the brine flowing through the plant during the time period considered. The subscript D represents the dump (sink) conditions, taken to be 80°F and 14.7 psia herein. Thus, the magnitude of B is dependent on the properties of the geothermal fluid and the dump temperature, T_D, and the magnitude of the thermal source. It may be noted here that η_{RU} can be determined for any geothermal energy conversion process and therefore process details are not required for the intercomparison of processes on this basis. This is an attractive feature of the resource utilization efficiency, since net thermodynamic cycle efficiency, η_c, and other thermal efficiencies are inadequate for broad intercomparison of geothermal energy conversion processes.

Another measure of how well the brine is utilized for energy conversion is the brine effectiveness, W_{NP}/M_H, which is the net plant work per unit mass of brine. It can be noted that maximizing the brine effectiveness, W_{NP}/M_H, corresponds to maximizing the resource utilization efficiency, η_{RU}, does not necessarily correspond to maximizing the cycle thermal efficiency, η_c.[7]

CHAPTER II

SENSITIVITY ANALYSIS OF THERMODYNAMIC AND PROCESS UNIT OPERATIONAL PARAMETERS

Cycle State Points

In the thermodynamic analysis of processes, the usual approach is to define various process or cycle efficiencies, and then discuss the sensitivities of these efficiencies to other process or economic parameters. There seems nothing wrong with this kind of analysis except that a specific value cannot be assigned to any process or cycle efficiency in advance of a calculation for given process conditions. However, a cycle efficiency, for example net thermodynamic cycle efficiency η_c, depends on the cycle state points, eg., turbine inlet pressure, temperature, condenser dew point temperature, etc. Turbine inlet pressure and temperature can be specified and controlled in the binary cycle operation by means of control devices; whereas, η_c cannot be specified or controlled arbitrarily. Therefore, it seems appropriate here to study and discuss the effects of variation of cycle state points on η_c or other cycle efficiencies. It may be mentioned here that cycle state points like condenser outlet T and P and cycle pump outlet conditions (T and P) are dependent on the

cycle state points mentioned earlier; i.e., turbine inlet P and T and condenser dew point temperature, and other process constraints. This section, therefore, will be restricted to the sensitivities of the latter three cycle state points to the other cycle parameters.

Turbine Inlet Temperature

The turbine inlet temperature (T.IN.T.) of a working fluid is fixed by specifying an approach temperature difference (DTHWI) between the working fluid and the given georesource (e.g., brine) at the brine inlet to the brine heat exchanger (BHE). Since isobutane is currently being considered as the top candidate pure fluid to be used in the first U.S. geothermal binary cycle power plant,[17] isobutane was chosen for most of the analyses. Figure 7.0 shows on a temperature-entropy (T-S) diagram an isobutane reversible cycle where the expansion and compression through the turbine and the cycle pump have been assumed to be isentropic. The isobutane cycle with the operating conditions shown in Figure 7.0, will be considered here as the base case (or basis) for some later comparisons. Here the turbine inlet temperature (state point 1) at pressure P_1 (= 200 psia) was chosen to be slightly greater than the dew pcint temperature (@ P_1) such that the turbine isentropic expansion path (represented by the path 1-2) will avoid the retrograde condensation region. State point 2 represents the turbine exhaust. The path 3-4 in Figure 7.0

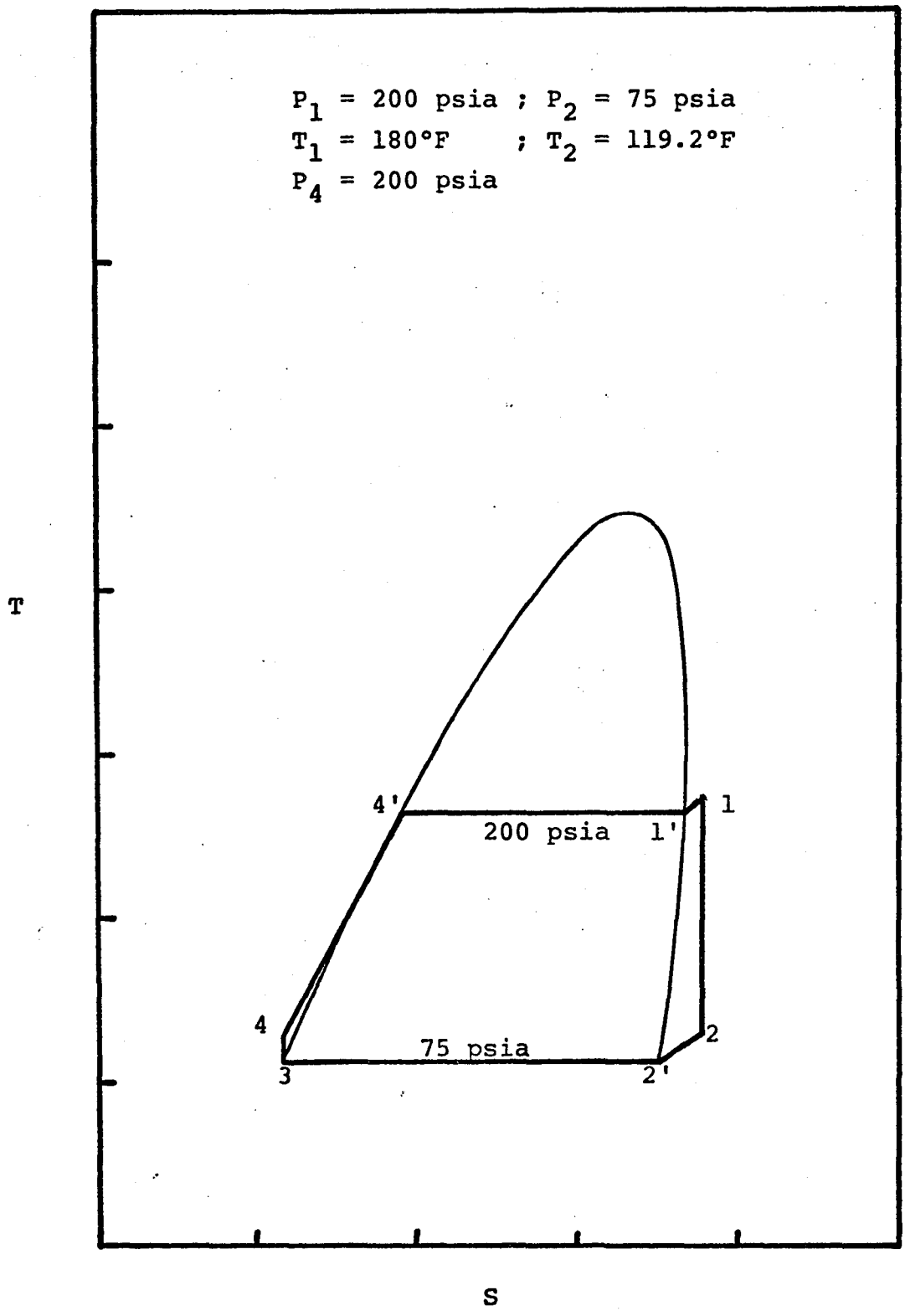

Figure 7.0 T-s diagram of isobutane reversible cycle (base case).

represents the cycle pump isentropic compression path. Similarly the heat transferred to the working fluid is the area under 4-4'-1'1 and the heat rejected by the working fluid is the area under 3-2'-2. Viscous pressure drops in the heat exchanger and the condenser have been neglected in order to simplify the analysis work.

In this section the effects of increasing the T.IN.T. on the following cycle parameters will be discussed: (1) turbine enthalpy change, (2) net thermodynamic cycle specific work, $\underline{W}_N$, and (3) net thermodynamic cycle efficiency, η_c. We know that

$$\underline{W}_N = \underline{W}_T + \underline{W}_P = \underline{Q}_H + \underline{Q}_C \qquad (1)$$

and

$$\eta_c = \frac{\underline{W}_N}{\underline{Q}_H} \qquad (2)$$

where

$\underline{W}_T$ = Turbine Specific Work, Btu/lb_m working fluid

$\underline{W}_P$ = Cycle Pump Specific Work, Btu/lb_m working fluid

$\underline{W}_N$ = Net Cycle Specific Work, Btu/lb_m working fluid

$\underline{Q}_H$ = Specific BHE Duty, Btu/lb_m working fluid

$-\underline{Q}_C$ = Specific Condenser Duty, Btu/lb_m working fluid

From equation (1) it is obvious that $\underline{W}_N$ can be increased two-ways: (1) increase $\underline{W}_T$ or (2) decrease $\underline{W}_P$. Because a higher working fluid turbine inlet temperature results in a greater enthalpy drop in the turbine[20], the

effect on increasing T.IN.T. on $\underline{W}_T$ can now be studied. The T.IN.T. can be increased in two fundamental ways: (1) increasing T.IN.T. while keeping turbine inlet pressure (T.I.P.) constant, (2) increasing T.IN.T. by increasing T.I.P. The two cases are shown on a pressure-enthalpy (P-h) diagram for isobutane in Figure 8.0, where a 20°F temperature increase (ΔT) was assumed for both cases.

Turbine inlet temperature and enthalpy change in turbine. In Figure 8.0 state points 1, b, and e represent turbine inlet temperatures and state points 2,2', and 2" represent turbine outlet temperatures for the base case, case 1 and case 2, respectively. From the first law of thermodynamics, for a change in the state of the system, the turbine enthalpy change depends only on the initial and final states and not on the path followed between the two states. Thus, if Δh across turbine for any specific path between the initial and final states is evaluated, the result must be the same for all other paths between the same initial and final states. However, it may be noted here that the change in a state property over any path may be evaluated as the sum of the changes of the property over all segments of the original path.[21]

A multi-step process for the evaluation of Δh across the turbine may now be established for the base case, case 1, and case 2 as indicated in Figure 9.0. The total enthalpy change, Δh, for all three cases can now be written:

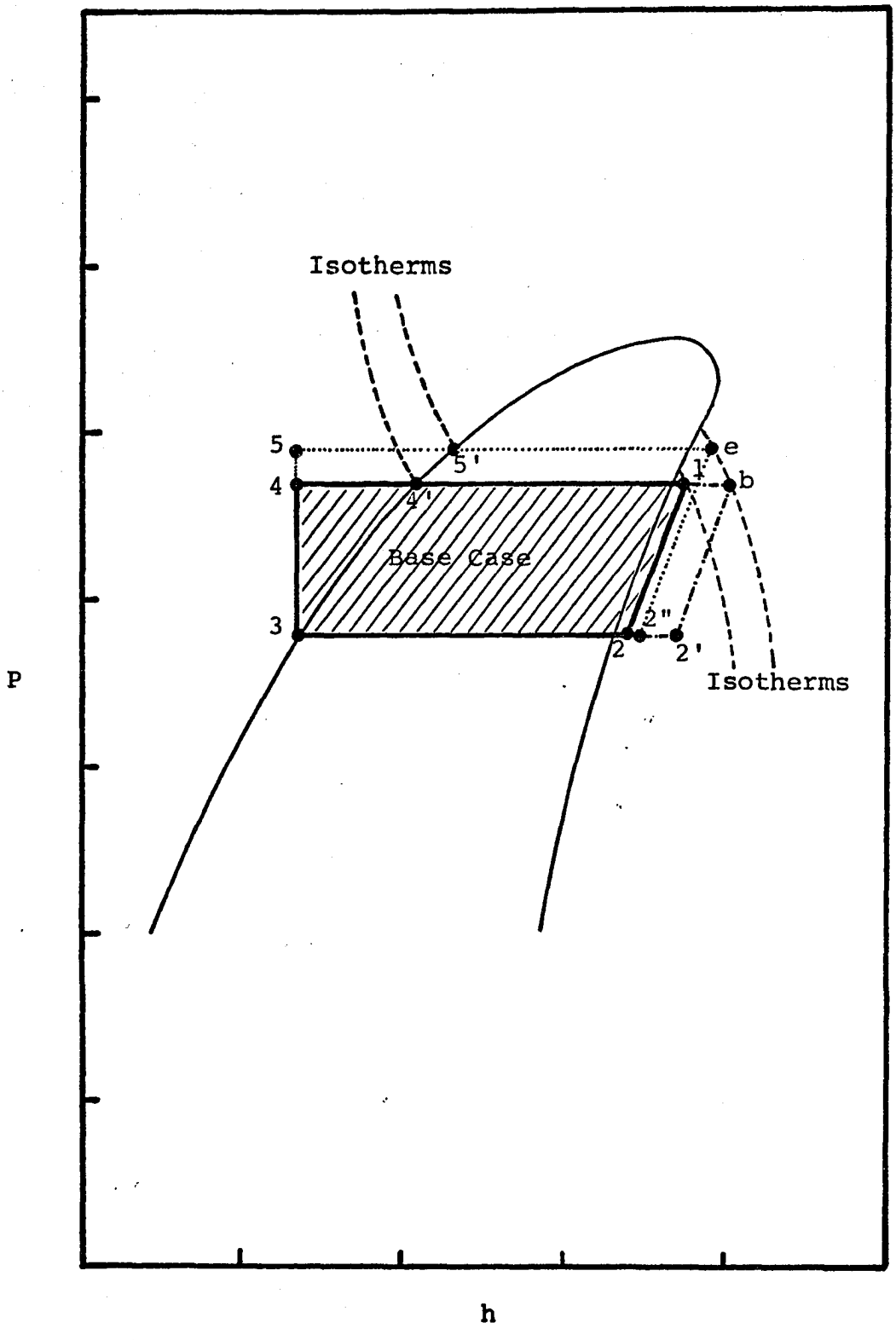

Figure 8.0 P-h diagram for isobutane ideal cycles

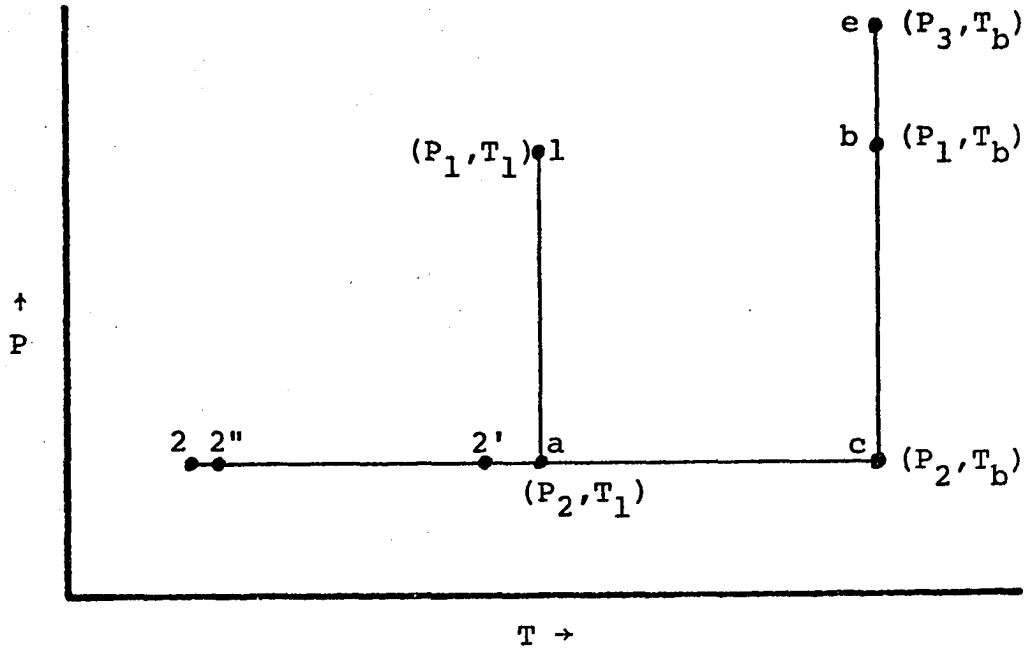

Figure 9.0 Pressure-Temperature Plot of Base Case, Case 1 and Case 2 Isobutane Cycles

Base Case:

$$\Delta h_{1-2} = \Delta h_{1-a} + \Delta h_{a-2} \tag{3}$$

Case 1

$$\Delta h_{b-2'} = \Delta h_{b-c} + \Delta h_{c-a} + \Delta h_{a-2'} \tag{4}$$

Case 2

$$\Delta h_{e-2"} = \Delta h_{e-b} + \Delta h_{b-c} + \Delta h_{c-a}$$

$$+ \Delta h_{a-2'} + \Delta h_{2'-2"} \tag{5}$$

Since

$$h = h(T,P)$$

the enthalpy change between any two states can be derived from thermodynamics as

$$\Delta h_{1-2} = \int_1^2 C_p dT + \int_1^2 [v - T(\frac{\partial v}{\partial T})_p] dP \tag{6}$$

Thus, Δh for equations (3), (4) and (5) can now be written using the sign convention of Reference 21 as follows:

$$-\Delta h_{1-2} = \int_{P_1}^{P_2} [v - T_1(\frac{\partial v}{\partial T})_p] dP - \int_{T_2}^{T_1} C_p \, dT \tag{7}$$

$$-\Delta h_{b-2'} = \int_{P_1}^{P_2} [v - T_b(\frac{\partial v}{\partial T_p})] dP - \int_{T_1}^{T_b} C_p \, dT - \int_{T_2'}^{T_1} C_p \, dT \tag{8}$$

$$-\Delta h_{e-2''} = \int_{P_3}^{P_1} [v - T_b(\frac{\partial v}{\partial T})_p] dP + \int_{P_1}^{P_2} [v - T_b(\frac{\partial v}{\partial T})_p] dP - \int_{T_1}^{T_b} C_p \, dT - \int_{T_2'}^{T_1} C_p \, dT - \int_{T_2''}^{T_2'} C_p \, dT \tag{9}$$

In order to compare the Δh for case 1 and case 2, the change in Δh between equations (9) and (8) can be taken. Let

$$-\Delta h_T = \Delta h_{e-2''} - \Delta h_{b-2'}$$

Then from equations (8) and (9) the following result is obtained after cancelling out the equal terms:

$$-\Delta h_T = \int_{P_3}^{P_1} [v - T_b(\frac{\partial v}{\partial T})_p] dP - \int_{T_2''}^{T_2'} C_p \, dT \tag{10}$$

For the operating conditions shown in Figures 7.0 and 8.0, the following results were obtained by hand calculation for isobutane ideal cycles, using Reference 24:

P_1 = 200 psia ; T_1 = 182°F

P = 251 psia ; T_b = 202°F

v = 24.265 cu.ft/lb mole; T_2, = 141.3 °F

$(\frac{\partial v}{\partial T})_P$ = 0.09596 $\frac{\text{cu. ft}}{\text{lb mole °R}}$; $T_{2"}$ = 121.7°F

C_p = 26.764 Btu/lbmole °R

$-\Delta h_T$ = -155.085 Btu/lbmole

or Δh_T = 2.668 Btu/lb_m

Thus, the turbine enthalpy change for case 2 is greater than that of case 1 by approximately 2.7 Btu/lb_m, when the T.IN.T. is increased by 20°F for both cases. Table 2 shows the results of the isobutane ideal cycle calculations for the three cases using the GEO4 simulator (although the same calculations could also be done by hand, the GEO4 simulator was used to save time!). The calculated enthalpy change between case 2 and case 1, Δh_T, is 2.66 Btu/lb_m compared to the previously hand calculated value of 2.668 Btu/lb_m.

The result shown above suggests that the turbine inlet temperature should be increased by increasing the pressure simultaneously rather than by adding superheat along the isobar at the turbine inlet. One may question the validity of this statement since a Δh of 20.40 Btu/lb_m as shown in Table 2 for

Table 2

EFFECTS OF TURBINE INLET TEMPERATURE ON THE IDEAL BINARY CYCLE PERFORMANCE

Cases Parameters	Base Case	Case 1	Case 2
Turbine			
Inlet T, °F	182	202	202
Inlet P, psia	200	200	251
Δh, Btu/lb_m	16.66	17.74	20.4
Δh Ratio	1.0	1.06	1.22
Cycle Pump			
Δh, Btu/lb_m	0.707	0.707	0.995
Heat Exchanger			
Δh, Btu/lb_m	156.9	168.3	161.5
Condenser			
Δh, Btu/lb_m	140.9	151.2	142.0
Overall			
Net Work, Btu/lb_m	15.95	17.03	19.4
Net Thermo. Eff. (η_c)%	10.2	10.1	12.0

case 2 could also be gotten if a sufficient amount of superheat were added at the turbine inlet (let us refer to this calculation as case 3). However, for fluids with I=1 or I<1 (such as isobutane), the addition of superheat at the turbine inlet would result in a corresponding amount of superheat ΔT at the turbine outlet. The consequences of the superheat at the turbine inlet and outlet would be the increases in the enthalpies at the turbine inlet and outlet and a decline in the net cycle efficiency η_c (as will be shown later).

Alternately, it could be argued that a turbine Δh of 17.74 Btu/lb_m as shown in Table 2 for case 1 could also be obtained for case 2 by relatively small increases of P and T at the turbine inlet (let us refer to this calculation as case 4). Table 3 shows a summary of the results of the calculations for case 3 and case 4. The corresponding values of pertinent parameters for case 1, case 2 and the base case also are included in Table 3 for comparison purposes. From Table 3, it is evident that even though the turbine Δh for case 2 and case 3 are the same, the net cycle efficiency for case 2 is approximately 21.6% higher than case 3. Similarly, the η_c for case 4 is approximately 5.9% higher than case 1. In comparing the claculations of case 2 (minimal superheat at turbine inlet) and case 3 (large amount of superheat at turbine inlet and outlet), it may be mentioned here that relative to the base case additional heat transfer surface area would be needed for case 3 whereas none would be required

Table 3

SUMMARY OF THE EFFECTS OF TURBINE INLET TEMPERATURE
ON THE IDEAL BINARY CYCLE PERFORMANCE

Parameters \ Case #	Base Case	Case 1	Case 2	Case 3	Case 4
Turbine					
Inlet T, °F	182	202	202	257	188
Inlet P, psia	200	200	251	200	213
Δh_T, Btu/lb_m	16.66	17.74	20.40	20.4	17.75
Superheat ΔT at Inlet, °F	1.0	21.0	1.0	76.0	1.0
Superheat ΔT at Outlet, °F	14.0	26.0	16.4	94.4	15.4
Cycle Pump					
Δh, Btu/lb_m	0.707	0.707	0.995	0.707	0.78
Heat Exchanger					
Δh, Btu/lb_m	156.9	168.3	161.5	199.2	158.5
Condenser					
Δh, Btu/lb_m	140.9	151.2	142.0	179.5	141.6
Overall					
Net Work, Btu/lb_m	15.95	17.03	19.40	19.66	16.97
Net Thermo. Eff. %	10.2	10.1	12.0	9.87	10.7

for case 2.

In conclusion, it can be stated that the increase in turbine inlet temperature results in an increase in turbine enthalpy change for a given fluid in the binary cycle, but the manner in which this increase in turbine inlet temperature is obtained is of importance.

Turbine inlet temperature and net cycle specific work. For any cycle, if viscous effects are ignored, the net cycle specific work obtained form the working fluid is the difference in the areas under the working fluid warming and cooling curves on a temperature-entropy diagram. This is easily illustrated, since from the relation

$$\underline{W}_N = \underline{Q}_H + \underline{Q}_C$$

it follows that if there are no viscous effects then

$$W_N = M_W \int_4^1 T \, ds + M_W \int_2^3 T \, ds \qquad (11)$$

where M_W is the mass of the working fluid, W_N is the net cycle work and s is the specific entropy and points 1, 2, 3 and 4 are state points in Figure 7.0. If the cycle is ideal, that is if expansion and compression are reversible, $s_1 - s_4 = s_2 - s_3$, and the net cycle specific work (per pound of working fluid) is the area enclosed by the working fluid cycle on the T-s diagram.

Figure 10.0 shows on a temperature-entropy diagram the state points for the base cycle, case 1 and case 2. The net cycle work for the three cycles can now be represented by areas

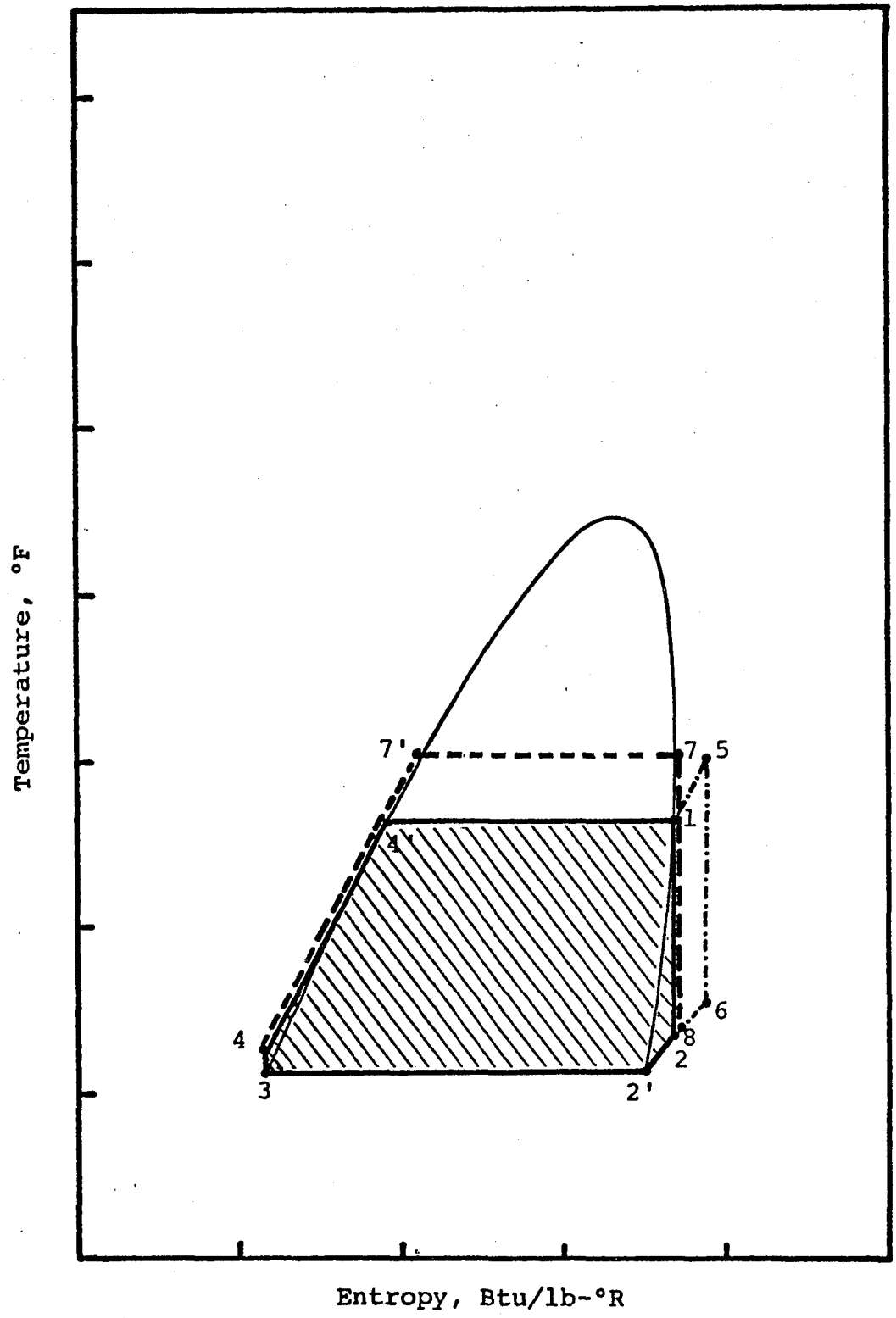

Figure 10.0 Temperature-entropy diagram for isobutane ideal binary cycles

enclosed by state points as follows:

net cycle specific work, base cycle = area 1-2-2'-3-4-4'-1

net cycle specific work, case 1 = area 5-6-2'-3-4-4'-1-5

net cycle specific work, case 2 = area 7-8-2'-3-4-7'-7

From Figure 10.0 the net cycle specific work for the base cycle (shown by the cross-hatched area) is common to the net cycle specific work obtained from case 1 and case 2. Therefore, the difference in the net cycle specific work between case 2 and case 1 will be represented by the difference in the areas 7-1-4'-7'-7 and 5-6-8-1-5. However, it is evident from Figure 10.0 that the area 7-1-4'-7'-7 is larger than the area 5-6-8-1-5. Therefore, the net cycle specific work obtained from case 2 should be larger than that of case 1. This can be verified from Table 1, where the net cycle specific work for case 2 was calculated as 19.4 Btu/lb_m compared to 17.0 Btu/lb_m for case 1, a 14% improvement over case 1 net cycle specific work.

It should be noted that at some higher pressure condition (depending on the working fluid) increasing the turbine inlet temperature while holding the turbine inlet pressure fixed (case 1) may yield a greater increase in cycle work than increasing the turbine inlet temperature to the same level while also increasing the turbine inlet pressure (case 2). However, for turbine inlet pressures far below the critical pressure, case 2 will yield more cycle work than case 1 for most fluids.

Turbine inlet temperature and net thermodynamic cycle efficiency. The net thermodynamic cycle efficiency for a cycle is given by

$$\eta_C = \frac{\underline{Q}_H + \underline{Q}_C}{\underline{Q}_H} = 1 + \frac{\underline{Q}_C}{\underline{Q}_H} \qquad (12)$$

also

$$\eta_C = \frac{\underline{W}_N}{\underline{Q}_H}$$

where $\underline{Q}_H$ and $-\underline{Q}_C$ are the heat received and rejected by the working fluid respectively in the cycle. Figure 11.0 shows on a temperature-enthalpy diagram the state points for the three ideal cycles considered in this analysis. In Figure 11.0, $\underline{Q}_H$, $\underline{Q}_{H1}$, $\underline{Q}_{H2}$ represent the heat transferred to the working fluid in the base case, case 1 and case 2 cycles respectively. Similarly $-\underline{Q}_C$, $-\underline{Q}_{C1}$, $-\underline{Q}_{C2}$ represent the heat rejected by the working fluid in the base case, case 1 and case 2 cycles respectively.

From the relationship of η_C, $\underline{Q}_H$ and $\underline{Q}_C$, it is evident that for a specified net work ($\underline{W}_N = \underline{Q}_H + \underline{Q}_C$), the net thermodynamic cycle efficiency is inversely proportional to $\underline{Q}_H$ and directly proportional to $\underline{W}_N$. From the relationships presented in equation (12) it is obvious that η_C can also be increased by decreasing $\underline{Q}_C$. Let

$$\eta_C = \frac{\underline{Q}_H + \underline{Q}_C}{\underline{Q}_H} = 1 + \frac{\underline{Q}_C}{\underline{Q}_H}$$

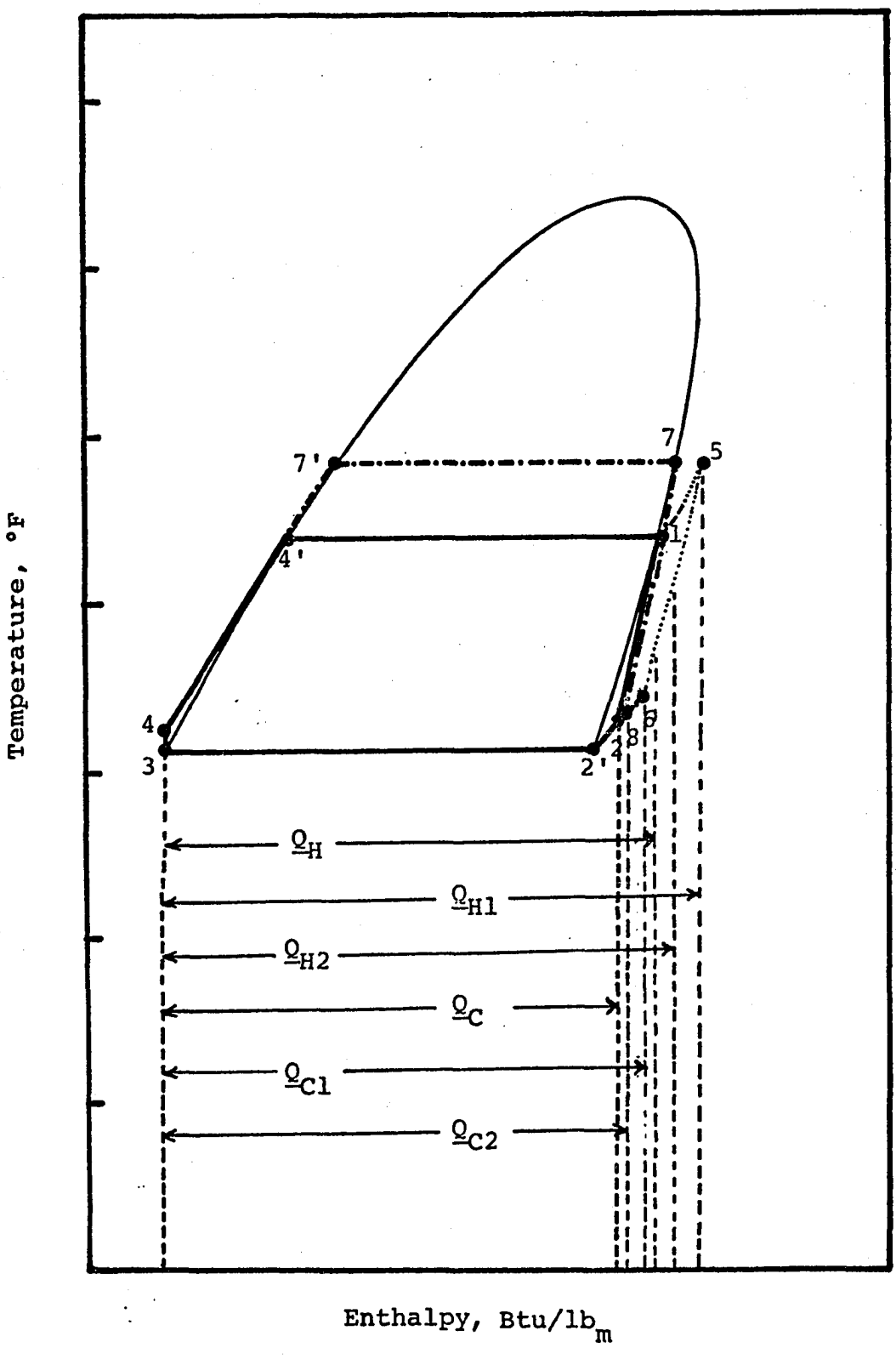

Figure 11.0 Temperature-enthalpy diagram of the isobutane ideal binary cycle

$$\eta_{C1} = \frac{\underline{Q}_{H1} + \underline{Q}_{C1}}{\underline{Q}_{H1}} = 1 + \frac{\underline{Q}_{C1}}{\underline{Q}_{H1}}$$

$$\eta_{C2} = \frac{\underline{Q}_{H2} + \underline{Q}_{C2}}{\underline{Q}_{H2}} = 1 + \frac{\underline{Q}_{C2}}{\underline{Q}_{H2}}$$

where η_C, η_{C1} and η_{C2} represent the net thermodynamic cycle efficiencies for the base case, case 1 and case 2 respectively. Referring to Figure 11.0, since $\underline{Q}_{C2} \simeq \underline{Q}_C$, it follows, since $\underline{Q}_{H2} > \underline{Q}_H$ that

$$\eta_{C2} > \eta_C \tag{13}$$

On the other hand, for case 1 the increases in the duties of the heat exchangers, $\underline{Q}_{H1} - \underline{Q}_H$ and $|\underline{Q}_{C1}| - |\underline{Q}_C|$ are nearly equal, so that

$$\eta_{C1} \leq \eta_C \tag{14}$$

Thus, from equations (13 and (14),

$$\eta_{C2} > \eta_{C1} \tag{15}$$

In Table 2, the net thermodynamic cycle efficiencies for the base case, case 1 and case 2 are shown to be 10.2%, 10.1% and 12.0% respectively, which is in accord with Equations (14) and (15).

The analyses presented in this section suggests that in order to obtain maximum turbine and net cycle work for sub-critical cycles, the turbine inlet temperature should be along the locus of the constant entropy (or isentropic) line which

just avoids the retrograde region (assuming the wet region is to be avoided in the turbine). This also yields the minimum amount of superheat at both ends of the turbine.

Turbine Inlet Pressure

For a given pressure, the turbine inlet temperature of any fluid can be determined if the georesource temperature and the approach temperature at the brine inlet of the brine heat exchanger (DTHWI) are specified. For the discussion from this point on, the turbine inlet temperature for a given pressure will be assumed to be obtained following the guidelines established in the previous section.

In this section, the effects of increasing the turbine inlet pressure (T.I.P.) on the following cycle parameters will be discussed: (1) turbine enthalpy change, (2) net thermodynamic cycle specific work, $\underline{W}_N$, and (3) net thermodynamic cycle efficiency, η_C. Here, the previously considered base case and case 2 will be used for comparison purposes. Only subcritical cycles are considered.

Turbine inlet pressure and turbine enthalpy change. Figure 12.0 shows on a temperature-enthalpy diagram the base case (P_1 = 200 psia) and case 2 (P_5 = 251 psia). As turbine inlet pressure is increased, the turbine inlet temperature is also increased in order to keep the turbine expansion path in the single-phase vapor region. Thus, the enthalpy at turbine inlet is increased because of an increase in T.I.P. For an isentropic expansion, the turbine outlet temperature

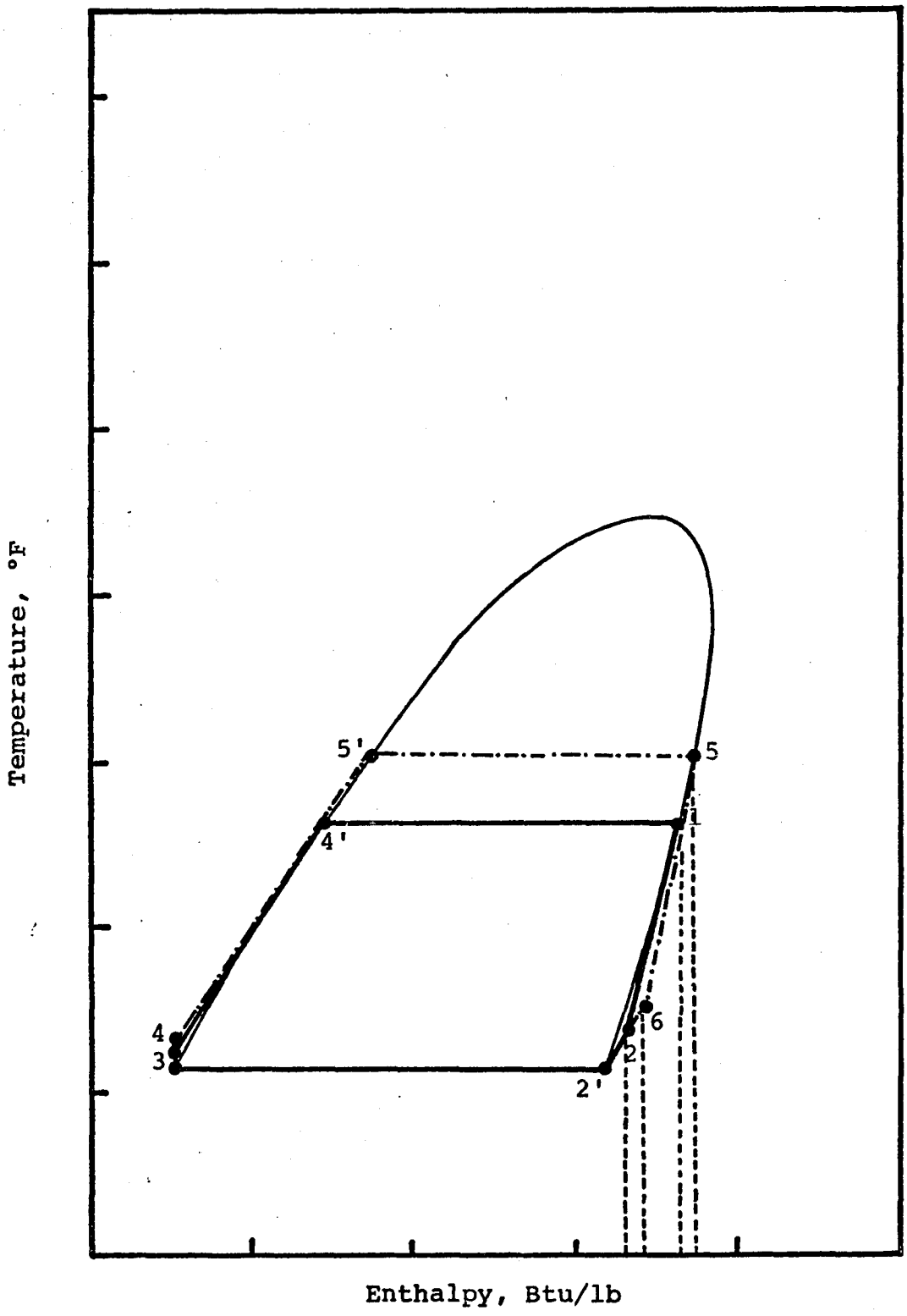

Figure 12.0 Temperature-enthalpy diagram of the isobutane ideal binary cycles

will be dependent on the saturated vapor locus or I-factor of the fluid. For fluids with I > 1, the entropy at the turbine inlet is dictated by the outlet conditions, and so remains unchanged; therefore the turbine Δh will increase for any increase in T.I.P. For fluids with I = 1, the entropy at the turbine outlet will not change, resulting in an increase in turbine Δh for any increase in T.I.P. For fluids with I < 1, like isobutane, the entropy at the turbine inlet is the controlling entropy and it increases for any increase in T.I.P. (for subcritical cycles well below the critical pressures). The increase in entropy at the turbine inlet results in an increase in entropy and temperature at the turbine outlet. Thus, for fluids with I < 1, the enthalpy at both the turbine inlet and outlet will increase because of an increase in T.I.P. However, the increase in the enthalpy will be larger at the turbine inlet than the turbine outlet and therefore the turbine Δh will increase. This is shown in Figure 12.0; the enthalpy change in the turbine for case 2 (Δh_2) is larger than the turbine Δh for the base case. In Table 2, the turbine Δh for case 2 is 20.40 Btu/lb_m when the T.I.P. is increased from 200 psia to 251 psia. Thus, for a 25% increase in T.I.P., the turbine enthalpy change increased by approximately 22%.

Turbine inlet pressure and net thermodynamic cycle specific work. It has been discussed earlier that in the absence of any viscous effects, the net thermodynamic cycle

specific work is given by the difference in the areas under the working fluid warming and cooling curves on a temperature-entropy (T-s) diagram

$$\underline{W}_N = \underline{Q}_H + \underline{Q}_C$$

Therefore, to compare the net cycle specific work for two binary cycles, the T-s diagrams for both cycles were utilized, as shown in Figure 13.0. The net cycle specific work, $\underline{W}_{N2}$ for case 2 (P_5 = 251 psia) is the area enclosed by the state points 5-6-2'-3-4-5'-5 and $\underline{W}_N$ for the base case (P_1 = 200 psia) is the area enclosed by the state points 1-2-2'-3-4-4'-1. It is quite obvious from Figure 13.0 that the area enclosed by 5-6-2'-3-4-5'-5 is greater than the area enclosed by 1-2-2'-3-4-4'-1, so that

$$\underline{W}_{N2} > \underline{W}_N$$

In other words, an increase in T.I.P. results in an increase in the net thermodynamic cycle work. In Table 2, the net cycle specific work obtained for case 2 is 19.4 Btu/lb_m compared to the 15.95 Btu/lb_m for the base case. Thus, for a 25% increase in the isobutane T.I.P. the net cycle specific work was increased by 21.6%.

Turbine inlet pressure and net thermodynamic cycle efficiency. The net thermodynamic cycle efficiency, η_C, for the base case is

$$\eta_C = \frac{Q_H + Q_C}{Q_H}$$

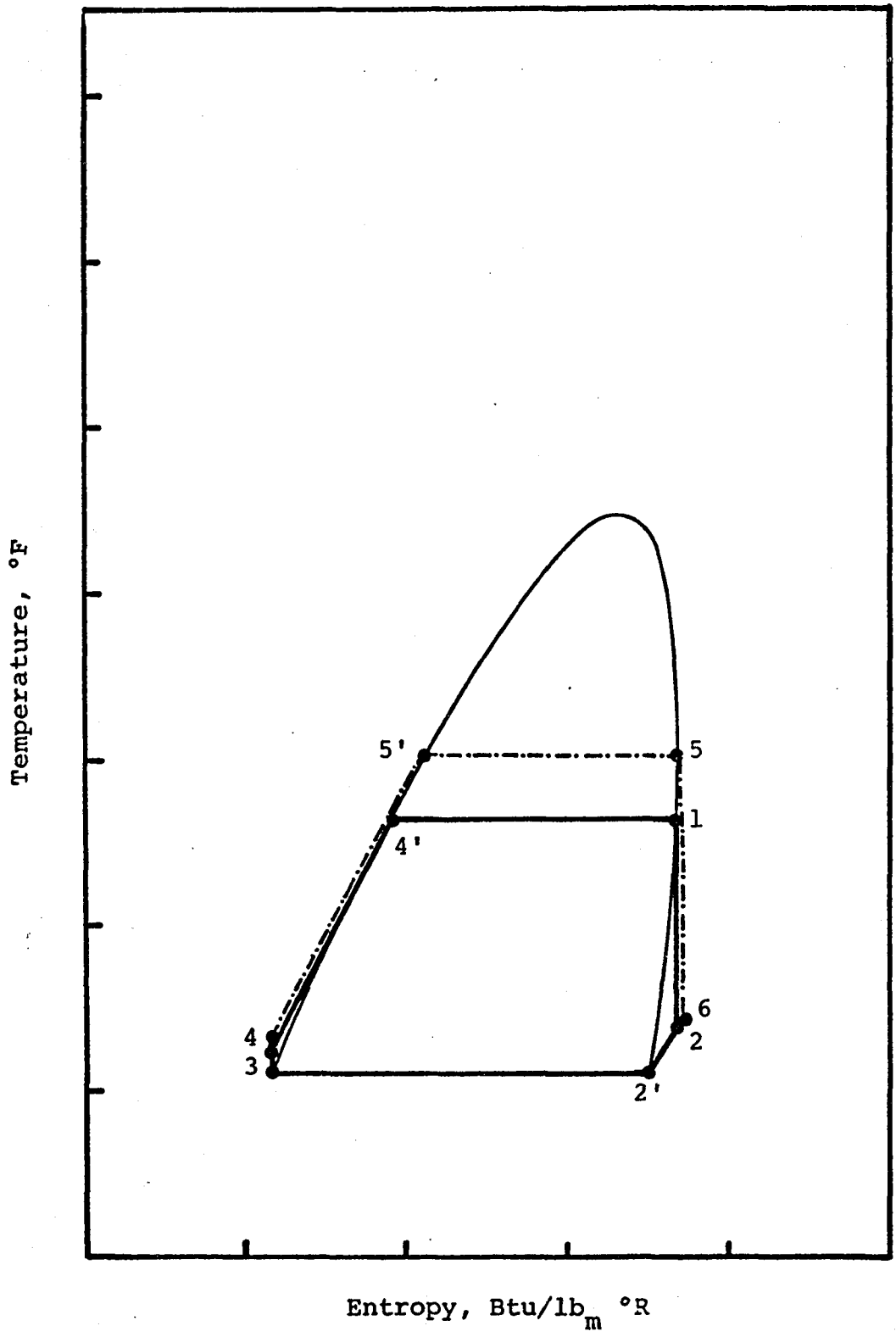

Figure 13.0 Temperature-entropy diagram of the isobutane ideal binary cycles

while that for case 2 is

$$\eta_{C2} = \frac{Q_{H2} + Q_{C2}}{Q_{H2}}$$

However,

$$Q_H = M_W \times \Delta h_{(H.E.)}^{*} \tag{16}$$

$$-Q_C = M_W \times \Delta h_{(cond.)}^{*} \tag{17}$$

$$\eta_C = 1 - \frac{M_W \times \Delta h_{(cond.)}}{M_W \times \Delta h_{(H.E.)}} = 1 - \frac{\Delta h_{(cond.)}}{\Delta h_{(H.E.)}} \tag{18}$$

and

$$\eta_{C2} = 1 - \frac{M_{W2} \times \Delta h_{(cond.)2}}{M_{W2} \times \Delta h_{(H.E.)2}} = 1 - \frac{\Delta h_{(cond.)2}}{\Delta h_{(H.E.)2}} \tag{19}$$

From Figure 12.0 we know that

$$\Delta h_{(H.E.)2} > \Delta h_{(H.E.)}$$

and

$$\Delta h_{(cond.)2} \simeq \Delta h_{(cond.)}$$

Therefore,

$$\eta_{C2} > \eta_C \tag{20}$$

that is, the net thermodynamic cycle efficiency increases for an increase in the T.I.P.

---

* Subscripts H.E. and cond. stand for heat exchanger and condenser, respectively.

Thus, it can be concluded that an increase in T.I.P. results in an increase in the turbine enthalpy change, net cycle work, and net thermodynamic cycle efficiency. On the other hand, for a specified net cycle work, the heat exchanger duty, Q_H, would decrease for an increase in T.I.P. In other words, when

$$W_N = W_{N2}$$

since

$$W_N = \eta_C \, Q_H$$

$$W_{N2} = \eta_{C2} \, Q_{H2}$$

it follows that

$$\eta_C \, Q_H = \eta_{C2} \, Q_{H2}$$

or

$$Q_{H2} = (\eta_C/\eta_{C2}) \, Q_H$$

But since

$$\eta_C/\eta_{C2} < 1$$

it follows that

$$Q_{H2} < Q_H \tag{21}$$

which verifies the statement that $Q_{H2} < Q_H$.

Condenser Dew Point Temperature

The condenser dew point temperature (D.P.T.) is fixed by specifying an approach temperature difference (DTCWO) between the working fluid and the cooling water at the cooling

water exit of the condenser. As the condenser dew point temperature is increased, its dew point pressure is also increased. The effect of condenser dew point temperature (and pressure) on the Ranking cycle can be studied by drawing the cycle state points on T-s and T-h diagrams. The cycle parameters to be considered in the analysis are the enthalpy change in the turbine, net cycle specific work and the net thermodynamic cycle efficiency.

Condenser dew point temperature and enthalpy change in turbine. In this section the effect of increasing the condenser dew point temperature on the enthalapy change in the turbine will be discussed. Figure 14.0 shows on a temperature-enthalpy diagram the effect of increasing the dew point temperature in the condenser on the turbine enthalpy change.

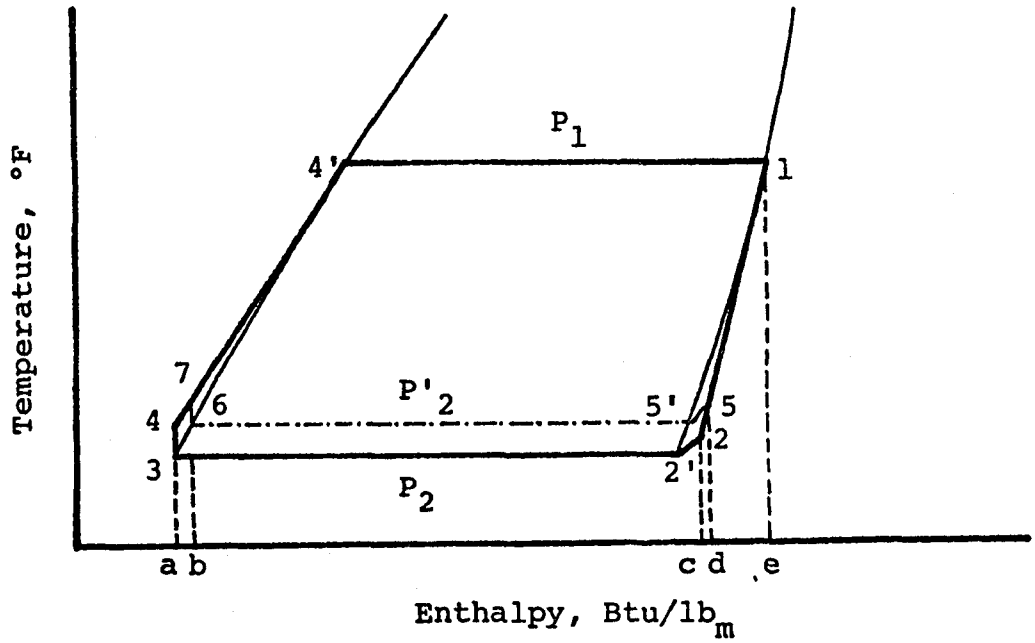

Figure 14.0 Effect of condenser dew point temperature on turbine enthalpy change

In Figure 14.0, the base cycle D.P.T. is represented by state point 2', and the turbine enthalpy change between state points 1 and 2 is represented by Δh_1. However, when the D.P. temperature is increased to state point 5', the condenser dew point pressure increases from P_2 to P_2'. Since the expansion is isentropic and for fluids with $I < 1$, s_1 is the controlling entropy, the turbine outlet temperature also increases from T_2 to T_5. The enthalpy change across the turbine for the second case is shown in Figure 14.0 to be Δh_2. Here the turbine outlet conditions have been exaggerated on the diagram in order to simplify the analysis. It is evident from this T-h diagram that $\Delta h_1 > \Delta h_2$; in other words, the increase in the dew point temperature of the condenser results in a decrease in the turbine enthalpy change. The reverse is true for a decrease in the condenser dew point temperature. For a specified gross turbine power, an increase in the condenser D.P.T. would mean a reduction in gross turbine power unless the working fluid flow rate were increased to compensate for the loss in the working fluid specific enthalpy change in the turbine. For a turbine inlet condition of 200 psia and 182°F and condenser dew point temperature of 110°F, the isobutane ideal cycle enthalpy change was calculated to be 15.5 Btu/lb_m. When the condenser D.P. temperature was increased to 115°F, the turbine enthalpy change decreased to 14.2 Btu/lb_m, which verifies the prediction stated earlier.

Condenser dew point temperature and net thermodynamic cycle work. The effect of the condenser dew point temperature on the net thermodynamic cycle work can be explained fairly easily with reference to the cycle state points on a temperature-entropy diagram. Figure 15.0 represents on a T-s diagram the effect of increasing the condenser D.P.T. on the net thermodynamic cycle work. Here again the turbine outlet conditions have been exaggerated. Since the expansions and compressions are reversible and no viscous pressure drops are assumed, the net thermodynamic cycle specific work is the area enclosed by the heating and cooling curves. Thus, when the condenser D.P.T. is increased form state point 2' to 5' the net cycle specific work decreases from the base cycle

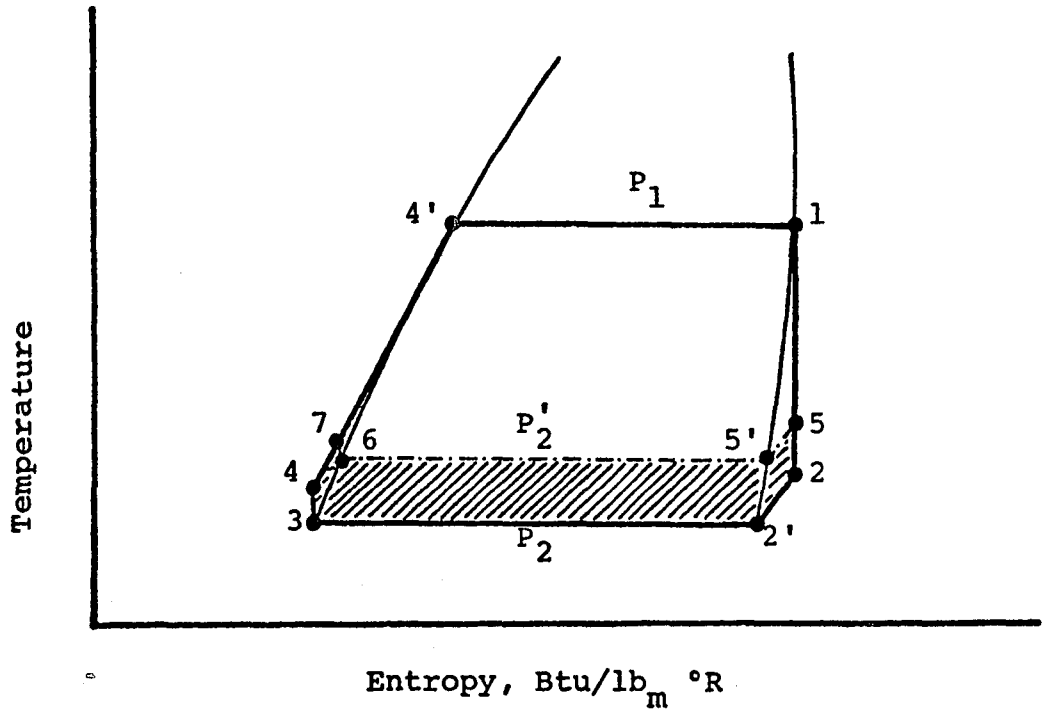

Figure 15.0 Effect of condenser dew point temperature on the net thermodynamic cycle work

area 1-2-2'-3-4-4'-1 to the area 1-5-5'-6-7-4'-1. The decrease in the area is shown cross-hatched in Figure 15.0. This means that an increase in the condenser dew point temperature results in a decrease in the net thermodynamic cycle specific work. The reverse would be true for a decrease in the condenser dew point temperature. However, the condenser dew point temperature is limited by ambient conditions. Table 4 shows the results of the isobutane ideal Rankine cycle calculation. In Table 4, the net cycle specific work, $\underline{W}_N$, decreased from 14.8 Btu/lb_m to 13.6 Btu/lb_m when the condenser D.P.T. is increased from 110°F to 115°F. On the other hand, $\underline{W}_N$ increases from 14.8 Btu/lb_m to 16.0 Btu/lb_m when the condenser D.P.T. is decreased from 110°F to 105°F.

For a specified net power, the decrease in the net cycle specific work (caused by an increase in the condenser dew point T) would have to be compensated for by circulating a larger amount of working fluid and using a larger amount of brine in the binary cycle.

Condenser dew point temperature and net thermodynamic cycle efficiency. Let the net thermodynamic cycle efficiency for the base case considered here be given by

$$\eta_{C1} = \frac{\underline{W}_{N1}}{\underline{Q}_{H1}}$$

Let η_{C2} be the net cycle efficiency when the condenser dew point temperature is increased. Then

Table 4

EFFECT OF CONDENSER DEW POINT TEMPERATURE ON THE PERFORMANCE OF THE BINARY CYCLE

Parameters \ Condenser Dew Point T, °F	105	110	115
Condenser			
Dew Point P, Psia	74.7	80.3	86.3
ΔH, Btu/lb_m	141.0	139.3	137.6
Heat Exchanger			
ΔH, Btu/lb_m	157.0	154.1	151.2
Turbine			
Inlet Pressure, psia	200	200	200
Inlet Temperature, °F	182	182	182
ΔH, Btu/lb_m	16.7	15.5	14.2
Cycle Pump			
ΔH, Btu/lb_m	0.7	0.68	0.65
Overall			
Net ΔH, Btu/lb_m	16.0	14.8	13.6
Net Thermo. Efficiency, %	10.2	9.6	9.0

$$\eta_{C2} = \frac{\underline{W}_{N2}}{\underline{Q}_{H2}}$$

We know that

$$\underline{W}_{N2} < \underline{W}_{N1}$$

and although also

$$\underline{Q}_{H2} < \underline{Q}_{H1}$$

the percentage change in the net thermodynamic cycle specific work is greater than the percentage change in the specific heat input, so that

$$\eta_{C2} < \eta_{C1}$$

In Table 4, the net thermodynamic cycle efficiency is shown to decrease from 10.2% to 9.6% when the condenser dew point temperature is increased from 110°F to 115°F. It can be concluded that an increase in the condenser dew point temperature results in a decrease in the turbine enthalpy change, net cycle work and net thermodynamic cycle efficiency.

Process Equipment and Unit Operational Characteristics

The process equipment and unit operational characteristics are cycle major equipment related parameters which are either influenced by or can influence the working fluid operating conditions in the cycle. For example, the brine heat exchanger duty is dependent on the cycle operating

conditions. Conversely, the turbine efficiency determines the percentage of the reversible work which can be expected from the turbine for the given turbine operating conditions for a given working fluid. Since no viscous pressure drops have been considered in the simplified analysis here, the turbine inlet pressure becomes the operating pressure for the heat exchanger. Similarly, the turbine outlet pressure is the operating pressure for the condenser.

This section is concerned with the effects of these and other process unit operational characteristics on the performance of the working fluid and vice versa. The operational characteristics to be considered are: (1) brine heat exchanger and condenser duties, (2) working fluid heat transfer coefficient in brine heat exchanger, (3) working fluid heat transfer coefficient in condenser, and (4) turbine and cycle pump efficiencies.

Brine Heat Exchanger and Condenser Duties

For Rankine cycles with efficiencies as low as geothermal binary cycles, the heat exchanger duties (for a specified net work) are roughly inversely proportional to the net thermodynamic cycle efficiency. For the thermodynamic cycle, the net cycle work, W_N is

$$W_N = Q_H + Q_C$$

where Q_H is the brine heat exchanger duty and $-Q_C$ is the condenser duty. Also the net thermodynamic cycle efficiency

is given by

$$\eta_C = \frac{W_N}{Q_H}$$

or

$$Q_H = \frac{W_N}{\eta_C} \tag{22}$$

The following relationship can be written for Q_C,

$$Q_C = W_N - Q_H = W_N - \frac{W_N}{\eta_C}$$

$$= \frac{W_N}{\eta_C} \quad (\eta_C - 1)$$

or

$$-Q_C = \frac{W_N}{\eta_C} \quad (1 - \eta_C) \tag{23}$$

From the above relationships in Equations (22) and (23) it can be stated that for a specified W_N, Q_H is inversely proportional to η_C and if η_C is small, $-Q_C$ is roughly inversely proportional to η_C. For example, consider the cases shown in Table 4. For a fixed net plant power (where power, $\dot{W}$, is the product of specific work, $\underline{W}$, in Btu/lb_m and the working fluid flow rate, $\dot{M}_W$ expressed in lb_m/hr, i.e., $\dot{W} = \underline{W} \times \dot{M}_W$), $\dot{W}_{NPl}$ (= $\dot{W}_N + \dot{W}_{parasitic}$) of 25.0 MW, the values of η_C, $\dot{Q}_H$ and $-\dot{Q}_C$ are 9.43%, 30.03MW, and 27.196 MW, respectively for a condenser D.P. temperature of 110°F. For a condenser D.P.T. of 115°F, the values of η_C, $\dot{Q}_H$ and $-\dot{Q}_C$ are 8.84%, 32.12 MW and 29.28 MW respectively. Thus, for a 6.3% reduction in η_C, the brine heat exchanger and condenser duties increased by

approximately 6.7% and 7.7% respectively (to yield the same net power output).

Working Fluid Heat Transfer Coefficient in Brine Heat Exchanger

In this preliminary analysis of the working fluid heat transfer coefficient, the discussion will be limited to the effects which are caused by changes in the value of two transport properties, namely the viscosity and thermal conductivity and one thermodynamic property, the heat capacity, due to changes in the operating pressure and temperature of the heat exchanger. The example calculations discussed earlier in the section on turbine inlet temperature are used here for illustration purposes.

The design equations from the University of Oklahoma GEO4 simulator were utilized to show the heat transfer effects. No claim is made as to the correctness of these equations. Although the same procedure could be applied to alternate design equations in order to determine the sensitivity of viscosity, thermal conductivity, and heat capacity changes on them. In the GEO4 simulator, the working fluid is on the shell side and the brine is on the tube side.

For the <u>single phase</u> (gas or liquid) section of the the correlation used for the heat transfer coefficient of the working fluid is

$$h_{WF} = A \left[\frac{G_s D_e}{\mu}\right]^b \left[\frac{C_p \mu}{k}\right]^c \frac{k}{D_e} \qquad (24)$$

or

$$h_{WF} = (A/D_e)(G_s D_e)^b (C_p)^c (\mu)^{c-b} (k)^{1-c} \qquad (25)$$

where

h_{WF} = working fluid heat transfer coefficient, Btu/hr. ft^2 °F

A = constant

D_e = equivalent shell side diameter, ft

G_s = mass velocity of the working fluid, lb_m/ft^2-hr

C_p = heat capacity, Btu/lb_m °F

μ = viscosity, lb_m/ft-hr

k = thermal conductivity, Btu/hr-ft °F

For the <u>two-phase</u> section of the heat exchanger, Chen's boiling correlation is utilized. Viscous pressure drops are ignored for the analysis here, so Chen's boiling correlation reduces to

$$h_{WF} = F \times \left[A \left(\frac{G_s D_e}{\mu_\ell} \right)^{b'} \left(\frac{C_p \mu_e}{k_\ell} \right)^c \frac{k_\ell}{D_e} \right] \qquad (26)$$

where the parameter F accounts for the forced convection contribution to the working fluid heat transfer and has been explained in reference 10. The subscript "ℓ" refers to liquid.

For the single phase section, equation (25) can be differentiated with respect to μ, k and C_p and then rearranged to recover functional groups. The results are

$$\frac{\partial h_{WF}}{\partial \mu} = A \left(\frac{G_s D_e}{\mu_\ell}\right)^b \left(\frac{C_p \mu}{k_\ell}\right)^c \left(\frac{k}{D_e}\right)\left(\frac{c-b}{\mu}\right) \tag{27}$$

$$\frac{\partial h_{WF}}{\partial k} = A \left(\frac{G_s D_e}{\mu}\right)^b \left(\frac{C_p \mu}{k}\right)^c \left(\frac{k}{D_e}\right)\left(\frac{1-c}{k}\right) \tag{28}$$

$$\frac{\partial h_{WF}}{\partial C_p} = A \left(\frac{G_s D_e}{\mu}\right)^b \left(\frac{C_p \mu}{k}\right)^c \left(\frac{k}{D_e}\right)\left(\frac{c}{C_p}\right) \tag{29}$$

which is the same as

$$\frac{\partial h_{WF}}{\partial \mu} = h_{WF} \left(\frac{c-b}{\mu}\right) \tag{30}$$

$$\frac{\partial h_{WF}}{\partial k} = h_{WF} \left(\frac{1-c}{k}\right) \tag{31}$$

$$\frac{\partial h_{WF}}{\partial C_p} = h_{WF} \left(\frac{c}{C_p}\right) \tag{32}$$

For small changes in μ, k or C_p

$$\Delta h_{WF} = h_{WF} \left(\frac{c-b}{\mu}\right) \Delta\mu \tag{33}$$

$$\Delta h_{WF} = h_{WF} \left(\frac{1-c}{k}\right) \Delta k \tag{34}$$

$$\Delta h_{WF} = h_{WF} \left(\frac{c}{C_p}\right) \Delta C_p \tag{35}$$

Combining equations (33), (34) and (35)

$$\Delta h_{WF} = h_{WF} \left[\frac{(c-b)\Delta\mu}{\mu} + \frac{(1-c)\Delta k}{k} + \frac{c\ \Delta C_p}{C_p}\right] \tag{36}$$

For this work, b = 0.8 and c = 0.4

$$\Delta h_{WF} = h_{WF} \left[\frac{-0.4\ \Delta\mu}{\mu} + \frac{0.6\ \Delta k}{k} + \frac{0.4\ \Delta C_p}{C_p} \right] \tag{37}$$

Similarly for the two-phase section of the heat exchanger,

$$\Delta h_{WF} = F\ h_{WF} \left[\frac{-0.4\ \Delta\mu_\ell}{\mu_\ell} + \frac{0.6\ \Delta k_\ell}{k_\ell} + \frac{0.4\ \Delta C_{p\ell}}{C_{p\ell}} \right] \tag{38}$$

Thus, the change (increase or decrease) in the working fluid heat transfer coefficient will depend on the changes in transport and thermodynamic properties and the parameter F.

To evaluate the effect of a change in h_{WF} on the overall heat transfer coefficient, the following equation is used:

$$U = \frac{1}{\frac{1}{h_{WF}} + \frac{1}{h_B} + R_{fB} + R_{fWF} + \frac{t}{k_m}} \tag{39}$$

where

U = overall heat transfer coefficient, Btu/hr-ft^2 °F

h_B = brine side heat transfer coefficient, Btu/hr-ft^2 °F

R_{fB} = fouling factor for brine, hr-ft^2-°F/Btu

R_{fWF} = fouling factor for working fluid, hr-ft^2 °F/Btu

t = tube wall thickness, ft

k_m = conductivity of tube metal, Btu/hr-ft-°F

For the example calculations of turbine inlet temperature, the following values were used for the base case, case 1 and case 2:

Enthalpy Weighted Average, $h_{WF} = 790$

$h_B = 2300$

$R_{fB} = 0.002$

$R_{fWF} = 0.0001$

$k_m = 93$

$t = 0.0138$

$U = 253.2$

Table 5 shows the effect of temperature and pressure on the working fluid heat transfer coefficient. It is evident from this Table that when the temperature in the brine heat exchanger is increased such that there is a minimal amount of superheat at the heat exchanger outlet (case 2), the working fluid heat transfer coefficient, h_{WF}, changes by +4.0% compared to a mere +0.25% change with 20.6 degrees of superheat. The +4.0% change in h_{WF} yields for U

$$U = \left[\frac{1}{1.04(790)} + \frac{1}{2300} + 0.002 + 0.0001 + 0.000148\right]^{-1}$$

or $U = 256.4$ Btu/hr-ft^2-°F, a change of + 1.3%. This is assuming that all other system parameters remained stable (which is doubtful). Only if the fouling from the brine were reduced to a level of pure water, would the overall heat transfer coefficient be affected appreciably by these changes in h_{WF}.

Table 5

EFFECT OF TEMPERATURE AND PRESSURE ON THE WORKING FLUID HEAT TRANSFER COEFFICIENT IN THE BRINE HEAT EXCHANGER

Parameters \ Case No.	Base Case	Case 1	Case 2
Overall			
BHE Inlet T, °F	105.9	105.9	106.3
BHE Outlet T, °F	182.	202	202
Superheat at Outlet, °F	0.6	20.6	0.2
Average Design P, psia	200	200	251
Section I (Liquid Phase)			
Avg. design T, °F	144.0	144.0	154.0
μ_ℓ, lb/ft-hr	0.2238	0.2238	0.2148
k_ℓ, Btu/hr-ft °F	0.04399	0.04399	0.04336
$C_{p\ell}$, Btu/lb-°F	0.62899	0.62899	0.64156
Enthalpy Change, Btu/lb_m	47.72	47.72	62.05
h_{WF}, Btu/hr-ft^2-°F	467	--	--
Δh_{WF}, (%)	--	0.0	+1.6
Section II (Two-Phase)			
Avg. design T, °F	181.4	181.4	201.8
μ_ℓ, lb/ft-hr	0.18532	0.18532	0.16486
k_ℓ, lb_m/ft-hr	0.040963	0.040963	0.039314
$C_{p\ell}$, Btu/lb-°F	0.6993	0.6993	0.75935
Enthalpy Change, Btu/lb_m	108.8	108.8	99.29
h_{WF}, Btu/hr-ft^2-°F	1136	--	--
Δh_{WF}, (%)	--	0.0	+5.6
Section III (Gas-Phase			
Avg. design T, °F	181.7	192.0	201.9
μ_g, lb_m/ft-hr	0.02471	0.02491	0.026285
k_g, Btu/hr-ft-°F	0.012347	0.012794	0.01292
C_{pg}, Btu/lb	0.7001	0.7336	0.7598
Enthalpy Change, Btu/lb_m	0.35	11.75	0.13
h_{WF}, Btu/hr-ft^2-°F	548	--	--
Δh_{WF}, (%)	--	+3.5	+3.4
Avg. Overall Δh_{WF}, (%)	--	+0.25	+4.05

It can be observed from Table 5 that the change in the working fluid heat transfer coefficient due to changes in temperature and pressure of the working is strongly damped by: (1) the nature of the defining equations for heat transfer, Equations 24, 26, 37 and 38, and (2) the self cancelling of the viscosity and thermal conductivity effects.

Working Fluid Heat Transfer Coefficient in Condenser

In this section, the discussion will be limited to those effects which are caused by changes in working fluid viscosity and thermal conductivity. Following the procedure of the previous section and using the design equation:

$$h_{WF} = A \left[\frac{g_c \, \rho(\rho-\rho_g) \, k_\ell^3 \, h'_{fg}}{d \, \mu_\ell \, \Delta T} \right]^{1/4} \tag{40}$$

we get

$$\frac{\partial h_{WF}}{\partial \eta_\ell} = \frac{-h_{WF}}{4 \, \mu_\ell} \tag{41}$$

$$\frac{\partial h_{WF}}{\partial k_\ell} = \frac{3h_{WF}}{4k_\ell} \tag{42}$$

and:

$$\Delta h_{WF} = \frac{h_{WF}}{4} \left[\frac{-\Delta\mu_\ell}{\mu_\ell} + \frac{3\Delta k_\ell}{k_\ell} \right] \tag{43}$$

Here the example calculations discussed earlier in the section on condenser dew point temperature are used for

the heat transfer effects. The following parameter values from the simulator were utilized:

$$h_{WF} = 290$$

cooling water side, $h_{CW} = 1500$

cooling water side, $R_{fCW} = 0.001$

$$R_{fWF} = 0.0001$$

$$t/_{km} = 0.000148$$

$$U = \left[\frac{1}{290} + \frac{1}{1500} + 0.001 + 0.0001 + 0.000148\right]^{-1}$$

$$U = 186.5 \text{ Btu/hr-ft}^2\text{-°F}$$

Table 6 shows the effects of temperature and pressure on h_{WF} in the condenser. It is evident from Table 6 that small changes in the T and P in the condenser have negligible effect on the value of h_{WF}, even though the indication is that increasing T and P results in the reduction of h_{WF}. This reduction in h_{WF} due to increases in the working fluid T and P is caused by: (1) the reduction in h_{fg} as P increases (since h_{fg} is in numerator), (2) the self cancelling effects of viscosity and thermal conductivity changes, and (3) an increase in the ΔT between the working fluid and the cooling water average design temperatures.

It is important to note that the working fluid heat

Table 6

EFFECT OF WORKING FLUID HEAT TRANSFER COEFFICIENT IN CONDENSER

Parameters \ Condenser D.P.T., °F	105	110	115
Overall			
Condenser Inlet T,°F	119.0	123.2	127.3
Condenser Outlet T,°F	104.8	109.8	114.8
Avg. design P, psia	74.7	80.3	86.3
Avg. design T, °F	104.9	109.9	114.9
μ_ℓ, lb_m/ft-hr	0.2610	0.25596	0.2509
k_ℓ, Btu/hr-ft °F	0.04668	0.046304	0.04593
h_{fg}, Btu/lb_m	141.04	139.3	137.6
h_{WF}, Btu/hr-ft^2 °F	290	---	---
Δh_{WF}, %	---	-0.001	-0.002

transfer coefficient, h_{WF}, is the controlling coefficient in the overall heat transfer coefficient equation. Therefore, the procedure outlined here can be very useful for fluids which may be sensitive to composition changes. For example, in the ocean thermal energy conversion cycles, ammonia is considered the top candidate working fluid. But ammonia properties are very sensitive to the mixing of water (due to leakage) in heat exchange equipment. The effects of changes in ammonia-water mixtures properties have been discussed in reference 25.

Turbine and Cycle Pump Efficiencies

It is obvious that for given operating conditions for a working fluid, the efficiencies of the turbine and the cycle pump determine the actual work obtained or required. However, what is not obvious is the effect of the turbine and the cycle pump efficiencies on the cycle operating conditions, or their effect on the determination of the optimum operating conditions (for the given objective function) of the cycle. In this section, the only objective function to be considered is the net thermodynamic cycle work, W_N. The actual turbine work is given by

$$W_T^{act} = m\ \Delta H_T\ \eta_T \tag{44}$$

where

ΔH_T = Isentropic enthalpy change in turbine, Btu/lb_m

η_T = Turbine efficiency expressed as a fraction

m = mass of working fluid, lb_m

W_T^{act} = Actual turbine work, Btu

When $\eta_T = 1.0$, the ideal or isentropic work is equal to

$$W_T^{ideal} = m \, \Delta H_T \tag{45}$$

and since

$\eta_T < 1$,

$$W_T^{act} < W_T^{ideal} \tag{46}$$

Similarly, the cycle pump work is

$$-W_P^{act} = \frac{m \times \nu(P_1 - P_2)}{\eta_P} \times \frac{144}{778} \tag{47}$$

$-W_P^{act}$ = Actual cycle pump work, Btu

ν = Working fluid specific volume at cycle pump inlet, cu-ft/lb

P_1 = Cycle pump outlet pressure, psia

P_2 = Cycle pump inlet pressure, psia

η_P = Cycle pump efficiency expressed as a fraction

When $\eta_P = 1.0$, the ideal cycle pump work is given by

$$-W_P^{ideal} = m \, \nu(P_1 - P_2) \times \frac{144}{778} \tag{48}$$

and since

$$\eta_P < 1.0$$

$$W_P^{act} > W_P^{ideal} \tag{49}$$

When viscous pressure drops are ignored, the cycle pump outlet pressure, P_1, becomes the turbine inlet pressure, and P_2 becomes turbine outlet pressure. Thus, any change (increase or decrease) in P_1 or P_2 would affect both W_T^{act}/m and $-W_P^{act}/m$. However, if P_2 is specified, then W_T^{act}/m or $-W_P^{act}/m$ would be dependent on P, alone. The net cycle work can then be written as

$$W_N = W_T^{act} + W_P^{act}$$ **

or

$$W_N = m\left[\Delta H_T\ \eta_T - \frac{\nu(P_1 - P_2)144}{778\ \eta_P}\right] \tag{50}$$

From the above it is evident that W_N/m will increase or decrease according to the corresponding increase or decrease in η_T or η_P for the given operating conditions. Therefore for specified W_N, as η_T decreases to $\acute{\eta}_T$, the net

---

** In GE04 simulator, the actual cycle pump work is calculated using:

$$-W_P^{act} = \frac{m\ \Delta H_P}{\eta_P}$$

where ΔH_P is the isentropic enthalpy change in cycle pump. The use of simplified expression for W_P^{act} in Equation (47) is made to simplify the discussion.

work decreases to W_N, either m or P_1 must be increased (or perhaps both P_1 and m may have to be increased). Since P_1 also determines the design pressure of the brine heat exchanger, the decrease in η_T would increase the design pressure rating of the heat exchanger if P_1 is increased. The increase in working fluid flow rate would result in higher viscous pressure drops in the heat exchange equipment, and depending on the size of the increase in the working fluid flow rate, η_T may be further reduced. The size of the heat exchange equipment would increase as well (unless the brine flow rate were increased to maintain the original LMTD).

A decrease in the cycle pump efficiency, η_P, would result in an increase in the cycle pump work; and for a specified net work, $\dot{W}_N$, the working fluid flow rate would have to increase to overcome the decrease in the net specific work, $\dot{W}_N/m$. The increase in working fluid flow rate would also cause the viscous pressure drops to increase.

For an actual binary cycle, the parasitic power requirements of the brine and cooling water must be added to the net thermodynamic cycle power W_N in order to obtain the net plant power, W_{NP}. However, the inclusion of the parasitic power requirements would not change any of the conclusions drawn earlier regarding the changes in the turbine and the cycle pump efficiencies. Tables 7 and 8 show the effects of turbine and cycle pump efficiencies on the binary cycle for a goeresource temperature of 300°F.

Table 7

EFFECT OF TURBINE EFFICIENCY ON THE PERFORMANCE OF THE BINARY CYCLE

Working Fluid: Isobutane — Georesource T = 300°F

Turbine Efficiency (%) / Cycle Parameters	(Base Case) 86	80	75	70
Cycle				
Net Plant Power, MW	25.0	25.0	25.0	25.0
Gross Power, MW	31.07	31.66	32.25	32.94
Net Thermo. Eff. %	10.8	10.05	9.36	8.67
Turbine				
Inlet P, psia	300	300	300	300
Inlet T, °F	220	220	220	220
ΔH_T^{act}, Btu/lb$_m$	19.37	18.01	16.89	16.0
Working Fluid Flow, lb/kw	219.0	240.0	261.0	285.0
Cycle Pump				
Cycle Pump Power, MW	2.51	2.75	2.99	3.27
Efficiency, %	85	85	85	85
Brine Heat Exchanger				
Brine Flow, lb/kw	300	329	358	391
Brine Pump Power, MW	0.50	0.54	0.58	0.62
Area, (10^4) ft^2	11.27	12.34	13.40	14.67
Condenser				
Cooling Water Flow, lb/kw	1770	1960	2146	2367
Cooling Pump Power, MW	3.05	3.37	3.67	4.04
Area, (10^4) ft^2	26.54	29.23	31.89	35.04

Table 8

EFFECT OF CYCLE PUMP EFFICIENCY ON THE PERFORMANCE OF THE BINARY CYCLE

Working Fluid: Isobutane — Georesource T = 300°F

Cycle Parameters \ Cycle Pump Efficiency (%)	(Base Case) 85	80	75	70
Cycle				
Net Plant Power, MW	25.0	25.0	25.0	25.0
Gross Power, MW	31.07	31.27	31.49	31.75
Net Thermo. Eff. %	10.8	10.8	10.76	10.70
Turbine				
Inlet P, psia	300	300	300	300
Inlet T, °F	220	220	220	220
Efficiency, %	86	86	86	86
ΔH_T^{act}, Btu/lb_m W.F.	19.37	19.37	19.37	19.37
Working Fluid Flow, lb_m/kw	219.0	220.	222.	224.
Cycle Pump				
Cycle Pump Power, MW	2.51	2.68	2.88	3.12
Brine Heat Exchanger				
Brine Flow, lb/kw	300.	302.	305.	307.
Brine Pump Power, MW	0.50	0.50	0.51	0.51
Area, (10^4) ft^2	11.27	11.33	11.41	11.49
Condenser				
Cooling Water Flow, lb/kw	1770.	1784.	1797.	1812.
Cooling Pump Power, MW	3.05	3.07	3.09	3.12
Area, (10^4) ft^2	26.54	26.71	26.90	27.13

The heat exchanger and condenser were assumed to be single-pass, counter-current shell-and-tube exchangers with brine on the tube side of the BHE and the cooling water on the tube side of condenser respectively. The turbine and cycle pump efficiencies for the base case of isobutane (as working fluid) were fixed to be 86% and 85% respectively.

From Table 7, for a decrease in turbine efficiency of about 18.6% (86% to 70%) when the net plant power was specified to be 25.0 MW, the working fluid flow rate increased by about 2.8%. The increase in working fluid flow rate resulted in an increase in brine heat exchanger and condenser areas of approximately 2.6 and 2.8% respectively.

For a 17.6% decrease in the cycle pump efficiency (i.e., from 85-70%), the cycle pump power requirements increased by 24% compared to the working fluid flow rate increase of merely 2.3%. The rest of the parameters in Tables 7 and 8 are self-explanatory. It may be added here that the cases considered in Tables 7 and 8 can actually be encountered in a real plant; for example, the turbine efficiency specified by the vendor may not be achieved in actual operation.

In order to determine the drop in the net plant power due to changes in the turbine efficiency, a fixed plant simulation was performed (see Appendix B for changes made in GE04 simulator for fixed plant simulator) for decreased turbine efficiencies. For approximately 7% and 13% decreases

in the turbine efficiencies, the net plant power decreased by 8.5% and 16.4%, respectively for the base case isobutane cycle.

The results in Tables 7 and 8 demonstrate the fact that the power plant efficiency is almost proportional to the turbine efficiency. This would be anticipated from equation (50), since the pump work (and also all parasitic work contributions) are more than an order of magnitude smaller than the gross turbine work. Thus, it is important to use turbines with the highest possible efficiencies in geothermal binary cycles.

CHAPTER III

SENSITIVITY ANALYSIS OF THE TOTAL SYSTEM COMPONENT COSTS

Total System Cost

The total system considered here is the geothermal power cycle consisting of the following primary elements:

1. Brine heat exchanger
2. Condenser and cooling system
3. Turbine-generator
4. Cycle pump
5. Geothermal wells and gathering system
6. Auxiliaries

The first four primary cost elements are collectively termed here as the power plant and cost element number five as the brine system. The cost of auxiliaries is proportional to the other cost elements. In this section, the effects of the power plant and brine system cost changes on the total system cost will be discussed. Also, the sensitivity of the working fluid molecular weight (isobutane-isopentane systems only) to the total system component costs is discussed.

The cycle working fluids considered here are isobutane,

isopentane, and two binary mixtures of these fluids. The discussion of more than one working fluid in the total system cost analysis presented here was felt necessary to show the possibility of a relationship between the locus of the optimum working fluid molecular weight and the total system component costs.

A net power of 25.0 MW was chosen as the basis for this cost analysis which was carried out for the georesource temperature of 300°F. However, some of the conclusions drawn from this study may be also applied to other georesource temperature binary cycles.

Power Plant Cost

The capital cost of each major process unit of the power plant and the total power plant capital cost were obtained by the cost estimation method described in Appendix A. The total system capital cost is then simply the sum of the total power plant and the brine system costs. Since the design correlations and the factored-estimation method (used here) have an uncertainty of approximately $\pm$ 20% each, the total system cost calculated does not represent the actual capital expenditures which would be obtained if actual vendor bids were obtained. The difference in the calculated and the actual power plant cost (or, conversely, brine system cost) represents an important consideration with respect to the total system capital cost.

As an example, consider the hypothetical case of XYZ Utility Company which supplies power to its customers from its conventional steam power plants. About three years ago, the company decided to study the feasibility of constructing and operating a geothermal binary cycle power plant based on the hot brine discovered in that region. The feasibility study recommended a more detailed design and cost optimization of the binary cycle. XYZ Company obtained the existing cost data from the vendors of the respective process unit, and carried out the detailed study. The detailed optimization study took almost a year. However, the decision to build the binary cycle power plant was not finalized until a few months ago. XYZ Company asked its purchasing department to invite the bids for the design and construction of the power plant equipment from the vendors. The bids were received by the company and then came the bombshell. The cost of most of the power plant major equipment had doubled from their previously estimated values! The increase in the cost of the power plant equipment was attributed to the higher cost of raw materials and the fabrication charges. Now, what should XYZ Company do in such a situation? Well, a similar question can be asked if the cost of the power plant equipment had been decreased by half due to some advances in technology. These are some of the typical situations which a company can encounter and for which satisfactory and economical solutions are desired.

Table 9 and Figure 16.0 show the sensitivity of the total system capital cost to percentages changes in the power plant cost for isobutane, mixture I (75% isobutane, 25% isopentane), mixture II (50% isobutane, 50% isopentane), and isopentane as working fluids for the georesource temperature of 300°F. For no change in the power plant cost (i.e., for the base case), mixture II has the lowest capital cost compared to isobutane, isopentane and mixture I primarily due to lower turbine cost compared to isopentane and lower heat exchange equipment costs compared to isobutane. For all the working fluids shown in Table 9, the power plant cost is roughly 55-60% of the total system cost. Therefore, any significant change in the power plant cost will have a corresponding effect on the total system cost, as is evident from Figure 16.0. Another point to note from Table 9 is that when the power plant cost is reduced by 50%, the brine system cost becomes the major cost item (approx. 57-63%) of the total system cost.

The effect of the power plant cost on the optimum molecular weight of the working fluid is shown in Figure 17.0. It may be mentioned here that the base cases for all the working fluids (i.e., when the change in the power plant cost is zero) were optimized with respect to the total system cost expressed in dollars per kilowatt for a power plant producing 25.0 MW net power. The other cases shown in Figure 17.0 were not optimized. Even with unoptimized cases, the general

Table 9

SENSITIVITY OF TOTAL SYSTEM COST* TO POWER PLANT COST

Working Fluid and Cost Parameters \ Percent Change in Power Plant Cost	-50	-25	0	+25	+50	+75	+100
Isobutane:							
Power Plant Cost, $/kw	434	651	868	1085	1302	1519	1736
Cost as Percent of Total System	42.6	52.7	59.7	65.0	69.0	72.2	74.8
Total System Cost, $/kw	1018	1235	1453	1669	1886	2103	2320
Mixture I:							
Power Plant Cost, $/kw	404	606	808	1010	1212	1414	1616
Cost as Percent of Total System	39.5	49.5	56.7	62.0	66.2	69.6	72.3
Total System Cost, $/kw	1022	1224	1425	1628	1830	2032	2234
Mixture II:							
Power Plant Cost, $/kw	387	581	775	969	1162	1356	1550
Cost as Percent of Total System	38.1	48.0	55.2	60.6	64.9	68.3	71.1
Total System Cost, $/kw	1016	1210	1404	1598	1791	1985	2179
Isopentane:							
Power Plant Cost, $/kw	409	614	819	1024	1228	1433	1638
Cost as Percent of Total System	37.4	47.2	54.4	59.9	64.2	67.6	70.5
Total System Cost, $/kw	1094	1299	1504	1709	1913	2118	2323

*Cost in 1976 dollars

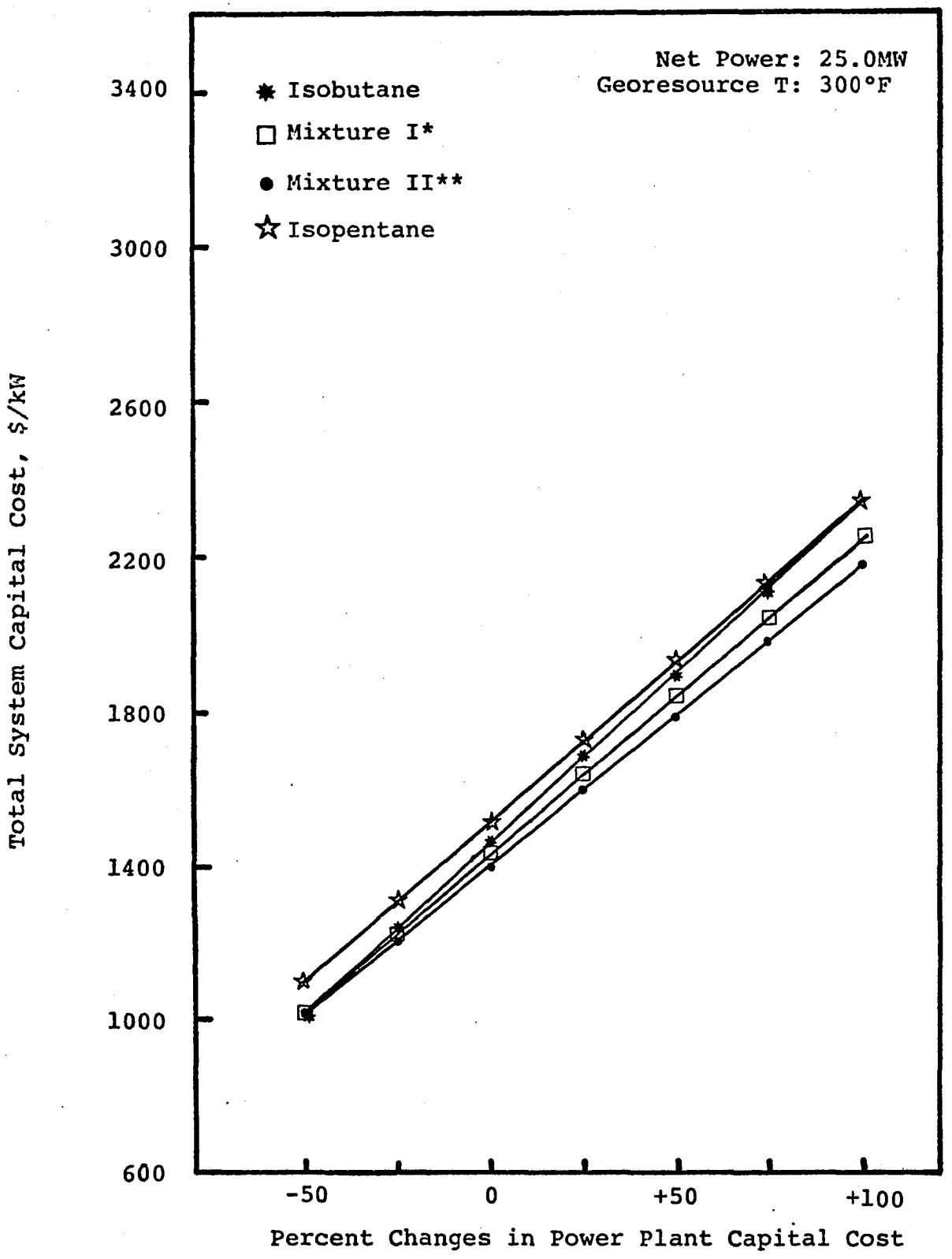

Figure 16.0 Sensitivity of Total System Capital Cost to Power Plant Capital Cost

* 75% isobutane, 25% isopentane
** 50% isobutane, 50% isopentane

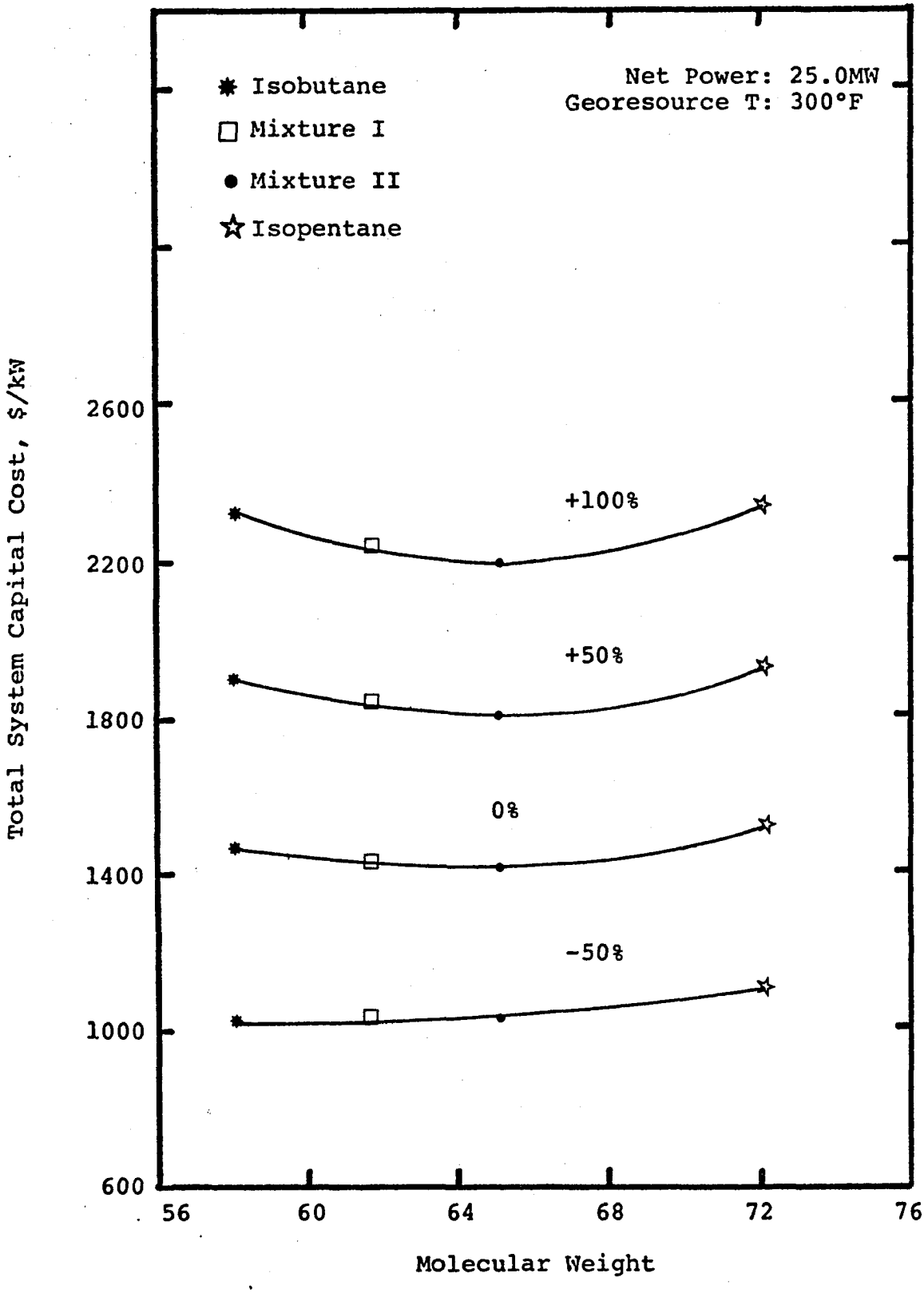

Figure 17.0 Effect of Power Plant Capital Cost on the Optimum Molecular Weight of the Working Fluid

trend seems to favor mixture working fluids when the power plant cost is increased by 100%. Thus, mixture II has significantly lower cost than either isobutane or isopentane. The reason is that for increased power plant cost, lower subcritical turbine operating pressures are optimal, and for subcritical operation, mixtures give better performances than pure fluids.[20,26] For the 50% reduction in power plant cost, the total system costs for isobutane, mixture I and mixture II become nearly identical, but the slope of the 50% plant cost reduction curve generally favors isobutane. This behavior seems logical since for decreased power plant cost, higher turbine inlet pressures would be economical; and for supercritical operating pressures, mixtures may either be only marginally lower in cost (i.e., total system cost) than isobutane or even slightly higher in cost than isobutane. In both situations, isobutane would be chosen as the optimum working fluid over mixture I or mixture II. It may be added here that for the 300°F georesource, of the fluids considered in this section, only isobutane can be operated at a supercritical turbine inlet pressure and temperature condition (since the critical temperature of isobutane is ∿275 °F) whereas mixtures I and II cannot (since mixture I and mixture II have pseudo critical temperatures of approximately 298.5°F and 322°F respectively).

From the above discussion, the hypothetical case of XYZ Company can be analyzed. Since the cost of the power

plant major equipment had increased by 100%, the first thing to note is that the working fluid originally chosen may or may not remain the optimum working fluid. Secondly, the working fluid operating conditions for the binary cycle would have to be optimized with new costs. Similar conclusions can be drawn for a significant reduction in the power plant cost. For example, if isobutane was the original working fluid choice, then for the 50% reduction in power plant cost, isobutane would be the final choice for the cost model utilized here. However, the operating conditions of the binary cycle would require revision to obtain the most economic utilization of the georesource.

The analysis presented in this section suggests a universal relationship between the power plant cost and brine system cost with respect to the total system cost. For example, if the power plant cost and the brine system cost were roughly identical for the base case, then, a 100% increase in the power plant cost would correspond to a 50% decrease in the brine system cost (and vice versa). This is probably universal because the total system cost is just the sum of power the plant cost and the brine system cost.

Brine System Cost

The brine system cost includes the cost of production and reinjection wells, as well as the brine pumping and piping system. Although the brine system cost is dependent

on the negotiated agreement between the producer and user (e.g., utility), the brine system cost to the producer is expected to be a direct function of the mass flow rate, while user charges may be made on a combined mass and thermal energy basis. The brine cost model used in this research (given in Appendix A) is a direct function of the brine flow rate.

For a utility, the brine delivery cost is likely to vary (normally increase) e.g., on a year to year basis, depending on the estimated brine production cost to the producer. Such rate increases likely would be built into the negotiated agreement between the utility and the producer. This would mean that the power plant fuel charges (i.e., brine delivery cost) would increase annually and so, therefore would power production cost (expressed in mills/kWh). For such a situation, the utility would need to know the "break-even point", defined here as the time in years after which the utility would not make any profit under the same operating conditions. It is not the purpose of this discussion to predict the break-even point or to calculate the power production cost (even though these could be determined); but rather to predict the possible shifting of the optimum molecular weight (isobutane in isopentane) with respect to the changes in the brine system cost.

Another example of the importance of brine system cost variation is the case of a utility which owns the rights

to the brine in the land area where the geothermal brine was discovered. However, in order to produce a specific net power, additional producing wells are needed. At this point, the utility can only estimate the brine production cost from its previous experiences. But these estimates may have large uncertainties. For such a case, the utility would need to know the effect of changes in the brine system cost on the selection of the optimum working fluid and its operating conditions, and of course, on the total system cost. The analysis presented here would correspond to this second case.

Figure 18.0 and Table 10 show the sensitivity of the total system capital cost to the brine system cost. From Table 10 it is evident that the brine system cost increases with working fluid molecular weight for the georesource temperature of 300°F. However, since the power plant costs of mixture I and mixture II are lower than either pure isobutane or isopentane, their total system costs are slightly lower. But when the brine system cost is increased by 100%, the small differences between the power plant costs of mixture I and II and isobutane are taken up by the increased brine system costs of the mixtures compared to isobutane. The net result is that the total system cost is almost the same for isobutane, mixture I and mixture II, but the isopentane total system cost remains high due to the 100% increase in brine system cost. The general trend favors the

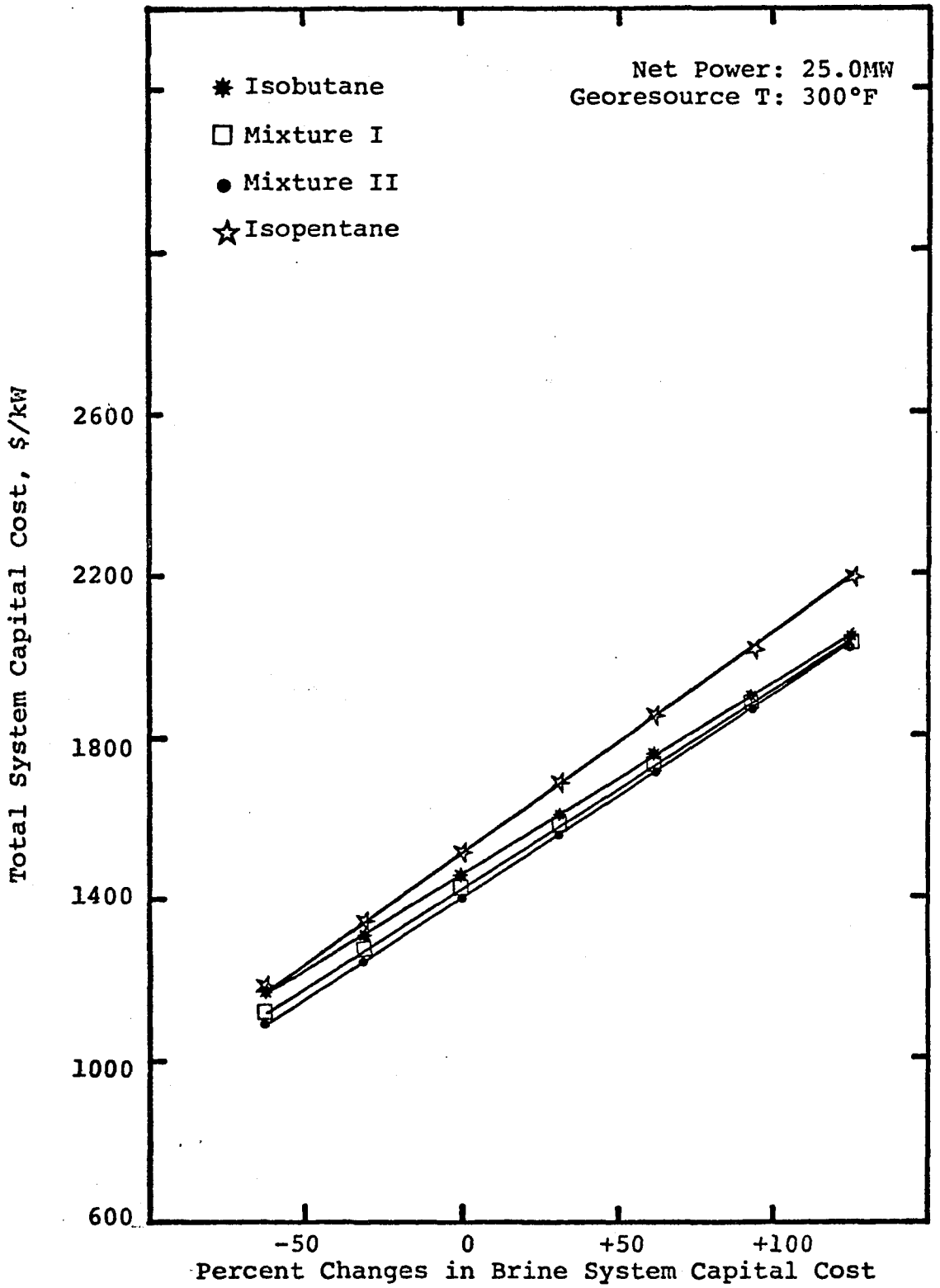

Figure 18.0 Sensitivity of Total System Capital Cost to Brine System Cost

Table 10

SENSITIVITY OF TOTAL SYSTEM COST TO BRINE SYSTEM COST

Georesource Temperature = 300°F Net Power = 25.0 MW

Working Fluid and Cost Parameters \ Percent Change in Brine System Cost	-50	-25	0	+25	+50	+75	+100
Isobutane:							
Brine System Cost, $/kw	292	438	584	730	876	1022	1168
Cost as Percent of Total System	25.2	33.5	40.2	45.7	50.2	54.1	57.4
Total System Cost, $/kw	1160	1306	1453	1598	1744	1890	2036
Mixture I:							
Brine System Cost, $/kw	309	463	618	772	927	1081	1236
Cost as Percent of Total System	27.7	36.4	43.4	48.8	53.4	57.2	60.5
Total System Cost, $/kw	1117	1271	1425	1580	1735	1889	2044
Mixture II:							
Brine System Cost, $/kw	314	472	629	786	943	1101	1258
Cost as Percent of Total System	28.8	38.2	44.8	50.3	54.9	58.7	61.9
Total System Cost, $/kw	1089	1247	1404	1561	1718	1876	2033
Isopentane:							
Brine System Cost, $/kw	342	514	685	856	1027	1198	1370
Cost as Percent of Total System	29.4	38.5	45.5	51.1	55.6	59.4	62.6
Total System Cost, $/kw	1161	1333	1504	1675	1846	2017	2189

lower molecular weight fluids when the brine system cost is increased by 100%. The reverse is true when the brine system cost is reduced by 50% or more. This is evident from Figure 19.0, which shows the effect of brine system capital cost on the optimum molecular weight of the working fluid.

Power Plant Component Costs

The primary cost components of the power plant are the brine heat exchanger, condenser, turbine-generator, cooling tower, working fluid (W.F.) and cooling water (C.W.) pumping equipment and auxiliaries. The cost of auxiliaries is proportional to the other cost elements. In this section, the sensitivity of the total system cost to the power plant component costs will be detailed.

Figure 20.0 illustrates the costs of major power plant equipment components as percentages of the total system cost for isobutane, isopentane and mixture II (an equimolar mixture of isobutane and isopentane) for the 300°F georesource. It can be noted that the largest equipment component cost variations occur for the condenser, brine heat exchanger and turbine-generator. To a good extent, the differences in costs are due to differences in thermodynamic behavior from fluid to fluid. For mixture II, many aspects of property behavior fall almost linearly between the behavior of isobutane and isopentane. However, the fact that the turbine specific enthalpy drop is greater for

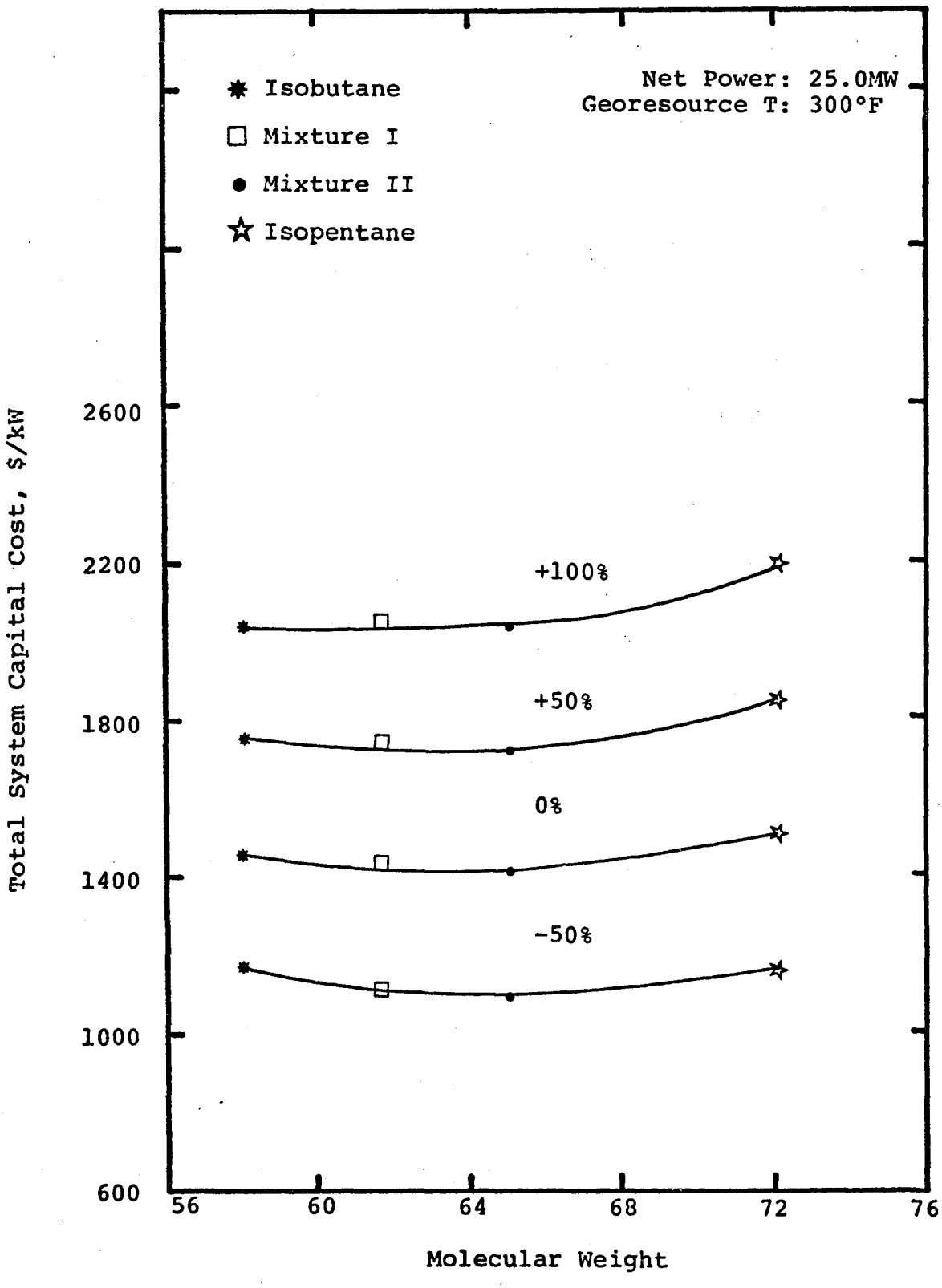

Figure 19.0 Effect of Brine System Capital Cost on the Optimum Molecular Weight of the Working Fluid

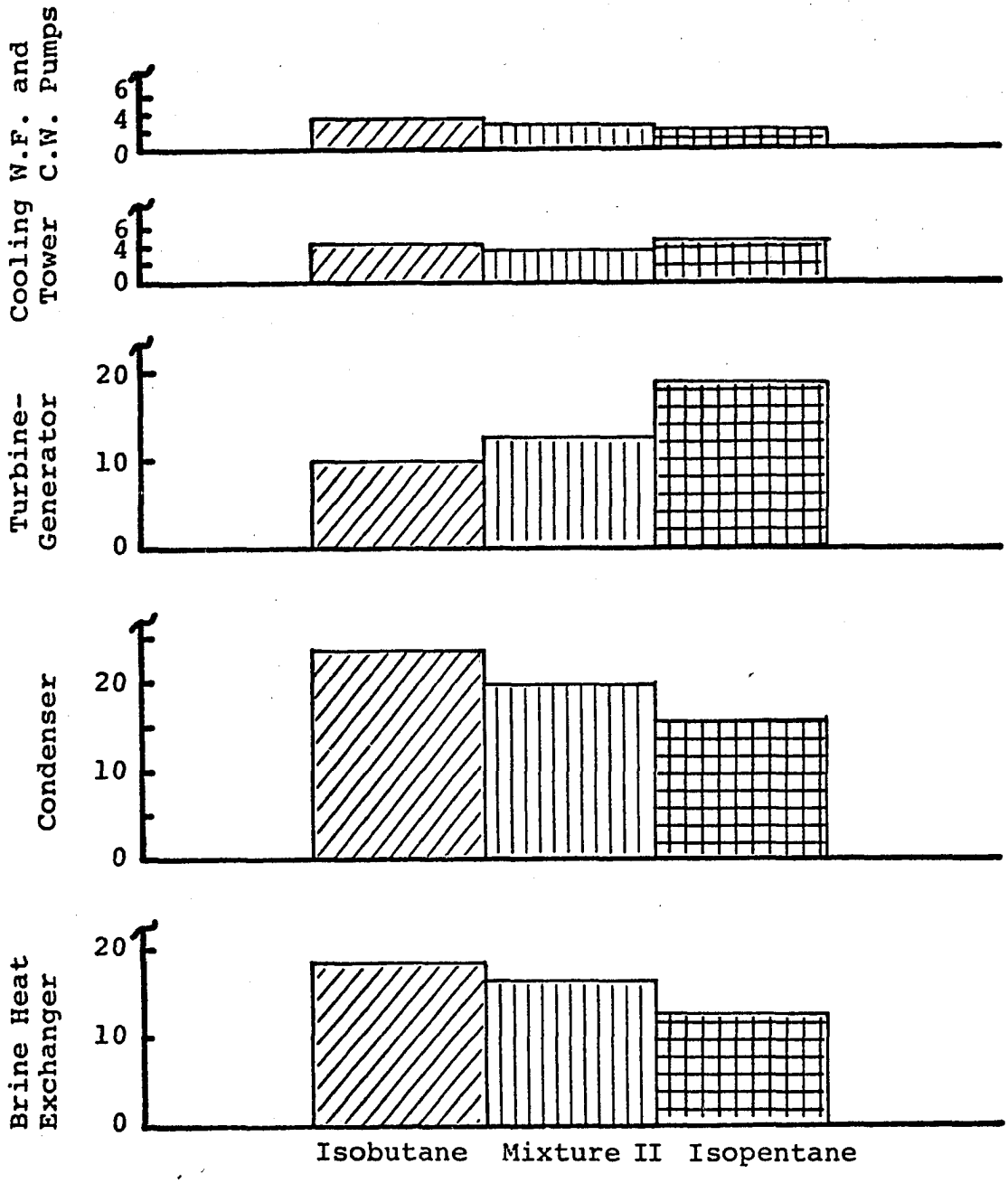

Figure 20.0 Power Plant Component Costs as Percentages of Total System Cost

the mixture than either pure fluid leads to a lower turbine-generator cost for the mixture than would be predicted from interpolation between the turbine-generator costs for the isobutane and isopentane cycles.[7] This is a major reason for the lower total system cost for the mixture cycle at 300°F relative to the isobutane and isopentane total system costs.

It can be noted from Figure 20.0 that the brine heat exchanger and condenser costs decrease with increasing molecular weight, whereas turbine costs increase with increasing molecular weight. Therefore, a trade-off exists between these major cost items for the power plant equipment.

The effects of increases and decreases in individual power plant component costs on the total system cost for isobutane, mixture II, and isopentane cycles are illustrated in Figures 21.0, 22.0 and 23.0, respectively, Figure 21-(a), 22-(a) and 23-(a) show the power plant component cost variations for percentage changes in their respective costs. Figures 21-(b), 22-(b) and 23-(b) show the total system cost variations for percentage changes in the individual power plant component costs. It is clearly evident that the largest equipment component cost variations occur for the condenser, heat exchanger and turbine generator as previously indicated for the base cases in Figure 20.0. Also, when the component costs decrease by 50%, the contribution of cooling tower and fluid pumping costs to the total system cost become even

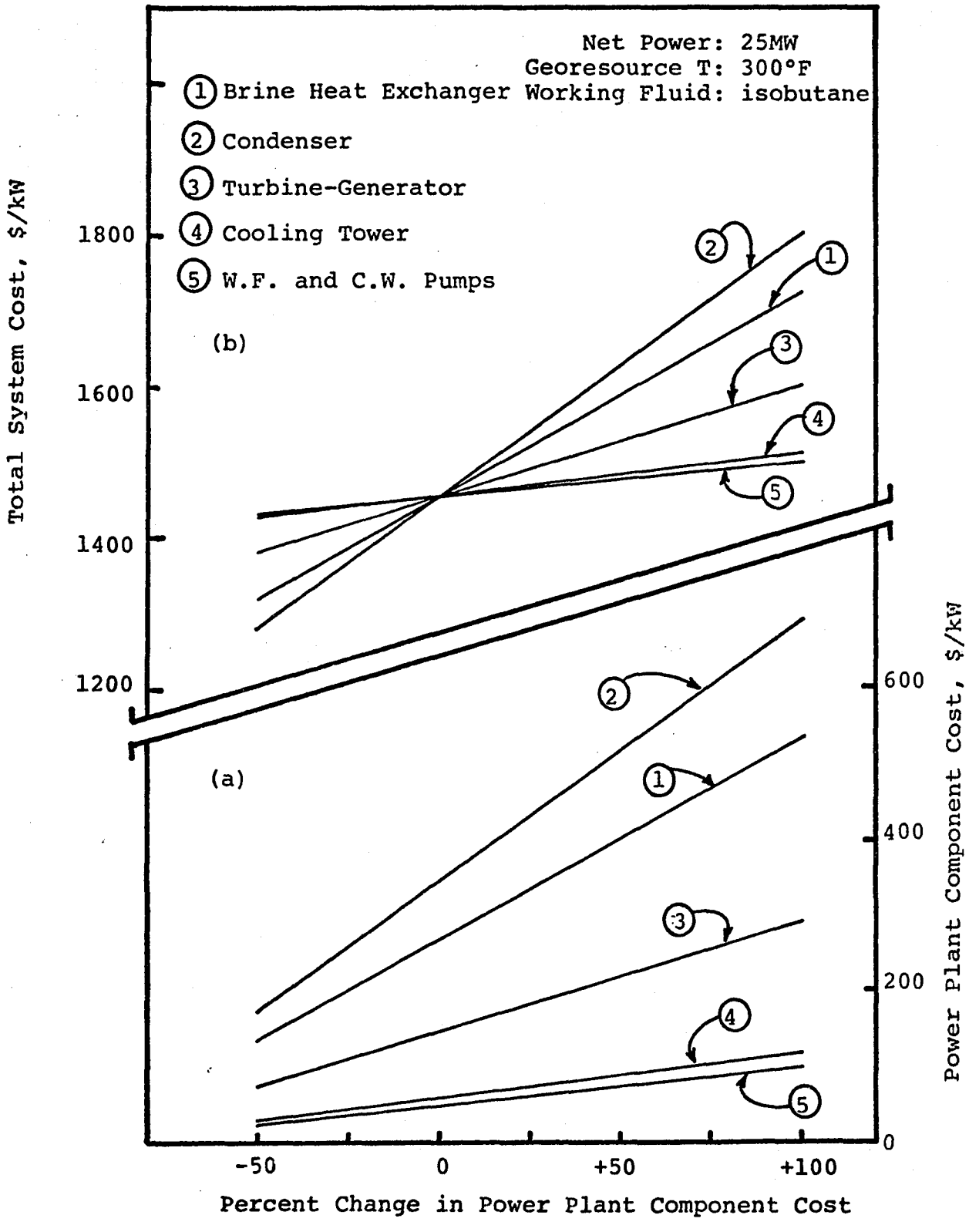

Figure 21.0 Sensitivity of Total System Cost to Power Plant Component Cost

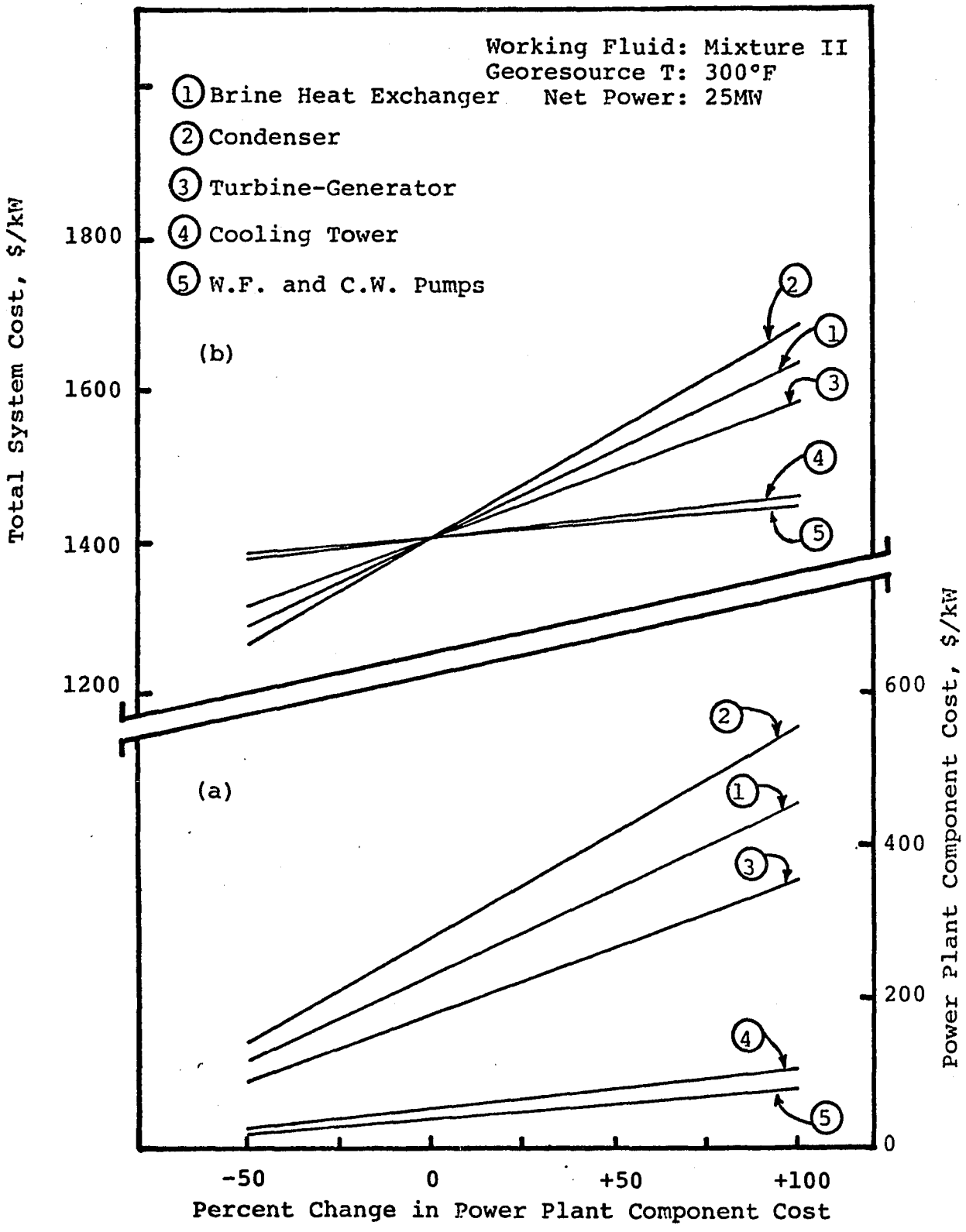

Figure 22.0 Sensitivity of Total System Cost to Power Plant Component Cost

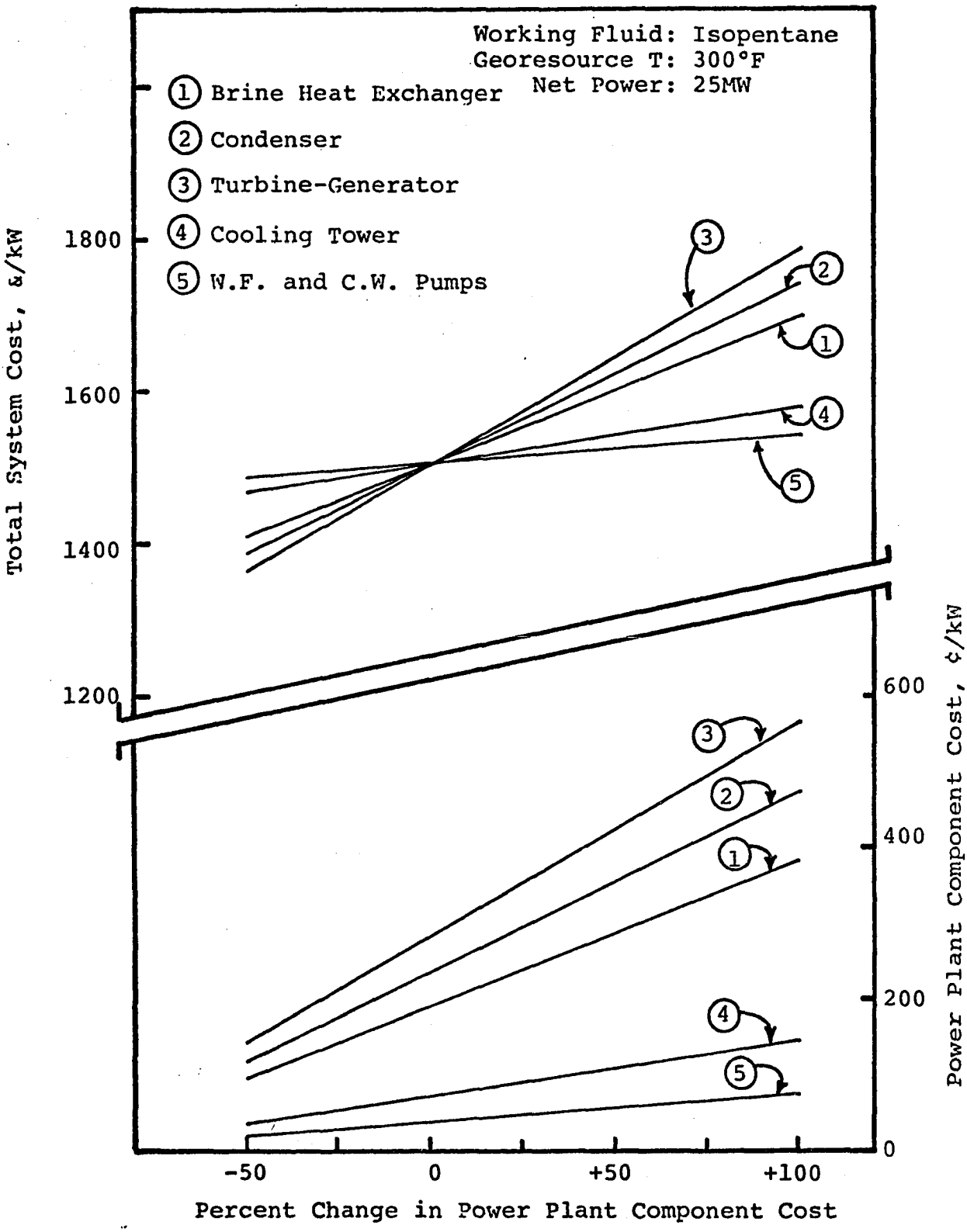

Figure 23.0 Sensitivity of Total System Cost to Power Plant Component Cost

smaller as is evident from Figures 21.0, 22.0 and 23.0. This can be generally expected since a 50% decrease in the power plant component costs (and hence power plant cost) means a 100% increase in the brine system cost (for equal power plant and brine system costs as the basis). Thus, increased brine system cost contribution automatically reduces the percentage contribution of the power plant component costs.

Unfortunately, Figures 21.0, 22.0 and 23.0 do not show the effect of power plant component costs on the optimum operating conditions of the working fluid. In the earlier discussion of power plant cost it was predicted that a decrease in power plant cost would result in higher optimum operating pressures. To verify this prediction, the isobutane base case was optimized again for a 50% reduction in the brine heat exchanger cost (and approximately 15.4% reduction in the power plant cost) with respect to the total system cost for a 25.0 MW net power plant. The new optimum turbine inlet pressure was 400 psia (and 234°F inlet T) compared to the base case pressure of 300 psia (and 220°F inlet T), a 33% increase in operating pressure. Of course, the increase in operating pressure would vary from fluid to fluid for an equivalent percent decrease in the brine heat exchanger cost. The differences in the optimum operating pressures and brine heat exchanger costs, will be primarily due to the differences in thermodynamic behavior from fluid to fluid. A 17.0% decrease in the total system cost for the new optimized case

was obtained, compared to 15.4% if the cycle were not re-optimized. The greater cost decrease is due primarily to the smaller sizes of the brine heat exchanger and condenser and corresponding lower equipment costs for the revised operating conditions and secondly due to decreased costs of the brine system due to higher efficiency.

From the above discussion, it can be stated that the increase in the optimum operating pressure for a given fluid (for a decrease in power plant component cost) would depend on two factors: (1) the percentage contribution of the component of the power plant cost and (2) the extent of the decrease in the component cost. Similar conclusions can be drawn for a decrease in optimum operating pressure for an increase in a power plant component cost. However, the increase in the optimum operating pressure for a given fluid will be generally directly proportional to the percentage contribution of the power plant component and inversely proportional to the decrease of the component cost. For example, if the percentage contribution of the component of the power plant is X%, the percent decrease in the component cost is Y%, then, the percent increase in the optimum operating pressure, ΔP, will be given by

$$\Delta P = \frac{X}{(100-Y)} \times 100$$

A similar formula can be derived from an increase in the component of the power plant cost.

CHAPTER IV

INTERRELATIONSHIP OF THERMODYNAMIC AND OPERATIONAL AND COST PARAMETERS

The sensitivity of the net thermodynamic cycle work and net thermodynamic cycle efficiency to thermodynamic process unit operational parameters was discussed earlier, in Chapter II. In Chapter III, the sensitivity of the total system cost to the total system component costs was presented without any significant reference to the thermodynamic and process unit operational parameters. The main objective of the discussion presented in this chapter is to discuss the relationships between these thermodynamic, operational and cost parameters.

In previous sensitivity studies carried out at the University of Oklahoma,[20,22] it was pointed out that for a given georesource temperature and specified net plant power, the variables which have large effects on the working fluid binary cycle capital cost are the following:

1. Turbine inlet temperature and pressure
2. Brine heat exchanger and condenser LMTD
3. Cooling water temperature range in condenser
4. Brine flow rate

To analyze the effects of these variables on the total system cost, choices are needed for: (1) the objective function for optimization, and (2) a common basis for comparison purposes. The commonly used objective functions for optimization in the geothermal energy conversion literature are: (1) maximization of the net plant work per unit mass of brine, (2) maximization of the net thermodynamic cycle efficiency and (3) minimization of the total system capital cost in dollars per kilowatt ($/kw) for a specified net electrical power output. The first objective function represents a resource utilization optimum, the second represents a thermodynamic optimum and the third represents an economic optimum. The objective function chosen for this research was the capital cost in $/kw for a power plant producing 25 MW_e net electrical output, unless otherwise stated. The working fluid selected for this study was pure isobutane, and most of the work was done for a 300°F georesource. A similar procedure, described later, can be followed for analyzing other binary cycle working fluids and other brine temperatures.

Resource Utilization Optimum and Cost Optimum and Thermodynamic Optimum

In this study, the resource utilization optimum corresponds to the binary cycle operating conditions which provide the maximum net plant work per unit mass of brine; the cost optimum corresponds to the binary cycle operating

conditions which require minimum total system capital investment per kilowatt of the net plant power output; and the thermodynamic optimum corresponds to the binary cycle operating conditions which provide the maximum net thermodynamic cycle efficiency.

Resource Utilization Optimum

In searching for the resource utilization optimum, it will be assumed that the initial state of the geothermal brine is that prevailing at the wellhead. The change in the thermodynamic state which occurs between the reservoir and the wellhead is ignored here (but it must be taken into account when the design and operation of the geothermal well itself is incorporated into the overall scheme). The sink pressure and temperature are assumed constant at 14.7 psia and 80°F, respectively. Under these conditions, the limiting (unattainable) resource utilization optimum will correspond to the amount of work available, i.e., the specific availability (per unit mass of brine), b,

$$b = (h - h_D) - T_D(s - s_D) \tag{52}$$

The availability provides a convenient measure of the maximum extent to which the geothermal resource can be utilized in a geothermal energy conversion process. The brine effectiveness, i.e., net plant work per unit mass of

brine (W_{NP}/M_H), is another measure of resource utilization. Therefore, maximizing W_{NP}/M_H will result in maximum resource utilization.

Consider the hypothetical idealized Rankine cycle, in Figure 24(a), a reversible cycle in which the working fluid high pressure and low pressure temperature profiles on a temperature-entropy diagram can be made to exactly parallel the brine and cooling water temperature profiles. In Figure 24(a), T_{HI} and T_{HO} are the brine temperatures at the brine heat exchanger inlet and outlet and T_{CI} and T_{CO} are the cooling water temperatures at the condenser inlet and outlet, respectively. When the expansions and compressions are reversible, i.e., $s_1 - s_4 = s_2 - s_3$, and in the absence of viscous effects, the net cycle specific work, $\underline{W}_N$, is the area enclosed by the working fluid cycle on a T-s diagram. Since $\underline{W}_N = \underline{Q}_H + \underline{Q}_C$, it follows that

$$W_N = M_W \int_4^1 Tds + M_W \int_2^3 Tds \tag{53}$$

For the above cycle, if the heat exchangers are adiabatic (again ignoring viscous effects), we have

$$Q_H = M_W \int_4^1 Tds = M_H \int_{S_{H(T_{HO})}}^{S_{H(T_{HI})}} T_H \, ds_H \tag{54}$$

and

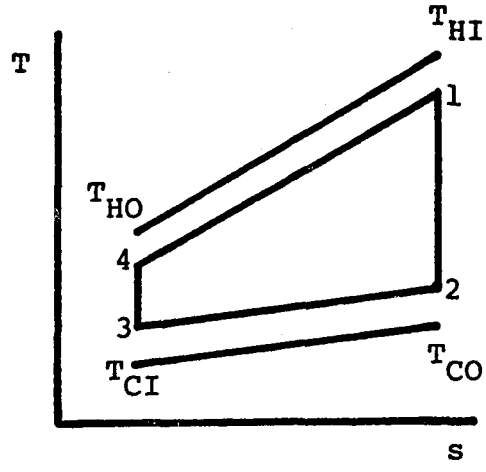

(a) Idealized Rankine Cycle for Hypothetical Fluid

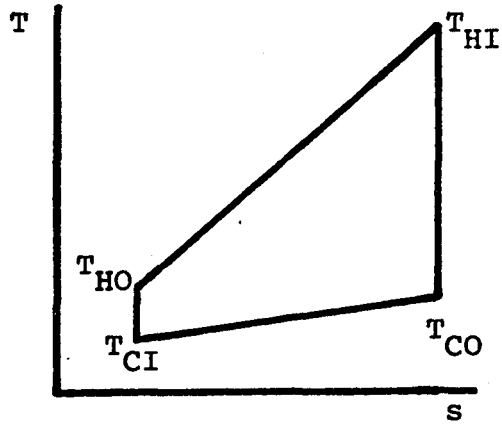

(b) Ideal Rankine Cycle with Reversible Heat Transfer for Hypothetical Fluid

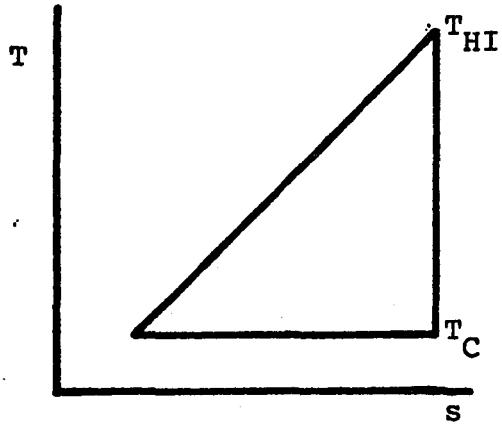

(c) Ideal Finite Resource Cycle

Figure 24.0 Ideal Cycles Using Finite Resources

$$Q_C = M_W \int_2^3 Tds = M_C \int_{S_{C(T_{CO})}}^{S_{C(TCI)}} T_C ds_C \qquad (55)$$

where the subscript H refers to the high temperature source (brine) and subscript C refers to the low temperature sink (cooling water). Thus,

$$W_N = M_H \int T_H \, ds_H + M_C \int T_C ds_C \qquad (56)$$

where the limits of integration are given in Equations 54 and 55.

Consider next the idealized limit of the ideal Rankine cycle for the hypothetical fluid in Figure 24(a) as the approach temperatures in the heat exchangers are allowed to approach zero (reversible heat transfer). This yields a cycle which is reversible both internally (flow, expansions and compressions) and externally (heat exchange with source and sink). In this limit, $T_1 = T_{HI}$, $T_2 = T_{CO}$, $T_3 = T_{CI}$ and $T_4 = T_{HO}$ and the T-s diagram for this cycle would appear as in Figure 24(b). The area enclosed by the cycle in Figure 24(b) is the maximum work which can be obtained with the finite cooling water (sink) temperature rise shown, for a working fluid which exhibits a temperature rise in isentropic compression in the liquid state.[10]

Consider finally the hypothetical case of the internally and externally reversible cycle and an infinite sink, such that the cooling water temperature rise approaches

This page is intentionally left blank.

zero (i.e., the sink temperature is constant) and further the idealized working fluid undergoes no temperature rise upon isentropic compression in the liquid state, as shown in Figure 24(c). This very idealized cycle yields the absolute maximum work for a finite source geothermal fluid and an infinite sink and will be referred to as the ideal finite resource cycle. Therefore, the net cycle work obtained from the second case, shown in Figure 24 (c), represents the resource utilization optimum for the hypothetical fluid binary cycle. A question can be asked at this point about the cost penalty for achieving this resource utilization optimum. To answer this question, consider the heat transfer relationship:

$$\dot{Q}_H = U_H A_H \Delta T_H \tag{57}$$

and

$$\dot{Q}_C = U_C A_C \Delta T_C \tag{58}$$

where

$\dot{Q}_H$, $\dot{Q}_C$ = Brine heat exchanger and condenser duty, respectively, Btu/hr

U_H, U_C = Overall heat transfer coefficient in brine heat exchanger and condenser, Btu/hr ft^2 °F

A_H, A_C = Brine heat exchanger and condenser heat transfer surface areas, ft^2

ΔT_H, ΔT_C = Log mean temperature differences of brine heat exchanger and condenser, °F

From Equations 57 and 58 it follows that:

$$A_H = \frac{\dot{Q}_H}{U_H \ \Delta T_H} \tag{59}$$

and

$$A_C = \frac{\dot{Q}_C}{U_C \ \Delta T_C} \tag{60}$$

But since $T_H \rightarrow 0$ and $T_C \rightarrow 0$

Therefore

$$A_H \rightarrow \infty$$

and (61)

$$A_C \rightarrow \infty$$

In other words, in order to achieve the hypothetical resource utilization optimum, infinite brine heat exchanger and condenser surface areas are required, which would mean infinite cost! However, for an actual power plant operation, some constraints on the approach temperatures between the working fluid and the heating (brine) and cooling (cooling water) fluids would be required. Moreover, geothermal binary cycle power plants will use real working fluids and their thermodynamic behavior will not correspond to that of the hypothetical fluid shown in Figure 24.0. For example, consider the case of an isobutane binary cycle for a 300°F georesource. The critical temperature of isobutane is approximately 275°F which is close to the resource temperature of 300°F. If minimum approach temperatures were specified to

be 10°F in both the brine heat exchanger and condenser, then in order to find the resource utilization optimum turbine inlet pressure for the isobutane cycle (for a specified net power), many cycle calculations would be required. Because the resource temperature is close to the critical temperature of isobutane, the pinch will occur near the bubble point temperature of the working fluid in the brine heat exchanger. If it is noted that the key to maximizing the net plant work per unit mass of brine is to optimize the brine outlet temperature (for given approach and pinch temperature differences) in the brine heat exchanger, then it becomes evident that subcritical turbine inlet pressures would be optimal. Conversely, it can be stated that for higher georesource temperatures (or working fluids such as propane, with lower critical temperatures), if the pinch occurs near the working fluid entrance to the brine heat exchanger, then the resource utilization optimum turbine inlet pressure will either be supercritical or close to the critical pressure of the fluid.

Thus, for the 300°F georesource temperature, the resource utilization optimum turbine inlet pressure for the isobutane cycle will be well below its critical pressure (since the pinch in the brine heat exchanger occurs near the bubble point temperature) as shown in the temperature-enthalpy diagram of isobutane binary cycles in Figure 25.0.

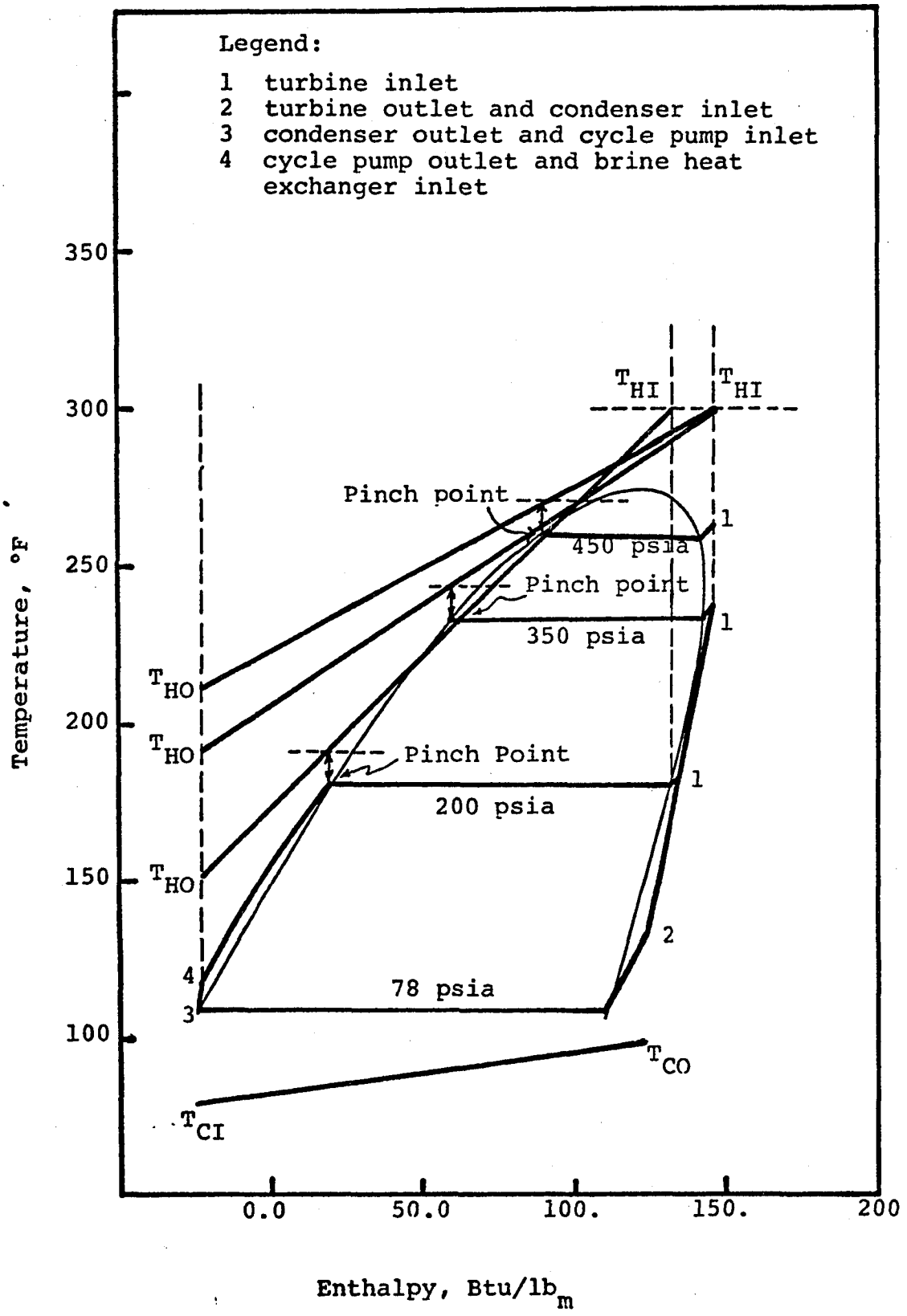

Figure 25.0 Isobutane binary cycles for various turbine inlet pressures for 300°F georesource

Economic Optimum

For calculations to determine the economic optimum, it will be assumed that the goethermal brine is self-flowing (so that no brine pumping is required). In addition, it will be assumed that cooling water also is available in abundance and at no cost to the utility (except for pumping costs). Since the brine heat exchanger, condenser and turbine are the major cost elements of the power plant, the minimization of the cost of these major equipment elements will give the cost optimum for a fixed brine delivery system cost.

Brine heat exchanger and condenser capital costs are primarily dependent on the design pressure rating and the heat transfer surface area requirements. To reduce their cost, the design pressures (above atmospheric pressure) and/or surface areas must be reduced. The heat transfer surface area requirements can be minimized by maximizing the log mean temperature differences (LMTD) in the brine heat exchanger and condenser. Consider the heat transfer relationship:

$$\dot{Q} = U\ A(LMTD)$$

or (62)

$$A = \frac{\dot{Q}}{U(LMTD)}$$

Since the LMTD is in the denominator, the surface area, A, is inversely proportional to the LMTD and therefore, maximization of the LMTD will minimize the surface area A.

To reduce the cost of the turbine, its physical size must decrease, by decreasing the working fluid specific volume at the turbine exit and/or reducing the flow rate of the working fluid. The reduction of the brine heat exchanger and condenser sizes (that is, areas) and consequently cost is the primary objective of this analysis, since the combined costs of these two pieces of equipment in geothermal binary cycles often amounts to 40-60% of the total system cost, depending on the resource temperature and the working fluid.

To maximize the brine heat exchanger and condenser LMTD's, the assumption of an infinite source and sink will be made, such that the brine temperature drop $(T_{HI} - T_{HO})$ and the cooling water temperature rise $(T_{CO} - T_{CI})$ both approach zero. This situation is shown in Figure 26.0, which illustrates on a temperature-entropy diagram an idealized Rankine cycle for infinite source and infinite sink conditions. If no constraint is put on the net power output, then the minimum power system cost will be obtained for a hypothetical ideal binary cycle with brine heat exchanger and condenser sizes approaching zero.

However, infinite sources or sinks do not exist. Morecver, any utility which is going to design, construct and operate a binary cycle has finite cash or credit available. Therefore, depending on the magnitude of the georesource, the utility's electrical power needs and financial

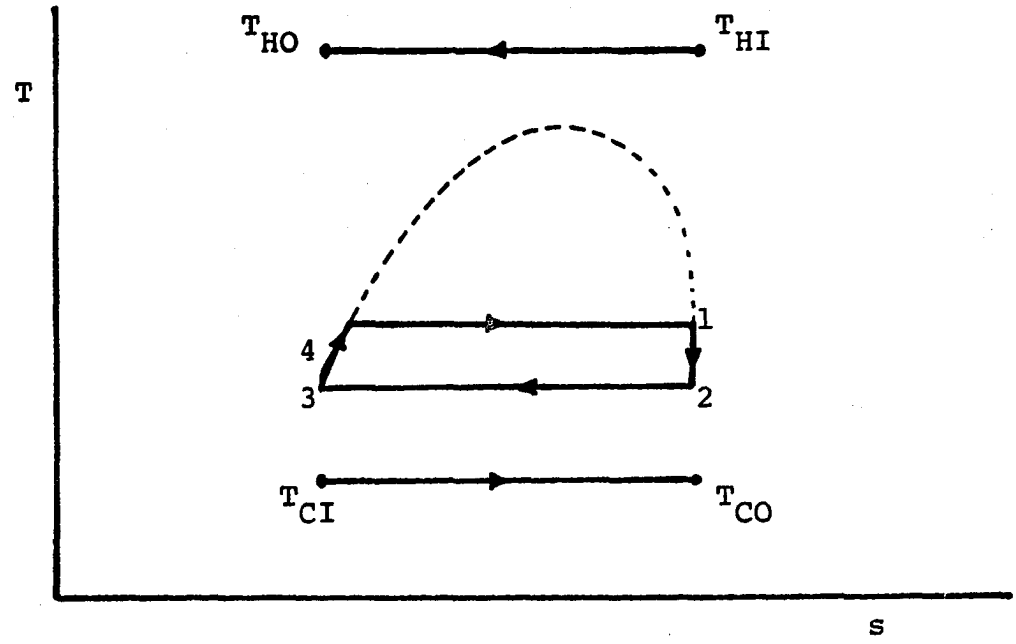

Figure 26.0 Ideal Rankine Cycle with Infinite Source and Infinite Sink

status, a finite net power will be produced. Of course, some other thermodynamic process and environmental constraints will also be put on any real binary cycle plant. For a specified net power and a given georesource temperature, the optimum cost of the total system is a trade-off between the power plant and the brine system costs.

It has been shown elsewhere[7,20] that for a 300°F georesource, the cost optimized brine heat exchanger and condenser LMTD's are very nearly independent of the working fluid used. In addition, the cost optimized pinch point temperature

differences are nearly equal to or slightly greater than the minimum specified value of 10°F. This suggests that for the 300°F georesource, the cost optimum and resource utilization optimum turbine inlet pressure and other cycle operating conditions for a given working fluid shculd be nearly the same or very close (for equal pinch and minimum approach temperature differences). On the other hand, for higher resource temperatures where the cost optimized pinch point temperature differences are much higher than the specified minimum for a given working fluid, the resource utilization optimum and cost optimum operating conditions will be correspondingly far apart. Of course, this result could be anticipated because larger LMTD's mean larger irreversibilities due to heat transfer and it is a general principle of thermodynamics that the reduction of irreversibilities at any point in a process increases the efficiency of the process.

Thermodynamic Optimum

In calculating the thermodynamic optimum operating conditions of a working fluid binary cycle, the assumption of an infinite source and an infinite sink will be made. The net thermodynamic cycle efficiency is given by the relation

$$\eta_c = \frac{W_N}{Q_H}$$

From the above equation, it is obvious that the net

thermodynamic cycle efficiency, η_c, can be increased in two fundamental ways: (1) by increasing the net thermodynamic cycle specific work, $\underline{W}_N$, and/or (2) by decreasing the specific brine heat exchanger duty, $\underline{Q}_H$. It may be noted here that η_c is determined by considering the internal cycle undergone by the working fluid.

Thus, maximizing η_c would require maximizing $\underline{W}_N$ and minimizing $\underline{Q}_H$. The net thermodynamic cycle specific work, $\underline{W}_N$, is given by

$$\underline{W}_N = \underline{W}_T + \underline{W}_P$$

where $\underline{W}_T$ and $\underline{W}_P$ are the specific turbine and pump work, respectively. To increase $\underline{W}_N$, the focus should be on $\underline{W}_T$, because it changes more quantitatively than $\underline{W}_P$. The specific turbine work, $\underline{W}_T$, can be increased in two ways: (1) by increasing the turbine inlet temperature or pressure or both (and therefore increasing specific enthalpy at turbine inlet), or (2) by decreasing the turbine outlet temperature (and therefore decreasing specific enthalpy at turbine outlet). For given source and sink conditions, the working fluid specific enthalpy at turbine inlet will be maximum when the turbine inlet temperature (for a given pressure) approaches the source temperature, and the specific enthalpy at the turbine outlet will be minimum when the turbine outlet temperature (for a given outlet pressure) approaches the sink temperature. Thus, maximum $\underline{W}_N$ will be obtained from a hypo-

thetical idealized Rankine cycle, in Figure 27.0, a reversible (internally) cycle in which the turbine inlet temperature of the hypothetical fluid approaches the source (brine) temperature, and the turbine outlet temperature approaches the sink temperature, such that the brine temperature drop and the cooling water temperature rise approach zero.

Thus, under steady state steady flow conditions and in the absence of working fluid viscous pressure drops, the area enclosed by the working fluid cycle in Figure 27.0 is the maximum net thermodynamic cycle work which can be obtained with an infinite source and an infinite sink. On the other hand, since the brine temperature drop approaches zero, the brine flow rate approaches infinity. For example, consider the heat transfer from the brine

$$Q_H = M_H \, C_p \, \Delta T$$

or

$$M_H = \frac{Q_H}{C_p \, \Delta T}$$

where Q_H is the heat transferred from the brine to the working fluid, C_p is the average heat capacity of the brine, ΔT is the brine temperature drop and M_H is the mass of brine. Thus, when

$$\Delta T \to 0$$

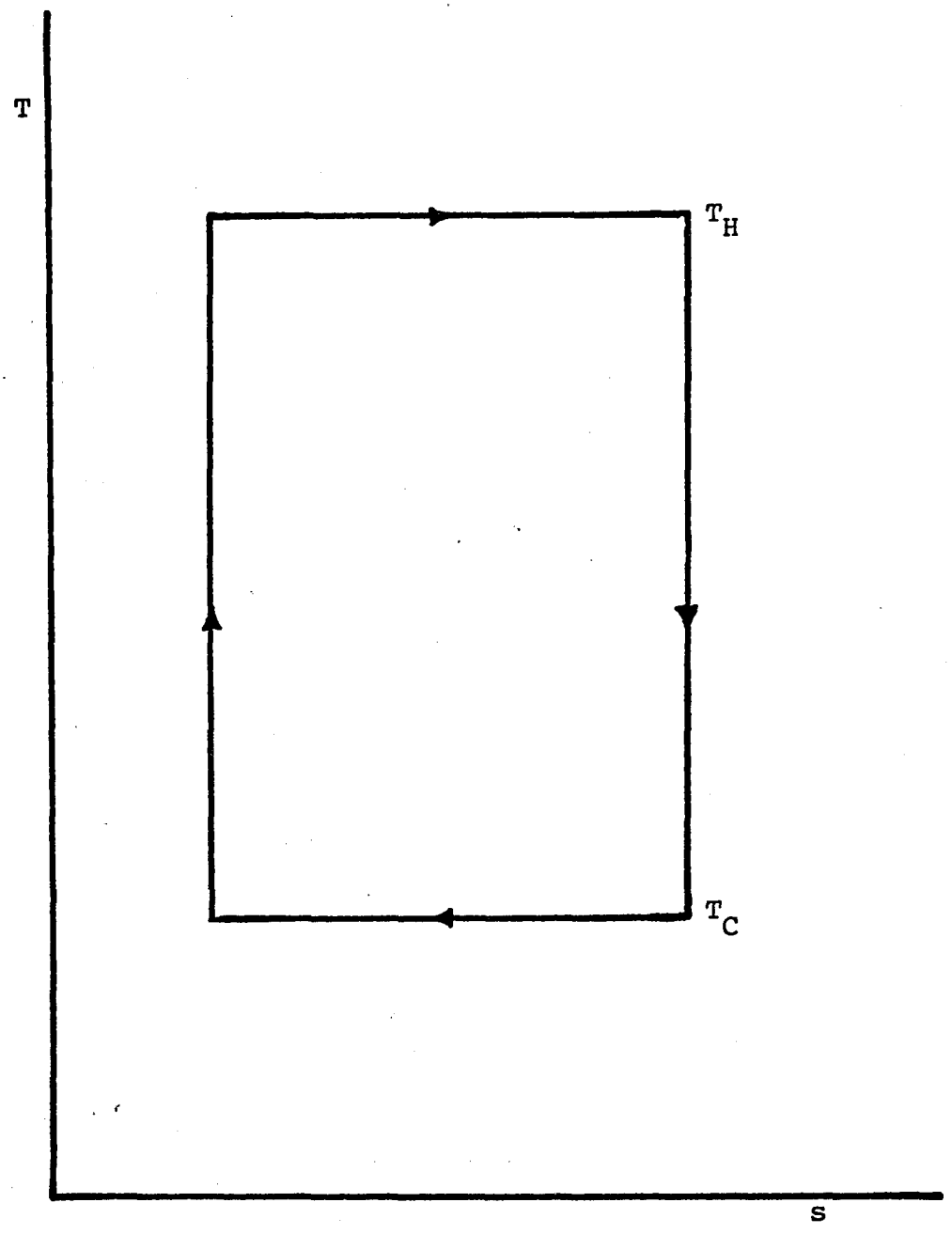

Figure 27.0 Ideal Rankine Cycle with Infinite Source and Infinite Sink

it follows that

$$M_H \rightarrow \infty$$

but since

$$\underline{W}_N \rightarrow (\underline{W}_N)_{max}$$

it follows that

$$\eta_c \rightarrow (\eta_c)_{max}$$

Therefore, the net thermodynamic cycle efficiency obtained from Figure 27.0 represents the thermodynamic optimum for the hypothetical fluid binary cycle. It is interesting to note that the thermodynamic cycle shown in Figure 27.0 is in effect a Carnot cycle. This means that the Carnot cycle efficiency represents the thermodynamic optimum for the binary cycle. Even though the Carnot cycle is perfectly reversible, η_c must have a value less than unity. This can be explained by the thermodynamic cycle efficiency of the Carnot cycle, η_{Car}, given by

$$\eta_{Car} = \frac{T_H - T_C}{T_H}$$

The equation for the Carnot cycle efficiency given above indicates that η_{Car} is a function solely of the absolute temperature levels at which the cycle receives and rejects heat. Complete conversion of heat to work is possible only if the cycle receives heat at infinite temperature or discards heat at an absolute temperature of zero. Obviously,

neither of these conditions is attainable in any practical cycle, so a value of η_{Car} of unity is not possible. Besides, reversible operation is both impossible and impractical to obtain and represents only a theoretical maximum against which a real system's performance can be compared. For example, for reversible heat exchanger and condenser operation, only an infinitesimal temperature difference (ΔT) would exist between the hot (brine) or cold (cooling water) and the respective portions of the working fluid. Thus, infinitely large heat exchangers (brine heat exchanger and condenser), which cost an infinite amount of money, would be required. Since this is clearly intolerable, it is necessary to provide a finite ΔT between the working fluid and the hot and cold sinks. It may also be mentioned here that even the best expanders and compressors available today do not operate reversibly.

For an actual power plant operation, only finite source and sink are available, and only real working fluids will be used. In any case, the thermodynamic optimum turbine inlet operating pressures and temperatures (limited only by the approach temperature ΔT between the source and the working fluid) will generally be dependent on the working fluid used. Moreover, the thermodynamic optimum operating conditions will generally be far away from the cost optimum and the resource utilization optimum.

To verify the prediction that the resource utilization and cost optimums are close for the 300°F georesource, but are away from the thermodynamic optimum, the GEO4 simulator was

used to find the resource utilization optimum, cost optimum and thermodynamic optimum operating conditions for the isobutane binary cycle. The minimum pinch point ΔT for all three cases was specified to be 10°F. The optimized net work per pound of brine is maximum and not sensitive to turbine inlet pressure between 300-325 psia; whereas the optimized cost is minimum and is not sensitive to turbine inlet pressure between 325-350 psia, as can be seen from Figure 28.0. If the resource utilization optimum turbine inlet pressure is picked as 325 psia, then the cost optimum will be identical, which verifies the previously stated assumption.

The plot in Figure 28.0 shows that net plant work per unit mass of brine, $^{W}N/M_{H}$, is quite different for resource utilization and cost optimums. This is due to the fact that the economically optimized brine flow rate is larger than the resource utilization optimized brine flow rate due to larger brine heat exchanger LMTD for the cost optimum case. The thermodynamically optimized isobutane turbine inlet pressure was 550 psia and net thermodynamic cycle efficiency was calculated to be 13.6 percent. This shows clearly that the thermodynamic optimum operating conditions are away from the resource utilization and economic optimum operating conditions at lower georesource temperatures.

Turbine Inlet Temperature and Pressure

For a given pressure, the turbine inlet temperature

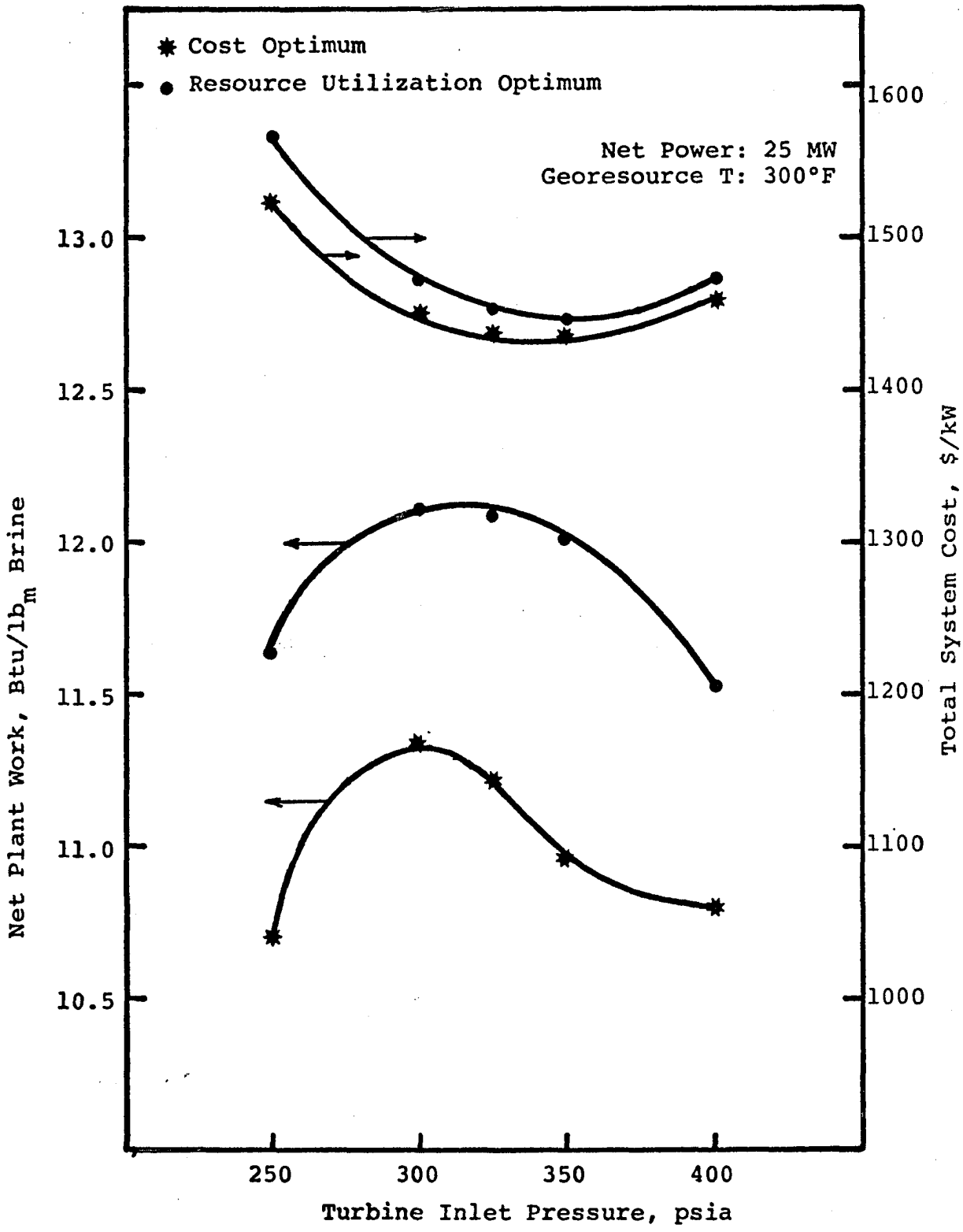

Figure 28.0 Resource Utilization Optimum and Cost Optimum Turbine Inlet Pressure Versus Net Plant Work and Total System Cost of Isobutane Binary Cycles

for any working fluid can be determined if the georesource temperature and approach temperature, DTHWI, are specified. The turbine inlet temperature is assumed to be obtained following the guidelines established earlier in Chapter II.

In this section, the basis of comparison is a plant with net power of 25.0 MW using georesource temperature of 300°F. Only subcritical cycles are considered in detail. The effects of increasing the turbine inlet temperature and pressure on the following thermodynamic, process unit operational and cost parameters of the geothermal binary cycle will be discussed: (1) turbine specific enthalpy change, (2) net thermodynamic cycle specific work, (3) net thermodynamic cycle efficiency, (4) brine heat exchanger and condenser duties, (5) brine heat exchanger and condenser overall heat transfer coefficients, (6) brine heat exchanger and condenser LMTD's (log mean temperature differences), (7) brine heat exchanger and condenser costs, (8) turbine-generator cost, (9) cooling tower cost, (10) brine system cost, and (11) total system cost.

In Chapter II, the following conclusions were drawn regarding the effects of increasing the turbine inlet temperature and pressure on the Rankine cycle:

(1) Turbine specific enthalpy change increases,

(2) Net thermodynamic cycle specific work increases,

(3) Net thermodynamic cycle efficiency increases,

(4) For a specified net work, W_N, the brine heat exchanger duty, Q_H, decreases.

In order to study the effects of increasing turbine inlet T and P on other cycle parameters, consider the isobutane cycle shown on a T-h diagram in Figure 29.0. The isobutane cycle operating conditions (except turbine inlet pressure) were optimized with respect to the total system capital cost in $/kw for a specified net plant power of 25.0 MW. The turbine efficiency was assumed to be 86% whereas an efficiency of 85% was assumed for the cycle pump, brine and cooling water pumps. Figure 30.0 shows on a temperature-enthalpy diagram the base case (P_1 = 300 psia, 220°F) and case 1 (P_5 = 350 psia, 235°F) for isobutane cycles.

Condenser Duty

A relationship between the net thermodynamic cycle work, W_N, net thermodynamic cycle efficiency η_c, and condenser duty, $-Q_c$ was derived earlier and can be written for the base case as

$$-Q_c = \frac{W_N}{\eta_c} (1 - \eta_c) \tag{63}$$

and for case 1

$$- Q_{c1} = \frac{W_{N1}}{\eta_{c1}} (1 - \eta_{c1}) \tag{64}$$

It follows then

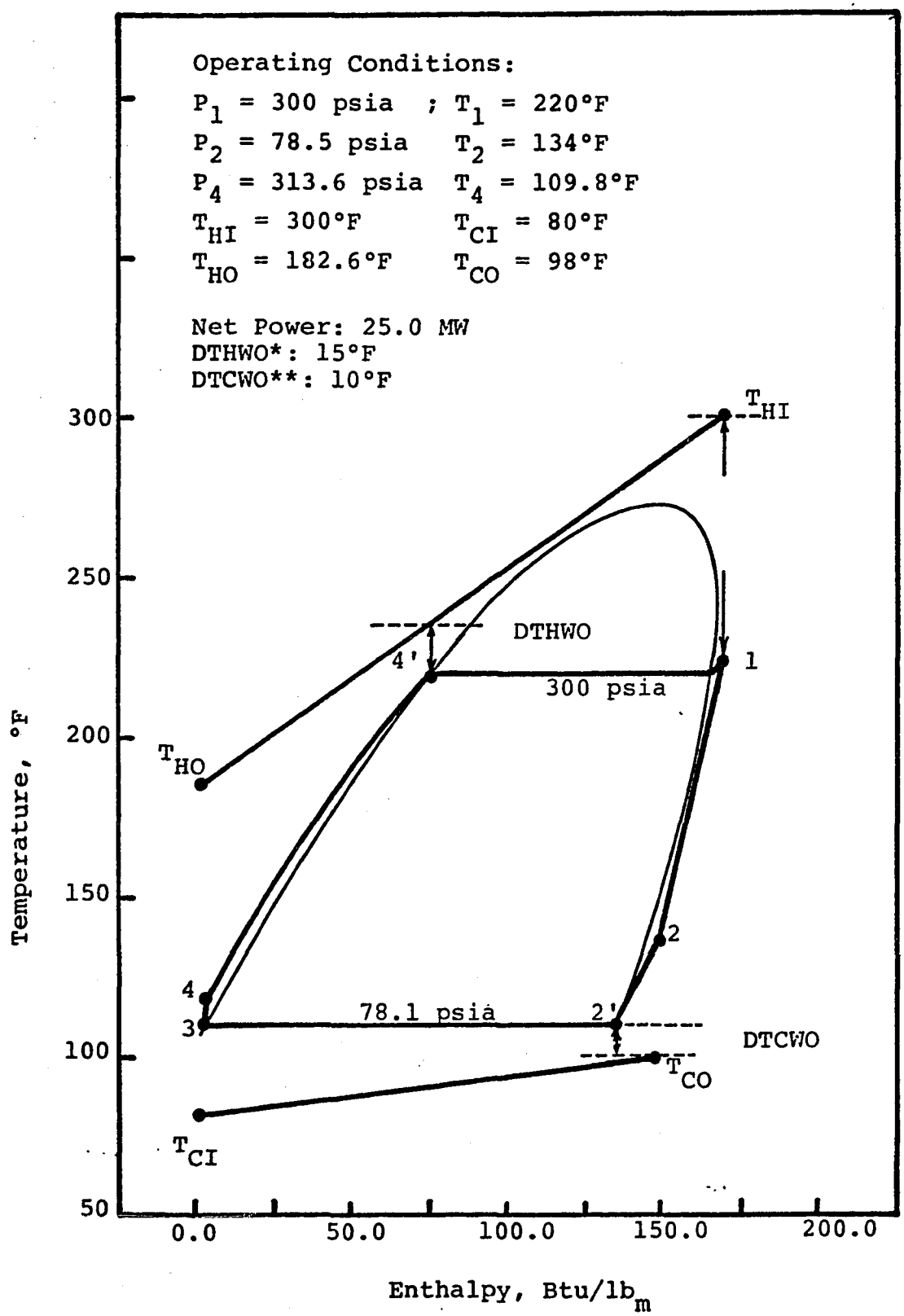

Figure 29.0 Temperature-Enthalpy Diagram of Isobutane Cycle (Base Case)

* DTHWO is the pinch point temperature ΔT in brine heat exchanger

** DTCWO is the pinch point temperature ΔT in condenser

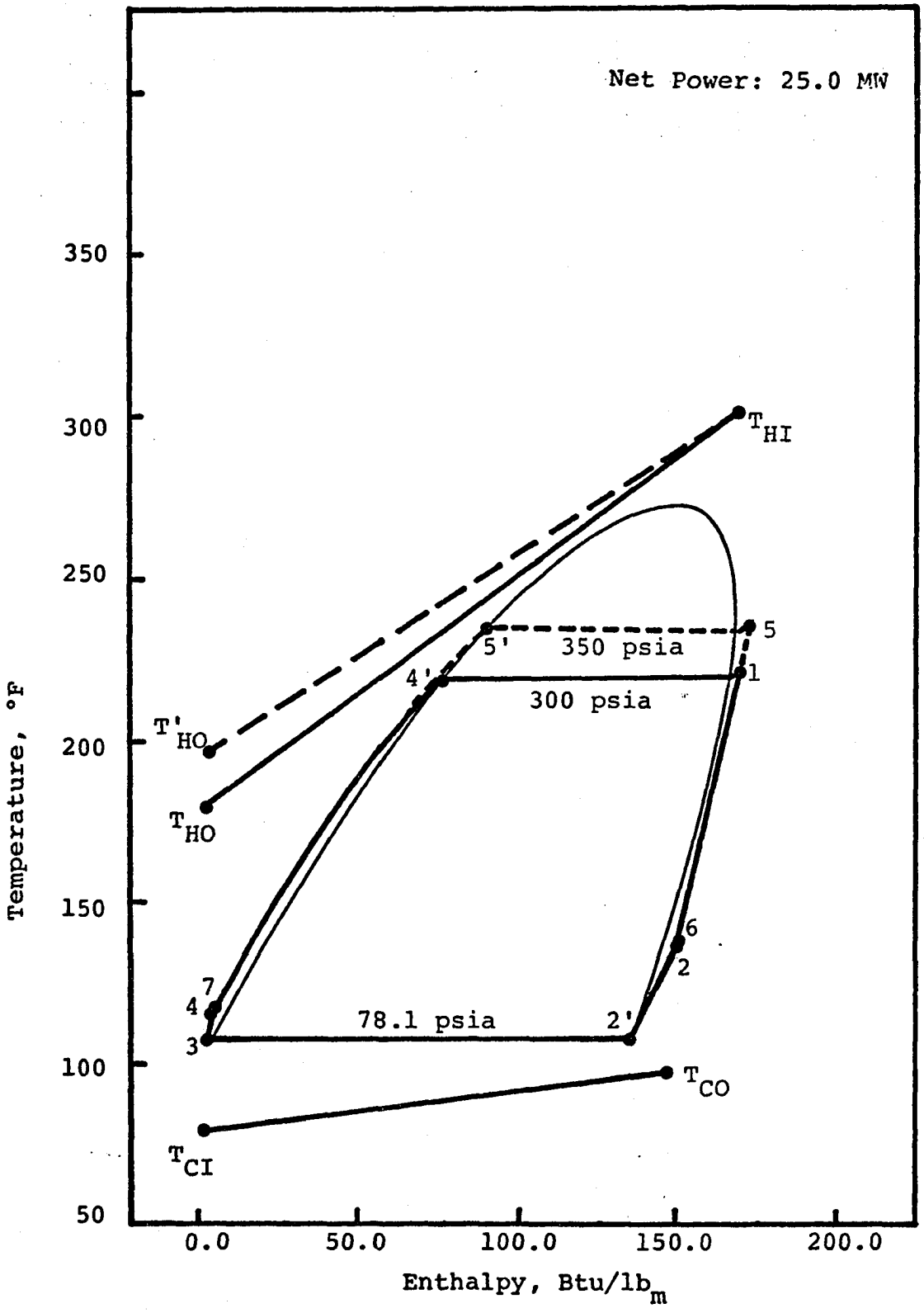

Figure 30.0 Temperature-Enthalpy Diagrams of Isobutane Cycles (Base Case and Case 1)

$$\frac{-Q_{c1}}{-Q_c} = \left(\frac{W_{N1}}{W_N}\right)\left(\frac{\eta_c}{\eta_{c1}}\right)\left(\frac{1-\eta_{c1}}{1-\eta_c}\right) \tag{65}$$

Let us now examine each ratio on the right hand side.

For fixed net plant work

$$W_{N1} = W_N$$

since

$$\eta_{c1} > \eta_c$$

it follows then

$$\frac{\eta_c}{\eta_{c1}} < 1$$

and

$$\frac{(1-\eta_{c1})}{(1-\eta_c)} < 1$$

hence

$$\frac{-Q_{c1}}{-Q_c} < 1$$

or

$$-Q_{c1} < -Q_c \tag{66}$$

It can therefore be stated that for an increase in turbine inlet temperature and pressure, the condenser duty will decrease. For specified cooling water temperature range in the condenser, the decrease in condenser duty will result in lower cooling water flow rate and lower pumping requirements.

The decrease in condenser duty for case 1 could have been anticipated from the examination of Figure 30.0. Although the specific enthalpy change in the condenser for case 1 is only marginally greater than the base case, the working fluid flow rate is much less than the base case resulting in a decrease in the condenser duty for case 1.

Brine Heat Exchanger and Condenser Overall Heat Transfer Coefficients

The brine heat exchanger overall heat transfer coefficient, U_H, is given by the relation

$$U_H = \left[\frac{1}{h_{WF}} + \frac{1}{h_B} + R_{fB} + R_{fWF} + \frac{t}{k_m} \right]^{-1} \qquad (67)$$

Since the brine side and working fluid side fouling resistances R_{fB} and R_{fWF}, and t/k_m are specified as input in these calculations, U_H is in fact a function of h_{WF} (working fluid) and h_B (brine), i.e.,

$$U_H = f\left[\frac{1}{h_{WF}}, \frac{1}{h_B} \right]^{-1} \qquad (68)$$

The brine side heat transfer coefficient, h_B, is basically a function of flow rate and temperature, and increases with increasing flow rate and/or temperature. However, the brine side heat transfer coefficient (using pure water properties) is usually two to three times larger than the working fluid heat transfer coefficient, h_{WF}. Therefore, if fouling is ignored, the overall heat transfer coefficient will be influenced more by h_{WF} than h_B.

For subcritical cycles, an increase in turbine inlet pressure results in a decrease in the two-phase (boiling) region in the heat exchanger, and consequently the compressed liquid region of the brine heat exchanger increases. Because of the small superheating section, the working fluid heat transfer coefficient is mainly influenced by the liquid and boiling side heat transfer coefficients.

As discussed earlier in Chapter II, the working fluid heat transfer coefficient (for fixed working fluid flow rates) increases slightly for an increase in the average design temperature and pressure of the working fluid. Since the working fluid flow rate for case 1 is lower than in the base case, both the liquid and boiling heat transfer coefficients will decrease for an increase in turbine inlet T and P. Thus, the working fluid heat transfer coefficient generally will decrease for an increase in turbine inlet temperature and pressure. The net result of a decrease in h_{WF} will be a decrease in the overall heat transfer coefficient of the brine heat exchanger, U_H.

The condenser overall heat transfer coefficient, U_c, is primarily influenced by the working fluid heat transfer coefficient. From Figure 29.0 it is evident that the condenser inlet temperature and pressure increase marginally for an increase in turbine inlet T and P. However, due to the lower working fluid flow rate, the working fluid heat transfer coefficient will decrease for case 1. However, the weighted (based on heat transfer surface area) average overall heat transfer coefficient for the condenser will either decrease very slightly or will remain unchanged depending on the size of increase in the turbine inlet T and P.

Brine Heat Exchanger and Condenser Log Mean Temperature Differences

If the brine flow rate is specified, then an increase in the turbine inlet temperature will decrease the brine heat exchanger log mean temperature difference (LMTD), because the approach temperature DTHWI decreases, as does the pinch point temperature difference DTHWO. For specified resource temperature and net plant power, the cost optimum value for DTHWO (within $\pm$ 5°F) does not change for a change in the turbine inlet temperature and pressure. Therefore, for a specified net power and pinch point temperature difference, DTHWO, the brine outlet temperature (and flow rate) must increase to satisfy the pinch point constraint. If the brine heat exchanger areas are fixed, then (since the brine

heat exchanger duty decreases) the brine heat exchanger LMTD will decrease for an increase in the turbine inlet T and P. This can be explained by the following equations.

For base case

$$\dot{Q}_H = U\ A\ \Delta T_m$$

or

$$\Delta T_m = \frac{\dot{Q}_H}{U\ A} \tag{69}$$

Similarly for case 1

$$\Delta T_{m1} = \frac{\dot{Q}_{H1}}{U_1 A_1} \tag{70}$$

where ΔT_m and ΔT_{m1} are the log mean temperature differences for base case and case 1, respectively. But since $\dot{Q}_{H1} < \dot{Q}_H$, $A_1 = A$, and assuming $U_1 = U$, it follows then that

$$\Delta T_{m1} < \Delta T_m \tag{71}$$

Thus, an increase in turbine inlet temperature and pressure will decrease the brine heat exchanger LMTD.

For isobutane, the condenser inlet temperature increases with increasing turbine inlet T and P for a good portion of the operating region, so that the condenser desuperheating section LMTD increases correspondingly. Fluids in the homologous series of normal paraffin hydro-

carbons have I-factor considerably different from unity. Thus, depending on operating conditions, normal paraffin hydrocarbons with I < 1 generally will have some superheat at the turbine exhaust (condenser inlet), whereas the fluids with I > 1 generally will have no superheat at the condenser inlet. For fixed dew point temperature of the working fluid in condenser, an increase in turbine inlet T and P, for fluids with I < 1, generally will increase the superheat at the condenser inlet. However, for specified (optimum) values of the approach temperature difference, DTCWO, the condensing section (two-phase) LMTD remains unchanged for an increase in turbine inlet T and P. Therefore, depending on the increase in condenser inlet temperature, the overall enthalpy averaged condenser LMTD will increase accordingly for any increase in turbine inlet temperature and pressure (for the isobutane cycle).

Brine Heat Exchanger and Condenser Costs

The cost of heat exchangers is primarily dependent on the design pressure rating and the heat transfer surface area requirements. It is common practice in the hydrocarbon industry to specify the design pressure rating somewhat above the normal operating pressure to avert relief valve operation in the event the cycle pump "backs up" the pump head curve. Therefore, a heat exchanger will usually have a higher (25% higher in this research) pressure rating than normal operation dictates.

The shell and tube heat exchanger cost correlation (presented in Appendix A) used in the GEO4 simulator indicates that the heat exchanger cost for a 300 psia shell and tube unit is approximately $\$10.7/ft^2$ of surface area. The cost increases to $\$12.2/ft^2$ (a 14% increase) for a 400 psia rated exchangers.

As noted earlier, an increase in turbine inlet T and P decreases the brine heat exchanger (BHE) duty and LMTD. Since

$$A_H = \frac{\dot{Q}_H}{U_H(LMTD)} \tag{72}$$

it follows that only if $\dot{Q}_H$ decreases more rapidly than U_H (LMTD) as turbine inlet P is increased will the brine heat exchanger area decrease. However, an increase in turbine inlet T and P would mean higher design pressure and higher $\$/ft^2$ of surface area rating. If the cost rating in $\$/ft^2$ increases more rapidly than the decrease in the brine heat exchanger area, the cost of the brine heat exchanger will increase, for an increase in turbine inlet temperature and pressure.

The condenser cost, on the other hand, will decrease with increasing turbine inlet T and P, for two reasons: (1) there is no change in the design pressure rating, (2) the decrease in condenser area due to lower condenser duty and slightly higher condenser LMTD (for the case of the isobutane cycles).

Therefore, it can be stated, for isobutane cycles with turbine inlet pressures well below the critical, that an increase in turbine inlet T and P will increase the brine heat exchanger cost but decrease condenser cost. If condenser cost decreases faster than brine heat exchanger cost increases, the total heat exchange equipment cost will decrease. For higher georesource temperatures, where supercritical cycles are optimum[20], the heat exchange equipment total cost may not change for an increase in the turbine inlet T and P because the increase in the brine heat exchanger cost will nullify the decrease in the condenser cost.

Turbine-Generator Cost

The turbine cost is a direct function of the last stage diameter of the turbine and the number of exhaust ends on a common shaft. Other factors include the blade tip speed and the turbine inlet pressure. The generator cost is a direct function of the net electrical output of the unit.

The turbine diameter is directly proportional to the square root of the turbine exhaust volumetric flow rate and inversely proportional to the one-fourth root of the turbine isentropic specific work. Thus, fluids with larger volumetric flow rates at the turbine exhaust and/or lower turbine isentropic specific work, will have larger turbine last stage diameter and cost. Conversely, fluids with smaller

volumetric flow rates at the turbine exhaust and/or larger turbine isentropic specific work will have smaller turbine diameter and cost.

It has been shown earlier for isobutane cycles that an increase in the turbine inlet pressure and temperature has the following effects: (1) the turbine isentropic specific work increases, (2) the turbine outlet temperature increases. Also, the turbine exhaust specific volume will increase slightly. However, for a specified net plant power, the working fluid flow rate decreases more rapidly than the specific volume increases so the volumetric flow rate will decrease for an increase in turbine inlet T and P. Therefore, the turbine diameter and cost will decrease for an increase in the turbine inlet T and P.

At lower georesource temperatures, relatively larger flow rates are needed for specified net plant power (since subcritical cycles are optimum) compared to the higher georesource temperatures where higher pressure (or supercritical) cycles are optimum. It can, therefore, be anticipated that for a specified increase in the turbine inlet pressure, the turbine cost will decrease more for lower georesource temperature cycles compared to higher georesource temperature cycles.

Cooling Tower Cost

The cooling towers considered in this study are wet cooling towers of the mechanical draft type. The cost model used is a direct function of the cooling water flow rate. Since the condenser duty decreases for an increase in the turbine inlet T and P, the cooling water flow rate will decrease (for a specified cooling range). For example, consider the following heat transfer relations:

For the base case we have

$$\dot{Q}_c = \dot{M}_c \, \bar{C}_p \, (T_{CI} - T_{CO}) \tag{73}$$

and for case 1

$$\dot{Q}_{c1} = \dot{M}_{c1} \, \bar{C}_p \, (T_{CI} - T_{CO}) \tag{74}$$

From Equations 73 and 74, we have

$$\frac{\dot{M}_{c1}}{\dot{M}_c} = \frac{\dot{Q}_{c1}}{\dot{Q}_c} \tag{75}$$

where $\dot{M}_c$ and $\dot{M}_{c1}$ are the cooling water flow rates (in lb_m/hr) for base case and case 1, respectively. But since

$$\frac{\dot{Q}_{c1}}{\dot{Q}_c} < 1$$

it follows that

$$\frac{\dot{M}_{cl}}{\dot{M}_c} < 1$$

or

$$\dot{M}_{cl} < \dot{M}_c \tag{76}$$

which verifies the statement made earlier.

Brine System Cost

Geothermal brine delivery costs are extremely site dependent but for a particular geothermal producing site, the geothermal fluid delivery cost increases as the required flow rate increases. Since the slope of the brine profile (shown as a straight line on the T-h diagram in Figure 29.0) decreases for an increase in the turbine inlet T and P, the brine delivery (and hence brine system) cost will increase. Consider for a fixed plant power the base case and case 1 duties for the brine heat exchanger

$$\dot{Q}_H = \dot{M}_H \bar{C}_p (T_{HI} - T_{HO}) \tag{77}$$

$$\dot{Q}_{Hl} = \dot{M}_{Hl} \bar{C}_p (T_{HI} - T'_{HO}) \tag{78}$$

where $\dot{M}_H$ and $\dot{M}_{Hl}$ are the brine flow rates (in lb_m/hr) for base case and case 1, respectively. If a constant average brine heat capacity, $\bar{C}_p$, of 1.0 Btu/lb°F is assumed, then we have

$$\frac{\dot{M}_{Hl}}{\dot{M}_H} = \frac{\dot{Q}_{Hl}}{\dot{Q}_H}\left[\frac{T_{HI} - T_{HO}}{T_{HI} - T'_{HO}}\right] \tag{79}$$

but

$$\frac{\dot{Q}_{Hl}}{\dot{Q}_H} < 1 \tag{80}$$

and

$$\frac{T_{HI} - T_{HO}}{T_{HI} - T'_{HO}} > 1 \tag{81}$$

It follows then that only if the ratio of temperature differences (Equation 81) increases more rapidly than the ratio of duties (Equation 80) decreases, would the ratio of brine flow rates ($\dot{M}_{Hl}/\dot{M}_H$) be greater than 1. For subcritical cycles, this will be the case, whereas for supercritical cycles the ratios of flow rates will be less than 1. For the subcritical isobutane cycle considered

$$\frac{\dot{M}_{Hl}}{\dot{M}_H} > 1$$

so that

$$\dot{M}_{Hl} > \dot{M}_H \tag{82}$$

which verifies the statement made earlier.

Total System Cost

The total system cost is simply the sum of the power plant cost and the brine system cost. The power plant cost is roughly inversely proportional to the net thermodynamic cycle efficiency, η_c. Therefore, an increase in η_c will result in a decrease in the power plant cost. The decrease in the power plant cost is primarily due to the decreases in the turbine and condenser costs. The increase in the brine heat exchanger cost (due to an increase in turbine inlet T and P) is roughly nullified by a corresponding decrease in the cooling system cost. However, an increase in the turbine inlet T and P results in an increase in the brine system cost, as shown earlier.

It can therefore be concluded that the operating conditions for an optimum total system cost occur via a trade off between the power plant cost and the brine system cost. Table 11 gives a summary of results for isobutane (base case and case 1) cycles for the 300°F georesource temperature. It can be noted from Table 11 that for an increase in the turbine inlet temperature and pressure of 15°F and 50 psia, the net thermodynamic cycle efficiency increased from 10.88% to 11.73% (a 7.8% increase). The turbine-generator and condenser costs decreased by approximately 34.9% and 9.3%, respectively; whereas the brine heat exchanger cost increased by approximately 3.8% compared to a 9.6% decrease in the cooling system cost. The brine system

Table 11

EFFECT OF TURBINE INLET TEMPERATURE AND PRESSURE ON THE ISOBUTANE CYCLE PARAMETERS FOR THE GEORESOURCE TEMPERATURE OF 300°F

Process Parameters \ Case No.	Base Case	Case 1
Cycle		
Net Power, MW	25.00	25.00
Gross Power, MW	31.08	31.01
Net Plant Work, Btu/lb_m brine	11.33	10.98
Net Thermo. Efficiency, %	10.88	11.73
Power Plant Cost, $/kw	864	830
Total System Cost, $/kw	1449	1434
Brine Delivery		
Brine Flow, lb/kw	301	311
Brine Exit T, °F	182.6	195.7
Brine Delivery Cost, $/kw	585	604
Brine Heat Exchanger (BHE)		
BHE LMTD, °F	36.7	35.4
Brine Load ΔH, Btu/lb_m W.F.	163.6	165.6
BHE Overall U, Btu/hr ft^2 °F	220	214
BHE Duty, 10^8 Btu/hr	8.961	8.228
Cost Rating, $/ft^2	12.04	12.78
BHE Area, 10^4 ft^2	11.08	10.824
BHE Cost, $/kw	264	274
Condenser		
Cond. LMTD, °F	18.6	18.7
Cond. Load ΔH, Btu/lb_m W.F.	145.8	146.1
Cond. Overall U, Btu/hr ft^2 °F	161	161
Cond. Duty, 10^8 Btu/hr	7.987	7.263
Cost Rating, $/$ft^2$	6.56	6.56
Condenser Area, 10^4 ft^2	26.552	24.122
Condenser Cost, $/kw	345	313
Turbine		
Turbine Inlet P, psia	300	350
Turbine Inlet T, °F	220	235
Turbine ΔH, Btu/lb_m W.F.	19.37	21.30
Working Fluid Flow, lb/kw	219	199
Exhaust Vol. Flow, ft^3/min/kw	4.5	4.1
Turbine-Generator Cost, $/kw	146	95
Cooling System		
Cooling Water Flow, lb/kw	1773	1613
Cooling Cost, $/kw	83	75
Cycle Pump		
Parasitic Power, MW	2.51	2.73
Pump Cost, $/kw	26	28

cost increased from \$585/kw to \$604/kw (a net increase of 3.2%), but the total power plant cost decreased from \$864/kw to \$830/kw (a net decrease of 3.9%). The net result is an overall decrease of about 1% in the total system cost. Other process parameters in Table 11 are self-explanatory.

Overall effects of increasing turbine inlet temperature and pressure are summarized in Figures 31.0 and 32.0. Figure 31.0 shown on the next page (and the analysis required to construct it) demonstrates that for fixed brine flow rate $\dot{M}_H$ and brine exit temperature T_{HO} (fixed $\dot{M}_H$ and T_{HO} fix $\dot{Q}_H$), an increase in turbine inlet T, P always yields an increase in $\dot{W}_N/\dot{M}_H$. For turbine inlet T, P below the optimum, increasing T, P will decrease the total system cost per kw; otherwise the cost per kw will increase.

Figure 32.0 demonstrates that for fixed net plant power $\dot{W}_N$, an increase in turbine T, P yields the following: (1) generally an increase in $\dot{W}_N/\dot{M}_H$ for high temperature source (e.g., 500°F) cycles and (2) generally a decrease in $\dot{W}_N/\dot{M}_H$ for low temperature source (e.g., 300°F) cycles. For turbine inlet T,P below the optimum, increasing T,P will decrease the total system cost per kw; otherwise the cost per kw will increase.

Brine Heat Exchanger Log Mean Temperature Difference

The cost optimization studies carried out at the University of Oklahoma for the geothermal binary cycle

Fixed $\dot{M}_H$ and $\dot{Q}_H$

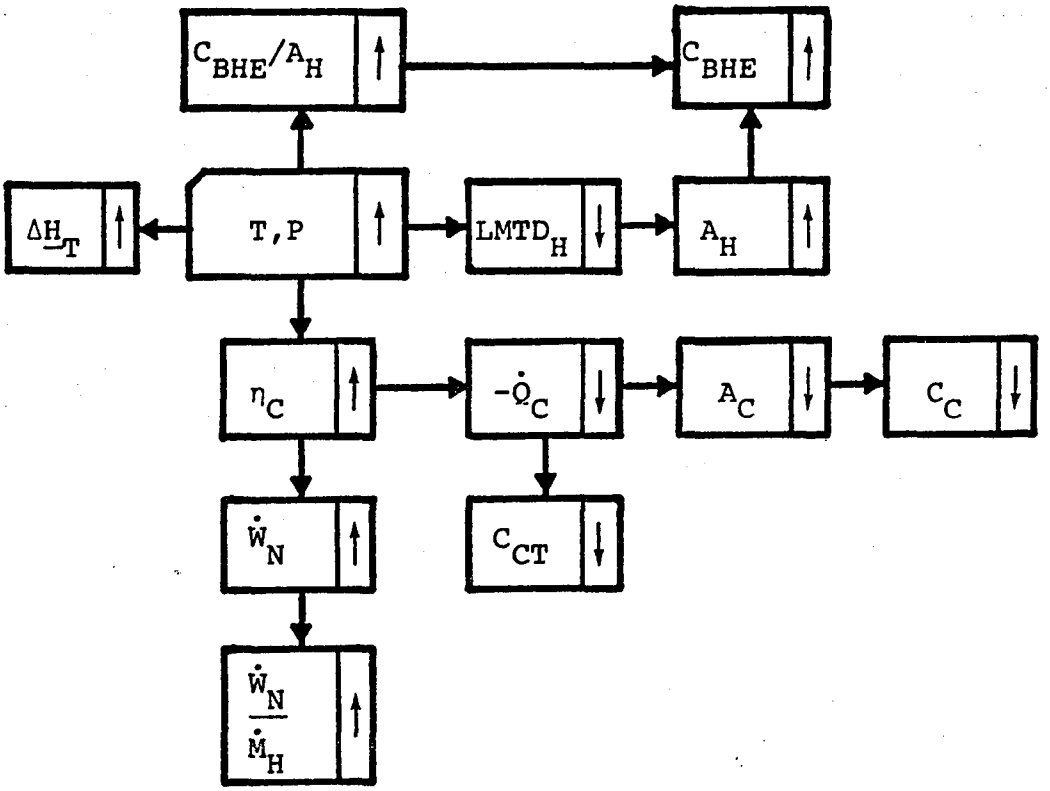

(a)

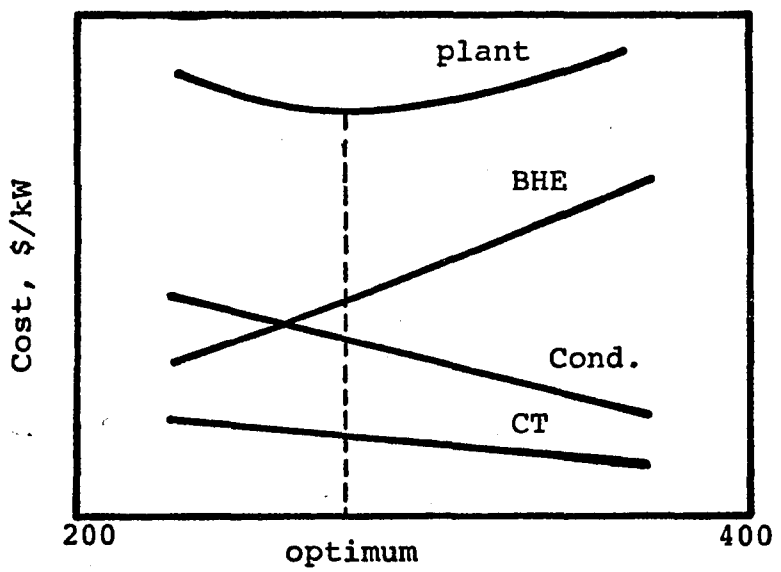

(b) Turbine Inlet Pressure Versus Cost in $/kW

Figure 31.0 Effects of Increasing Turbine Inlet T and P (fixed $\dot{M}_H$ and $\dot{Q}_H$) on Isobutane Cycle for 300°F georesource

Fixed $\dot{W}_N$

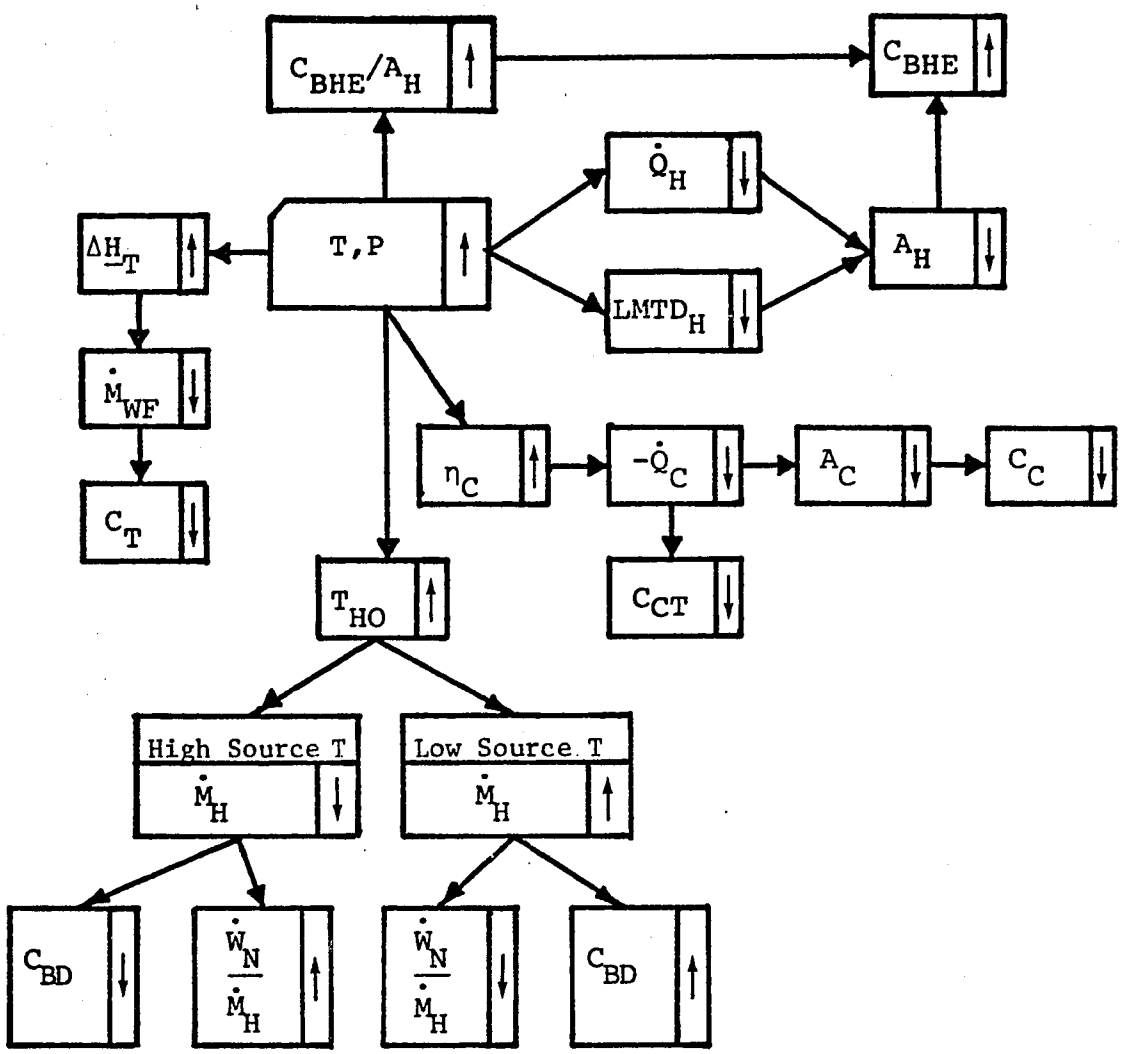

(a)

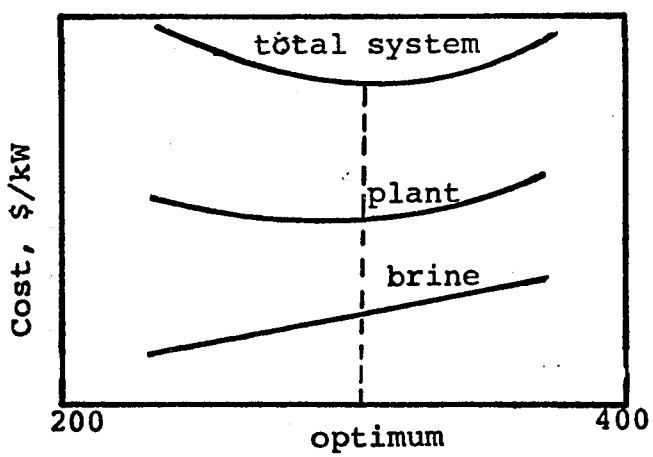

(b) Turbine Inlet Pressure Versus Cost in $/kW

Figure 32.0 Effects of Increasing Turbine Inlet T and P (fixed $\dot{W}_N$) on Isobutane Cycle for 300°F georesource

(without preheater) demonstrate that near optimal brine heat exchanger (BHE) LMTD's vary with georesource temperature and molecular weight (isobutane, isopentane and their binary mixtures)[20]. In this section, however, the discussion will be limited to only one working fluid, namely isobutane, and include (1) the effect of increasing the BHE LMTD from its optimal value on the process equipment cost and the brine system cost and (2) the relationship of the georesource temperature and the cost optimum BHE LMTD's and their effect on cycle parameters and cost.

The parameters which directly affect the BHE LMTD's are the inlet and exit approach temperatures and the pinch point (or minimum) temperature difference. Since the approach temperature at the brine inlet (DTHWI) is fixed for a specified turbine inlet pressure, while the approach temperature at the brine exit is a function of the minimum approach temperature or pinch point temperature difference (DTHWO), it is obvious that the pinch temperature difference is the parameter controlling the brine heat exchanger LMTD.

For lower georesource temperatures (e.g., 250-350°F) and subcritical cycles, the pinch occurs at or near the working fluid bubble point temperature in the BHE; whereas for higher georesource temperatures the pinch usually occurs at or near the brine exit of the BHE.

Figure 33.0 shows on a temperature-enthalpy diagram the base case (as shown earlier in Figure 38) and case 1

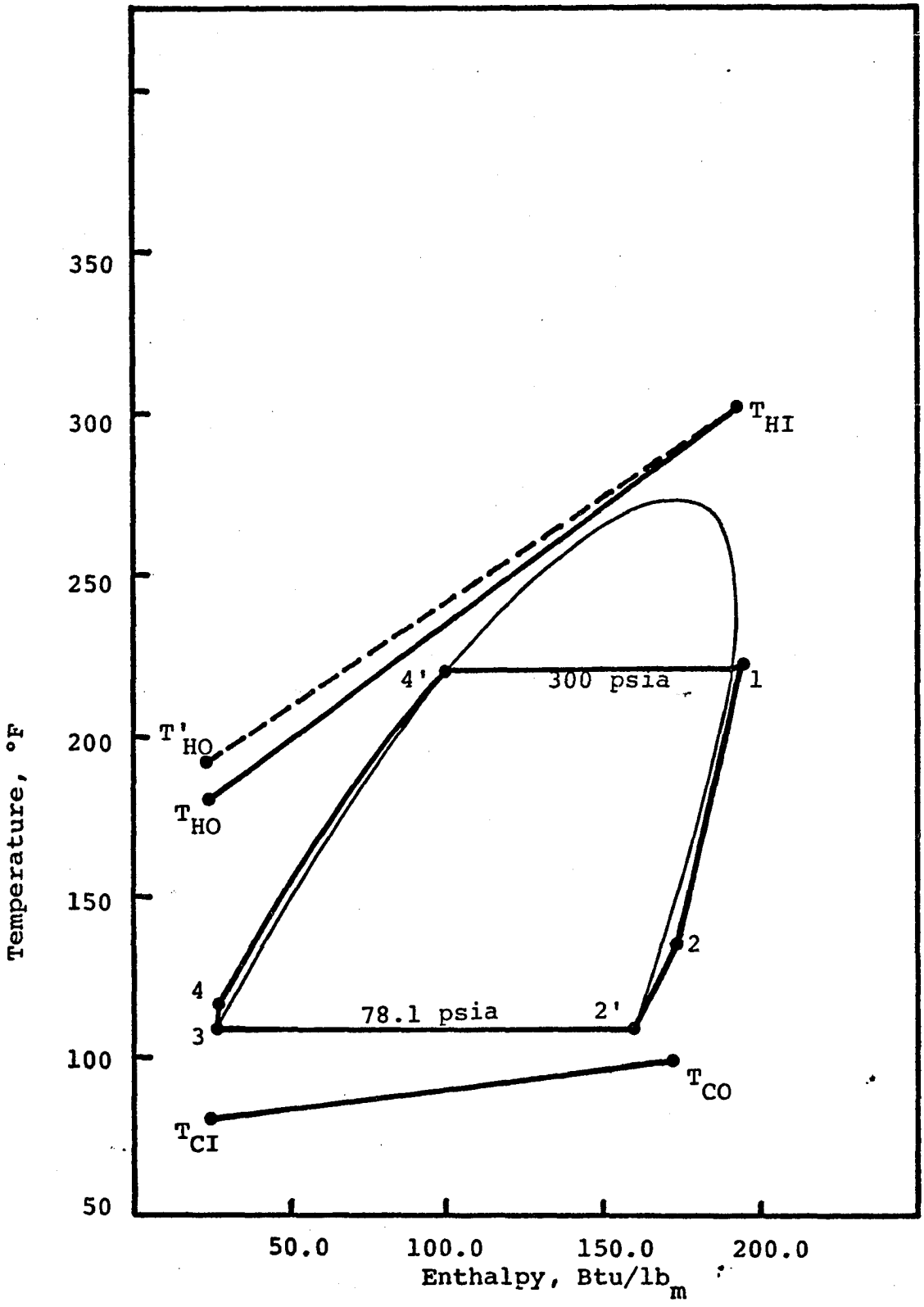

Figure 33.0 Effect of Increasing Brine Heat Exchanger LMTD on Isobutane Cycles (Base Case and Case 1)

(increased LMTD) for isobutane cycles. The increase in LMTD is brought about by increasing the pinch temperature difference, DTHWO. Since the turbine inlet T and P are the same for both cases, the turbine, condenser, cooling system and cycle pump will be unaffected with respect to performance and cost. Hence, only the brine heat exchanger and brine flow rate will be affected by an increase in the BHE LMTD.

The slope of the brine profile decreases for an increase in the BHE LMTD and therefore the brine flow rate will increase, and the brine heat exchanger area will decrease. Since the cycle operating conditions (except brine outlet T) do not change, there will be no effect on the net thermodynamic cycle efficiency. Because of the reduction in BHE area, the BHE cost will decrease for an increase in the BHE LMTD; however, the brine system cost will increase. Therefore, the optimum BHE LMTD will be a trade-off between the BHE cost and brine system cost.

Table 12 shows the effect of increasing the brine heat exchanger LMTD on the process parameters and cost for the isobutane cycles. It is evident from Table 12 that for the isobutane subcritical cycle, increasing the BHE LMTD from 36.7°F to 42.5°F (a 15.9% increase), the BHE area decreased from 11.08×10^4 ft^2 to 9.652×10^4 ft^2 (a 12.9% reduction), the brine flow rate increased from 301 lb_m/kw to 324 lb_m/kw (a 7.6% increase) and brine heat exchanger

Table 12

EFFECT OF BRINE HEAT EXCHANGER LOG MEAN TEMPERATURE DIFFERENCE ON CYCLE AND COST PARAMETERS

Process Parameters \ Case No.	Isobutane Cycle	
	Base Case	Case 1
Cycle		
Net Power, MW	25.00	25.00
Gross Power, MW	31.08	31.00
Net Plant Work, Btu/lb_m brine	11.33	10.53
Resource Utilization Efficiency %	31.53	29.30
Net Thermo. Efficiency, %	10.88	10.89
Power Plant Cost, $/kw	864	828
Total System Cost, $/kw	1449	1457
Brine Delivery		
Brine Flow, lb_m/kw	301.	324.
Brine Exit T, °F	182.6	191.2
Brine Pump Power, MW	0.503	0.477
Brine Delivery Cost, $/kw	585	629
Brine Heat Exchanger (BHE)		
BHE LMTD, °F	36.7	42.5
Brine Load H, Btu/lb_m W.F.	163.6	163.6
BHE Area, 10^4 ft^2	11.08	9.652
BHE Cost, $/kw	264	229
Condenser Cost, $/kw	345	344
Cooling System Cost, $/kw	83	82
Turbine-Generator Cost, $/kw	146	146
Cycle Pump Cost, $/kw	26	26

cost decreased from $264/kw to $229/kw. However, since the BHE LMTD for case 1 is removed from the optimum value (base case) the net effect of an increase in the BHE LMTD is an increase in the total system cost.

In order to understand the relationship between the georesource temperature and the optimal BHE LMTD, consider Figure 34.0, which shows that cost optimized BHE LMTD's increase with increasing georesource temperature for a given fluid (isobutane in this case). The brine heat exchanger brine flow rate as a function of georesource temperature is shown in Figure 35.0, while the BHE heat transfer surface area is shown as a function of georesource temperature in Figure 36.0. For a given fluid, the slope of the BHE brine flow rate (versus georesource temperature) is opposite in sign to the slope of the BHE LMTD (Figure 34.0). For lower georesource temperatures (e.g., 300°F), comparatively larger brine flow rates are needed to generate a specific net plant power output (e.g., 25.0 MW net for this study) because cycle efficiency is low. Because there is a relatively small temperature difference between the brine and the working fluid, the brine flow rate is very sensitive to changes in the BHE LMTD at the lower georesource temperatures. However, for the 500°F georesource, the brine flow rate required to produce the same net plant power output (e.g., 25.0 MW net) is only about one third georesource; thus, larger BHE LMTD's are achieveable without significant increases in the brine

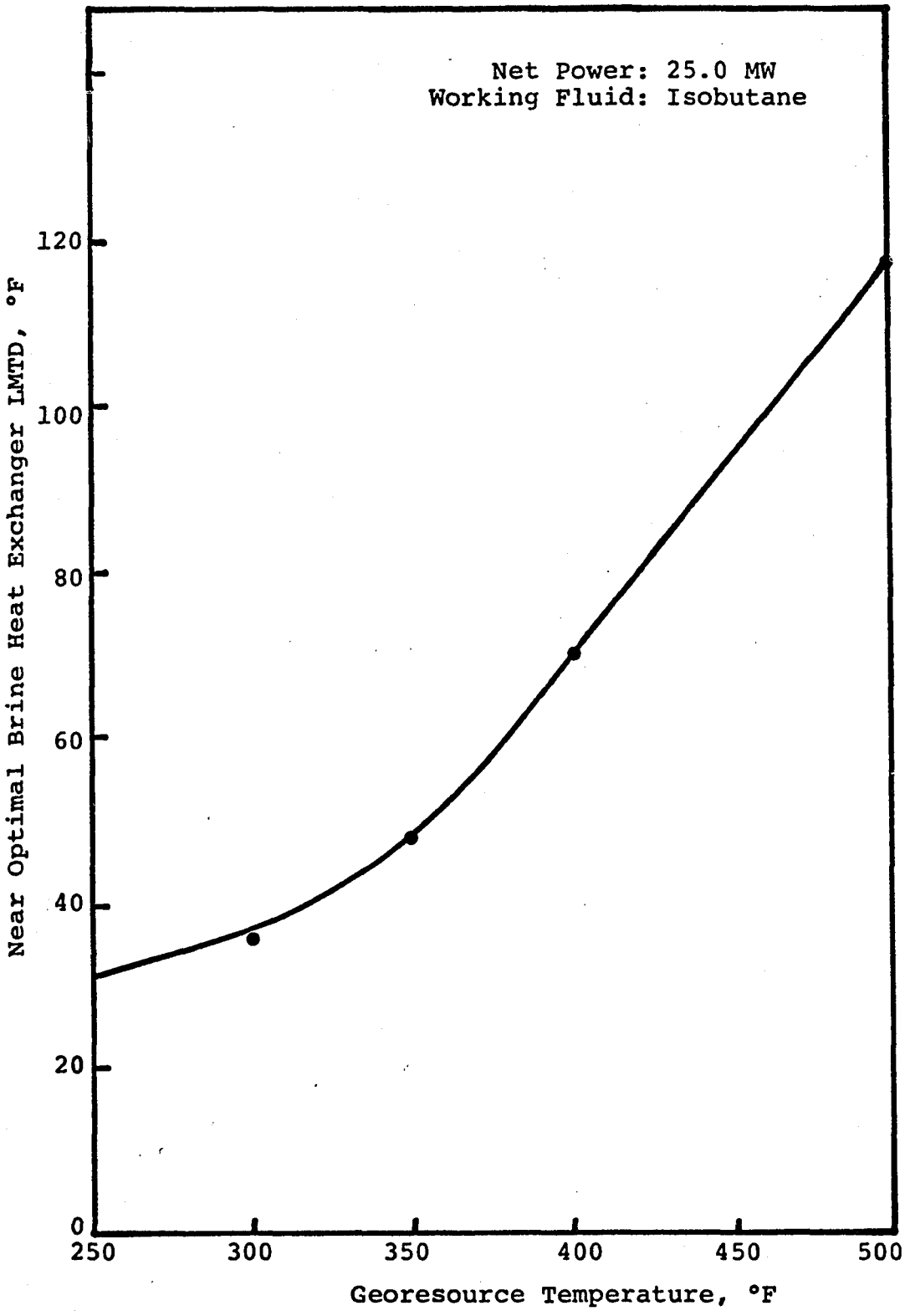

Figure 34.0 Brine Heat Exchanger LMTD as a Function of Georesource Temperature

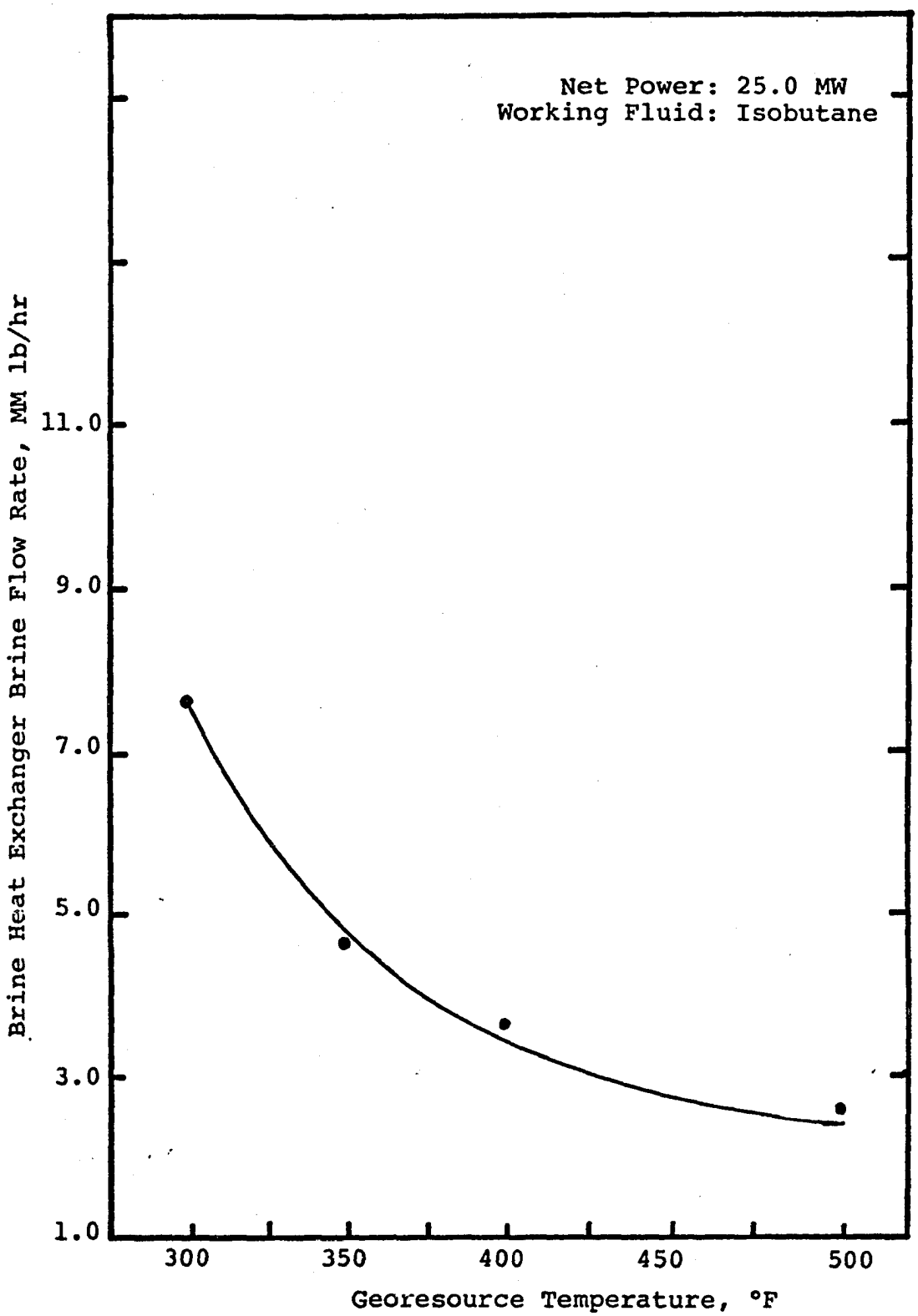

Figure 35.0 Brine Heat Exchanger Brine Flow Rate Versus Georesource Temperature

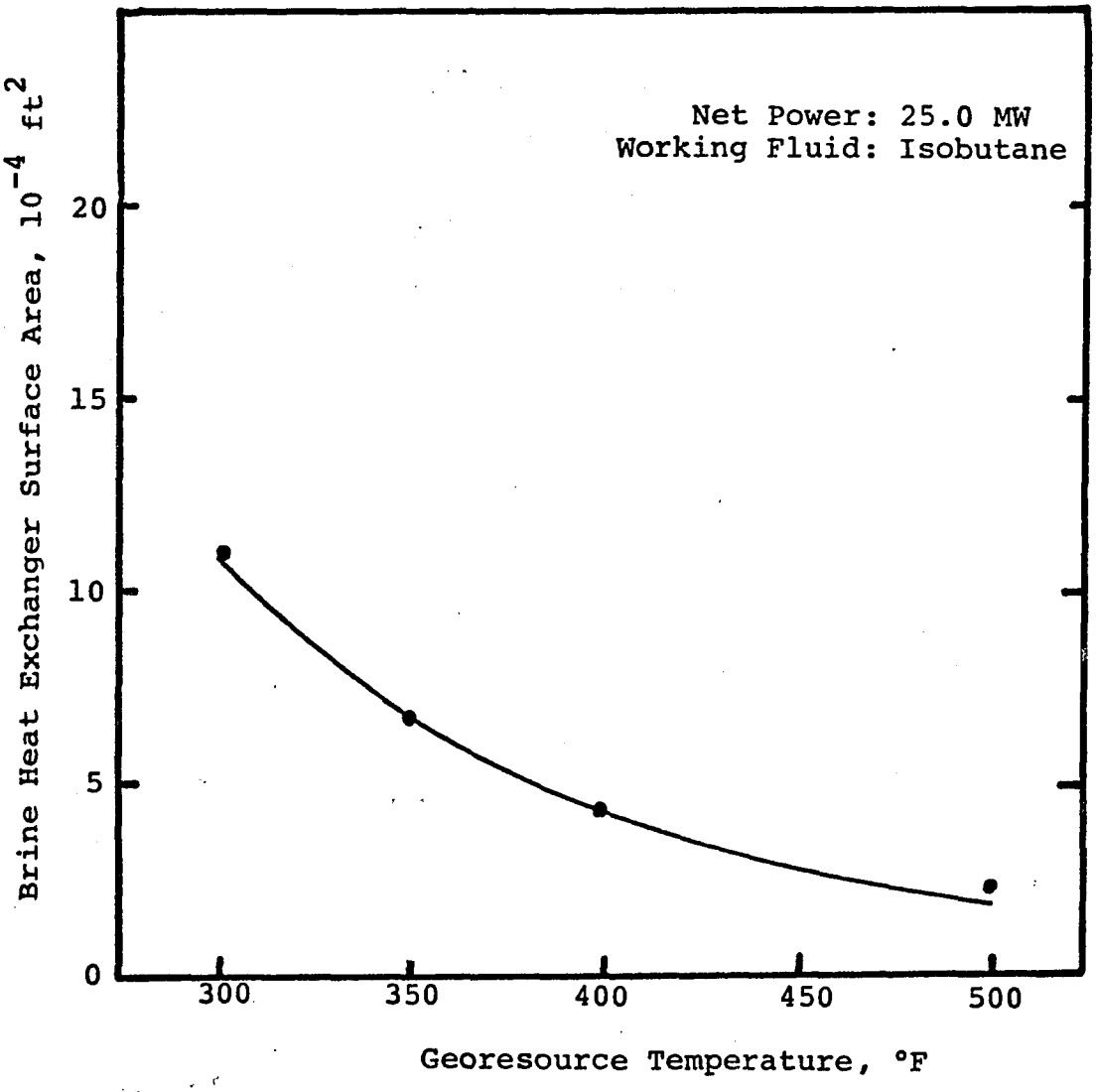

Figure 36.0 Brine Heat Exchanger Surface Area as a Function of Georesource Temperature

flow rate. The overall effect of larger BHE LMTD and lower brine flow rate for high temperature georesources is much smaller BHE heat transfer surface areas (e.g., for the 500°F georesource). This behavior is shown in Figure 36.0.

The trade-off between heat transfer surface area and LMTD for a given working fluid is shown clearly in Figures 34.0 and 36.0. It may be added here that for a given georesource temperature and a given working fluid, the equipment cost will dominate for small LMTD's, whereas for large LMTD's brine system cost will dominate. At 500°F georesource, cost optimized BHE LMTD's are large, and consequently high brine exit temperatures are obtained. The thermodynamic cycle efficiency is also highest for the cost optimized cycle. This suggests that maximizing thermodynamic cycle efficiency corresponds closely to the cost optimum for a 500°F georesource. Thus, geothermal binary cycles for the 500°F or higher georesource temperatures may actually correspond more closely to a conventional power plant situation.

Figure 37.0 (and the analysis required to construct it) demonstrates that for fixed net plant power $\dot{W}_N$, an increase in brine heat exchanger (BHE) LMTD (for fixed turbine inlet T,P) results in a decrease in $\dot{W}_N/\dot{M}_H$. For BHE LMTD below the optimum, increasing BHE LMTD will decrease BHE and total system costs per kw; otherwise the cost/kw will increase.

Fixed $\dot{W}_N$

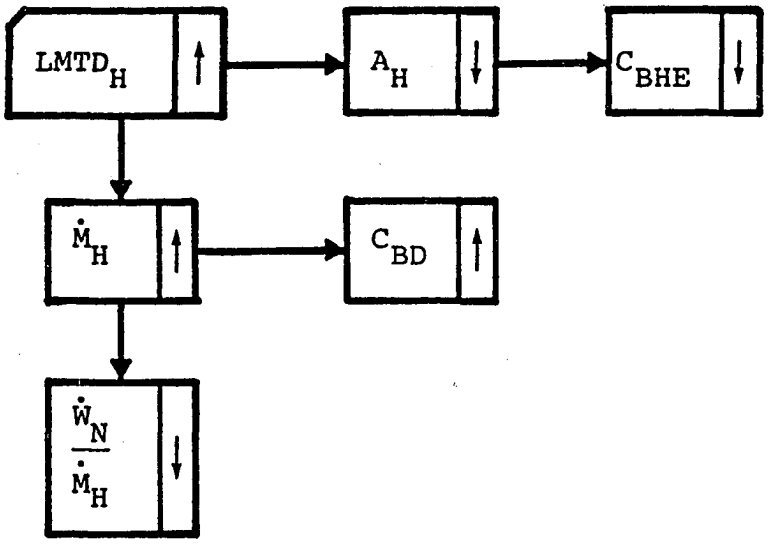

(a)

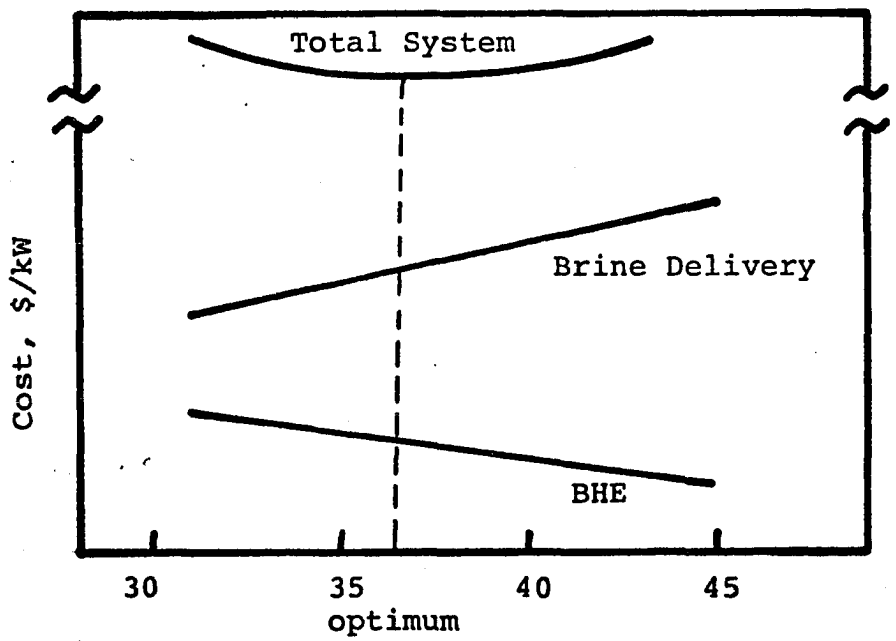

(b) BHE LMTD Versus Cost

Figure 37.0 Effects of Brine Heat Exchanger LMTD (Fixed $\dot{W}_N$)

Condenser Log Mean Temperature Difference

The condenser LMTD can be controlled by the approach temperature at the working fluid dew point (DTCWO) or the approach temperature at the working fluid bubble point (DTCWI). The approach temperature at the working fluid dew point (DTCWO) is the pinch point temperature difference for pure fluids and mixtures for which the working fluid temperature drop is less than the cooling water temperature rise in the condensing region. The approach temperature at the working fluid bubble point (DTCWI) is the pinch point temperature difference for mixtures for which the working fluid temperature drop is greater than the cooling water temperature rise in the condensing region.

The objectives of this subsection are to study the effects on cycle state points, process parameters and total system cost of increasing the condenser LMTD from its optimal value. Since the approach temperature difference at the working fluid dew point (DTCWO) is the parameter controlling the condenser LMTD, this study could also be considered to be an analysis of the effect of the working fluid dew point temperature in condenser on the cycle parameters.

From the analysis of the condenser dew point temperature in Chapter II, the following effects of increasing the condenser dew point temperature were noted:

(1) a decrease in the turbine specific enthalpy change.

(2) a decrease in the net thermodynamic cycle specific work, $\underline{W}_N$.

(3) a decrease in the net thermodynamic cycle efficiency.

(4) a decrease in the condenser specific duty.

Figure 38.0 shows on a temperature-enthalpy diagram the base case (cycle state points 1-2-2'-3-4-4'-1) and case 1 (cycle state points 1-5-5'-6-7-4'-1) for isobutane cycles. The increase in the approach temperature (DTCWO) results in an increase in the working fluid dew point temperature and pressure and turbine outlet temperature as well. Thus, the condenser LMTD increases because of the increase in the approach temperature, DTCWO. The decrease in the net thermodynamic cycle efficiency, η_c, results in an increase in the working fluid flow rate in order to generate a specified net power.

The condenser specific duty, $-\underline{Q}_C$ (Btu/lb of working fluid), decreases for an increase in the condenser LMTD, but since the percentage increase in the working fluid flow rate is larger than the percentage decrease in the condenser specific duty, the condenser duty, $-\dot{Q}_C$ (expressed in Btu/hr), will increase. The brine heat exchanger duty, $\dot{Q}_H$, is inversely proportional to the net thermodynamic cycle efficiency, and will increase. This can be verified by considering the following thermodynamic relations:

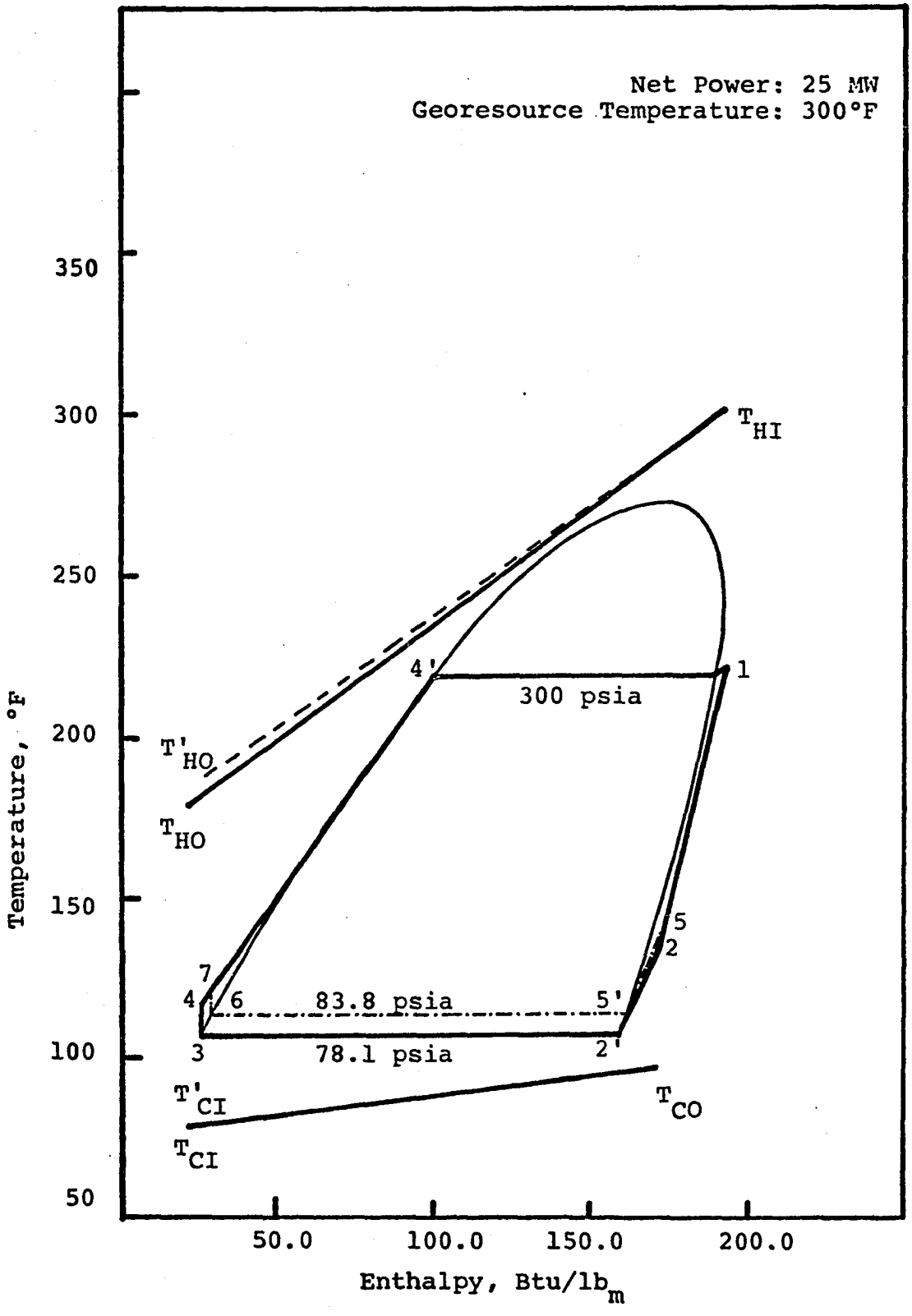

Figure 38.0 Effect of Increasing Condenser LMTD on Isobutane Cycles (Base Case and Case 1)

For the base case

$$\eta_c = \frac{\dot{W}_N}{\dot{Q}_H}$$

or

$$\dot{Q}_H = \frac{\dot{W}_N}{\eta_c} \tag{83}$$

and for case 1

$$\dot{Q}_{H1} = \frac{\dot{W}_{N1}}{\eta_{c1}} \tag{84}$$

$$\frac{\dot{Q}_{H1}}{\dot{Q}_H} = \left[\frac{\dot{W}_{N1}}{\dot{W}_N}\right]\left[\frac{\eta_c}{\eta_{c1}}\right] \tag{85}$$

For fixed net power

$$\dot{W}_{N1} = \dot{W}_N$$

and since

$$\frac{\eta_c}{\eta_{c1}} > 1$$

it follows that

$$\frac{\dot{Q}_{H1}}{\dot{Q}_H} > 1$$

or

$$\dot{Q}_{H1} > \dot{Q}_H \tag{86}$$

For fixed net power, if the brine temperature drop (i.e., $T_{HI} - T_{HO}$) were held constant, then the brine heat exchanger brine flow rate would have to increase because of an increase in the brine heat exchanger duty. The slope of the brine profile can be decreased to compensate for the reduction in LMTD in the compressed liquid section of the brine heat exchanger (caused by the increase in the condensing temperature of the working fluid). Thus, the brine outlet temperature increased from T_{HO} to T'_{HO} in Figure 38.0. The brine heat exchanger surface area requirements will increase due to the increased duty (since the percent changes in the BHE LMTD and overall heat transfer coefficient, U_H, are insignificant).

The condenser LMTD increases more rapidly than does the condenser duty with increasing condensing temperature and this would mean lower surface area requirements for the condenser with the increased LMTD. The net result of increasing condenser LMTD is a reduction in the condenser cost, but an increase in the brine heat exchanger and brine system cost. But since the decrease in the condenser cost is larger than the increase in the brine heat exchanger cost, the power plant cost will decrease.

The total system cost optimum will be determined by

a trade-off between decreasing power plant cost and increasing brine system costs. Table 13 gives a summary of isobutane binary cycles for the base case and case 1 using the GEO4 simulator. For a 5°F increase in the approach temperature difference (DTCWO), the condenser LMTD increased from 18.65°F to 23.86°F (a 28% increase) whereas the condenser duty increased from 7.9866×10^8 Btu/hr to 8.3648×10^8 Btu/hr (a 4.7% increase) and the condenser area decreased from 2.655×10^5 ft^2 to 2.267×10^5 ft^2 (a 14.6% reduction). On the other hand, the brine heat exchanger duty and areas increased by approximately 4.2% and 5.0%, respectively. The total system cost increase was less than 1% due to almost equal changes in the power plant and the brine system cost.

The optimized condenser LMTD's (and approach temperature DTCWO) increase with increasing georesource temperature for a given working fluid,[20] so that there is a trade-off between the heat transfer surface area and LMTD (for a given fluid).

Figure 39.0 (and the analysis required to construct it) demonstrates that an increase in the condenser LMTD, for fixed net plant power (for fixed turbine inlet T,P), always yields a decrease in $\dot{W}_N/\dot{M}_H$. For condenser LMTD below the optimum, increasing condenser LMTD will decrease condenser and total system costs per kw; otherwise the cost per kw will increase.

Table 13

EFFECT OF CONDENSER LOG MEAN TEMPERATURE DIFFERENCE ON CYCLE AND COST PARAMETERS

Process Parameters \ Case No.	Isobutane Cycle	
	Base Case	Case 1
Cycle		
Net Power, MW	25.0	25.0
Gross Power, MW	31.08	31.19
Net Plant Work, Btu/lb_m Brine	11.33	10.68
Net Thermo. Efficiency, %	10.88	10.44
Power Plant Cost, $/kw	864	839
Total System Cost, $/kw	1449	1460
Brine Delivery		
Brine Flow, lb/kw	301.1	319.6
Brine Exit T, °F	182.6	184.7
Brine Delivery Cost, $/kw	585	621
Brine Heat Exchanger (BHE)		
BHE Duty, (10^8 Btu/hr)	8.9613	9.3395
BHE LMTD, °F	36.67	36.27
BHE Load ΔH, Btu/lb_m W.F.	163.6	160.7
BHE Area, 10^4 ft^2	11.08	11.64
BHE Cost, $/kw	264	277
Condenser		
Cond. Duty, (10^8 Btu/hr)	7.9866	8.3648
Cond. LMTD, °F	18.65	23.86
Cond. Superheat ΔT, °F	26.0	24.5
Cond. Dew Point T, °F	108.0	113.
Cond. Dew Point P, psia	78.1	83.8
Cond. Load ΔH, Btu/lb_m W.F.	145.8	143.9
Cond. Area, 10^4 ft^2	26.552	22.669
Cond. Cost, $/kw	345	304
Cooling System		
Cooling Water Flow, lb/kw	1773	1857
Cooling Cost, $/kw	83	85
Turbine		
Turbine Inlet P, psia	300	300
Turbine Inlet T, °F	220	220
Turbine ΔH, Btu/lb	19.37	18.31
Working Fluid Flow, lb/kw	219.	232.5
Turbine-Generator Cost, $/kw	146	146
Cycle Pump		
Parasitic Power	2.51	2.62
Pump Cost, $/kw	26	28

Fixed $\dot{W}_N$

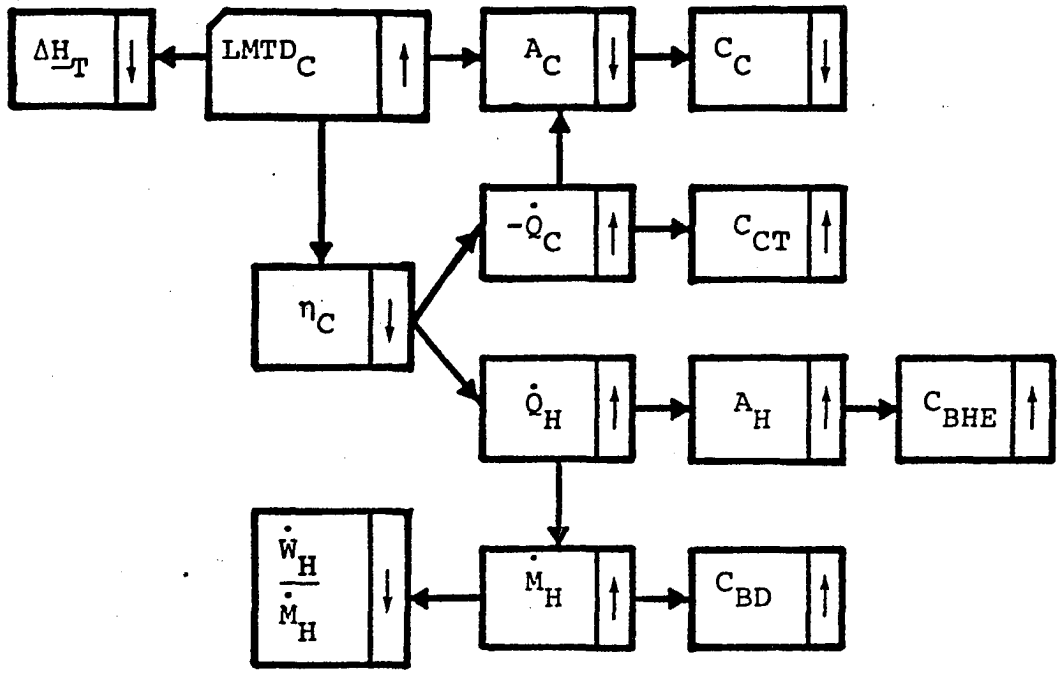

(a)

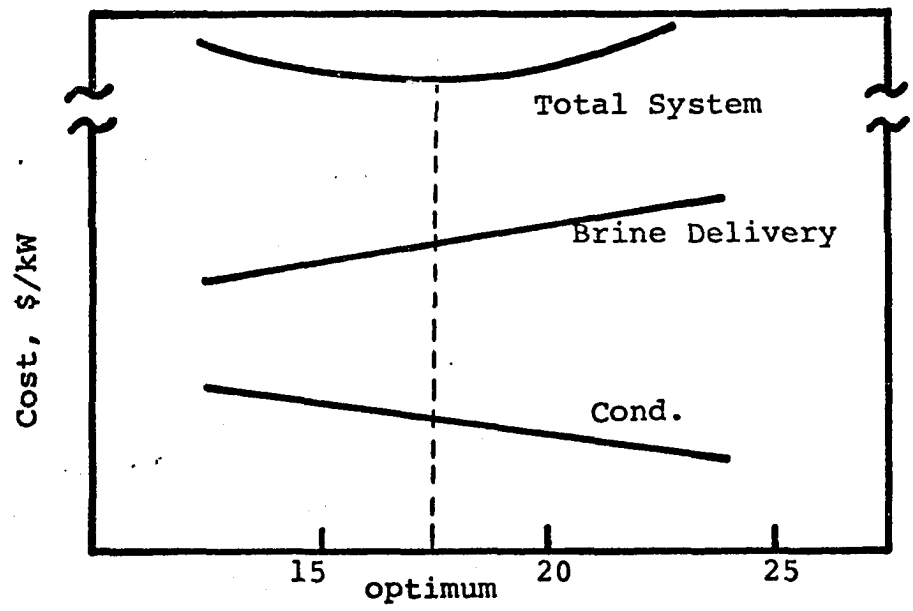

(b) Condenser LMTD Versus Cost in $/kW

Figure 39.0 Effects of Increasing Condenser LMTD (fixed $\dot{W}_N$) on Isobutane Cycle for 300°F Georesource

Cooling Water Temperature Range in Condenser

The cooling water temperature range (or temperature rise as it is sometimes called) in the condenser is primarily a function of the condenser duty and the cooling water flow rate. It is obvious, however, that increasing the cooling water temperature range would decrease cooling water requirements, but would also decrease the gross turbine specific work because of the resultant increase in the turbine outlet pressure (and temperature). The purpose of this discussion is to study the effects of increasing the cooling water temperature range on the process unit operational and equipment parameters and on the total system cost.

The base case isobutane cycle, as considered earlier, is an optimized cycle for 300°F georesource. The optimized cooling range for this isobutane cycle is 18°F for a cooling water condenser inlet temperature of 80°F. A 5°F increase in the cooling water temperature range is used for case 1. Figure 40.0 shows on a temperature-enthalpy diagram the effect of increasing the cooling water temperature range on the cycle state points.

Since increasing the cooling water temperature range in the condenser also increases the working fluid dew point temperature (for fixed approach temperature, DTCWO) in the condenser, the following conclusions can be drawn from the previous section as effects of increasing the cooling water temperature range:

(1) a decrease in the turbine specific enthalpy change.

(2) a decrease in the net thermodynamic cycle

(3) a decrease in the net thermodynamic cycle efficiency

(4) a decrease in the condenser specific duty

(5) a decrease in the brine heat exchanger specific duty (per pound of working fluid).

From Figure 40.0 it is evident that because of the increase in the working fluid bubble point temperature in the condenser, the approach temperature DTCWI has increased. Thus, the condenser LMTD will increase because of the increase in DTCWI. The decrease in the net thermodynamic cycle efficiency (for fixed net plant power) will have the following effects:

(1) an increase in the working fluid flow rate

(2) an increase in the brine heat exchanger duty, $\dot{Q}_H$.

(3) an increase in the condenser duty, $-\dot{Q}_C$.

(4) an increase in the brine flow rate, and a decrease in the net plant specific work expressed in Btu/lb_m brine.

The brine heat exchanger surface area (and cost) will increase because of the increase in the brine heat exchanger duty. On the other hand, the condenser surface

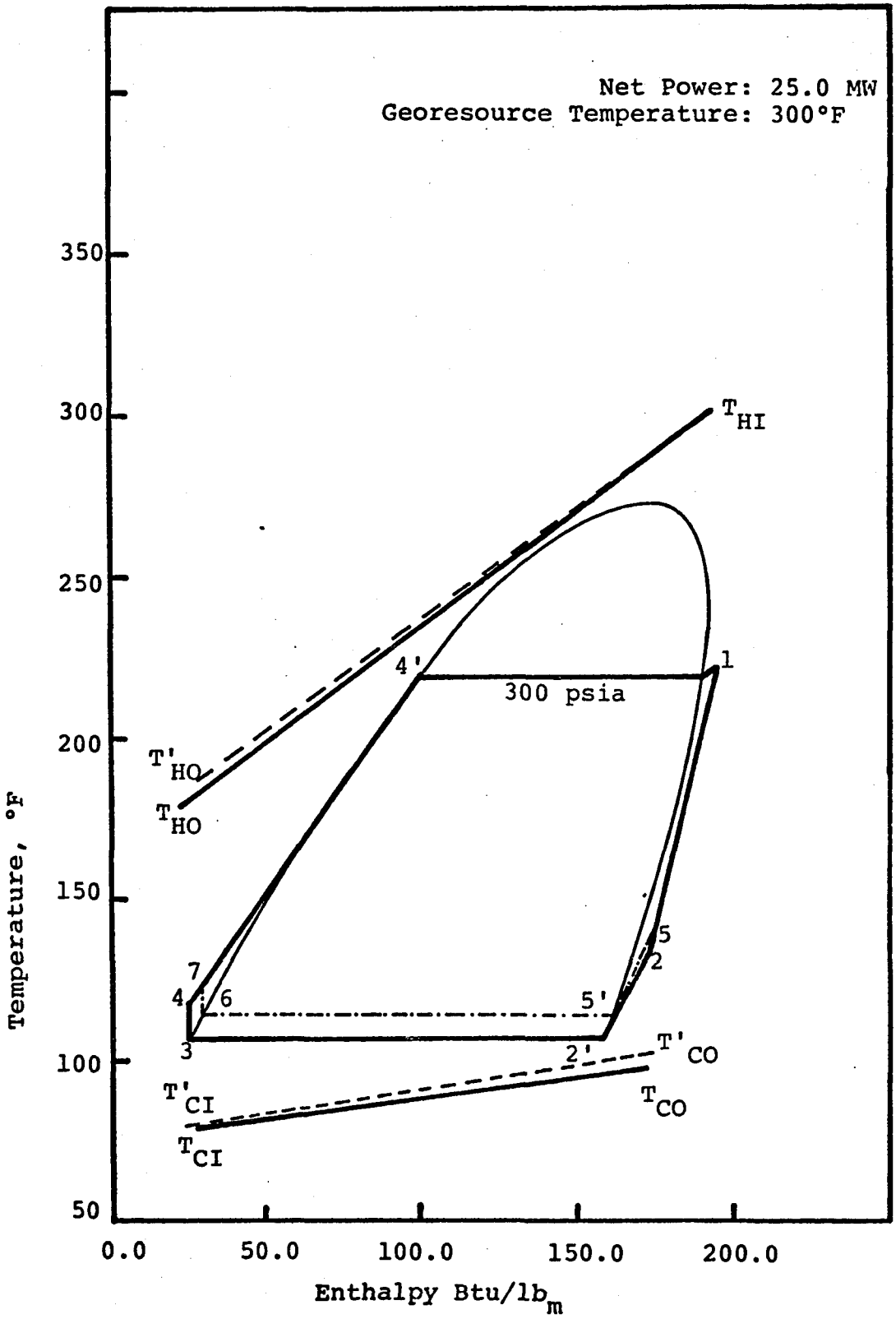

Figure 40.0 Effect of Increasing Cooling Water Temperature Range on Isobutane Cycles (Base Case and Case 1)

area will decrease because the percent increase in the condenser LMTD is larger than the percent increase in the condenser duty. Even though there is a slight increase in the condenser cost rating in $\$/ft^2$ of surface area due to an increase in the working fluid due point pressure in the condenser, the condenser cost will decrease due to a decrease in the condenser area.

The cooling system cost (cooling tower plus parasitic power system requirements) will decrease sharply due to a decrease in the cooling water flow rate. The optimum power plant cost is therefore obtained in a trade-off between the decreasing condenser and cooling system cost and the increasing brine heat exchanger cost. This cost trade-off is governed by another trade-off between the two important parameters, the cooling water temperature range and the turbine exhaust pressure. If the cooling water temperature range is removed (i.e., increased) from the cost optimum value the cooling system and condenser costs will decrease sharply than the increase in the brine heat exchanger cost and therefore the power plant cost will decrease. Conversely, the power plant cost will increase for a decrease in the cooling water temperature range from the optimum value.

The brine system cost will increase or decrease according to the decrease or increase in the net thermodynamic cycle efficiency. The total system cost will therefore depend on the percent changes in the power plant and brine system costs.

Table 14 provides a summary of isobutane cycle calculations using the GEO4 simulator. For a 5°F increase in the cooling water range, the condenser LMTD increased from 18.6°F to 20.6°F (an increase of 10.5%), the cooling water flow requirements decreased from 1773 lb_m/kw to 1438 lb_m/kw (a decrease of approximately 19%), the condenser duty increased by only 3%, resulting in decreased condenser surface area and cost by 6.4% and 3.5%, respectively. The brine heat exchanger duty increased by 3% whereas the BHE LMTD actually decreased from 36.67°F to 36.27°F (a decrease of approximately 1%), the net result being an increase in BHE area and cost of roughly 3.8% in both. The brine system cost increased by approximately 5%. The power plant cost decreased by approximately 1.8%. The total system cost increased by 0.9% for a 5°F increase in the cooling water range.

Figure 41.0 summarizes the analysis of the cooling water temperature range increase. This diagram demonstrates that for an increase in the cooling water temperature range (for fixed net plant power and for fixed turbine inlet T,P) always yields a decrease in $\dot{W}_N/\dot{M}_H$. Increasing cooling water temperature range below the optimum decreases the total system cost per kw, otherwise the cost per kw increases.

Brine Flow Rate

Geothermal brine flow rates and temperatures are extremely site specific, but for particular geothermal

Table 14

EFFECT OF COOLING WATER TEMPERATURE RANGE
ON CYCLE AND COST PARAMETERS

Case No. / Process Parameters	Isobutane Cycle	
	Base Case	Case 1
Cycle		
Net Power, MW	25.0	25.0
Gross Power, MW	31.08	31.71
Net Work, Btu/lb_m Brine	11.33	10.80
Net Thermo. Efficiency, %	10.88	10.39
Power Plant Cost, $/kw	864	848
Total System Cost, $/kw	1449	1462
Brine Delivery		
Brine Flow, lb/kw	301.1	315.9
Brine Exit T, °F	182.6	184.7
Brine Delivery Cost, $/kw	585	614
Brine Heat Exchanger (BHE)		
BHE Duty, 10^8 Btu/hr	8.9613	9.2336
BHE LMTD, °F	36.67	36.27
BHE Load ΔH, Btu/lb_m W.F.	163.6	160.7
BHE Area, 10^4 ft^2	11.08	11.508
BHE Cost, $/kw	264	274
Condenser		
Cond. Duty, 10^8 Btu/hr	7.9866	8.2741
Cond. LMTD, °F	18.6	20.6
Cond. Dew Point T, °F	108.	113.
Cond. Dew P	78.1	83.8
Cond. Load ΔH, Btu/lb_m W.F.	145.8	144.01
Cond. Area, 10^4 ft^2	26.552	24.846
Cond. Cost, $/kw	345	333
Cooling System		
Cooling Water Flow, lb/kw	1773	1438
Cooling Pumping Power, MW	2.22	1.92
Cooling Cost, $/kw	83	69
Turbine		
Turbine Inlet P, psia	300	300
Turbine Inlet T, °F	220	220
Turbine ΔH, Btu/lb_m W.F.	19.37	18.24
Working Fluid Flow, lb_m/kw	219.	229.8
	146	144
Cycle Pump		
Cycle Pump Power, MW	2.51	2.60
Cycle Pump Cost, $/kw	26	27

Fixed $\dot{W}_N$, T_{CI}

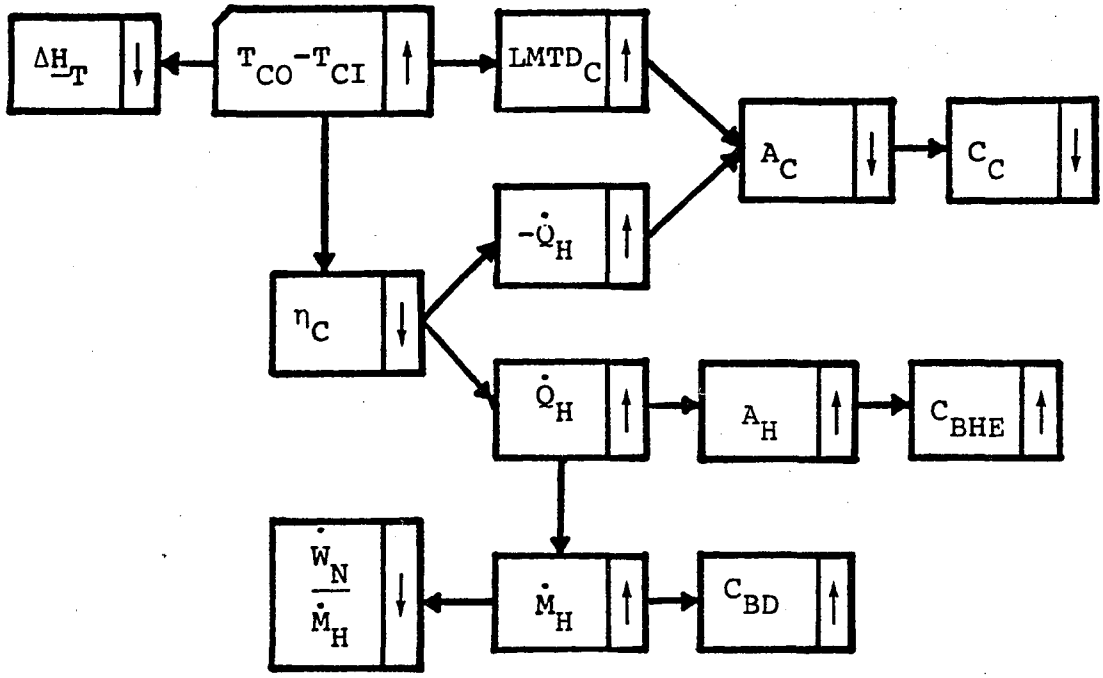

(a)

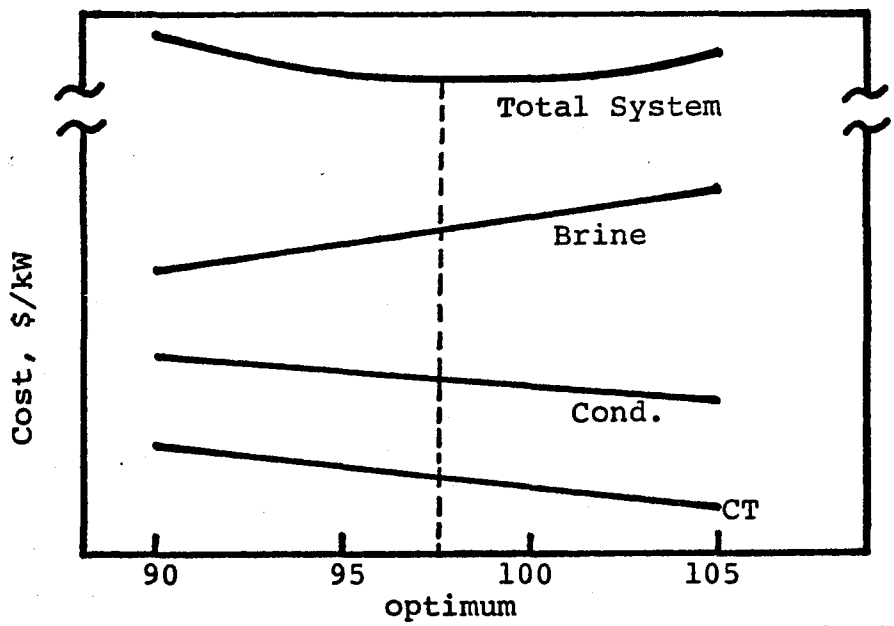

(b)

Figure 41.0 Effects of Cooling Water Temperature Range (for fixed $\dot{W}_N$) on Isobutane Cycle for 300°F Georesource

producing areas, the optimum brine flow rates required to produce a specified net power using the binary cycle will depend (for a given working fluid) on the choice of the objective function and the sink conditions. The objective function commonly used by industry is the minimization of the total system cost in dollars per kilowatt of the specified net plant power. The brine flow rate analysis can be carried out to perform the following tasks:

(1) Analysis of the effect of brine flow rate on net power (for fixed brine heat exchanger and condenser surface areas).

(2) Cost of optimization of brine flow rate for a given georesource temperature and a given working fluid and for a specified net power.

The studies relating to the second task were carried out earlier at the University of Oklahoma,[20] and indicate that cost optimized brine flow rates generally increase with increasing molecular weight for paraffinic hydrocarbon working fluids (isobutane in isopentane) and decrease with increasing georesource temperature. The behavior of brine flow rate for isobutane binary cycles, cost optimized ($/kw) for various georesource temperatures, was shown in a previous section in Figure 35.0. It may be mentioned here that the net extractable energy in the brine decreases sharply at the lower georesource temperatures, so that large brine flow rates are needed to generate the specified net power.

The purpose of this discussion is to analyze task I, since such an analysis should benefit the operator of the geothermal binary cycle power plant. The objective function is, therefore, the maximization of the net plant power. In this small study, however, no attempt is made to determine the optimum brine flow rate for the generation of maximum net plant power. Instead, this study is directed toward the understanding of the effects of increasing the brine flow rate on the binary cycle power plant operating conditions, the net power, and the performance of power plant equipment.

Brine Flow Rate and Brine Heat Exchanger

For a given working fluid, an increase in brine flow rate (for fixed heat transfer area) will result in higher brine heat exchanger duty and larger BHE LMTD's. Consider for example

the base case:

$$\dot{Q}_H = U_H \, A(LMTD)_H \tag{87}$$

and the case of increased brine flow rate, i.e., Case 1:

$$\dot{Q}_{H1} = U_{H1} \, A(LMTD)_{H1} \tag{88}$$

so that

$$\frac{\dot{Q}_{H1}}{\dot{Q}_H} = \left[\frac{U_{H1}}{U_H}\right]\left[\frac{A}{A}\right]\left[\frac{(LMTD)_{H1}}{(LMTD)_H}\right] \tag{89}$$

Since BHE areas have been assumed fixed, the overall heat transfer coefficients can also be assumed constant. Therefore, since $\dot{Q}_{H1} > \dot{Q}_H$, it follows that

$$\frac{(LMTD)_{H1}}{(LMTD)_H} > 1$$

so that

$$(LMTD)_{H1} > (LMTD)_H \tag{90}$$

which verifies the statement made earlier. It may be mentioned here again that by fixing the heat transfer surface area, the power plant operation can be approximated as a fixed plant operation. Since the original heat exchange equipment was designed for some optimum fluid velocities, the increase in the brine (or working fluid) flow rate can only be handled in the plant by higher fluid velocities. This would mean increased parasitic power requirements. Moreover, the working fluid and cooling water flow rates will increase due to increased brine heat exchanger and condenser duties. The condenser duty will increase due to the decrease in the net thermodynamic cycle efficiency of the cycle caused by increased parasitic power requirements.

However, the brine heat exchanger duty will increase more rapidly than the condenser duty, resulting in an increase in net plant power output. The condenser log mean temperature difference also will increase due to an increase in the condenser duty, $-\dot{Q}_c$. To prove this, compare the base case

$$- \dot{Q}_c = U_c \, A_c (LMTD)_c \tag{91}$$

and case 1

$$-\dot{Q}_{c1} = U_{c1} \, A_c \, (LMTD)_{c1} \tag{92}$$

to note

$$\frac{(LMTD)_{c1}}{(LMTD)_c} = \left[\frac{-\dot{Q}_{c1}}{-\dot{Q}_c}\right]\left[\frac{U_c}{U_{c1}}\right]\left[\frac{A_c}{A_c}\right]$$

But

$$-\dot{Q}_{c1} > -\dot{Q}_c$$

and

$$U_{c1} \simeq U_c$$

so that

$$\frac{(LMTD)_{c1}}{(LMTD)_c} > 1$$

and therefore

$$(LMTD)_{cl} > (LMTD)_{c} \tag{93}$$

Since the cooling water temperature range is fixed, the only way the condenser LMTD can increase (for pure isobutane) is by increasing the approach temperature at the working fluid dew point, DTCWO. The increase in the approach temperature, DTCWO, would mean a reduction in the turbine specific work due to the increase in the turbine outlet pressure. However, the turbine gross power will increase due to the larger amount of working fluid which will have to be circulated in order to receive the additional energy from the increased brine flow rate. In order to check these conclusions, fixed plant type simulations (only heat transfer surface areas are fixed) were performed using a modified GEO4 simulator, the details of which are provided in Appendix B. However, there are some other features of this modification which need to be mentioned here in order to understand the simulation results. First of all, only one heat exchanger subroutine (using the single-phase heat transfer correlation) and one condenser subroutine (using the condensing heat transfer correlation) are used regardless of the turbine inlet pressure (whether subcritical or supercritical). This means that for subcritical cycles, the heat exchanger and condenser must be divided into a large number of sections (with respect to temperature) in the order to obtain reasonable results. In GEO4 simulator, the number of sections

are controlled by input parameters, so that a maximum of 75 heat exchanger sections and a maximum of 20 condenser sections can be used.

The isobutane cycle base case considered in previous sections was chosen for this study. However, the base case calculations were revised using heat transfer surface areas from the base case. The brine flow rate also was fixed at 7.5284×10^6 lb_m/hr. Since only the single phase heat transfer correlation in brine heat exchanger is used, and working fluid flow rate cannot be fixed in the simulator, the values of the heat transfer coefficient and net power are slightly in error. On the other hand, the increased brine flow rate care (case 1) can also be considered in slight error. If the error is in the same direction for both the cases (i.e., positive or negative), then it can be argued that the conclusions drawn from this analysis will be valid.

Figure 42.0 shows on a temperature-enthalpy diagram the effect of increasing the brine flow rate on the cycle state points. The brine flow rate was increased by 10% from the base case. Table 15 provides the results from the fixed plant simulator for the revised base case and case 1. It is evident from Table 15 and Figure 42.0 that the increase in the brine flow rate resulted in an increased condenser dew point temperature and pressure and a slightly higher brine outlet temperature. The turbine specific enthalpy change decreased by approximately 1.8%, the net power increased from

Table 15

EFFECT OF BRINE FLOW RATE ON THE CYCLE PARAMETERS AND COST

Process Parameters \ Case No.	Isobutane Cycle	
	Rev. Base Case	Case 1
Cycle		
Net Power, MW	24.57	25.58
Gross Power, MW	30.45	32.22
Net Plant Work, Btu/lb_m Brine	11.14	10.54
Net Thermo. Efficiency, %	10.88	10.72
Brine Delivery		
Brine Flow, lb/kw	306.3	323.7
Brine Exit T, °F	184.7	187.7
Brine Pump Power, MW	0.504	0.678
Brine Heat Exchanger		
BHE Duty, 10^8 Btu/hr	8.7906	9.4234
BHE LMTD, °F	39.96	41.4
BHE Load ΔH, Btu/lb_m W.F.	164.4	163.6
BHE Area, 10^4 ft^2	11.124	11.119
BHE Overall U_H, Btu/hr ft^2 °F	200	205
Condenser		
Cond. Duty, 10^8 Btu/hr	7.8337	8.4125
Cond. LMTD, °F	17.75	19.10
Cond. Superheat ΔT, °F	25.6	25.2
Cond. Superheat ΔH, Btu/lb	12.0	11.83
Cond. Load ΔH, Btu/lb_m W.F.	146.5	146.02
Cond. Overall U_C, Btu/hr ft^2 °F	167	165
Cond. Dew Point T, °F	108.1	109.1
Cond. Cost, $/kw		
Cooling System		
Cooling Water Flow, lb/kw	1769	1825
Cooling Water Pump Power, MW	2.14	2.48
Turbine		
Turbine Inlet P, psia	300	300
Turbine Inlet T, °F	220	220
Turbine ΔH, Btu/lb_m W.F.	19.44	19.09
Working Fluid Flow, lb/kw	217.6	225.3

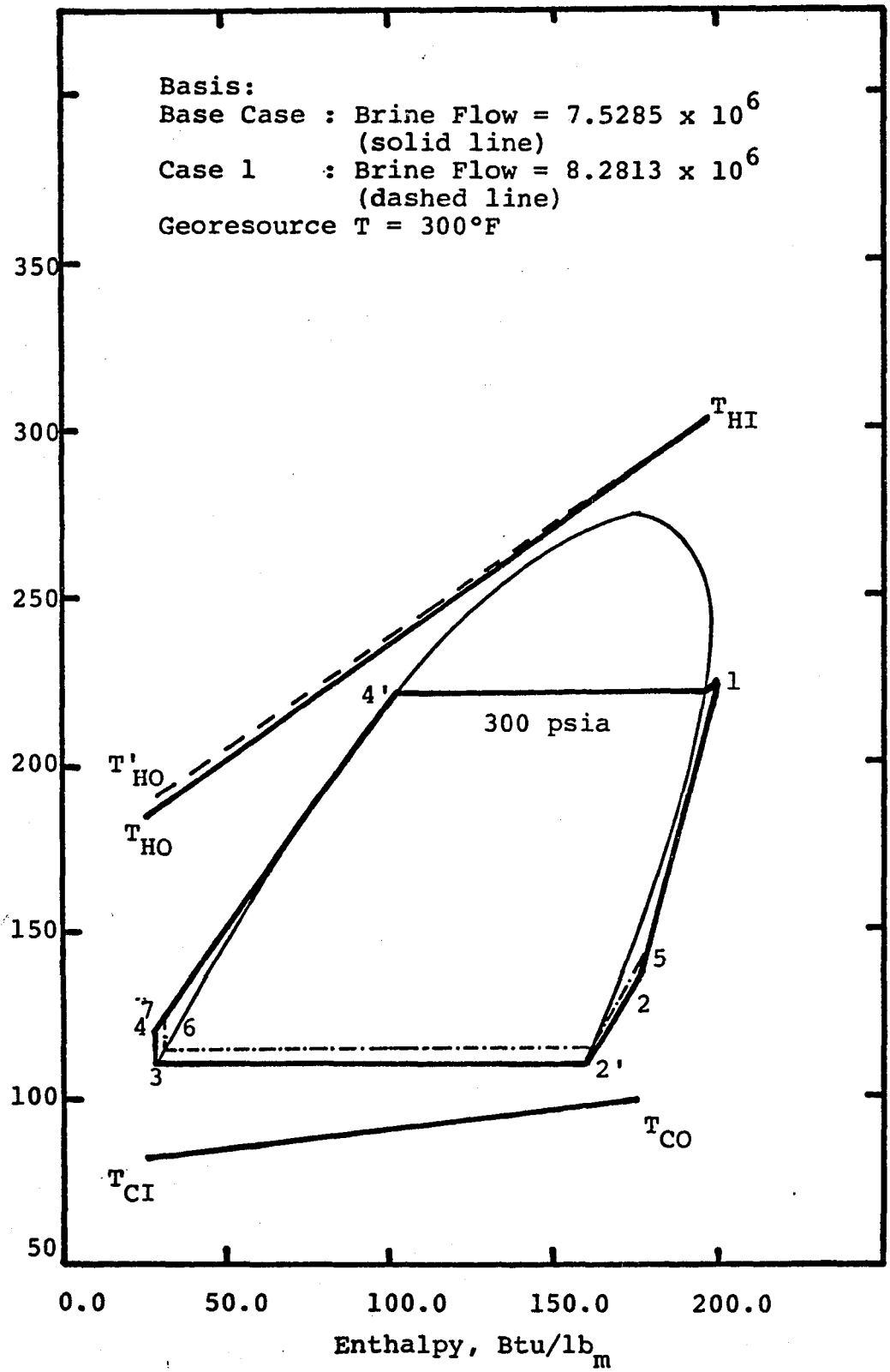

Figure 42.0 Effect of Increasing Brine Flow Rate on Isobutane Cycles (Revised Base Case and Case 1)

24.57 MW to 25.584 MW (a 4.1% increase), the net thermodynamic cycle efficiency decreased from 10.88% to 10.72% (a mere 1.4% decrease). However, the brine heat exchanger and condenser duties increased by 7.2% and 7.4% respectively. Even though the percent increase in condenser duty is higher than the brine heat exchanger duty, the magnitude of increase in brine heat exchanger duty is higher than that of condenser duty.

If there is no provision in the geothermal power plant to increase the working fluid flow rate (i.e., to increase the working fluid velocity), then the increase in the brine flow rate will result in an additional amount of superheat in the working fluid at the working fluid exit of the BHE. Of course, this implies here that the residence time of brine and working fluid are assumed to be sufficient for complete heat transfer between them. If the residence time is not sufficient, then the brine exit temperature will further increase resulting in even more decreased utilization of the georesource. Assuming sufficient residence time for both fluids, the working fluid superheat at brine heat exchanger working fluid exit will mean additional superheat at the turbine inlet and a corresponding amount of superheat at turbine exhaust. The turbine specific work will increase due to the increase in the turbine inlet temperature. The increase in the brine flow rate would then mean a reduction in the net thermodynamic cycle efficiency (due to exessive

amount of superheat at the turbine inlet and exit). The overall results would be similar to the conclusions drawn earlier in this section.

Figure 43.0 shows the effects of increasing the brine flow rate in a fixed plant (fixed heat transfer areas of brine heat exchanger and condenser) operation. Figure 43.0 demonstrates that an increase in the brine flow rate (for fixed A_H and A_C) beyond the optimum flow rate will always yield a decrease in $\dot{W}_N/\dot{M}_H$.

Fixed A_H, A_C

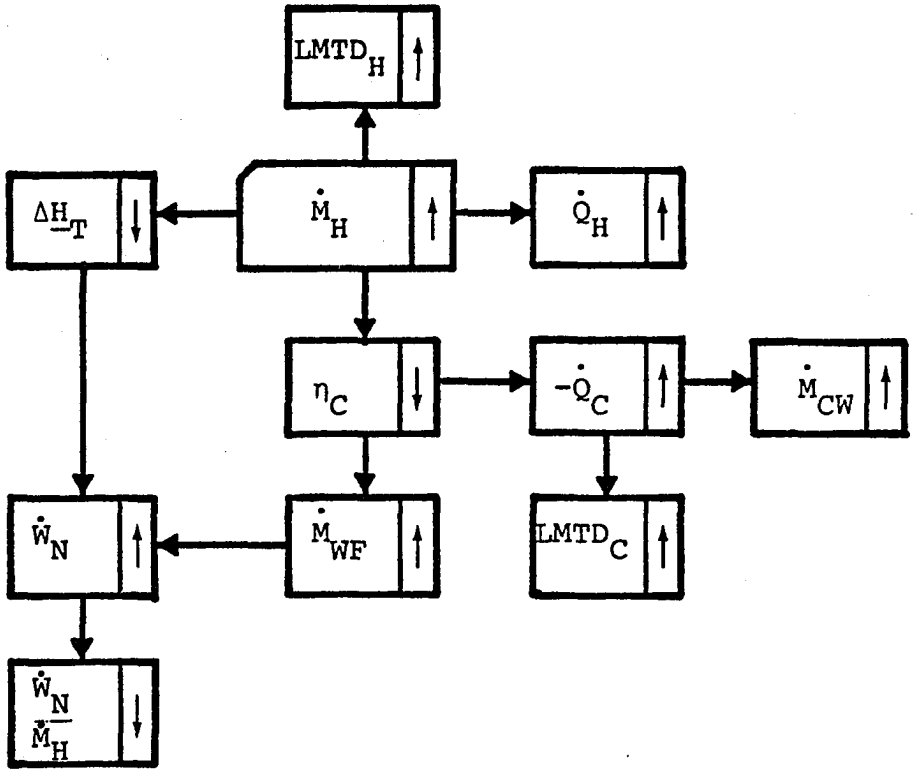

(a)

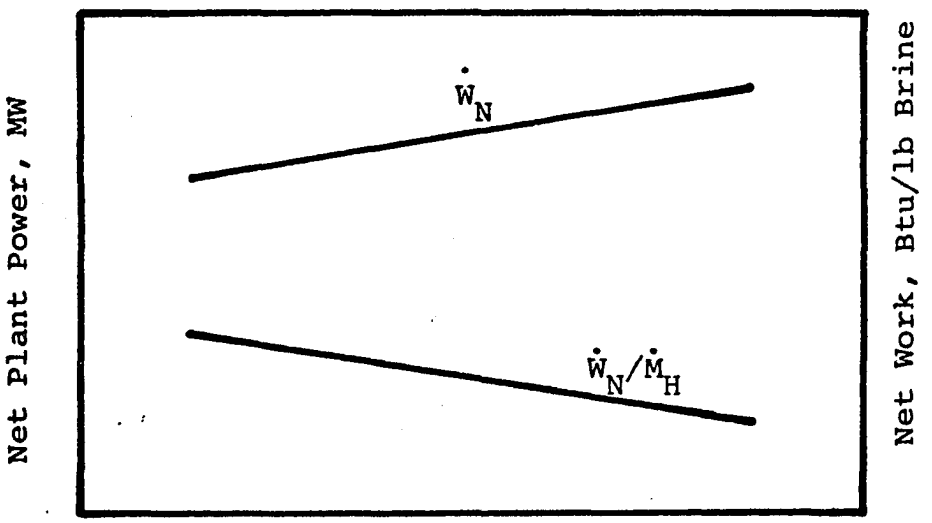

(b)

Figure 43.0 Effects of Increasing Brine Flow Rate (For Fixed A_H and A_C) on Isobutane Cycle for 300°F Georesource

CHAPTER V

ADVANTAGES AND DISADVANTAGES OF THE USE OF MIXTURES IN GEOTHERMAL BINARY CYCLES

The use of hydrocarbon mixture working fluids in the conventional geothermal binary cycle has been advocated in research carried out at the University of Oklahoma[7,26,27]; however, only isobutane-isopentane binary mixtures were considered in these studies. This study broadens the scope of investigation to other hydrocarbon systems (pure fluids and mixtures) and the use of these systems in cascade (multi-boiler) binary cycles. Advantages and disadvantages of the use of mixtures in the geothermal binary cycles are summarized.

A fixed plant simulator, the discussion of which is provided in Appendix B, was used in a preliminary study of the effects of georesource temperature decline on the performance of the pure and mixture binary cycles. A scoping study was also carried out for the hardware(equipment) evaluation of mixtures in the geothermal binary cycle.

Major Differences Between Pure and Mixture Fluid Cycle Parameters

The purpose of this discussion is to point out the major differences between pure and mixture fluid cycle parameters. Isobutane-iospentane mixture cycles are compared with pure isobutane and pure isopentane cycles on temperature-entropy (T-s) diagrams for supercritical cycles in Figure 44.0 and subcritical cycles in Figure 45.0. Reversible cycles are shown to simplify the analysis and diagrams; irreversible behavior is similar.

The important behavioral characteristics of mixtures compared to the pure fluids can be noted in Figures 44.0 and 45.0 as follows:

(1) At a constant pressure, mixtures condense nonisothermally whereas pure fluids condense isothermally.

(2) At a constant pressure, mixtures vaporize nonisothermally whereas pure fluids vaporize isothermally.

(3) The binary mixture condensation pressure lies between the condensation pressures of the constituent pure fluids (for a given dew point temperature).

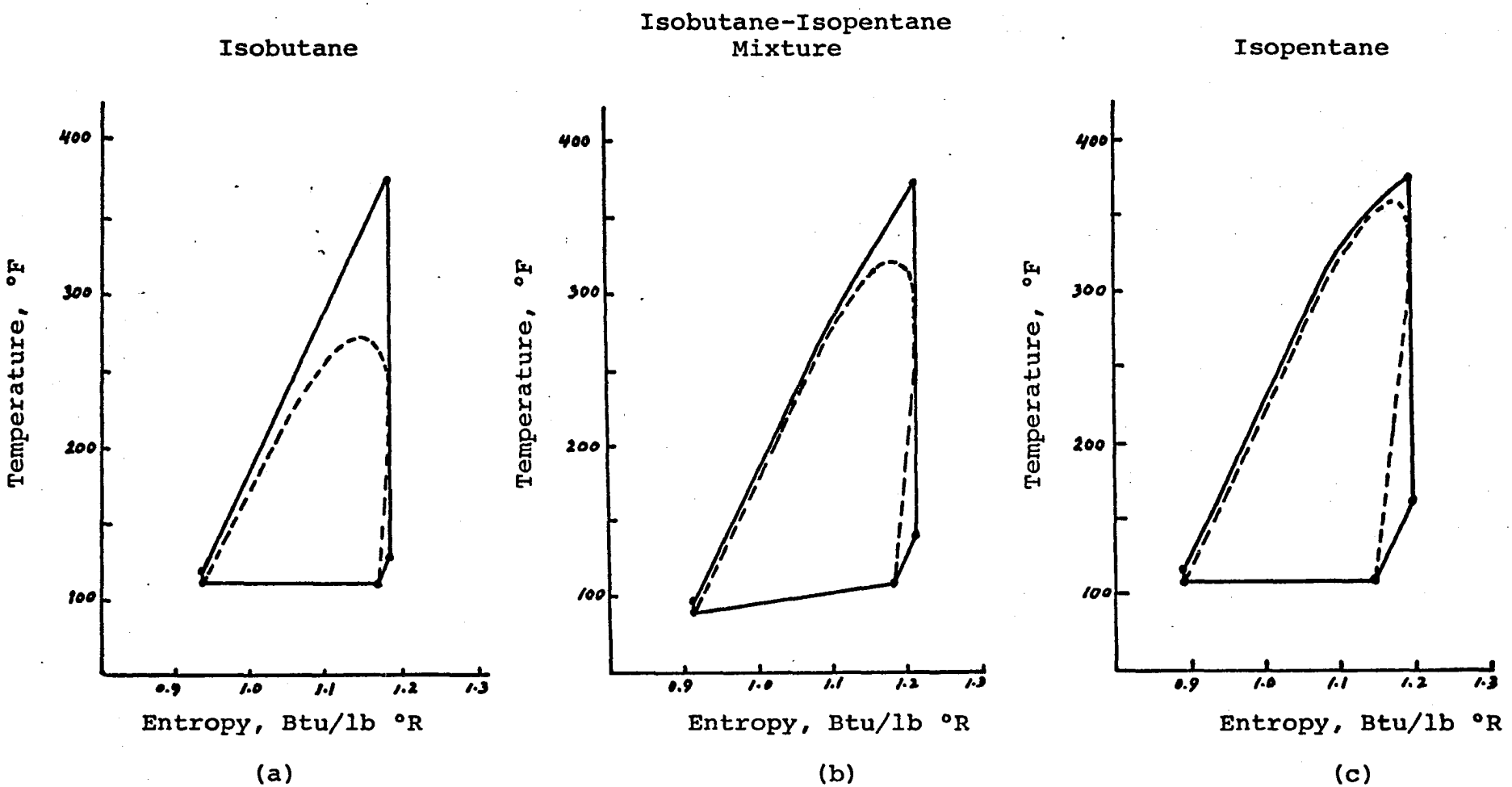

Figure 44.0 Supercritical Cycles

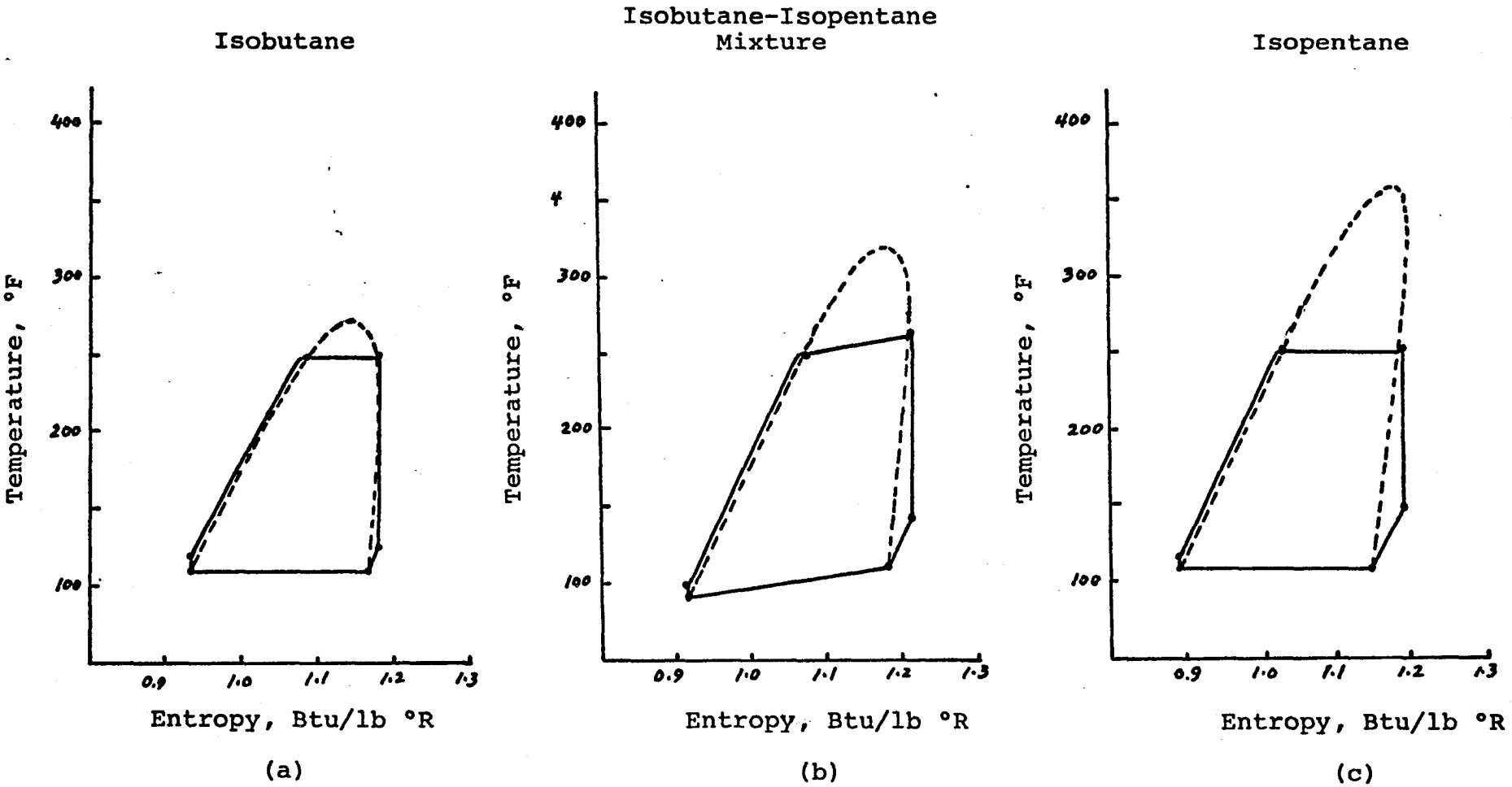

Figure 45.0 Subcritical Cycles

(4) The binary mixture turbine exit superheat lies between the turbine exit superheats of the constituent pure fluids (for a given dew point temperature).

(5) The cost optimized turbine inlet pressures for mixture binary cycles lie between the turbine inlet pressures of the constituent pure fluids (for a given georesource temperature and specified net power).[20]

(6) The cost optimized brine heat exchanger and condenser LMTD's lie between the LMTD's of the constituent pure fluids (for a given georesource temperature and specified net power).

The first two behavioral characteristics are of primary importance when process and economic considerations are ignored, i.e., when only thermodynamic optimization is considered. The latter four behavioral characteristics are of primary importance when process and economic factors are considered. However, when process and economic considerations are ignored, a large fraction of the availability in the resource brine can be converted to power, as was pointed out previously.

Advantages and Disadvantages of Mixtures

The use of mixtures as working fluids in geothermal binary cycles provides certain advantages over cycles using

pure component working fluids. In most of the studies carried out at the University of Oklahoma, the comparisons of mixture and pure fluid cycles have ignored mass transfer effects. Ignoring mass transfer effects the heat transfer coefficients, obtained through the use of standard heat transfer correlations, are virtually equal for similar mixture and pure fluid cycles in these studies. The purpose of this discussion is to provide some understanding of the expected mass transfer effects on mixture binary cycles, and to show the advantages of mixtures in specific terms.

Basis of Comparison

For comparing various working fluid binary cycles, a common basis is needed to draw meaningful conclusions. In the cost optimization studies, carried out for single boiler binary cycles, the total system cost expressed in dollars per kilowatt net plant electrical output (25.0 MW for this study) was chosen as the basis. Other design basis engineering parameters are given in Appendix A. In the preliminary study of cascade (or multi-boiler) binary cycles, the basis of comparison is the net thermodynamic cycle work per unit mass of brine (for a specified brine flow rate, 1.04×10^6 lb_m/hr).

Single Boiler Conventional Binary Cycle

The GEO4 simulator was used in all the calculations carried out for the single boiler conventional binary cycle. In this study, only binary mixtures of isobutane and isopentane are considered, for comparison with pure isobutane and pure isopentane cycles. To simplify the analysis, only one equimolar mixture of isobutane and isopentane is used here. The temperature of the resource brine chosen for the cost optimization study was 300°F and net plant power was specified to be 25.0 MW. A comparison between mixture and pure fluid cycle state points is given in Figure 46.0 on a superimposed temperature-enthalpy diagram for isobutane and the equimolar isobutane-isopentane mixture cycles for the case of the 300°F georesource temperature. The turbine inlet temperature and enthalpy for the mixture are both considerably higher than for isobutane. However, the mixture also has greater superheat and a higher enthalpy than isobutane at the turbine exit. Because the gain at the turbine inlet exceeds the loss at the turbine exit, the mixture cycle yields more gross turbine work per unit mass of working fluid than the isobutane cycle.

For the equimolar mixture of isobutane and isopentane, the turbine exit superheat would be greater than for isobutane and less than for isopentane. Thus, the overall

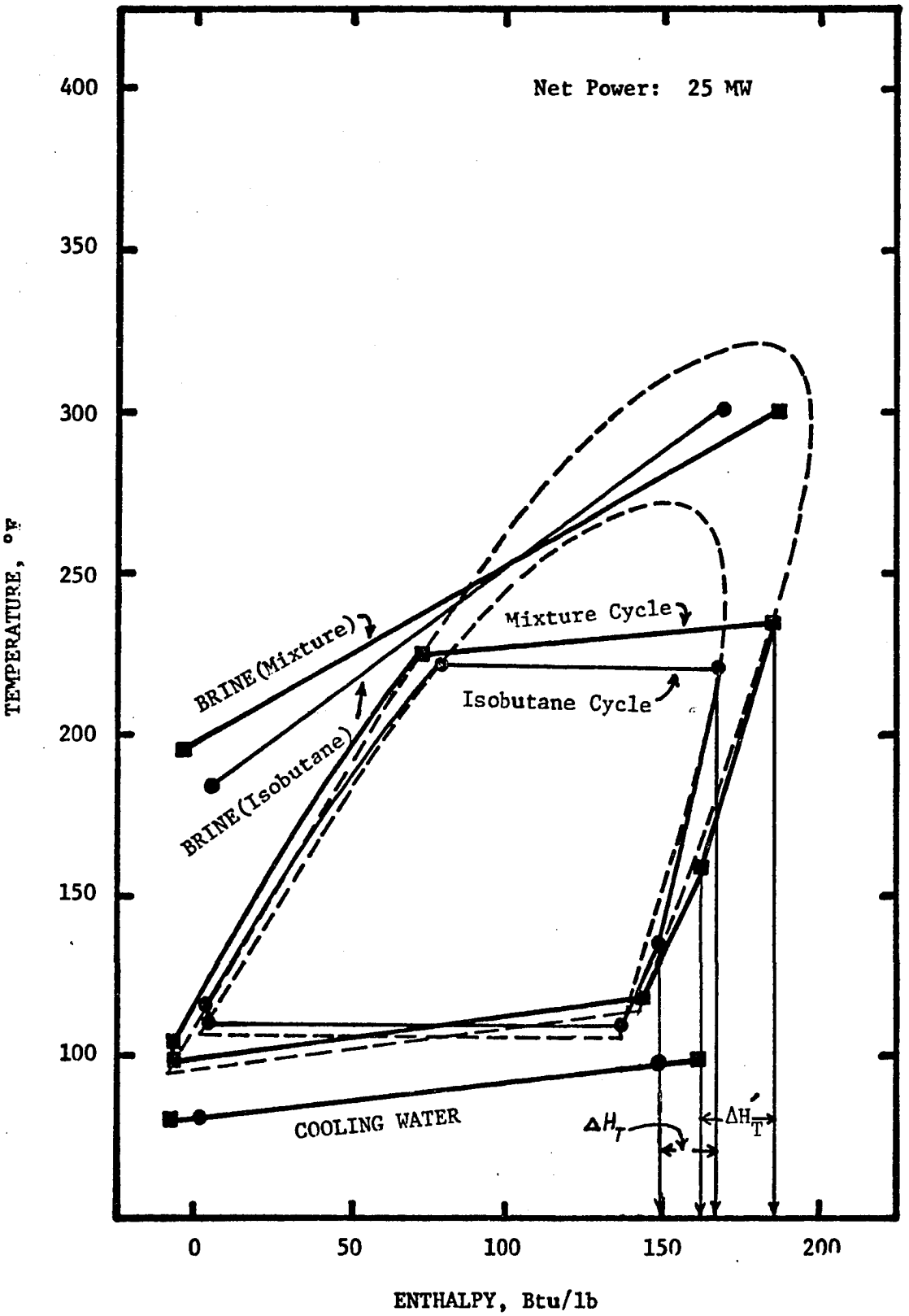

Figure 46.0 Superimposed Temperature-Enthalpy Diagram of Isobutane and Mixture (50% isobutane-50% isopentane) Cycle

condenser LMTD for the binary mixture would be between the pure fluid cycle condenser LMTD's. With respect to the brine heat exchanger, the near optimal LMTD for isopentane is lower than for isobutane. This is because the turbine inlet pressure to achieve a given turbine inlet temperature is smaller for isopentane than isobutane (by a factor of about one third), leading to lower brine heat exchanger cost per unit area and a smaller LMTD for the isopentane cycle. This lower cost per unit heat transfer surface area for the brine heat exchanger also allows a larger brine exit temperature for the economic optimum for the isopentane cycle. For the equimolar mixture of isobutane and isopentane, the near optimal brine heat exchanger LMTD's and brine exit temperatures fall between the pure fluid cycle values. It is interesting to note that the bubble point temperature of the working fluid in the BHE is virtually independent of working fluid composition (withing a few degrees F) for a given georesource temperature (Figure 46.0). The fact that the isobutane-isopentane mixture vaporization curve is nonisothermal then yields a larger enthalpy at the turbine inlet than would be obtained for pure isobutane (Figure 46.0).

Thus, the larger enthalpy change across the turbine for the mixture cycle results in a larger net thermodynamic cycle specific work and higher net thermodynamic cycle efficiency, η_c, compared to pure isobutane or pure isopentane.

The increase in η_c implies a lower working fluid flow rate per unit brine flow rate for the mixture cycle. By lowering the working fluid to geothermal brine flow ratio, process equipment sizes and parasitic power requirements are reduced.

The cost advantages of mixtures considered here can be explained by referring to the effect of mixture properties on binary cycle operating conditions as noted in Table 16. By increasing the working fluid molecular weight (adding isopentane to isobutane) the dew point pressure is decreased below that of isobutane. This means that the condenser cost can be reduced compared to isobutane. The lower brine heat exchanger operating pressure compared to isobutane also permits a slightly lower required condenser operating pressure compared to isobutane to achieve a given net power output for the mixture cycles.

The quantity of cooling water required is smaller for the mixture cycle than the isopentane cycle because the turbine exit superheat for the mixture is smaller than for isopentane; mixture cycle cooling water requirements are smaller than the isobutane cycle because of larger cooling water rise in the condenser for the mixture cycle. The turbine-generator cost for the mixture cycle is lower than the isopentane cycle primarily because of the greater turbine enthalpy change and lower volumetric flow rate for the mixture cycle.

Table 16

COMPARISON OF PURE FLUID AND MIXTURE FLUID CYCLE PARAMETERS FOR THE GEORESOURCE TEMPERATURE OF 300°F

Process Parameters \ Fluid	Isobutane	Mixture: Isobutane - 50% Isopentane - 50%	Isopentane
Cycle			
Net Power, NW	25.00	25.00	25.00
Gross Power, MW	31.08	29.78	29.92
Net Plant Work, Btu/lb Brine	11.35	10.54	9.68
Net Thermo. Efficiency, %	10.80	11.02	10.28
Power Plant Cost, $/kw	864	775	819
Total System Cost, $/kw	1449	1405	1504
Brine Delivery			
Brine Flow, lb/kw	301.	323.8	352.6
Brine Exit T, °F	182.6	193.1	192.0
Brine Delivery Cost, $/kw	585	629	685
Brine Heat Exchanger (BHE)			
BHE LMTD, °F	36.7	35.3	37.8
BHE Load ΔH, Btu/lb_m W.F.	163.6	189.2	180.2
BHE Cost, $/kw	264	229	191
Condenser			
Cond. LMTD, °F	18.6	20.7	21.8
Cond. Superheat ΔT, °F	26.0	39.8	43.2
Cond. Superheat ΔH, Btu/lb	11.95	18.12	18.97
Cond. Dew Point T, °F	108.0	119.3	109.0
Cond. Dew Point P, psia	78.1	43.7	23.6
Cond. Load ΔH, Btu/lb_m W.F.	145.8	168.3	161.6
Cond. Cost, $/kw	345	278	236
Cooling System			
Cooling Water Flow, lb/kw	1773	1562	2164
Cooling Cost, $/kw	83	52	72
Turbine			
Turbine Inlet P, psia	300	200	100
Turbine Inlet T, °F	220	235	210
Turbine ΔH, Btu/lb_m W.F.	19.37	21.90	19.05
Working Fluid Flow, lb/kw	219.	185.7	214.4
Exhaust Vol. Flow, ft^3/min/kw	4.5	6.6	12.6
Turbine-Generator Cost, $/kw	146	177	283
Cycle Pump			
Parasitic Power, MW	2.51	1.414	0.845
Pump Cost, $/kw	26	16	10

Cascade Binary Cycle

This study was made primarily for the Idaho National Engineering Laboratory for the low temperature brine available at the proposed Raft River 5-MW geothermal pilot plant dual boiler binary cycle plant.[3] The purpose of the study was the selection of a working fluid and suitable operating conditions for maximizing the net plant work per unit mass of brine in the Raft River geothermal dual boiling (cascade) binary cycle. Since it is believed that mixtures offer possible advantages over pure fluids for use as working fluids in cascade binary cycles, both pure fluids and mixtures are considered as working fluids in this study.

In the absence of a cascade binary cycle simulator, a simplified procedure for evaluation of the dual boiler binary cycle was developed. This procedure, outlined in Appendix C, utilizes the single boiler geothermal binary cycle simulator, GEO4, in the calculations for both pure fluids and mixtures as working fluids. The working fluids considered here include isobutane, cis-2-butene, and binary mixtures of cis-2-butene, propane and cyclopentane.

Dual boiler binary cycle process. The major elements of the dual boiler binary cycle power plant are shown in Figure 47.0. Other process units not shown in Figure 47.0

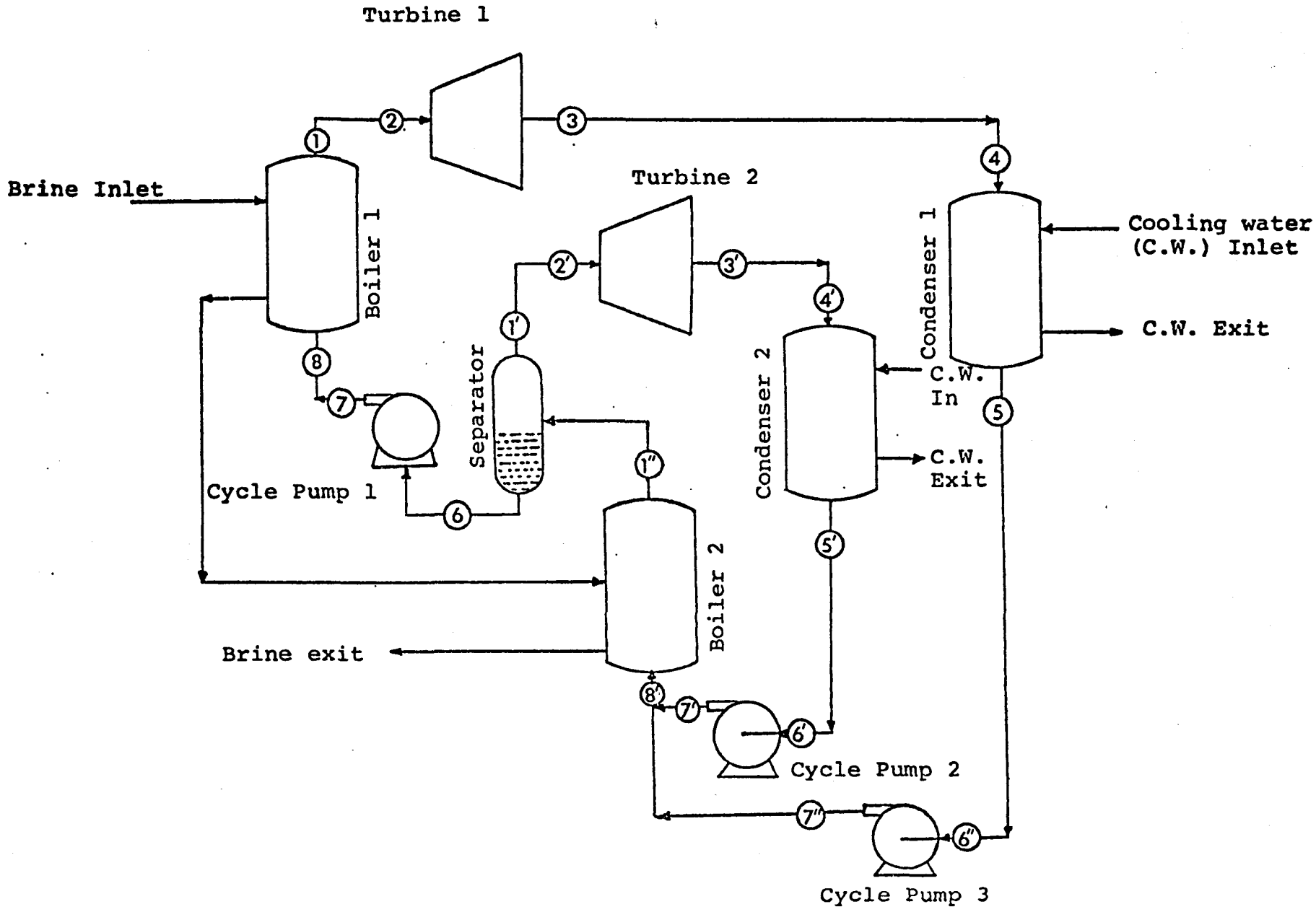

FIGURE 47.0 Dual Boiler Binary Cycle State Points

include brine wells and gathering system, cooling system and auxiliary plant equipment. The nodal points indicated in Figure 47.0 correspond to the process state points used in the calculation. The dual boiler process was described earlier, in chapter I; here the dual boiler binary cycle will be explained with reference to a T-$\dot{Q}$ diagram. To understand the dual boiler binary cycle shown in Figure 47.0, consider first a single boiler ideal binary cycle on a temperature-entropy diagram in Figure 48.0 (represented by solid lines). Since the objective here is the maximization of the net plant work per unit mass of brine, one would like to select the highest temperature and pressure conditions at turbine inlet (state point 1) without violating the pinch criterion in the heat exchanger (in order to increase the net plant work for specified brine flow rate conditions).

Consider now the revised single boiler ideal binary cycle (shown by dotted lines in Figure 48.0) where the turbine inlet temperature and pressure are increased to state point 5. But for this revised subcritical cycle, the brine flow rate would have to be increased in order to avoid the pinch occuring around state point 7'. The new brine outlet temperature will then be T'_{HO} (Figure 48.0). Neglecting the changes due to kinetic and potential energy, and assuming no viscous pressure drops, the net thermodynamic cycle specific work obtained form the working fluid will be

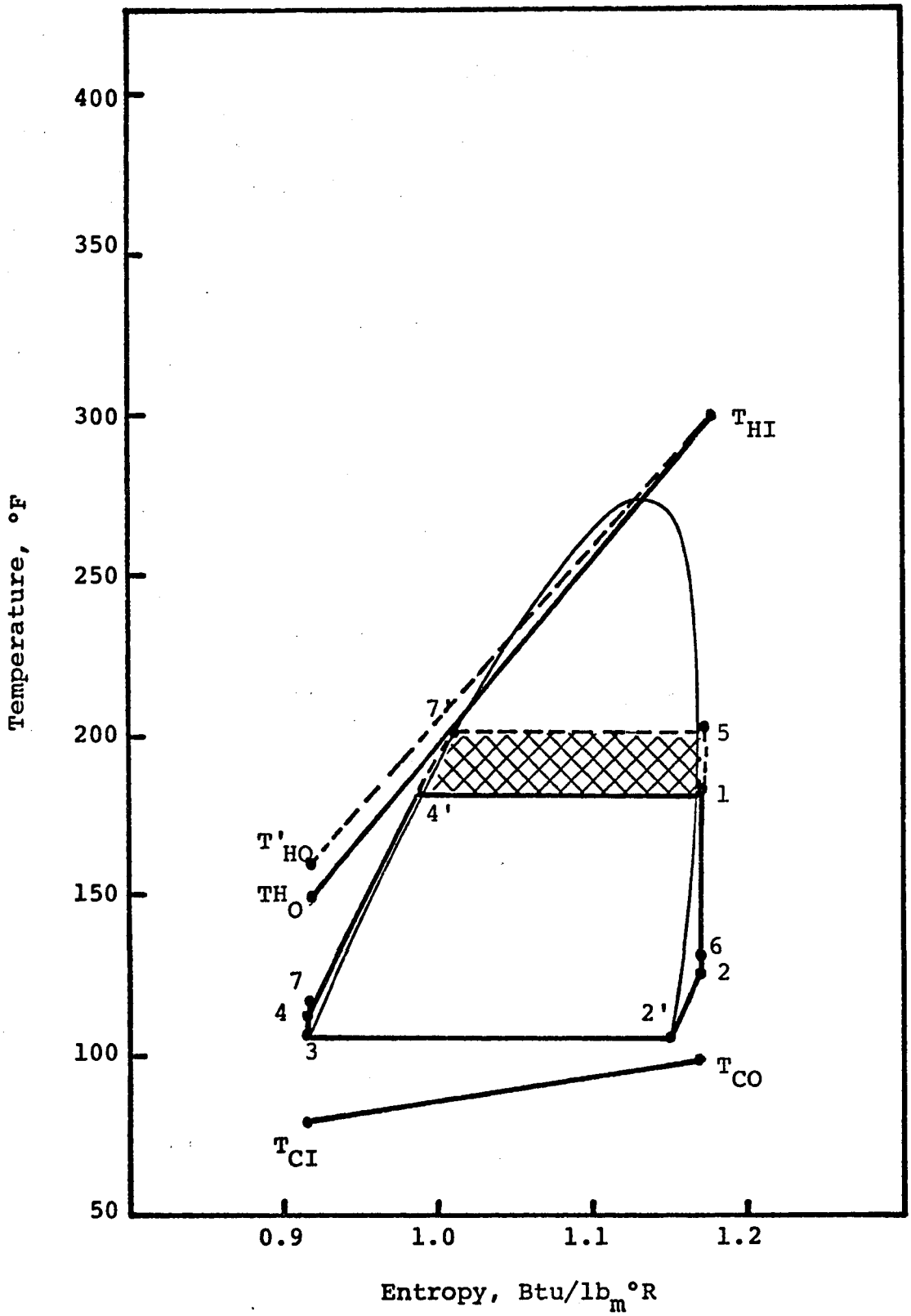

Figure 48.0 Temperature-Entropy Diagram of Single Boiler Binary Cycles

the difference in areas under the working fluid warming and cooling curves on a temperature-entropy diagram. The net cycle specific work obtained form the revised case and the original case will be represented by the difference in the areas 5-6-2'-3-7-7'-5 and 1-2-2'-3-4-4'-1. It is evident from Figure 48.0 that the area 5-6-2'-3-7-7'-5 is larger than the area 1-2-2'-3-4-4'-1. The difference in these areas is shown cross-hatched in Figure 48.0. Thus, the net cycle specific work, $\underline{W}_N$, increases for any increase in temperature and pressure of the working fluid at the turbine inlet. For subcritical cycles (such as the one shown in Figure 48.0), the pinch usually occurs (depending on the georesource temperature) near the bubble point temperature of the working fluid in the brine heat exchanger. For a fixed brine flow rate, the pinch will occur at the bubble point shown by state point 7' in Figure 48.0 when the pressure is increased. Therefore, the brine flow rate would have to be increased to avoid the violation of the pinch temperature criterion. This will result in a higher brine outlet temperature and, if the pressure is increased beyond the optimum, a decrease in resource utilization. Thus, maximization of the net plant work per unit mass of brine, W_N/M_H is a trade-off between the higher turbine inlet pressure (for increasing the net cycle work) and lower brine flow rate (for increasing resource utilization).

For specified brine flow rate and brine outlet temperature (T_{HO}), the net cycle work also can be increased by utilizing cascade (or multi-boiler) binary cycles. To simplify this discussion, only the dual boiler binary cycle will be explained here with reference to the working fluid temperature profiles in the dual boilers. Figure 49.0 shows on a T-$\dot{Q}$ diagram the dual boiler binary cycle with reference to the brine heat exchanger. This diagram will also be used in reference to Figure 47.0 to keep the discussion short. The working fluid is partially vaporized by brine up to state point 6 in a low pressure boiler 2. The partially vaporized working fluid (pure fluid for this discussion) is then taken to a separator (Figure 47.0) where the working fluid vapor at state point 6 is taken form the top of the vessel and expanded in low pressure turbine 2 in Figure 47.0. The liquid working from the separator at state point 6 is then pumped to a higher pressure and passed through a high pressure boiler 1 (Figure 47.0) where the working fluid is vaporized and converted to saturated vapor or superheated gas, by heat transfer with the incoming brine from the production wells. This process of warming and vaporization is shown by the working fluid state points (temperature profile) 6-7-5 in Figure 49.0. The high pressure gas phase working fluid (at state point 5 in Figure 49.0) is then expanded through turbine 1 (Figure 47.0) for power generation.

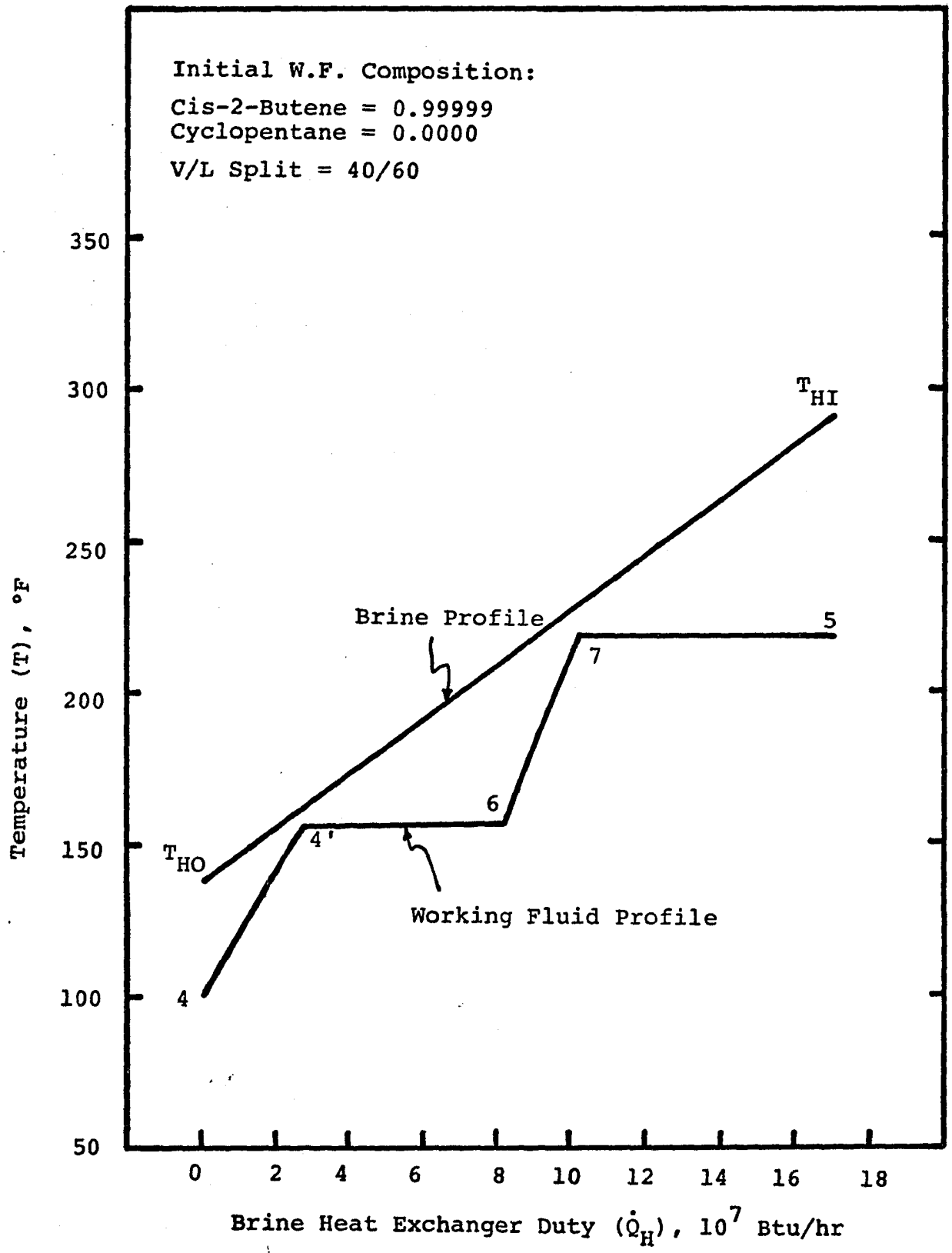

Figure 49.0 T-Q Diagram of Cis-2-Butene

The nonisothermal vaporization and condensation behavior of mixtures (at constant pressure) can be utilized to advantage here by making the working fluid temperature profiles (in both boilers) come closer to being parallel to the brine profile and the working fluid temperature profiles in condensers come closer to being parellel to the cooling water profiles to obtain more area under the warming and cooling curves for the mixture cycle compared to the pure fluid cycle. This behavior of mixtures will be further discussed in the comparison of pure fluid and mixture dual boiler binary cycle parameters. However, the point to keep in mind is that more work is obtained per unit mass of brine in going form the single boiler binary cycle to the dual boiler binary cycle. Theoretically, an infinite number of boilers would make the working fluid profile exactly parallel to the brine profile, even for a pure fluid. A very sufficiently wide boiling range mixture can do the same job, i.e., make the working fluid and brine profiles parallel with a finite number of boilers. However, the wide boiling mixture will have an even wider condensing range, which would be disadvantageous to a single or perhaps even dual boiler mixture cycle. Cascade cycles using more than two boilers will not be discussed here. Instead, the advantages of mixtures in the dual boiler binary cycles will be addressed.

Comparison of pure hydrocarbon and mixture working fluid for the dual boiler binary cycle. The objective function for comparing pure hydrocarbon and mixture working fluids was chosen as the net thermodynamic cycle work (turbine work-cycle pump feed work) per unit mass of brine. This choice was made because cost calculations for the dual boiler cycle would not be made easily. However, as noted earlier, for the lower georesource temperatures, the cost optimum and resource utilization optimum nearly coincide. The cycle operating conditions were determined using the simplified hand calculation procedure outlined in Appendix C. The design parameters used to conduct this sensitivity study also are listed in Appendix C.

The parameters which can be chosen for optimization in the dual boiler process include the following:

(1) Working Fluid Starting Composition

(2) Vapor/Liquid Split in Boiler 1

(3) Turbine Inlet Temperature and Pressure in Low and High Pressure Cycles

(4) Brine Outlet Temperature

(5) Cooling Range in Condensers 1 and 2

(6) Pinch Point Temperature Differences

A few calculations were performed to optimize the vapor-liquid split in boiler 2 for one binary mixture of propane-cis-2-butene. The semi-optimum vapor/liquid split

obtained for this mixture was then utilized for other binary mixtures. A mixture of 60 mole per cent cis-2-butene and 40 mole per cent cyclopentane was chosen for the first calculation, because both fluids have I-factors close to unity. The vapor-liquid split for this mixture was chosen so as to give approximately an equimolar mixture of cis-2-buten and cyclopentane in the high pressure cycle. The selection of a 50-50 mixture was based on the fact that such mixtures give the maximum slope on the temperature-enthalpy vaporization curve and thus higher turbine inlet temperature. However, because of the greater slope of the saturated liquid locus, for this mixture compared to cis-2-butene, the latent heat of vaporization at a given temperature was greater than that of pure cis-2-butene resulting in a higher brine outlet temperature for this mixture (than cis-2-butene). To reduce the slope of the saturated liquid locus, propane and cis-2-butene mixtures were chosen for further study.

No attempt was made in this preliminary study to optimize the parameters 4, 5 and 6 mentioned above.

Table 17 gives a summary of the most significant parameters for the comparison of pure and mixture dual boiler cycles. Table 18 provides a more detailed comparison of various other cycle parameters. Pure cis-2-butene was selected as the basis of comparison. Two mixtures (i.e.

Table 17

SUMMARY OF THE DUAL BOILER BINARY CYCLE
PRELIMINARY CALCULATIONS

Working Fluid / Parameters	Cis-2-Butene	Isobutane	Mixture I*			Mixture II	Mixture III	Mixture IV
	Vapor Fraction† (40%)	Vapor Fraction† (40%)	Vapor Fraction† (29%)	Vapor Fraction† (40%)	Vapor Fraction† (51%)	Vapor Fraction† (41%)	Vapor Fraction† (41%)	Vapor Fraction† (38.6%)
Net Plant Work, Btu/lb_m brine	18.49	20.16	21.85	22.46	21.87	22.27	20.85	20.17
Ratio of Net Plant Work**	1.00	1.09	1.18	1.21	1.18	1.20	1.13	1.09
Net Power, MW	6.046	6.595	6.966	6.952	7.055	7.349	6.784	6.594
Gross Power, MW	6.315	7.005	7.470	7.516	7.582	8.008	7.187	6.685
Brine Flow, $(10^6)lb_m/hr$	1.116	1.116	1.088	1.056	1.101	1.126	1.110	1.116
Brine Exit T, °F	137.	138.5	132.5	130.	132.5	132.5	139.	144.5

*Mixture I Initial Composition: Propane, 60%; Cis-2-Butene, 40%.
Mixture II Initial Composition: Propane, 70%; Cis-2-Butene, 30%.
Mixture III Initial Composition: Propane, 50%; Cis-2-Butene, 50%.
Mixture IV Initial Composition: Cis-2-Butene, 60%; Cyclopentane, 40%.

**Net Plant Work in Btu/lb_m brine.

†Vapor Fraction is the Vapor Split used in Boiler 2.

Table 18

COMPARISON OF PURE AND MIXTURE FLUID DUAL BOILER BINARY CYCLE PRELIMINARY CALCULATIONS

Parameters \ Working Fluid	Cis-2-Butene	Isobutene	Mixture I*			Mixture II	Mixture III	Mixture IV
	Vapor Fraction (40%)	Vapor Fraction (40%)	Vapor Fraction (29%)	Vapor Fraction (40%)	Vapor Fraction (51%)	Vapor Fraction (41%)	Vapor Fraction (41%)	Vapor Fraction (38.6%)
Net Plant Work, Btu/lb_m brine	18.49	20.16	21.85	22.46	21.87	22.27	20.85	20.17
Net Power, MW	6.046	6.595	6.966	6.952	7.055	7.349	6.784	6.594
Gross Power, MW	6.315	7.005	7.470	7.516	7.582	8.008	7.187	6.685
Net Thermo. Efficiency, %	12.08	13.31	13.87	14.04	13.88	14.14	13.81	13.86
Brine Flow, $(10^6)lb_m/hr$	1.116	1.116	1.088	1.056	1.101	1.126	1.110	1.116
Brine Exit T, °F	137.	138.5	132.5	130.	132.5	132.5	139.	144.5
Total Boiler Duty, (10^7)Btu/hr	17.078	16.912	17.143	16.9049	17.342	17.7384	16.7676	16.2332
Boiler 1 Duty, (10^7)Btu/hr	8.9052	7.4976	8.4484	6.9029	6.0701	7.4762	7.2588	8.1455
Boiler 2 Duty, (10^7)Btu/hr	8.1733	9.4140	8.6945	10.002	11.2717	10.2621	9.5088	8.0876
Total Cond. Duty, (10^7)Btu/hr	14.984	14.661	14.776	14.538	14.935	15.410	14.4972	13.9705
Condenser 1 Duty, (10^7)Btu/hr	9.015	8.8484	10.5907	8.676	7.4398	9.2732	8.7827	8.7049
Condenser 2 Duty, (10^7)Btu/hr	5.968	5.8122	4.1850	5.0618	7.4957	6.1368	5.7145	5.2655
Turbine 1 Inlet Pressure, psia	220.4	372.0	470.0	560.0	572.2	620.0	438.7	132.0
Turbine 1 Inlet Temp., °F	218.0	240.0	242.0	260.0	275.0	275.0	262.0	240.0
Turbine 2 Inlet Pressure, psia	104.3	190.0	312.0	312.0	312.0	310.0	275.0	81.4
Turbine 2 Inlet Temp., °F	156.0	177.0	180.7	183.0	185.0	182.6	185.8	175.4
Turbine 1 $\Delta\bar{H}$, Btu/lb_m W.F.	29.08	27.57	30.69	32.73	35.63	35.41	34.38	35.22
Turbine 2 $\Delta\bar{H}$, Btu/lb_m W.F.	15.09	17.07	20.25	20.60	20.94	19.49	20.29	20.82
Total W.F. Flow, (10^5) lb_m/hr	9.1783	10.23	9.2142	9.2142	9.2142	9.450	8.5691	7.6915
W.F. Flow in Turbine 1, $(10^5)lb_m/hr$	5.5070	6.138	6.5476	5.4981	4.4819	5.5995	5.0690	4.7236
W.F. Flow in Turbine 2, $(10^5)lb_m/hr$	3.6713	4.092	2.6667	3.7161	4.7324	3.8505	3.500	2.9680

*Mixture I Initial Composition: Propane, 60%; Cis-2-Butene, 40%.
Mixture II Initial Composition: Propane, 70%; Cis-2-Butene, 30%.
Mixture III Initial Composition: Propane, 50%; Cis-2-Butene, 50%.
Mixture IV Initial Composition: Cis-2-Butene; 60%; Cyclopentane, 40%.

mixtures I and II) of propane and cis-2-butene provide 20% or more net plant work compared to pure cis-2-butene and almost 11% more than pure isobutane. The overall improvement in net plant work of all other mixtures over cis-2-butene ranges between 9 and 18%. Mixture IV gives almost identical results to isobutane. However, the operating pressures for the heat exchanger and condenser are much lower (almost 1/3) than those for the isobutane cycle. This would mean lower costs for heat transfer units. However, somewhat higher turbine costs can be expected for this mixture compared to isobutane. Although cost calculations were not performed, it is evident that whether the objective is maximum utilization of the resource or cost of major equipment, mixtures do offer advantages over the pure fluids considered. The net power obtained form mixture cycles is also equal to or significantly greater than the pure fluids considered in this analysis, as can be noted in Table 17.

Figure 50.0 illustrates on a T-$\dot{Q}$ diagram the brine and working fluid profiles of pure cis-2-butene and a propane-cis-2-butene mixture. The cycle lost work is minimized by the use of mixtures because of their non-isothermal vaporization profiles in the brine heat exchangers (at a constant pressure).

It is interesting to note from Table 17 that the brine outlet temperature for mixture I (vapor fraction of 40%) is the lowest for all mixtures and pure fluids

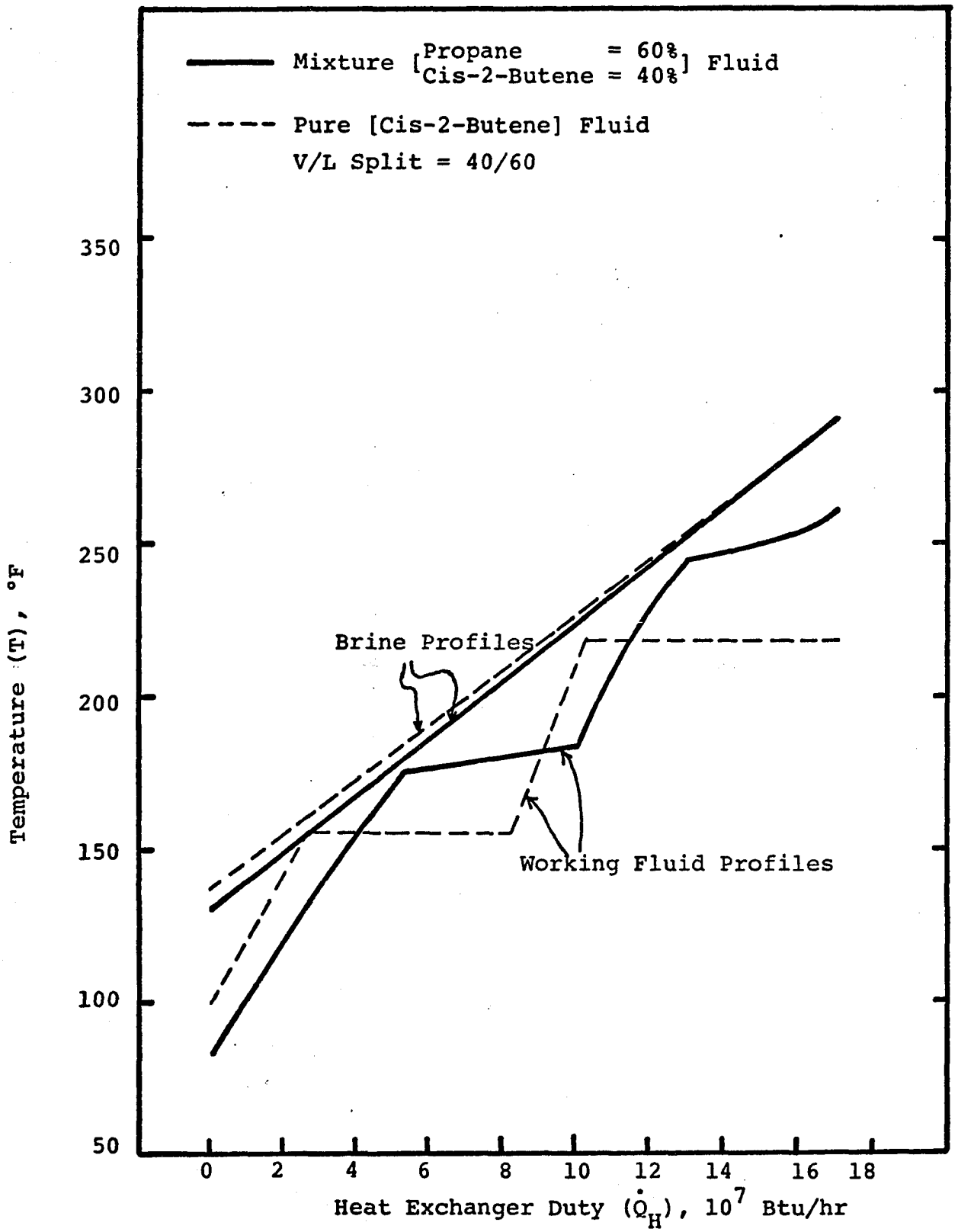

Figure 50.0 T-$\dot{Q}$ Diagram of Pure and Mixture Fluid

considered in this study, and at the same time it gives the best performance. Since minimizing the geothermal brine outlet temperature simultaneously aids both power conversion goals, resource utilization efficiency and minimum cost, the brine outlet temperature is an important parameter in cycle optimization studies. Another factor which should be noted is the fact that it is possible to adjust the cooling range for a mixture, thus reduction the cooling water flow requirements, whereas it is not possible to adjust the cooling range for a pure fluid.

Another significant result to note from Table 17 is the compositions of mixture I and II. Both mixtures give almost the same amount of improvement over the pure fluids. Mixture I is a subcritical cycle whereas mixture II is a supercritical cycle, so that there is a range of operating conditions and working fluid compositions which give the best performance. Such a range of operating conditions is not possible for a pure fluid. In other words, the performance of these mixtures are relatively insensitive to changes in composition between 60 and 70 mole per cent propane in cis-2-butene. This fact can be of immense value in adjusting the working fluid composition to match changes in the geothermal resource temperature over the plant lifetime. Other parameters given in Tables 17 and 18 are self explanatory and so will not be discussed here.

Comparison of pure hydrocarbon and mixture working fluids for multiple boiler binary cycle. The purpose of this discussion is to show the relationship of the number of boilers (in the multiple boiler binary cycle) versus the net plant work per unit mass of brine, and versus net thermodynamic cycle efficiency. The working fluids for comparison in this study are pure isobutane and a mixture of 60% propane and 40% cis-2-butene (referred to as mixture I, with vapor fraction of 0.4 in Table 17).

Tables 19 and 20 give a summary of the results for isobutane and mixture I multiple boiler cycles. Only isobutane triple boiler calculations were performed. From Tables 19 and 20 the following points can be noted:

(1) For the single boiler binary cycle, mixture I yields approximately 18% greater net plant work than isobutane. The net thermodynamic cycle efficiency is about 13% higher for the mixture cycle. The single boiler binary cycle calculations were not optimized. However, the conclusions should not change for optimized cases.

(2) For the dual boiler cycle, mixture I provides approximately 11% more net plant work than isobutane. The increase in the net plant work from the single boiler cycle to the dual boiler cycle is about 18% for the mixture I and 25% for isobutane.

Table 19

NET PLANT WORK PER POUND OF BRINE

No. of Boilers / Working Fluid	1	2	3
Mixture I*	19.04	22.46	---
Isobutane	16.15	20.16	22.33

Table 20

NET THERMODYNAMIC CYCLE EFFICIENCY, PERCENT

No. of Boilers / Working Fluid	1	2	3
Mixture I*	11.74	14.0	---
Isobutane	10.36	13.3	13.13

*Mixture I initial composition:

Propane = 60%

cis-2-Butene = 40%

(3) For the triple boiler cycle, only isobutane was considered. The net plant work for this cycle is 22.3 Btu/lb_m of brine, which is 10% greater than the isobutane dual boiler cycle, but still less than the dual boiler mixture cycle. The slight decrease in η_c for triple boiler cycle is due to the fact that brine heat exchanger duty increases as the number of boilers are increased. However, the isobutane cycle is not optimized and therefore η_c is inconsistent with increase in W_N.

Figure 51.0 and 52.0 show the results in Tables 19 and 20 graphically. It can be seen from Figure 51.0 that the net plant work gained from a triple boiler binary cycle is very close to the maximum work which can be obtained from an infinite boiler binary cycle. Also, the increase in net plant work is greater when the number of boilers is increased from 1 to 2. From the slope of the curve in Figure 51.0 it can be anticipated that mixture I will yield a greater net plant work than isobutane for the triple boiler cycle. However, the percentage of excess work will decrease as the number of boilers is increased until mixture and pure fluid cycles become equal. A point to note is the fact that as the number of boilers is increased, the number of optimization variables also will increase. Mixture cycles will always have more variables to be optimized than pure

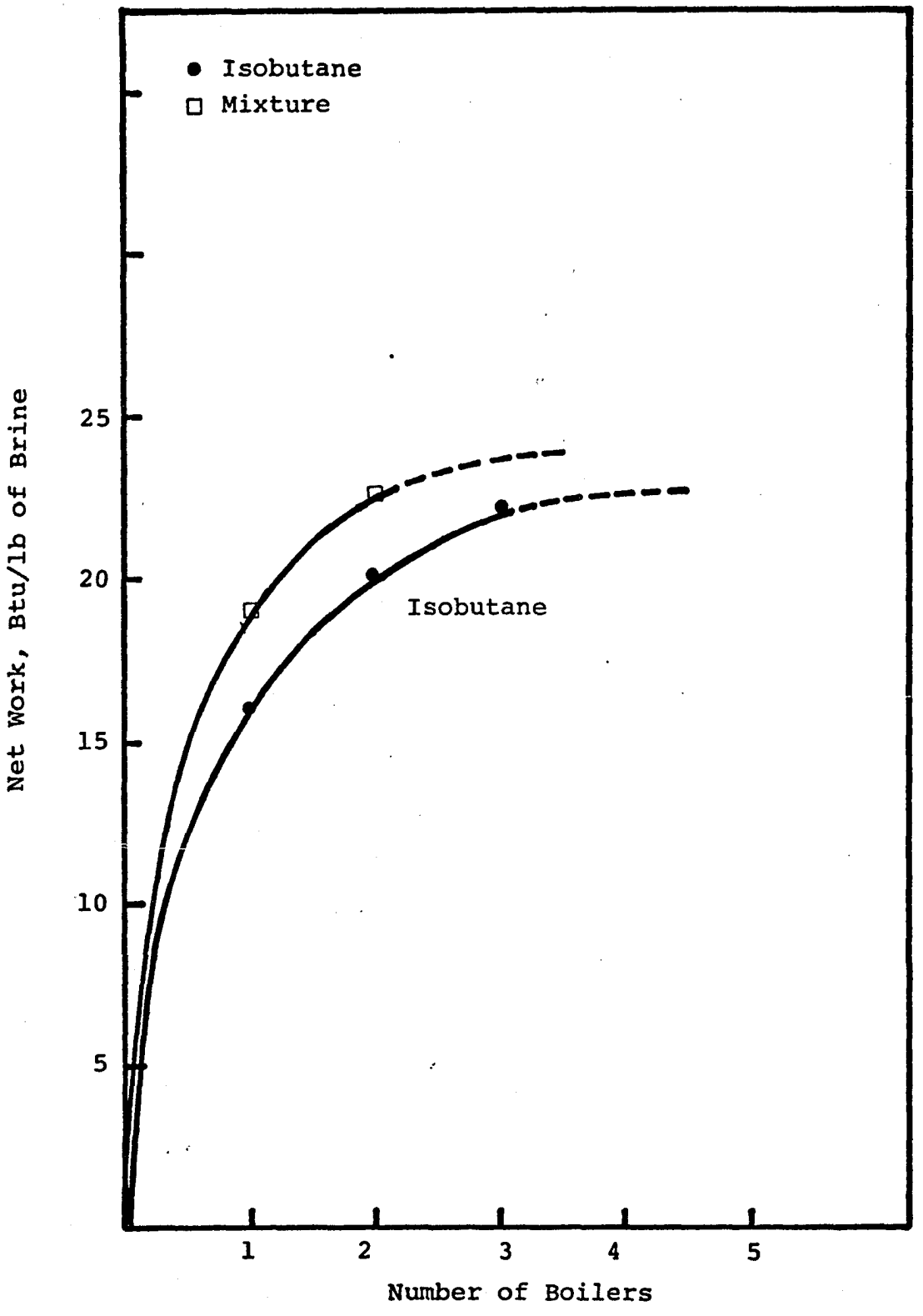

Figure 51.0 Net Plant Work Versus Number of Boilers for Multiple Boiler Binary Cycles

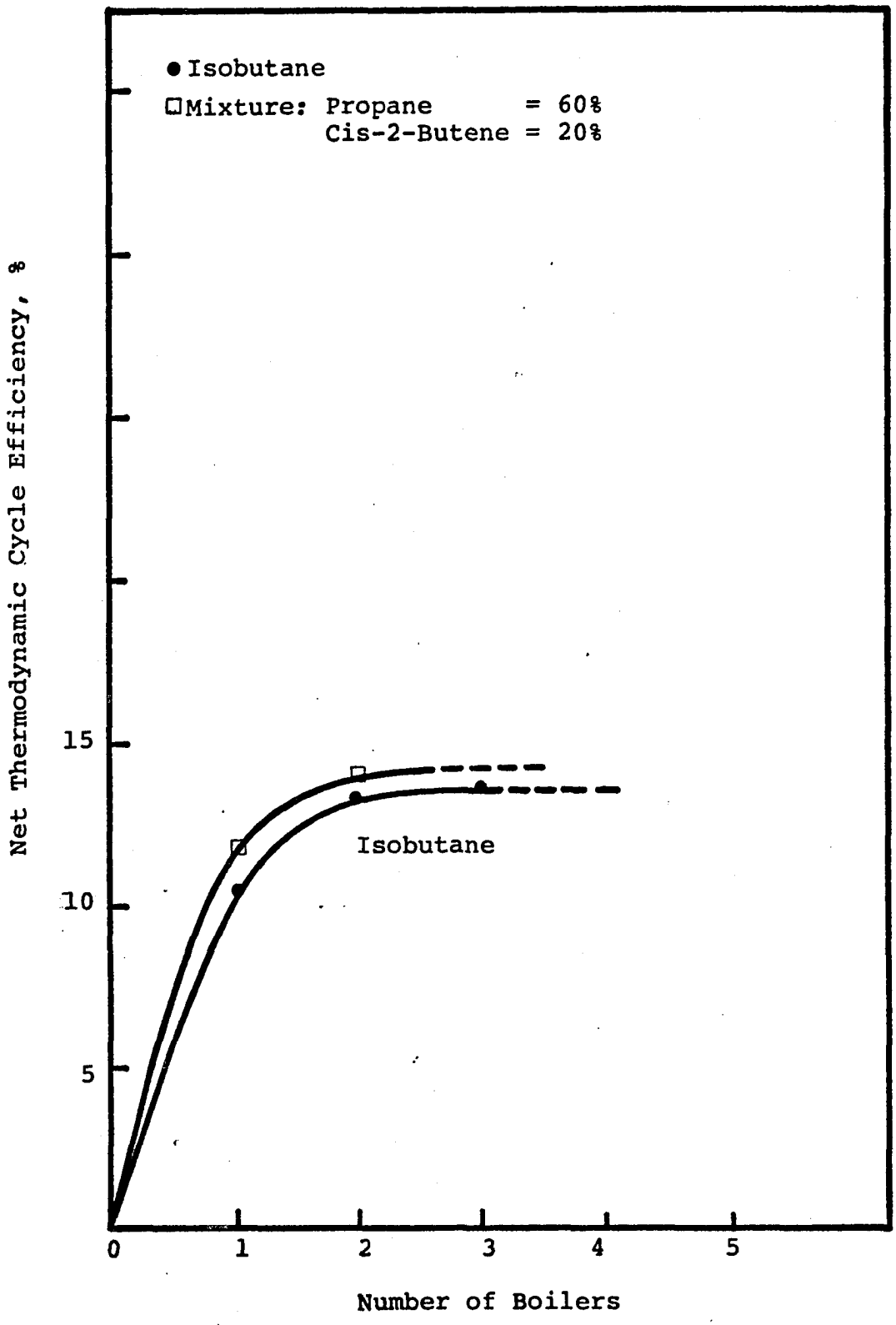

Figure 52.0 Net Thermodynamic Cycle Efficiency versus Number of Boilers for Multiple boiler Binary Cycle

fluid cascade cycles. Therefore, the mixture cycles beyond the dual boiler cycle will become quite complicated for computer simulation and/or optimization.

In summary, the net plant work and thermodynamic efficiency for the mixture dual boiler cycle are greater than for the isobutane triple boiler cycle.

Disadvantages of the use of mixtures in single boiler and multiple boiler binary cycles. The comparisons presented for mixture and pure fluid cycles have so far ignored mass transfer effects. Standard heat transfer correlations have yielded heat transfer coefficients which are within a few percent for similar mixture and pure lfuid cycles in these case studies.[20] Thus, only mass transfer effects and the related fact that vapor and liquid in two-phase flow are of different composition would be expected to detract from the advantages of mixture cycles over pure fluid cycles noted in these case studies (which ignored mass transfer effects).

Mass transfer effects which have the major influences on cycle performance are those mass transfer effects which occur in the two-phase regions of the brine heat exchanger and condenser. Two types of mass transfer occur, (1) bulk mass transfer occurs for both mixtures and pure fluids in evaporation and condensation and is not considered here. Diffusive mass transfer occurs only for mixtures in evaporation

and condensation. Because for mixtures, the coexisting vapor and liquid (at equilibrium) are of different compositions, concentration gradients are established in both the vapor and liquid phases (as the system attempts to achieve equilibrium). Because the major driving force for the diffusive mass flux of a component in a single phase mixture is the component concentration, it follows that mass transfer effects will be greatest when composition differences between liquid and vapor are greatest. Thus, mass transfer effects would be expected to be larger for mixtures of widely different fluids, such as ammonia-water mixtures than for mixtures of similar fluids, such as propane normal butane mixtures.

In a very preliminary study carried out at the University of Oklahoma regarding the diffusive mass transfer effects in geothermal binary cycles,[22] it was pointed out that there is a probability that for many working fluid mixtures, mixture boilers will be slightly smaller than boilers for the corresponding pure fluids (for equivalent heat transfer coefficients and LMTD's). On the other hand, it was concluded that because of the resistance to diffusive mass transfer in the vapor phase (of working fluid in condenser), mixture condensers will be larger than in the absence of diffusive mass transfer. However, the net disadvantages of the diffusive effects of mixtures in geothermal binary cycle should be offset by the advantages

mixtures exhibit with respect to their thermodynamic behavior. Besides these considerations, it should be noted that the commercial grades of isobutane and other pure working fluids actually are mixtures. Thus, mixture effects will occur even in "pure fluid" cycles.

Since working fluid heat transfer coefficients in the condenser are smaller than for pure fluids,[20] the negative effects of mass transfer will further increase the mixture fluid condenser sizes.

Effects of the Georesource Temperature Decline on Pure Fluid and Mixture Conventional Binary Cycle Performance

The effects on the net plant plant power, net plant work per unit mass of brine, net thermodynamic cycle efficiency and cooling water requirements, caused by an anticipated decline in the geothermal brine temperature (also design temperature) over the lifetime of power plants, are described with reference to pure isobutane and mixture (an equimolar mixture of isobutane and isopentane referred here as mixture I) binary cycles. Both pure isobutane and mixture cycles were cost optimized ($/kw) for the 350°F georesource and are used here as the base cases.

Geothermal reservoirs are finite sources of thermal energy. The rate of decline of the available brine temperature with time depends on the withdrawal rate of brine and

the thermal energy which it carries. If the withdrawal rate of the brine exceeds the replacement (i.e., brine reinjection) rate, the temperature of the brine would be expected to decline with time. Thus, geothermal power plants of larger capacities would cause greater reservoir temperature decline and require greater unit design modifications. Hankin and others[29] utilized a reservoir computer model to study the effects of reservoir temperature decline on the two-stage flashed steam energy conversion process for various plant capacities. Hankin determined that for their base case plant, designed to produce 200 MW_e under assumed constant brine temperature conditions, the net plant output dropped to 68 percent of the initial capacity in 30 years if subjected to time-wise brine temperature decline. This declining power output resulted in a decrease in lifetime electrical energy output of almost 14 percent and an increase in levelized bus-bar electric energy cost (in mills/kwh) of over 12 percent compared to constant brine temperature operation.

It can be anticipated that a decline in the available temperature of geothermal brine as a function of time would either cause the power output of the plant to also decline, or the flow rate of brine would have to be increased in order to maintain the initial rated plant capacity. The objective of this preliminary study is to present a simplified analysis of the reservoir temperature decline (for fixed brine flow rate condition) on the performance of pure and

mixture binary cycles, and then to check the conclusions using the fixed plant simulator developed by the author (see Appendix B for details).

Consider first brine heat exchanger duty, $\dot{Q}_H$, which for the base case can be written as

$$\dot{Q}_H = U_H \, A_H (LMTD_H) \tag{94}$$

For decreased brine temperature, case 1

$$\dot{Q}_{H1} = U_{H1} \, A_H (LMTD_H)_1 \tag{95}$$

Because of decline in T_{HI} (brine temperature)

$$(LMTD_H)_1 < LMTD_H$$

and

$$U_H \simeq U_{H1}$$

it follows then

$$\dot{Q}_{H1} < \dot{Q}_H \tag{96}$$

Thus, brine heat exchanger duty decreases for a decrease in T_{HI}. We also know that for the base case

$$\dot{Q}_H = \dot{M}_H \, \bar{C}_p \, (T_{HI} - T_{HO}) \tag{97}$$

and for case 1

$$\dot{Q}_{H1} = \dot{M}_H \bar{C}_p (T'_{HI} - T'_{HO}) \tag{98}$$

therefore

$$\frac{\dot{Q}_{H1}}{\dot{Q}_H} = \frac{T'_{HI} - T'_{HO}}{T_{HI} - T_{HO}}$$

since

$$\frac{\dot{Q}_{H1}}{\dot{Q}_H} < 1$$

it follows that

$$\frac{T'_{HI} - T'_{HO}}{T_{HI} - T_{HO}} < 1$$

or

$$(T'_{HI} - T'_{HO}) < (T_{HI} - T_{HO})$$

But

$$T'_{HI} < T_{HI}$$

therefore

$$T'_{HO} > T_{HO} \tag{99}$$

The brine exit temperature, therefore, increases for a decrease in resource temperature. The condenser duty, $-\dot{Q}_c$, also decreases because of decrease in $\dot{Q}_H$. To verify this,

we have for the base case

$$\dot{Q}_H = \dot{M}_W \, \Delta\underline{H}_{BHE} \tag{100}$$

and for case 1

$$\dot{Q}_{H1} = \dot{M}'_{W1} \, \Delta\underline{H}'_{BHE} \tag{101}$$

since

$$\Delta\underline{H}_{BHE} \simeq \Delta\underline{H}'_{BHE}$$

where $\Delta\underline{H}_{BHE}$ and $\Delta\underline{H}'_{BHE}$ are, respectively, working fluid specific enthalpy change in the brine heat exchanger for the base case and case 1.

We have

$$\frac{\dot{M}_{W1}}{\dot{M}_W} = \frac{\dot{Q}_{H1}}{\dot{Q}_H}$$

or

$$\frac{\dot{M}_{W1}}{\dot{M}_W} < 1$$

Thus,

$$\dot{M}_{W1} < \dot{M}_W$$

The condenser duty for case 1 is

$$-\dot{Q}_{c1} = \dot{M}_{W1} \underline{\Delta H}_c$$

Because $\dot{M}_{W1} < \dot{M}_W$ and $\underline{\Delta H}_{c1} \simeq \underline{\Delta H}_c$

$$-\dot{Q}_{c1} < -\dot{Q}_c \tag{102}$$

where $-\dot{Q}_c$ is the condenser duty for the base case. This analysis shows that the condenser duty decreases for a decrease in the resource temperature. A related effect of condenser duty can be seen on the condenser $LMTD_{c1}$ as follows:

$$-\dot{Q}_{c1} = U_{c1} A_c LMTD_{c1} \tag{103}$$

Since

$$U_{c1} = U_c$$

and

$$-\dot{Q}_{c1} < -\dot{Q}_c$$

it follows that

$$LMTD_{c1} < LMTD_c \tag{104}$$

For the pure fluid, the condenser LMTD would decrease only if the approach temperature, DTCWO, would decrease. The decrease in DTCWO means a decrease in the dew point temperature and pressure of the condenser. The decrease in the dew

point temperature (for fixed turbine inlet T, P) means an increase in the turbine specific work and an increase in the net thermodynamic cycle efficiency (as was noted in Chapter II, earlier). Thus, a decrease in the resource temperature implies an increase in the net thermodynamic cycle efficiency. The working fluid flow rate decreases more rapidly than the increase in the turbine specific work, resulting in a decrease in the net plant power, $\dot{W}_{N1}$. The net plant work per unit mass of brine, $\dot{W}_{N1}/\dot{M}_H$ would therefore decrease, for a decrease in the resource temperature. The decrease in the condenser duty for case 1 implies less cooling water requirements for cooling purposes. Tables 21 and 22 show the effects of georesource temperature decline on the performance of pure isobutane and mixture I binary cycles. The base cases for the 350° resource were revised (as explained in Chapter IV, in the brine flow rate section) for both pure isobutane and mixture I cycles. Therefore, the results presented in Tables 21 and 22 are in slight error. However, the overall conclusions drawn on relative basis would still hold. It is evident from Tables 21 and 22 that $\dot{W}_N/\dot{M}_H$ decreases for both pure fluid (isobutane) and mixture I cycles when the resource temperature declines from 350°F to 330°F. The net power decreases by approximately 13% and 17% for isobutane and mixture cycles, respectively.

Table 21

EFFECT OF GEORESOURCE TEMPERATURE DECLINE ON THE PERFORMANCE OF ISOBUTANE BINARY CYCLE**

Georesource T, °F / Process Parameters	Isobutane		Mixture II*
	350	330	330
Cycle			
Net Power, MW	24.63	21.43	19.45
Gross Power, MW	30.70	26.29	22.07
Net Plant Work, Btu/lb_m brine	18.21	15.85	14.38
Net Thermo. Efficiency, %	12.10	12.52	12.65
Turbine			
Turbine Inlet P, psia	450	450	200
Turbine Inlet T, °F	260	260	254
Turbine ΔH, Btu/lb_m	21.90	22.90	26.26
Working Fluid Flow, 10^6 lb_m/hr	4.7838	3.919	2.8677
Brine Delivery			
Brine Flow, 10^6 lb_m/hr	4.6153	4.6153	4.6153
Brine Exit T, °F	187.4	194.4	208.8
Brine Heat Exchanger (BHE)			
BHE LMTD, °F	47.4	41.45	45.05
BHE Load ΔH, $_8$Btu/lb_m W.F.	159.92	162.56	198.93
BHE Duty, 10^8 Btu/hr	7.6504	6.3716	5.7048
Brine Velocity, ft/sec	7.0	7.0	7.0
Condenser			
Cond. LMTD, °F	23.67	19.18	19.51
Cond. Load ΔH, $_8$Btu/lb_m W.F.	140.58	142.20	173.76
Cond. Duty, 10^8 Btu/hr	6.7250	5.574	4.9829
Cond. Dew Point T, °F	115.5	110.8	114.6
Cond. Dew Point P, psia	86.9	81.2	31.7
Cond. Superheat ΔT, °F	17.1	18.4	52.6
Cooling Water Velocity, ft/sec	6.94	5.75	5.14
Cooling System			
Cooling Water Flow, 10^7 lb_m/hr	3.3597	2.780	2.4894
Cooling Water Pump Power, MW	1.55	1.12	0.94
Cycle Pump			
Cycle Pump Power, MW	3.586	2.92	0.917
Cycle Pump ΔH, Btu/lb_m	2.56	2.54	1.09

*Mixture II Composition: Isobutane, 25%; Isopentane, 75%

**Fixed Heat Transfer Surface Areas: BHE Area, 68260 ft^2; Condenser Area, 177,820 ft^2.

Table 22

EFFECT OF GEORESOURCE TEMPERATURE DECLINE ON THE PERFORMANCE OF MIXTURE BINARY CYCLE†

Georesource T, °F / Process Parameters	Mixture I*		Mixture II**
	350	330	330
Cycle			
Net Power, MW	24.41	20.21	20.65
Gross Power, MW	28.50	23.25	23.60
Net Plant Work, Btu/lb_m Brine	17.16	14.2	14.51
Net Thermo. Efficiency, %	13.02	13.54	12.66
Turbine			
Turbine Inlet P, psia	300	300	200
Turbine Inlet T, °F	273	273	254
Turbine ΔH, Btu/lb_m	26.79	28.83	26.37
Working Fluid Flow, 10^6 lb_m/hr	3.5511	2.752	3.0535
Brine Delivery			
Brine Flow, 10^6 lb_m/hr	4.854	4.854	4.854
Brine Exit T, °F	208.6	218.5	206.8
Brine Heat Exchanger			
BHE LMTD, °F	46.7	40.31	44.24
BHE Load ΔH, Btu/lb_m W.F.	197.05	200.83	199.67
BHE Duty, 10^8 Btu/hr	7.0189	5.528	6.0972
Brine Velocity, ft/sec	7.0	7.0	6.98
Condenser			
Cond. LMTD, °F	23.2	17.34	18.29
Cond. Load ΔH, Btu/lb_m W.F.	171.92	173.63	174.40
Cond. Duty, 10^8 Btu/hr	6.1051	4.779	5.3255
Cond. Dew Point T, °F	121.6	115.7	114.2
Cond. Dew Point P, psia	45.4	41.2	31.5
Cond. Superheat ΔT, °F	48.4	50.4	52.71
Cooling Water Velocity, ft/sec	6.74	5.28	5.88
Cooling System			
Cooling Water Flow, 10^7 lb_m/hr	3.050	2.752	2.6605
Cooling Water Pump Power, MW	1.47	0.963	1.155
Cycle Pump			
Cycle Pump Power, MW	1.72	1.322	0.98
Cycle Pump ΔH, Btu/lb_m	1.656	1.64	1.096

†Fixed Heat Transfer Surface Areas: BHE Area, 74062 ft^2; Condenser Area, 197310 ft^2

*Mixture I Composition: Isobutane, 50%; Isopentane, 50%

**Mixture II Composition: Isobutane, 25%; Isopentane, 75%

It was argued earlier, in Chapter IV, that a mixture composition can be changed over the plant lifetime to match the changing characteristics of the resource. The main objective of this section is to provide the understanding and discussion of the procedure used here for the selection of optimum working fluid mixture composition for a declining georesource temperature. Figure 53.0 (taken from reference 20) shows a plot of near optimum average molecular weight, MW, (for the special case of the paraffin hydrocarbon working fluids and cost formulas utilized) as a function of georesource temperature. Figure 54.0 shows other near optimal characterization parameters (critical temperature, T_c, critical density, ρ_c, and accentric factor, ω) as a function of georesource temperature. These quantities are calculated using the formulas

$$MW = \Sigma\ Z_i\ (MW)_i$$

$$T_c = \Sigma\ Z_i\ T_{c_i}$$

$$\rho_c = \Sigma\ Z_i\ \rho_{c_i}$$

$$\omega = \Sigma\ Z_i\ \omega_i$$

where $(MW)_i$, T_{c_i}, ρ_{c_i}, ω_i and Z_i are, respectively, molecular weight, critical temperature, critical density, acentric factor and mole fraction of the ith component and summations range over all components in the mixture (for a pure working fluid, there is only one term in the sum).

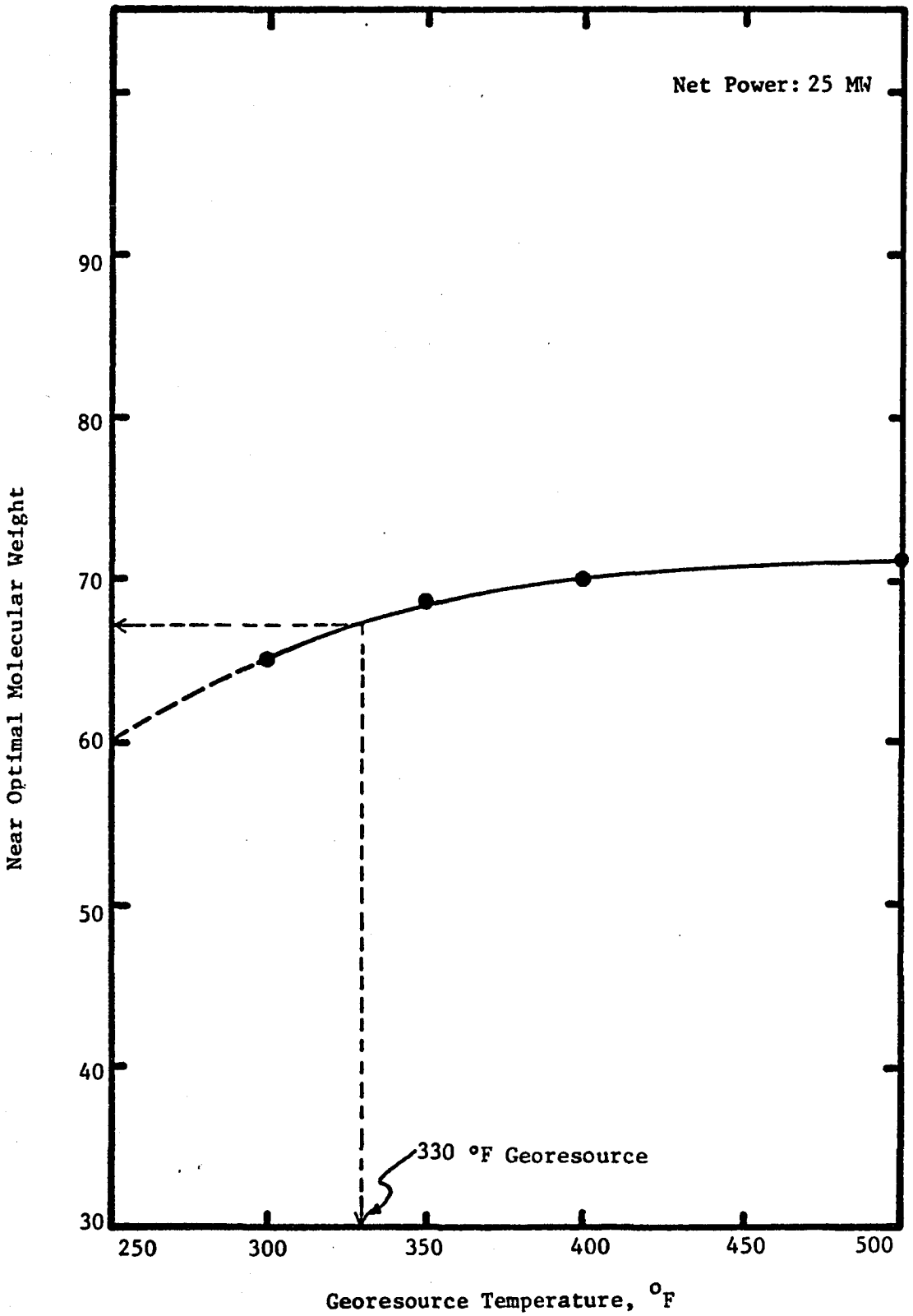

Figure 53.0 Molecular Weight as a Function of Georesource Temperature

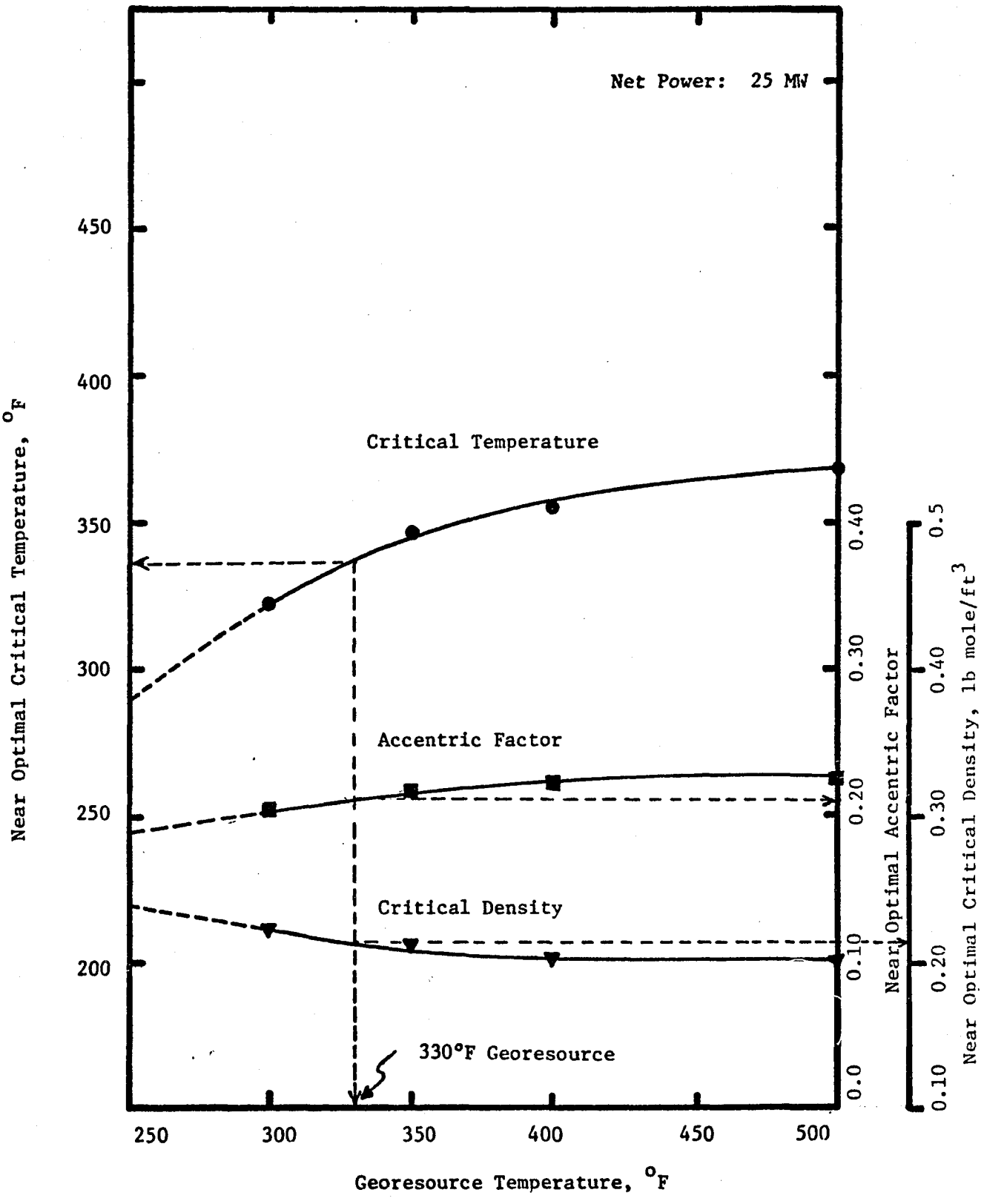

Figure 54.0 Critical Temperature, Critical Density and Accentric Factor as a Function of Georesource Temperature

Table 23.0 shows the values of these characterization parameters for the optimal working fluids determined in an earlier study.[20]

For a 20°F decline in the resource temperature, i.e., for the 330°F georesource, the optimum working fluid molecular weight was read from Figure 53.0 as 68.6. Other characterization parameters were read from Figure 54.0 as follows: T_c, 345.0; ρ_c, 0.211; ω, 0.21. These characterization parameter values correspond closely to a binary mixture of isobutane (25%) and isopentane (75%) in Table 23.0. This mixture will be referred to as mixture II. After selecting the near optimal mixture composition for the 330°F georesource, the near optimal turbine inlet pressure was determined to be 200 psia for mixture II from Figure 55.0; which shows near optimal turbine inlet pressure as a function of molecular weight and georesource temperature. Figure 56.0 is another way of representing Figure 55.0. The curve of near optimal molecular weight working fluids for the 330°F georesource was constructed using interpolated values of optimum turbine inlet pressures from Figure 55.0. Thus, Figures 53, 54, 55 and 56 suggest that at 330°F georesource, mixture II should give the best performance compared to other working fluids considered in these plots.

To verify the above prediction, mixture II was simulated using fixed heat transfer surface areas of mixture I and isobutane cycles and the results are shown in Tables 21

Table 23

NEAR OPTIMAL WORKING FLUID PARAMETERS FOR GEORESOURCE TEMPERATURE RANGE 300°F-500°F

Georesource Temperature (°F)	Compound	Molecular Weight	Pseudo Critical Density ($lb\ mole/ft^3$)	Pseudo Critical Temperature (°F)	Pseudo Accentric Factor
300	iC_4H_{10} = 50% iC_5H_{12} = 50%	65.133	0.220	321.98	0.2045
350	iC_4H_{10} = 25% iC_5H_{12} = 75%	68.639	0.21135	345.49	0.21525
400	iC_4H_{10} = 15% iC_5H_{12} = 85%	70.042	0.20789	354.89	0.22165
500	iC_5H_{12}	72.146	0.2027	369.0	0.226

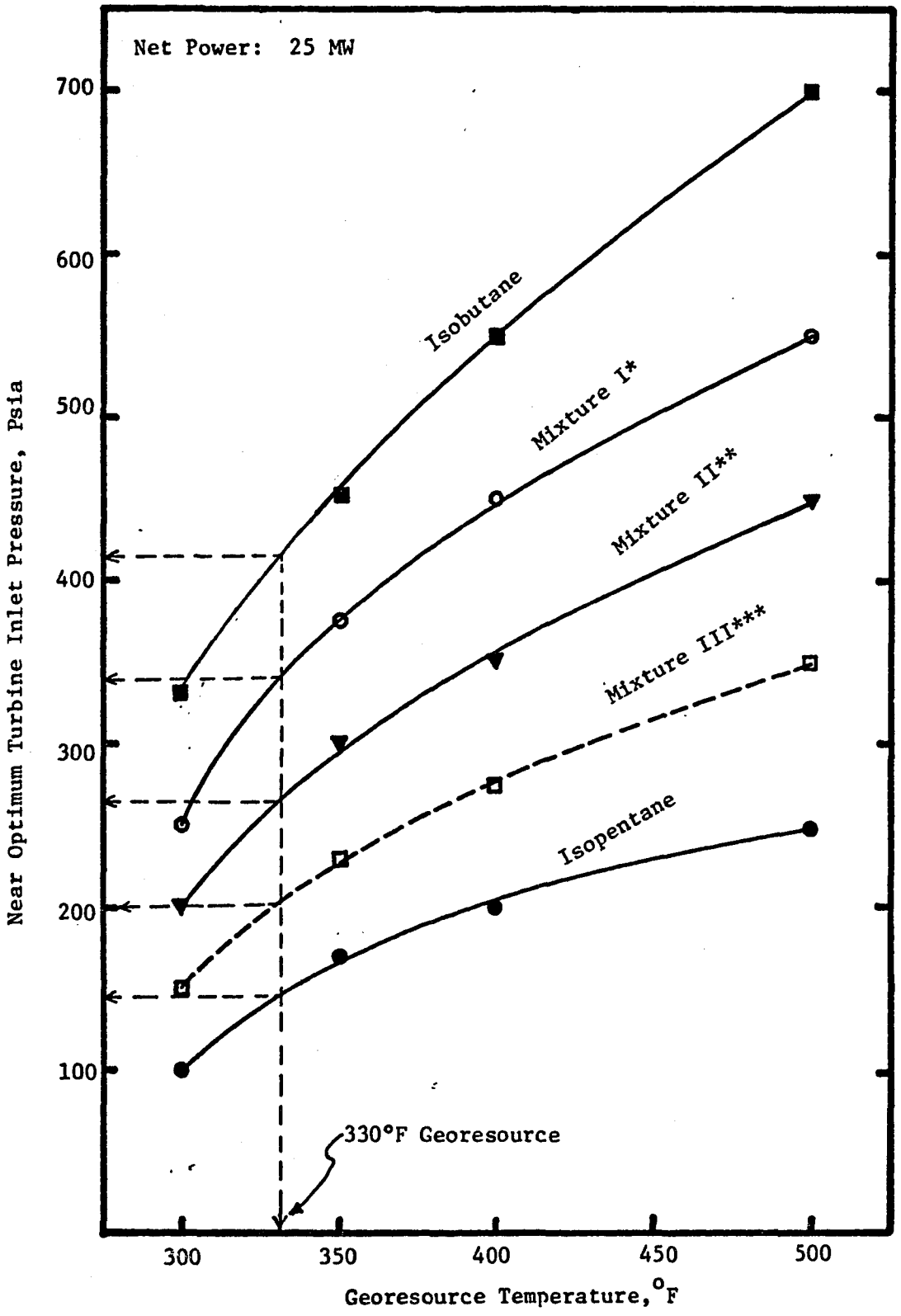

*Mixture I: 75 Mole % Isobutane - 25 Mole % Isopentane
**Mixture II: 50 Mole % Isobutane - 50 Mole % Isopentane
***Mixture III: 25 Mole % Isobutane - 75 Mole % Isopentane

Figure 55.0 Near Optimal Turbine Inlet Pressure Versus Molecular Weight and Georesource Temperature

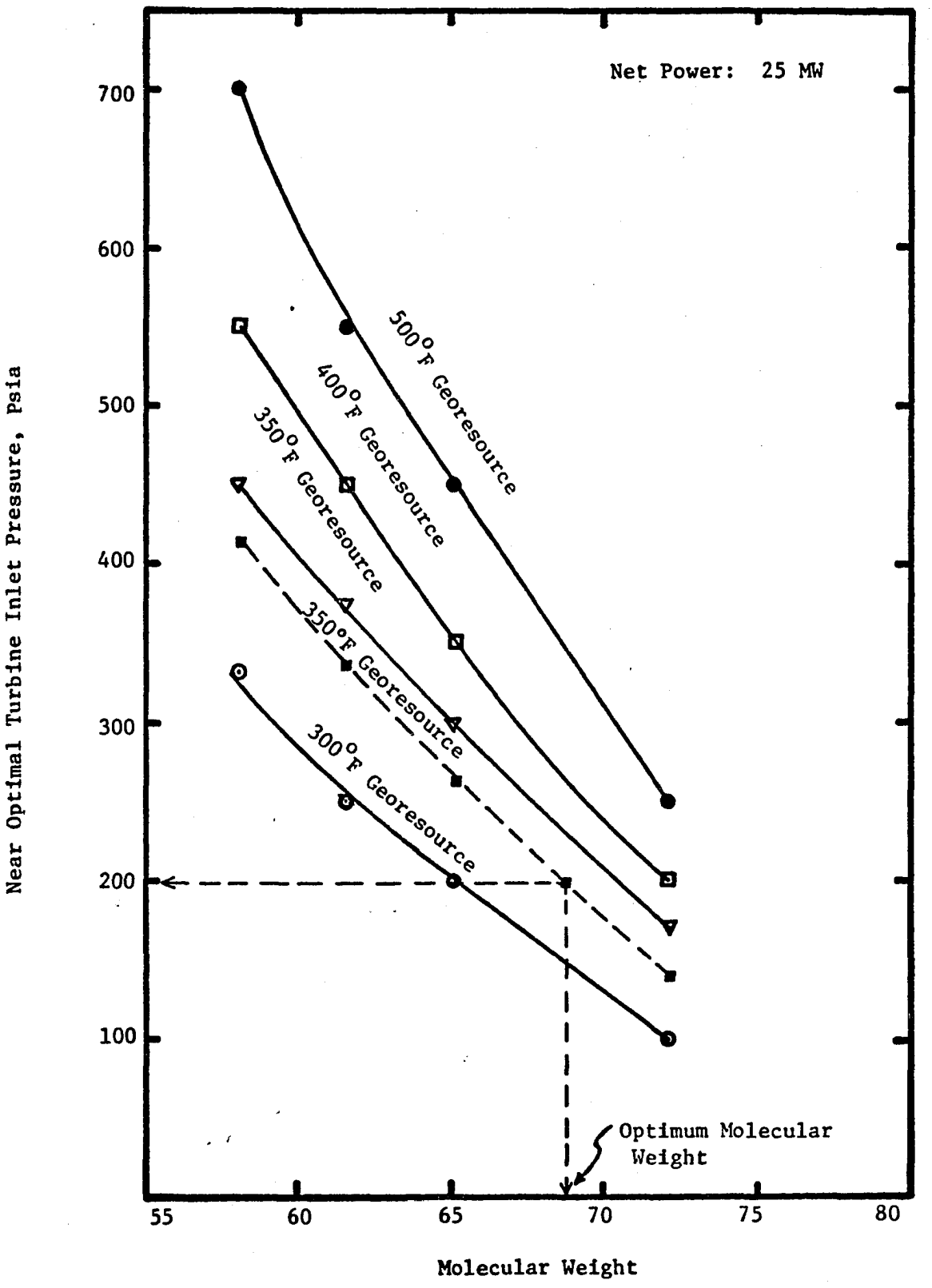

Figure 56.0 Near Optimal Turbine Inlet Pressure as a Function of Georesource Temperature and Molecular Weight

and 22. Mixture II yields approximately 2% (or 0.41 MW) more net plant power than for mixture I (when using mixture mixture I heat transfer areas and brine flow rate) for the 330°F georesource. When isobutane cycle brine flow rate and heat transfer areas were utilized, mixture II yielded approximately 4.2% less net power than for isobutane cycle for the 330°F georesource. Also, the net plant work per unit mass of brine increased for mixture II cycle compared to mixture I cycle, but decreased compared to isobutane cycle.

These preliminary results demonstrate the fact that mixture composition and cycle operating conditions can be varied over the lifetime of the plant to an advantage to match the changing resource characteristics. Another point to note is that power plant equipment which is originally designed for a mixture cycle would benefit other higher molecular weight mixtures and cycle operating conditions. On the other hand, the power plant equipment which is originally designed for a pure fluid may not benefit (higher molecular weight) mixture cycles.

Although Figures 53.0, 54.0, 55.0 and 56.0 can be used for working fluid selection and parameters such as turbine inlet pressure, caution should be exercised in such use of these results. The consideration of other classes of working fluids (such as halocarbons) will introduce additional factors (such as dipole moment effects) and the consideration of different equipment types and/or brine system

and equipment cost formulas will cause translation and warping of the plots of various parameters studied. Nevertheless, the study presented here provides perspective regarding the behavior and performance of binary mixtures compared to pure fluids in the binary cycle for a declining georesource temperature.

Figure 57.0 (shown on the next page and the analysis required to construct it) demonstrates that a decrease in the resource temperature always yields less net plant work per unit mass of brine, $\dot{W}_N/\dot{M}_H$ and that the net plant power decreases. This implies that a provision should be made for the georesource temperature decline in the design of geothermal power plant.

Equipment Needs Peculiar to Geothermal Binary Cycles Using Mixture Working Fluids

The use of mixture working fluids in geothermal binary cycles has been proposed in research at the University of Oklahoma[7,20,26,27]. To date, only horizontal, countercurrent, single pass shell and tube exchangers and condensers have been considered in these studies; with the working fluid on the shell side and brine and cooling water on the tube side of heat exchanger and condenser, respectively. In this report, other types of heat exchange equipment are considered which may enhance the performance of mixture working fluids in geothermal binary cycles. Other

Fixed A_H, A_C, $\dot{M}_H$

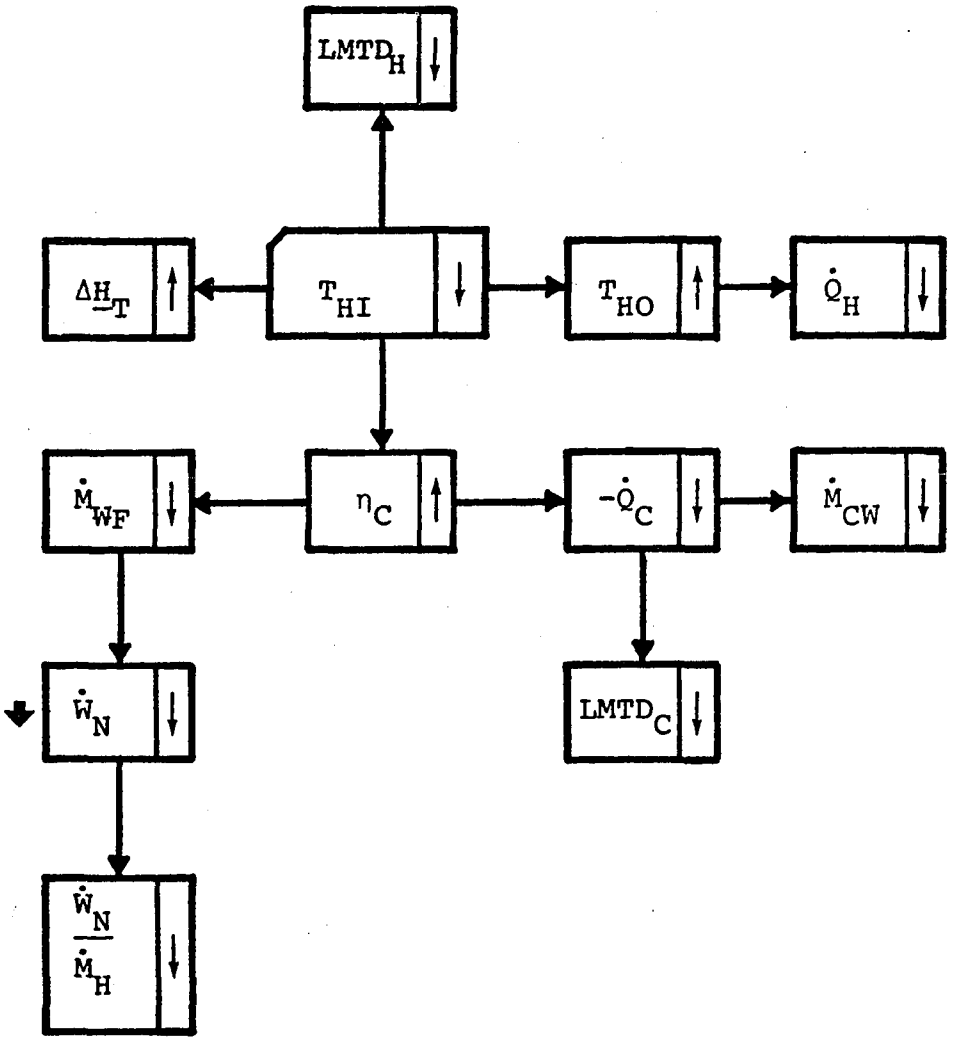

Figure 57.0 Effect of Georesource Temperature Decline (for Fixed A_H, A_C, $\dot{M}_H$) on Pure and Mixture Binary Cycles

factors taken into consideration are: types of flow, working fluid location, tube arrangement.

Brine Heat Exchanger

The conclusions from studies to date can be summarized as follows:

(1) Only one shell pass and one tube pass, horizontal, counter-current heat exchangers have been considered. Because of non-isothermal heat transfer between the working fluid and the hot brine, counter-current flow will have a distinct thermal advantage over the co-current flow because in co-current flow, the hot fluid (brine in this case) cannot be cooled below the cold fluid (working fluid in this case) outlet temperature (30).

(2) If brine fouling can be controlled, or if there is little fouling, then the working fluid should be on the tube side and the brine on the shell side. The assumption of working fluid phase equilibrium at each point in the two-phase section of the heat exchanger may be adequate if the working fluid is on the tube side. This would be a good assumption if the slip velocity, $V_s = V_g - V_\ell$, were zero; i.e., both gas and liquid phases travelling at the same velocity.

V_s is dependent on the flow regime, turbulence, fluid properties and the length of the conduit (31). The gas velocity, V_g, is usually higher than the liquid velocity, V_ℓ, as the fluid progresses in the two-phase section. The composition of the fluid therefore changes as it flows through the tube. Although the assumption that phase equilibrium exists is not exact, it is the best one that can be made without very tedious calculations. A survey by DeGance does not favor the flow-regime based correlations because of the additional errors associated with the calculation of flow regimes (32).

(3) The liquid/vapor ratio for mixture working fluids can be calculated for tube side flow, if the heat exchanger two-phase section is divided into large numbers of subsections with respect to pressure or temperature. The pressure or temperature interval midpoint may then be used to get the value of L/V by assuming phase equilibrium in each subsection. DeGance recommends Dukler's constant slip method for horizontal flow pressure drop calculations (33). Constant slip would mean that the slip velocity, V_s, is zero; or in other words, the velocities of gas and liquid phase are identical at each point in

the heat exchanger. The heat transfer coefficient correlation for two-phase flow used in the GEO4 simulator developed at the University of Oklahoma is probably adequate for the design purposes.

(4) Tubes are arranged in triangular, square or rotated square pitch. Triangular tube layouts result in better shell side coefficients and provide more surface area in a given shell diameter (30). The GEO4 simulator uses triangular tube pitch and therefore no change is needed.

(5) Higher circulation rates are possible on the tube side compared to the shell side, and the tube side flow distribution is more uniform. Mixture working fluid heat transfer coefficients are higher than pure fluids when the working fluid is on the shell side. Therefore, even higher heat transfer coefficients may be obtained for mixture working fluids flowing on the tube side because of higher circulation rates.

(6) It has been shown that sand fluidized by the geothermal brine on the shell side prevents scaling and increases the brine side heat transfer coefficient over conventional shell and tube heat exchangers (34). Both horizontal and vertical-tube bundle arrangements are being

considered (35). In preliminary evaluations, the vertical tube model appears to have more uniform flow distribution and slightly higher heat transfer coefficients than horizontal models (at the same cross-sectional velocity); the converse is true when no bed is involved. However, the heat transfer coefficient of the horizontal-tube model can be brought closer to the vertical-tube model by some design improvements. Since fluidized bed heat exchangers could reduce the size of the heat exchanger by as much as 50%, the development of such heat exchangers would definitely enhance the chances of working fluids being used on the tube side. Under such circumstances, the use of fluidized-bed vertical-tube heat exchangers must be given serious consideration.

(7) The use of direct contact heat exchangers for mixture cycles is attractive because a countercurrent flow situation can be achieved. In the Elgin type of brine heat exchanger, the working fluid is heated as it moves vertically upward in countercurrent flow with the brine. Because the height of the Elgin column is much greater in the liquid-liquid range than the boiling range, the fact that boiling is initiated

earlier by the mixture is a probable advantage (decreases size of heat exchanger).

Condenser

In earlier studies on the use of mixtures in geothermal binary cycles the heat transfer coefficients of the mixtures were calculated to be lower than the pure fluids in horizontal single pass shell and tube condensers. The working fluid mixtures were assumed to be condensing on the shell side with cooling water flowing counter-currently on the tube side. However, since the condensate drops from the tubes as it is formed in the horizontal condenser, a true counter-current flow behavior would not be achieved. In order to achieve true counter-current flow behavior, vertical vapor-in-tube down-draft condensers could be employed. Such condensers have several advantages over horizontal condensers, which will be discussed later in this section.

Many of the same advantages are offered by the vertical vapor-in-shell condensers that use baffles designed to permit condensate to remain on the tube (36). The condensing two-phase heat transfer coefficient can be increased by introducing turbulence, or in other words, by increasing Reynolds and Prandtl numbers. This may also be done by employing low-finned tubes or fluted tubes.

The mixture working fluid heat transfer coefficients can also be increased by employing vertical vapor-in-tube condensers. The vertical condenser could be of the conventional shell and tube exchanger type or the spool-wound exchanger shell type. A spool-wound exchanger consists of a layer of spirally wound tubes around a core with a fairly small pitch (37). The working fluid mixture would then condense downward within the tubes, while the cooling water would flow within the shell and between the tubes. This would require technology transfer from the LNG (liquefied natural gas) industry where spool-wound exchangers are used. Reference 37 indicates that mixtures may provide better heat transfer compared to pure fluids for identical pressure drop ratios of liquid and gas phases.

In spool-wound tube exchangers, the tube side working fluid mixture composition in liquid and gas phase at each point in the exchanger subsection can be assumed to be constant if the exchanger is subdivided into a large number of subsections. The vapor phase working fluid enters the exchanger at high velocity. As the mixture fluid condenses, the liquid phase (condensate) flows along with the uncondensed gas phase. Initially the gas and liquid phase velocities are different—the gas phase velocity being on the higher side. However, under the conditions of equilibrium (because of the increased turbulence and increased vapor liquid contact in spool-wound tubes) a constant slip may be assumed. The

Dukler correlation applies for vertical tubes, and can be modified for the spool-wound tubes (36,37).

In the conventional shell-and-tube vertical condenser, the condensate subcooling (for tube side cooling) is more efficiently accomplished due to falling-film heat transfer. Horizontal tube side cooling uses only a small portion of the available area. Appreciable horizontal shell side subcooling can be achieved only by flooding part of the shell.

The situation with respect to the direct contact condenser has not been considered in sufficient detail to make definite statements, but the fact that counter-current flow can be achieved offers an obvious advantage for mixtures compared to pure fluids in direct contact condensers.

CHAPTER VI

CONCLUSIONS AND RECOMMENDATIONS

Conclusions

Geothermal binary cycles using paraffin hydrocarbons as working fluids have been analyzed using principles of basic thermodynamics and in a relatively simple way. The complex interrelationships of thermodynamic, equipment and unit operational, and cost parameters have been developed and presented in a short form.

When the design objective is the maximization of the net plant work per unit mass of brine, mixtures provide more work than pure fluids. Although resource temperature decline will always result in a decrease in net plant power, mixture composition and behavior can be changed for better performance over the plant lifetime to match the changes in the geothermal resource.

At lower georesource temperatures, the cost optimum and resource utilization optimum nearly coincide, whereas at higher georesource temperatures they differ. The thermodynamic optimum always differs from the cost and resource utilization optima.

Recommendations

The methodology developed in this research using paraffin hydrocarbons may be used as a first step for analyzing other types of energy conversion processes as well as geothermal binary cycles. A preliminary but detailed thermodynamic analysis should be performed for any energy conversion process before any computer simulation. This relatively inexpensive task of thermodynamic analysis can save a lot of headaches which may not be understood by computer simulation alone.

Provision must be made for the georesource temperature decline in the design of geothermal power plants.

BIBLIOGRAPHY

1. Starling, K.E., et al. "Development of Geothermal Binary Cycle Working Fluid Properties Information and Analysis of Cycles," University of Oklahoma Annual Report No. OU/ID-1719-2, to Department of Energy, December 31, 1978.

2. Starling, K.E., et al. "Resource Utilization Efficiency Improvement of Geothermal Binary Cycles," Report No. ORO-4944-5, University of Oklahoma, December 1976.

3. Starling, K.E., West, H.H., Iqbal, K.Z., Chu, C.T., Subramanian, R. "Preliminary Evaluation of the Use of Pure Hydrocarbon and Mixture Fluid in the Dual Boiler Binary Cycle," Unpublished Report, from The University of Oklahoma to INEL, October 1978.

4. Eskesen, J. "Cost and Performance of Flash Binary and Steam Turbine Cycles for the Imperial Valley, California," Proc. 12th IECEC, 1, 842, 1977.

5. Kihara, D.H. and Fukunaga, P.S. "Working Fluid Selection and Preliminary Heat Exchanger Design for a Rankine Cycle Geothermal Power Plant," Proc. 2nd U.N. Symposium on The Development and Use of Geothermal Resources, 3, 2013, 1975.

6. Shepherd, D.G. "A Comparison of Three Working Fluids for the Design of Geothermal Power Plants," Proc. 12th IECEC, 1, 832, 1977.

7. Iqbal, K.Z., West, H.H., and Starling, K.E. "Hydrocarbon Working Fluid and Operating Conditions Selection for the Conventional Geothermal Binary Cycle," Proc. 13th IECEC, 2, 1114, 1978.

8. Palmer, D.A., Sirovich, B.E. "Selection of a Rankine Cycle Fluid for Recovery of Work from Heat at Moderate Temperature," Proc. 13th IECEC, 2, 1500, 1978.

9. Ingvarsson, I.J. and Turner, S.E. "Working Fluid and Cycle Selection Criteria for Binary Geothermal Power Plants with Resource Temperature in the Range 220 - 400°F", TREE - 1108, INEL, Idaho, 1977.

10. Starling, K.E., et al. "Resource Utilization Efficiency Improvement of Geothermal Binary Cycles," Report No. ORO-4944-3, University of Oklahoma, December 1975.

11. Iqbal, K.Z., Fish, L.W., Starling, K.E. "Development of a Geothermal Binary Cycle Simulator," Proc. Okla. Acad. Sci., 57, 1977.

12. Starling, K.E., Iqbal, K.Z., Fish, L.W., et al. "GEO4 - A Binary Cycle Simulator," Report No. OU/ID-1719-1, to DOE, University of Oklahoma, December 31, 1978.

13. Milora, S.L., Tester, J.W. Geothermal Energy as a Source of Electric Power. MIT Press, 1975.

14. Elliot, D.G. "Comparison of Geothermal Power Conversion Cycles," Proc. 11th IECEC, 1976.

15. Sheinbaum, I. "Power Production From High Salinity Geothermal Waters," Proc. 11th IECEC, 1976.

16. Anderson, J.H., Anderson, J.H., Jr. Mechanical Engineering, 88, No. 4, 41-46, 1966.

17. Dipippo, R. "A Summary of the Technical Specifications of the Geothermal Power Plants in the World: Revision 1," Brown University Report No. CATMEC/21, DOE Contract No. EY-76-S-02-4501. A001, July 1978.

18. Pope, W.L., Green, M.A., et al. "Multiparameter Optimiza- Studies on Geothermal Energy Cycles," Proc. 12th IECEC, 1, 865, 1977.

19. Holt, B, Hutchison, A.J.L., Coretz, D.S. "Geothermal Power Generation Using Binary Cycles," Geothermal Energy, 1, No. 1, August 1973.

20. Starling, K.E., et al. "Resource Utilization Efficiency Improvement of Geothermal Binary Cycles - Phase II," Report No. ORO-4944-7, University of Oklahoma, DOE Contract No. E-(40-1)-4944, December 1977.

21. Balzhiser, R. E., et al. Chemical Engineering Thermodynamics. New Jersey: Prentice-Hall, Inc., 1972.

22. Starling, K.E., et al. "Resource Utilization Efficiency Improvement of Geothermal Binary Cycles," Report No. ORO-4944-4, University of Oklahoma Annual Report, June 15, 1975 - June 15, 1976.

23. Anderson, J.H. "Working Fluids for the Sea Solar Power Processes," NSF/RANN/SE/GI-34979/TR/7316, University of Massachusetts (Amherst), May, 1973.

24. Starling, K.E. Fluid Thermodynamic Properties for Light Petroleum Systems, Gulf Publishing Co., Houston, Texas, 1973.

25. Starling, K.E., et al., "Use of Mixtures as Working Fluids in Ocean Thermal Energy Conversion Cycles - Phase II", Final Report, University of Oklahoma Final Report No. ORO-4918-11, 1978.

26. Starling, K.E., Fish, L.W., Iqbal, K.Z., and West, H.H., "The Use of Mixture Working Fluid in Geothermal Binary Power Cycles", 12th IECEC, 1, 850, 1977.

27. Iqbal, K.Z., Fish, L.W., Starling, K.E., "Advantages of Using Mixtures as Working Fluids in Geothermal Binary Cycles", Proc. Okla. Acad. of Sci., 1974.

28. Blake, G.L., Ed., "Semi-Annual Progress Report for Idaho Geothermal Program," INEL Report No. TREE-1278, July 1978.

29. Hankin, J.W., Hogue, R.A and Cassel, T.A.V., "Effect of Reservoir Temperature Decline on Geothermal Power Plant Design and Economics", 12th IECEC, 1, 870, 1977.

30. Lord, R.C., Minton, P.E., and Slusser, R.P., "Design of Heat Exchangers", Chemical Engineering, January 26, 1970.

31. DeGance, A.E., Atherton, R.W., "Phase Equilibria, Flow Regimes, Energy Loss", Chemical Engineering, April 20, 1970.

32. DeGance, A.E., et al., Chemical Engineering, October 5, 1970.

33. DeGance, A.E., et al., Chemical Engineering, March 23, 1970.

34. Allen, C.A. et al., "Liquid Fluidized-Bed Heat Exchanger Scale Control and Corrosion Tests", Proc. 13th IECEC, 1, 1109, 1978.

35. Allen, C.A. and Cole, C.T., "Liquid Fluidized-Bed Heat Exchanger Flow Distribution Models", Proc. 13th IECEC, 1, 1129, 1978.

36. Lord, R.C., et al., "Design Parameters for Condensers and Reboilers", Chemical Engineering, March 23, 1970.

37. Barbe, C., Roger, D., and Grange, A., Proc. 13th International Congress of Refrigeration, Washington, D.C., 2, 223, 1971.

APPENDIX A

APPENDIX A

DESIGN BASIS ENGINEERING PARAMETERS

As noted previously, the geothermal power plant can be divided into six primary process areas. Prior to detailed investigation of the sensitivity of various process parameters on thermodynamic or economic performance indicators, it is necessary to define all of the arbitrary process parameters used in the basic plant specification. The design basis specifications are simply a list of specific process parameters which were utilized in the project evaluation. Since there is no recommended set of design basis plant specifications yet developed by the geothermal industry to aid economic comparison, the selected process design parameters for each major process item are representative of available process equipment.

A 25 Mw net output was chosen as the base plant design. In order to meet this particular power output rating whole evaluation process alternatives, several key parameters are varied, including brine flow rate, cooling water flow rate, and working fluid flow rate.

The basic design parameters used in this study to define each major cycle process unit are detailed in Table A.1.

TABLE A-1

DESIGN BASIS ENGINEERING PARAMETERS

I. Brine Heat Exchanger

Type and Material of Construction:

shell and tube
horizontal
carbon steel construction

Shell:

single pass
ASME design pressure = 1.25 x max. operating pressure

Tube Bundle:

1.0 inch tube outside diameter
14 B.W.G.
1.4063 inch tube pitch
single pass

Other Selected or Assumed Parameters:

brine in tube side
working fluid in shell side
minimum allowable pinch point ΔT = 10°F
working fluid fouling factor = 0.0001
brine foulding factor = 0.002
velocity of brine through tubes = 7.0 ft/sec

Heat Transfer Coefficient Correlations:

1-phase	:	Dittus-Boelter	(1)
2-phase	:	Chen's boiling cor	(2)

Pressure Drop Correlations:

1-phase	:	Kern	(3)
2-phase	:	Degance	(4)

Friction Factor Correlations:

1-phase	:	Moody	(5)
2-phase	:	Starczewski	(6)

II. Condenser

Type and Material of Construction:

Shell and tube
horizontal
carbon steel construction

Table A-1 (continued)

Shell:

single pass
ASME design pressure = 1.25 x max. operating pressure

Tube Bundle:

1.0 inch tube outside diameter
14 B.W.G.
1.4063 inch tube pitch
single pass

Other Selected or Assumed Parameters:

cooling water in tube side
working fluid in shell side
minimum allowable pinch point ΔT = 10°F
working fluid fouling factor = 0.0001
cooling water fouling factor = 0.001
cooling water velocity through tubes = 7.0 ft/sec.

Heat Transfer Coefficient Correlations:

1-phase : Dittus-Boelter (1)
2-phase : Nusselt's top tube formula (1,7)

Pressure Drop Correlations:

1-phase : Kern (3)
2-phase : Degance (4)

Friction Factor Correlations:

1-phase : Moody (5)
2-phase : Starizewski (6)

III. Turbine

axial flow type
specific speed = 80
efficientcy of turbine-generator = 86%

Design Correlations:

turbine diameter, specific diameter, turbine wheel tip speed, RPM (8,9)

IV. Generator

efficiency of generator = 98%

Table A-1 (continued)

V. Working Fluid Pump

multi-stage centrifugal type
pump efficiency = 85%

VI. Brine System

equal number of brine production and
reinjection (or dry) wells
well casing diameter = 8.0 in.
brine flow rate per well = 500,000 lb/hr
brine pump efficiency = 85%
total brine system piping per
25 MW net power output = 5000 ft.

VII. Cooling System

mechanical draft cooling towers
wet bulb temperature range = 35-80°F
cooling temperature range ΔT = 10°-32°F
approach temperature = 8°F → variable
rating factor (R.F.) = 0.5 - 1.6
Design correlation : (10)

Tower Unit (TU) = GPM x R.F.
Fan Horsepower = 0.0125 BHP/TU
assumed value of R.F. = 1.0

TABLE A-2

DESIGN BASIS COST PARAMETERS

I. Power Plant

The factored estimate method described by Milora (11) and modified later (12) has been used:

$$C_t = \sum_i C_{ei}(1 + \sum_i f_i)(1 + \sum_j \bar{f}_j)$$

C_t = total capital investment in 1976 dollars

C_e = cost of major equipment (eg., heat exch., condenser, etc.)

f_i = factors for estimation of direct expenses, such as piping, control, etc.

$\bar{f}_j$ = factors for estimation of indirect expenses, such as fees, escalation, etc.

Cost Estimation Factors for Power Plant Used in GEO4

installation	0.50
instrument/control	0.15
piping/insulation	0.75
electrical	0.10
bldgs/structures/concrete	0.15
fire control	0.05
environment	0.05
land/improvement	0.10
start up	0.05
auxiliaries	0.10
Total Direct $(1 + \Sigma f_i)$	3.00
engineering/legal	0.15
contingency	0.10
working capital	0.15
environmental/safety	0.10
overhead/escalation	0.15
Total Indirect $(1 + \Sigma \bar{f}_j)$	
TOTAL	4.95

Table A-2 (continued)

I-a Heat Exchanger and Condenser

Cost Correlation:

$$\ln(\$/ft^2) = A \ln (P_{xhell}) - B \qquad (13)$$

where
for tube side pressure of 200-300 psia,
A=0.4383, B=0.1297
for tube side pressure of 300-1000 psia,
A=0.4092, B=0.0.3744
for tube side pressure of 1000-2000 psia,
A=0.3461, B=1.046

Note: The cost of condenser in ($/ft^2) is same for shell side pressure $\leq$ 50 psia.

I-b Turbine

Turbine cost based on Barber-Nichols Company (14,13)

$$C_{tur} = (1.04\ N_e - 0.04\ N_e^2) f_p (2.4858 \times 10^3\ \eta_s\ f_u\ D_T^{2.1}) + 4.7494 \times 10^2\ D_T^3 + 1.9248 \times 10^3\ D_T^2$$

where
C_{tur} = turbine cost in dollars
N_e = number of exhaust ends
η_s = number of internal stages (Pr/stage $\simeq$ 0.7)
D_T = last stage pitch diameter
f_u = cost multiplier for tip speed, V_T, ft/sec.
f_p = cost multiplier for inlet pressure

$$f_u = -2.469 + 0.009\ V_T - 7.991 \times 10^{-6}\ V_T^2 + 2.446 \times 10^{-9}\ V_T^3$$

$$f_p = 6.2857 \times 10^{-5}\ P_{max} + 0.9707$$

Note: The equation for C_{tur} is considered to be valid for h/D_T (last stage blade height to pitch diameter) values up to 0.11.

Table A-2 (continued)

I-d Working Fluid Pump

Cost correlation is a function of pump power rating (11,13)

$$\ln (\$) = 0.8751 \ln (MW_e) + 11.0$$

where

MW_e = working fluid pump power rating in mega watts

I-e Cooling Tower

Cost of Cooling Tower in dollars = 3.33 TU (10)

II. Brine System

The factored estimate method described by Milora (11) has been used:

$$C_B = \eta_w C_w (1 + f_w)(1 + f^*_I)$$

C_B = total brine system capital investment

C_w = cost of a geothermal production and/or reinjection well

η_w = number of wells required for a particular size plant

f_w = factor which accounts for piping from the wellhead to the power plant

f^*_I = indirect cost factors, eg., costs associated with drilling exploratory holes, contingencies, etc.

Cost Estimation Factors for Brine System used in GEO4

piping (wellhead to plant)	0.24
Total Direct (1t f_w)	1.24
land acquisiting (leasing, legal fees)	0.19
drilling exploratory holes (1 out of 4 successful)	0.14
surface exploration (geophysical-geochemical)	0.10
contingency	0.13
Total Indirect (1 + f^*_I)	1.56
TOTAL	1.934

Table A-2 (continued)

well cost:

a well cost (C_w) of $500,000/well was used with a brine flow rate of 500,000 lb/hr per well.

REFERENCES

1. McAdams, W.H., Heat Transmission, 3rd ed. McGraw-Hill Book Company, New York, 1954.

2. Tong, L.S., Boiling Heat Transfer and Two-Phase Flow, John Wiley and Sons Inc., New York, 1965.

3. Kern, D.Z., Process Heat Transfer, McGraw-Hill Book Company, New York, 1950.

4. Degance, A.C., Atherton, R.W., Chemical Engineering, March 23, 1970.

5. Moody in Parker, J.D. et.al., Introduction to Fluid Mechanics and Heat Transfer, Addison-Wesley Pub., p. 232, 1969.

6. Starczewski, J., Hydrocarbon Processing, p. 147, June, 1971.

7. Short, B.E., and Brown, H.E., 27, "General Discussion on Heat Transfer", London ASME, New York, 1951.

8. Anderson, J.H., Report No. NSF/RANN/SE/GI-34979/7317, University of Massachusetts, May, 1973.

9. Anderson, J.H., Report No. NSF/RANN/SE/GI-34979/3717, University of Massachusetts, June, 1973.

10. West, H.H., "Private Communication, Energy Analysts Inc., Norman, Oklahoma, 1977.

11. Milora, S.L. and Tester, J.S., Geothermal Energy as a Source of Electric Power, MIT Press Cambridge, Mass., 1976.

12. Starling, K.E. et.al., "Resource Utilization Efficiency Improvement of Geothermal Binary Cycles", ORO-4944-5, University of Oklahoma, June 15 - December 15, 1976.

13. Starling, K.E., et.al., "Resource Utilization Efficiency Improvement of Geothermal Binary Cycles", ORO-4944-3, University of Oklahoma, June 15 - December 15, 1975.

14. Nichols, K.E., "Turbine Prime Mover Cost Model Empirical Equation, P.O. 11Y-49428V", Barber-Nichols Engineering Co., Awada, Colorado, March, 1975.

APPENDIX B

APPENDIX B

FIXED PLANT SIMULATION MODIFICATION TO GEO4 SIMULATOR

The original motive behind this modification of the GEO4 simulator was to simulate as closely as possible fixed plant operation without extensive modification of GEO4. To accomplish this objective, the following parameters for the brine heat exchanger and condenser are specified as input:

(1) Heat transfer surface areas

(2) Shell inside diameter

(3) Number of tubes

For the remaining major equipment units (turbine, pumps, cooling tower) equipment sizes are not fixed, but are determined just as if the simulator were in a design mode rather than a fixed plant mode. This does not seriously limit the usefulness of the program in the fixed plant mode for studies of the effects of changes in georesource temperature, working fluid composition and other parameters, when the changes are not too large.

The fixed heat transfer surface area referred to here as fixed plant simulation, is controlled by the optimization control parameter "NOPT" and the areas. The main features

of this modification are as follows:

(1) When NOPT=0 and the areas are input as non-zero, the brine flow rate as specified in input remains unchanged. The approach temperature differences and the fluid pressure drops are then updated iteratively as follows:

$$DTHWO_{i+1} = \frac{A_{BHE}^{calc}}{A_{BHE}^{spec}} \; DTHWO_i \qquad (1)$$

$$DTCWO_{i+1} = \frac{A_{cond}^{calc}}{A_{cond}^{spec}} \; DTCWO_i \qquad (2)$$

and

$$DTCWI_{i+1} = \frac{A_{cond}^{calc}}{A_{cond}^{spec}} \; DTCWI \qquad (3)$$

No fluid pressure drop updating is needed if

$$\left| \frac{DP_{input} - DP_{calc}}{DP_{calc}} \right| \leq EPSDPW \qquad (4)$$

where the subscripts i and i+1 refer, respectively, to the iteration numbers i and i+1 and where

A_{BHE}^{calc} = Calculated brine heat exchanger area, ft^2

A_{BHE}^{spec} = Input specified value of BHE area, ft^2

A_{cond}^{calc} = Calculated condenser area, ft^2

A_{cond}^{spec} = Input specified value of condenser area, ft^2

DP_{input} = Fluid pressure drops in input, psia

DP_{calc} = Calculated fluid pressure drops, psia

EPSDPW = Convergence criteria for fluid pressure drops

DTHWO, DTCWO, DTCWI = Approach temperature differences in BHE and condenser

(2) When NOPT=-1 and the areas are input as non-zero, the brine flow rate, approach temperature differences, and fluid pressure drops are all updated in order to match the specified net power. This option in its present form takes an excessive amount of time for convergence and has not been used.

The details of these modifications is provided in the subroutines where such changes were made. However, there are some other features of this modification which need to be mentioned here in order to understand the results from this simulator. First of all, only one heat exchanger subroutine (using the single-phase heat transfer correlation) and one condenser subroutine (using the condensing heat tranfer correlation) are used regardless of the turbine inlet pressure

(whether subcritical or supercritical). This means that for subcritical cycles, the heat exchanger and condenser must be divided into a large number of sections (with respect to temperature) to obtain reasonable results.

In GEO4 simulator, the number of sections are controlled by input parameters, so that a maximum of 75 heat exchanger sections and a maximum of 20 condenser sections can be used. Since only single phase heat transfer correlation in brine heat exchanger is used, and working fluid flow rate cannot be fixed by the simulator, the values of heat tranfer coefficient and the net power will be slightly in error.

SUBROUTINE CONDSR

1. Insert common block XF for brine heat exchanger and condenser area inputs:

```
COMMON /XF / AREAE,AREAC                                    CNR 3150
```

2. Insert card number CNR 6650 for fixed plant simulation control and add a procedure step* CNR-11-a as follows:
CNR-11-a If the BHE (brine heat exchanger) and condenser areas are greater than zero, go to procedure step CNR-46.

```
IF ((AREAE+AREAC).GT.0.0) GO TO 2800                        CNR 6650
```

---

* The procedure steps correspond to the GEO4 simulator documentation (a published report) below:

Starling, K.E., Iqbal,K.Z., Fish, L.W., et al., "GEO4, A Geothermal Binary Cycle Simulator", Technical Report, Prepared for the U.S. Department of Energy, University of Oklahoma Report No. OU/ID-1719-1, December 31, 1978.

SUBROUTINE CONDTP

1. Insert common block XF for BHE and condenser areas.

```
      COMMON /XF / AREAE,AREAC                                    CNT 2950
```

2. Insert card number CNT 5950 for fixed plant simulation control.

```
      IF ((AREAE + AREAC).GT.0.0) GO TO 550                       CNT 5950
```

3. Replace card number CNT 6200 for the change made above.

```
  550 DO 600 I=2,K45                                              CNT 6200
```

4. Insert or replace the following cards for fixed plant simulation control.

```
      IF ((AREAE + AREAC).GT.0.0) GO TO 1350                      CNT 9910
 1350 DO 1400 I=2,K45                                             CNT10200
      IF ((AREAE + AREAC).GT.0.0) GO TO 2200                      CNT12650
      IF ((AREAE + AREAC).GT.0.0) GO TO 3400                      CNT21150
```

SUBROUTINE CYCLE

1. Insert common block XF for BHE and condenser areas.

```
      COMMON /XF / AREAE,AREAC                                    CYC 3250
```

2. Insert the following cards for fixed plant simulation control.

```
      IF ((AREAE + AREAC).GT.0.0) GO TO 1000                      CYC14750
      IF ((AREAE + AREAC).LE.0.0) GO TO 1350                      CYC18510
```

3. Insert card numbers CYC 18520 - CYC 18570 to initialize working fluid properties at the condenser inlet.

```
      TWF4=TWF3                                                    CYC18520
      PWF4=PWF3                                                    CYC18530
      HWF4=HWF3                                                    CYC18540
      SWF4=SWF3                                                    CYC18550
      DWF4=DWF3                                                    CYC18560
      VAPWF4=VAPWF3                                                CYC18570
 1350 PWF5=PWF3-DPWF35                                             CYC18700
```

4. Replace card number CYC 18700 to take care of the program internal sequence of calculations.

```
 1350 PWF5=PWF3-DPWF35                                             CYC18700
```

SUBROUTINE INOUT

Insert the following cards to take care of the new variables (i.e., BHE and condenser areas) input/out transfer.

```
      COMMON /XF/ AREAE,AREAC                                      INO 3450
      WRITE (6,7750) AREAE                                         INO11150
      WRITE (6,8950) AREAC                                         INO12350
 7750 FORMAT (T34,'BHE AREA (SQ.FT.)',T65,'AREAE',G17.6            INO35350
 8950 FORMAT (T34,'CONDENSER AREA (SQ.FT.)',T65,'AREAC',G17.6)     INO36550
```

SUBROUTINE INPUT

Insert/Replace the following cards to read/write two new variables (i.e., BHE and condenser areas) and for input/output tranfer.

```
      COMMON /XF/ AREAE,AREAC                                          INP 3350
      READ (5,1900)  DTPHI,DTPHO,AREAE,AREAC                           INP 8300
      WRITE (6,5600) DTPHI,DTPHO,AREAE,AREAC                           INP 8400
 5500 FORMAT (3X,5F10.2,3G10.2)                                        INP23100
C                                                                      INP23150
 5600 FORMAT (/4X,'DTPHI    DTPHO      AREAE     AREAC'/,2F10.4,       INP23200
     12G13.5)                                                          INP23250
```

SUBROUTINE MHWOPT

1. Insert common blocks DN, EF and XF for input/output tranfer.

```
      COMMON /DN/ FOULC,FOULEV,FOULHW,FOULCW,GC,DISEV,DISCND,STRESS,COR,MHW  910
     1DTHWO,MWF,NTUBEC,NTUBEV,NTPASS                                  MHW  920
      COMMON /EF/ EFFT,EFFC,EFFHWP,EFFCWP,VELCW,VELHW,PIPLCW,PIPLHW    MHW 1410
      COMMON /XF/ AREAE,AREAC                                          MHW 3250
```

2. Insert card numbers MHW 4510 - 4540 for fixed plant simulation control. Replace card number MHW 4600 for this change and revise procedurd step MHW-4 as follows:

   MHW-4 If BHE and condenser areas are nonzero and NOPT is zero, then set MRATION (ration of brine flow rates in two successive iterations) equal to

1.0, go to MHW-7. If I, the iteration counter for ITMAX, is greater than two, go to MHW-6 (MHW 4500 - MHW 4600)

```
      IF ((AREAE+AREAC).EQ.0.0) GO TO 250                    MHW 4510
      IF (NOPT.NE.0) GO TO 250                               MHW 4520
      MRATIO=1.0                                             MHW 4530
      GO TO 400                                              MHW 4540
  250 IF (I.GT.2) GO TO 300                                  MHW 4600
```

3. Insert card number MHW 5650 for fixed plant simulation control.

```
      IF ((AREAE+AREAC).GT.0.0) GO TO 500                    MHW 5650
```

4. Insert card numbers MHW 7810 - MHW 7860 for fixed plant simulation control. Replace card number MHW 7900 for this change and revise procedure step MHW-15 as follows:

   MHW-15 If BHE and condenser areas are nonzero and NOPT is not equal to zero, revise brine and cooling water velocities. The message "Parameters being changed", write pinch and approach temperature differences, and write the message "brine flow rate and pressure drops do not converge in ITMAX iterations". (MHW 7700 - MHW 7900)

```
      IF ((AREAE+AREAC).EQ.0.0) GO TO 1050                   MHW 7810
      WRITE (6,1700)                                         MHW 7820
      WRITE (6,1800)  DTHWO,DTCWO,DTCWI                      MHW 7830
      IF (NOPT.EQ.0) GO TO 1050                              MHW 7840
      VELHW=VELHW*MRATIO                                     MHW 7850
      VELCW=VELCW*MRATIO                                     MHW 7860
 1050 CALL CYCLE                                             MHW 7900
```

5. Insert following format statements for the above change.

```
1700 FORMAT (////4X,'***** PARAMETERS BEING CHANGED')                    MHW 9210
1800 FORMAT (/10X,'DTHWO = ',F10.4,/10X,'DTCWO = ',F10.4,/10X,'DTCWI = MHW 9220
     1',F10.4,//)                                                       MHW 9230
```

SUBROUTINE OPTIM

Revise procedure step OPT-2 and replace card number OPT 2400 as follows:

OPT-2 Call MHWOPT. Return (OPT 2300 - OPT 2500)

```
      CALL MHWOPT                                                       OPT 2400
```

SUBROUTINE RESLT

1. Insert common blocks DT and XF for input/output transfer.

```
      COMMON /DT/ DTWF12,DTWF56,DTWF78,DTCWI,DTCWO,DTHWI,VMIN           RES 2750
      COMMON /XF/ AREAE,AREAC                                           RES 5650
```

2. Insert card number RES 14950 for fixed plant simulation control.

```
      IF ((AREAE+AREAC).GT.0.0) GO TO 400                               RES14950
```

3. Revise procedure step RES-25 as follows:

RES-25 If optimization control is zero, go to RES-28

Replace card number RES 15500

```
  500 IF (NOPT.EQ.0) GO TO 510                                          RES15500
```

4. Replace card number RES 15700 and revise procedure step RES-27

   RES-27 If the work ratio is greater than the plant power convergence criteria and BHE and condenser areas are not greater than zero, go to RES-47

```
IF (DABS(WRATIO).GT.EPSW.AND.(AREAE+AREAC).LE.0.0) GO TO 1000     RES15700
```

5. Replace card number RES 15800 due to change in RES-25.

```
510 IF (DTPHI.GT.0.0.AND.DTPHO.GT.0.0) GO TO 600                  RES15800
```

6. Insert card numbers RES 15810 - RES 15830. Add procedure step RES-28-A

   RES-28-A If BHE and condenser areas are both zero, go to step 8; otherwise calculate area ratios of total BHE and condenser areas to the calculated areas.

```
IF ((AREAE+AREAC).EQ.0.0.) GO TO 580                              RES15810
RAEV =TOTAEV/AREAE                                                RES15820
RACND=TOTAC/AREAC                                                 RES15830
```

7. Insert card numbers RES 15840 - RES 15890 and add procedure step RES-28-B

   RES-28-B If the surface area convergence criteria is satisfactory, go to RES- , otherwise updated pinch and approach temperature differences; go to RES-47.

```
      IF (DABS(1.-RAEV).LE.0.005.AND.DABS(1.-RACND).LE.0.005) GO TO 650 RES15840
      DTHWO=RAEV*DTHWO                                                  RES15850
      DTCWO=RACND*DTCWO                                                 RES15860
      DTCWI=RACND*DTCWI                                                 RES15870
C                                                                       RES15880
C                                                                       RES15885
      GO TO 1000                                                        RES15890
```

8. Insert/Replace following cards due to internal statement changes.

```
  580 IF (NOPT.EQ.0) GO TO 1200                                         RES15895
      IF ((TWF3-1.).LE.TDEWF4) GO TO 700                                RES15900
  650 IF (NOPT.EQ.0) GO TO 700                                          RES16710
```

9. Insert/Replace following cards to take care of additional internal statement changes for fixed plant simulation control.

```
      IF (DABS(WRATIO).GT.EPSW) GO TO 1000                              RES16720
      IF ((AREAE+AREAC).GT.0.0) GO TO 2500                              RES28150
      IF ((AREAE+AREAC).GT.0.0) GO TO 2900                              RES30550
 3000 IF ((AREAE+AREAC).GT.0.0) GO TO 3050                              RES33300
 3050 DOTUBE=DOTUBE/12.                                                 RES33800
      IF (NOPT.EQ.0) WRATIO=0.0                                         RES33950
```

APPENDIX C

APPENDIX C

PROCEDURE USED FOR THE DUAL BOILER BINARY CYCLE PRELIMINARY CALCULATIONS

Step-1. Fix the following state points and parameters:

a) Brine Inlet Temperature = 290°F

b) Brine Outlet Temperature = 140°F (initial guess)

c) Cooling water inlet and outlet temperatures as 75° and 95°F

d) Turbine, cycle pump and other process pump efficiencies as 100%

e) Pinch point temperature differences:

DTHWO = DTCWO = DTCWI = 5°F

f) Turbine inlet temperature of working fluid for high pressure (H.P.) cycle to be 240°F. Note that this temperature is only an initial guess to be used for drawing a brine profile on a T-$\underline{H}$ diagram.

g) Zero viscous pressure drops

h) Brine Flow Rate (M_{HW}) = 1.04 x 10^6 lb_m/hr

Step 2. Choose a working fluid composition.

Step 3. Locate the brine inlet and outlet state points on a T-H diagram as follows:

a) Brine Outlet Location

Pure Fluids:

(i) Add DTCWO and TCW10 to get the dew point temperature (D.P.T.), and hence bubble point temperature (B.P.T.) of the pure fluid.

(ii) On a T-H diagram, mark the B.P.T. and then mark another point on the saturated liquid locus approximately 1° higher than the B.P.T. (this point represents the compressed liquid). Draw a vertical line from this point and locate the brine exit temperature on this vertical line.

Mixtures:

(i) Add DTCWI and TCW9 to get the B.P.T. of the mixture.

(ii) Repeat step (3a-ii) above to locate the brine exit temperature on a T-H diagram

b) Brine Inlet Location

(i) On the T-H diagram of the working fluid mark the turbine inlet temperature as a D.P.T. (or slightly superheated)

(ii) Find the brine inlet temperature location on the T-H diagram in a way similar to step (3a-ii)

Step-4. Draw a straight line by joining the brine inlet and outlet temperatures to get the brine profile through the brine heat exchanger.

Step-5. On a T-H diagram for a fixed DTHWO locate a B.P.T., T_{BP}, on the saturated liquid locus of the working fluid such that $(T_{Brine} - T_{BP}) = (DTHWO + 10°F)$. Then read/calculate B.P.P. and then read/calculate D.P.T. corresponding to B.P.P. (=D.P.P.)

Step-6. a) Using D.P.T. + t (where t is a very small value less than 2°) as the turbine inlet temperature and D.P.P. as turbine inlet pressure, make a Low Pressure Cycle run using GEO4 simulator.

b) Use the above output to get property value of state point 8'

c) Choose a vapor/liquid split (e.g., 40 mole per vapor and 60 mole percent liquid) from the detailed computer output and get property values at state points 1", 1' and 6

d) Use the above V/L split to calculate the working fluid flow rates for the H.P. and L.P. cycles (M_{WF}^{V} and M_{WF}^{L} respectively).

Step-7. Make a few hand calculations to determine optimum turbine inlet temperature and pressure for the H.P. cycle as follows:

a) From the T-$\underline{H}$ diagram read enthalpies of working fluid at turbine inlet temperature ($\underline{H}_1$) and at B.P.T. ($\underline{H}_{BP}$).

b) Calculate brine temperature (T_B') corresponding to the T_{BP} as follows:

$$T_B' = 290 - \frac{M_{WF}^L \times (\underline{H}_1 - \underline{H}_{BP})}{M_{HW}}$$

c) If $(T_B' - T_{BP}) = (DTHWO + 2)$, proceed to step-8. Otherwise go to next sub-step (d)

d) If $(T_B' - T_{BP})$ DTHWO, decrease D.P.T. (or turbine inlet temperature) by an amount equal to violation plus DTHWO then go back to sub-step (a)

e) If $(T_B' - T_{BP})$ $(DTHWO + 2)$, then increase D.P.T. (or turbine inlet temperature) by a corresponding amount then go back to sub-step (a)

Step-8. a) Make a H.P. cycle run using the simulator with turbine inlet conditions from step 7-c, and working fluid composition from step 6-d

b) Calculate T_B' using property values from (a) in a manner similar to step 7-b

c) Calculate brine temperature corresponding to state point 8, T_B'', using additional property values from step 6-c, as follows:

$$T_B'' = T_B' - \frac{H_{WF}^L \times (H_{BP} - H_8)}{M_{HW}}$$

where

H_8 = Working Fluid enthalpy at state point 8.

d) For supercritical operation, divide heat exchanger H into at least three sections and repeat steps 7 and 8.

e) Use T''_B as brine inlet temperature for the L/P cycle to calculate, by hand, the brine exit temperature from L/P boiler. Draw the overall brine profile on a T-$\underline{H}$ diagram. If the brine profile violates the pinch point criterion in the L/P loop, revise the turbine inlet temperature accordingly and go back to step 6.

Step-9. a) Make a L.P. cycle run using the GEO4 simulator as follows:

(i) Use T''_B as brine inlet temperature

(ii) Get turbine inlet temperature from step 6-c

b) Write down all property values of the working fluid on the dual boiler binary cycle diagram or make a table

Step-10. a) Calculate turbine work, pump work, boiler, and condenser duties for the H.P. and L.P. loops.

b) Calculate cycle efficiencies

Step-11. Repeat the whole procedure for non-zero values of

viscous pressure drops by assuming fixed values of viscous pressure drops, if so desired

Step 12. Repeat the whole procedure for other potential working fluids.

Methodology for the Preliminary Calculations

Pure Fluid Dual Boiler Cycle

A detailed procedure for the pure fluid dual boiler binary cycle calculation is already provided in pages 1 thru 6 of this Appendix. Therefore, only a brief summary of some of the important steps will be discussed here.

Figure 1.0 shows a temperature-enthalpy diagram of cis-2-Butene. Since no viscous pressure drops are assumed, the boiling and condensing profiles through the heat exchanger and condenser respectively will be isothermal. Keeping this fact in mind, and using fixed parameter values from step 1, the dew point temperature (D.P.T.) of cis-2-Butene in the condenser is obtained as 100°F which is also equal to its bubble point temperature (B.P.T.), as shown in Figure 1.0. Thus, brine outlet temperature location is marked following the procedure outlined in step 3a-(ii). Similarly mark the brine inlet temperature location corresponding to the D.P.T. of 240°F in the evaporator as shown in Figure 1.0. The initial brine profile in the brine heat exchanger would then be

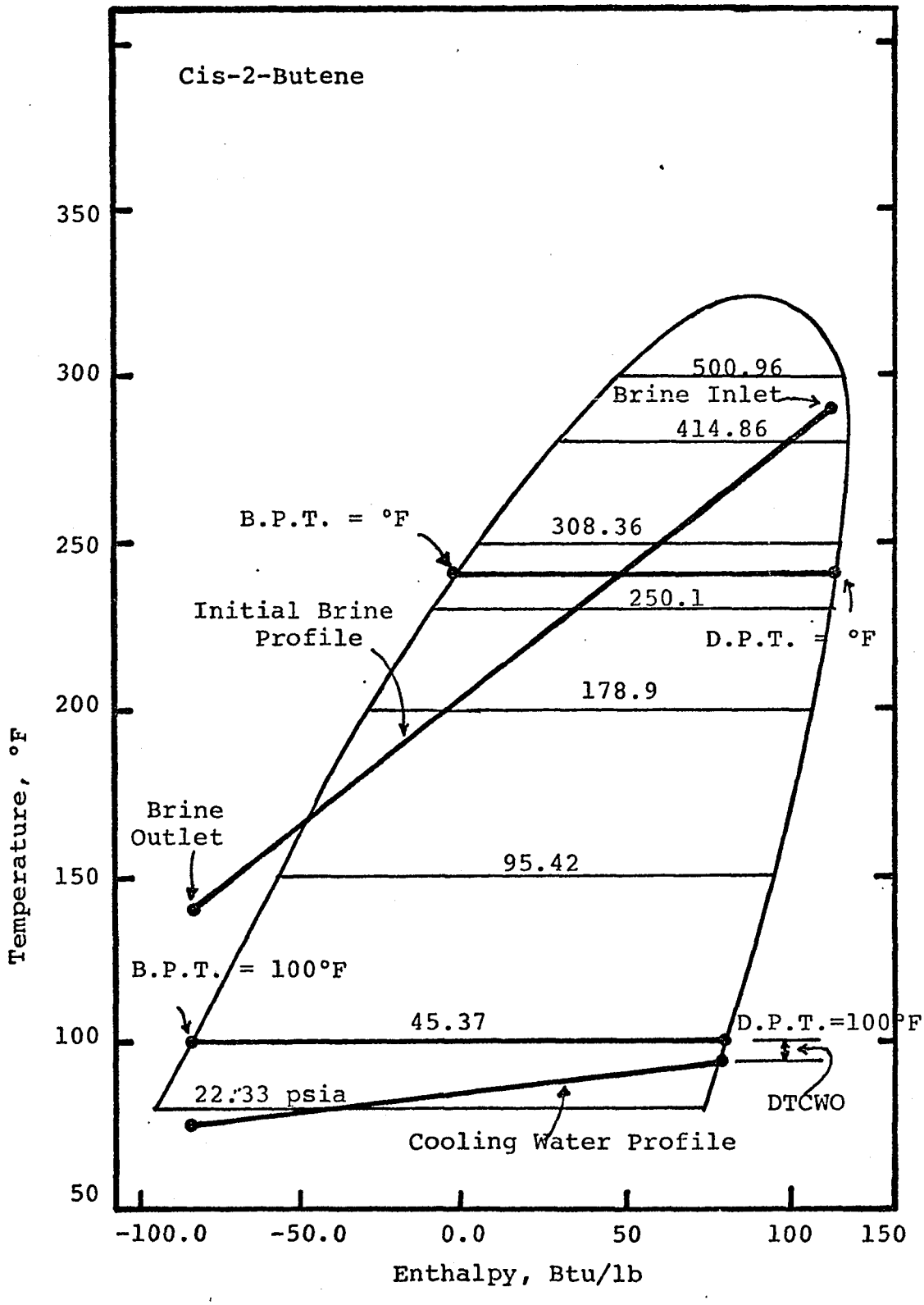

Figure C-1 Steps 3 and 4 Shown for a Pure Fluid, Cis-2-Butene, Cycle

represented by a straight line obtained by joining the brine inlet and outlet temperature.

Since the objective here is the maximization of net plant work per unit mass of brine, one would like to select the highest temperature and pressure conditions at turbine inlet (or heat exchanger outlet) without violating the pinch criterion in the heat exchanger. For subcritical operation, the pinch usually occurs at the B.P.T. of the working fluid in the heat exchanger. For a given value of the pinch point temperature difference, DTHWO, locate the B.P.T. and hence D.P.T. of the working fluid in boiler 1 as shown in Figure 2.0. Using bubble point pressure (B.P.P.) as the turbine inlet pressure and following step 6, first low pressure cycle calculation can either be done by hand for a pure fluid or with the help of a single boiler binary cycle simulator, as was done in this study. A suitable vapor-liquid split can then be chosen to calculate the working fluid flow rates for the high and low pressure cycle, thus completing step 6.

A turbine inlet temperature of 240°F was chosen as a first trial value for the high pressure cycle, as shown in Figure 2.0. Then the brine temperature corresponding to the B.P.T. of the working fluid, T_B', was calculated as outlined in step 7-b. However, a turbine inlet temperature of 218°F was found as an optimum temperature after two hand calculations as discussed in step 7-d and 7-e. The GEO4 simulator

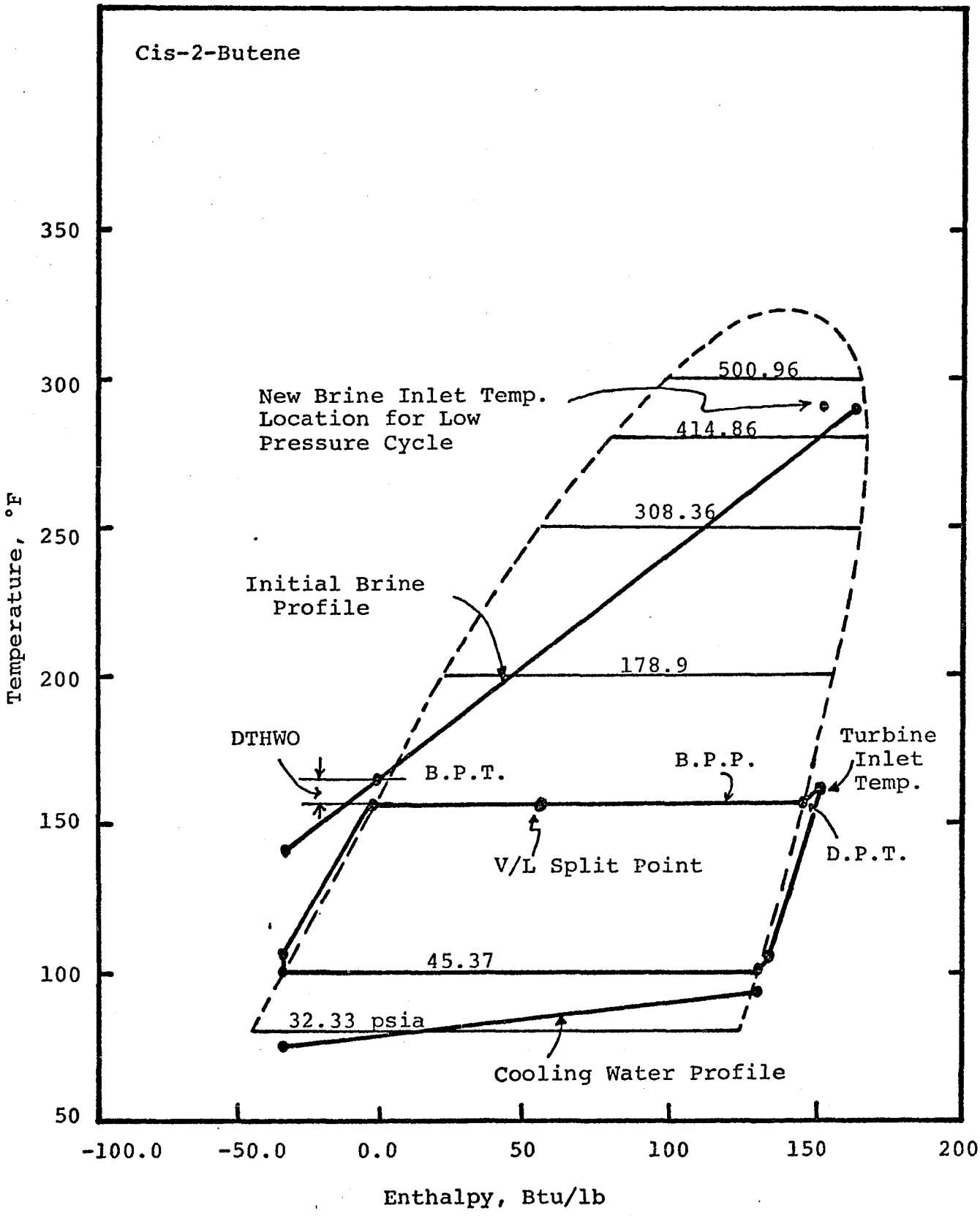

Figure C-2 Steps 5 and 6 Shown for a Pure Fluid Cycle

was used again at this step for the high pressure cycle calculation. It may be mentioned here that the turbine inlet pressure was chosen as the dew point pressure (D.P.P.) at 218°F for the cis-2-Butene high pressure cycle. Now a hand calculation can be made to calculate the brine temperature, T''_B, corresponding to the working fluid temperature at state point 8. Since for a pure fluid, the vapor and liquid phase compositions do not change in step 6-c, step 9-a is not needed. This is clearly shown in Table 1 which shows thermodynamic cycle state points for cis-2-Butene dual boiler cycle calculations.

Steps 10 thru 12 can now be carried out as required.

Mixture Fluid Dual Boiler Cycle

The overall procedure for a mixture dual boiling binary cycle calculation is more or less similar to that of a pure fluid cycle. However, due to the fact that at constant pressure the mixtures vaporize and condense nonisothermally, a few additional calculations are required for a mixture cycle.

Figure 3.0 shows a temperature-enthalpy diagram of a mixture of 60 mole percent cis-2-Butene and 40 mole percent cyclopentane. Since for this mixture, the pinch occurs at the condenser outlet end, the pinch point temperature difference, DTCWI, is added to the cooling water inlet temperature, TCW9, to get the B.P.T. of the mixture. The brine

Table C-1

THERMODYNAMIC CYCLE STATE POINTS

Initial Working Fluid: Cis-2-Butene (0.9999), Cyclopentane (0.0001)
Vapor Liquid Split in Boiler 2, % = 40/60

State Point	Location	Temperature (°F)	Pressure (psia)	Enthalpy (Btu/lb_m)	Entropy (Btu/lb_m °R)
	LOW PRESSURE CYCLE: [Z_1 = 1.0 ; Z_2 = 0.0]				
1"	Boiler 2 Outlet	156.04	104.30	55.578	1.105
8'	Boiler 2 Inlet	100.13	104.30	-33.472	0.958
8'	Bubble Point	156.03	104.30	- 3.3018	1.009
	LOW PRESSURE CYCLE: [Z_1 = 1.0 ; Z_2 = 0.0]				
1'	Separator Outlet	156.04	104.30	143.9	1.248
2'	Turbine 2 Inlet	156.04	104.30	143.9	1.248
3'	Turbine 2 Outlet	100.10	45.89	128.81	1.249
4'	Condenser 2 Inlet	100.10	45.89	128.81	1.249
4'	Dew Point	100.00	45.89	128.77	1.249
5'	Condenser 2 Outlet	99.80	45.89	-33.762	0.958
6'	Cycle Pump 2 Inlet	99.80	45.89	-33.762	0.958
7'	Cycle Pump 2 Outlet	100.01	104.3	-33.472	0.958
	HIGH PRESSURE CYCLE: [Z_1 = 1.0 ; Z_2 = 0.0]				
1	Boiler 1 Outlet	218.00	220.44	159.02	1.251
2	Turbine 1 Inlet	218.00	220.44	159.02	1.251
3	Turbine 1 Outlet	103.13	45.89	129.94	1.251
4	Condenser 1 Inlet	103.13	45.89	129.94	1.251
4	Dew Point	100.00	45.89	128.72	1.249
5	Condenser 1 Outlet	99.80	45.89	-33.762	0.958
6	Cycle Pump 1 Inlet	156.04	104.30	- 3.302	1.009
6"	Cycle Pump 3 Inlet	99.80	45.89	-33.762	0.958
7	Cycle Pump 3 Outlet	156.34	104.30	- 2.688	1.009
7"	Cycle Pump 3 Outlet	100.77	220.44	-32.897	0.958
8	Boiler 1 Inlet	156.34	104.30	- 2.688	1.009
8	Bubble Point	218.00	220.44	34.025	1.0066

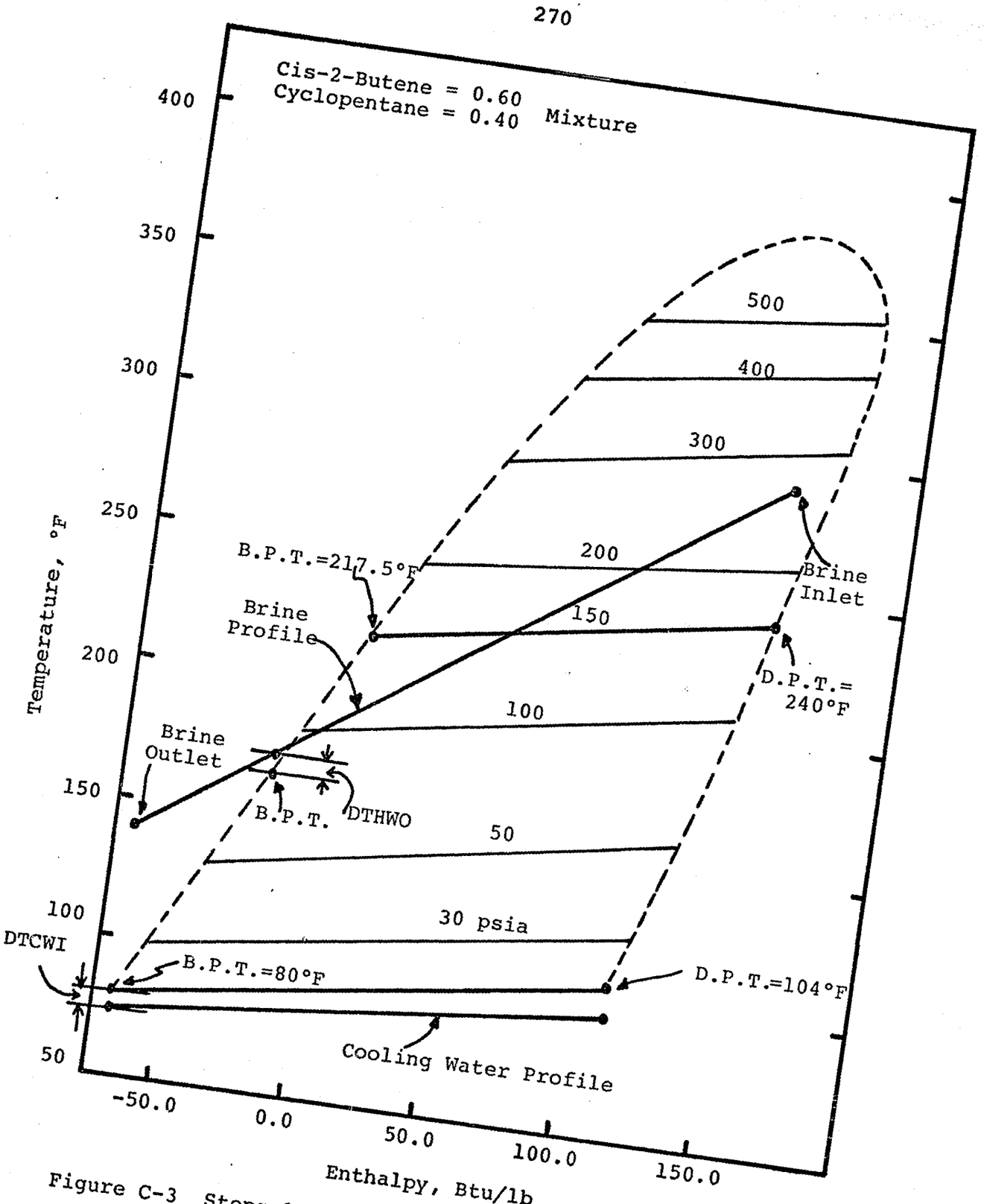

Figure C-3 Steps 3, 4, and 5 Shown for a Mixture Fluid Cycle

inlet and outlet temperature location is then determined in a manner similar to the pure fluid and is marked on the T-$\underline{H}$ diagram as illustrated in Figure 3.0. The brine profile is drawn next followed by a B.P.T. of the working fluid as outlined in step 5. Since mixtures vaporize nonisothermally at a constant pressure (less than the critical pressure of the mixture), a B.P.P. is calculated at the B.P.T. determined before this step. Then a D.P.T. @ B.P.P. is calculated. This completes the procedure up to step 5.

The next step is the use of GEO4 simulator to make a low pressure cycle calculation. A suitable vapor-liquid split (39/61 herein) can then be chosen to calculate the working fluid flow rates for the high and low pressure cycles. The vapor-liquid split choice also determines the liquid and vapor phase working fluid compositions for the high and low pressure cycles. The vapor-liquid split choice also determines the liquid and vapor phase working fluid compositions for the high and low pressure cycles respectively. For example, for a V/L split of 39/61, the working fluid vapor (low pressure cycle) and liquid phase (high pressure cycle) compositions are shown in Table 2, and are given below:

	cis-2-Butene (Mole Fraction) Z_1	Cyclopentane (Mole Fraction) Z_2
Low Pressure Cycle	0.758	0.242
High Pressure Cycle	0.50	0.50

Table C-2

THERMODYNAMIC CYCLE STATE POINTS

Initial Working Fluid: Cis-2-Butene (0.60), Cyclopentane (0.40)
Vapor Liquid Split in Boiler 2, % = 38.6/61.4

State Point	Location	Temperature (°F)	Pressure (psia)	Enthalpy (Btu/lb_m)	Entropy (Btu/lb_m°R)
	LOW PRESSURE CYCLE: [Z_1 = 0.60 ; Z_2 = 0.40]				
1"	Boiler 2 Outlet	175.40	81.40	43.490	1.023
8'	Boiler 2 Inlet	80.26	81.40	-61.660	0.851
8'	Bubble Point	166.00	81.40	-19.024	0.924
	LOW PRESSURE CYCLE: [Z_1 = 0.758 ; Z_2 = 0.242]				
1'	Separator Outlet	175.40	81.40	142.880	1.211
2'	Turbine 2 Inlet	175.40	81.40	142.880	1.211
3'	Turbine 2 Outlet	104.22	26.20	122.060	1.211
4'	Condenser 2 Inlet	104.22	26.20	122.060	1.211
4'	Dew Point	104.29	26.20	122.400	1.212
5'	Condenser 2 Outlet	80.00	26.20	-55.357	0.889
6'	Cycle Pump 2 Inlet	80.00	26.20	-55.357	0.889
7'	Cycle Pump 2 Outlet	80.26	81.40	-55.103	0.889
	HIGH PRESSURE CYCLE: [Z_1 = 0.50 ; Z_2 = 0.50]				
1	Boiler 1 Outlet	240.00	132.00	153.740	1.159
2	Turbine 1 Inlet	240.00	132.00	153.740	1.159
3	Turbine 1 Outlet	119.23	19.30	118.520	1.159
4	Condenser 1 Inlet	119.25	19.30	118.520	1.159
4	Dew Point	109.90	19.30	115.350	1.153
5	Condenser 1 Outlet	80.00	19.30	-65.766	0.827
6	Cycle Pump 1 Inlet	175.40	81.40	-18.938	0.905
6"	Cycle Pump 3 Inlet	80.00	19.30	-65.766	0.827
7	Cycle Pump 1 Outlet	175.70	132.00	-18.703	0.905
7"	Cycle Pump 3 Outlet	80.27	81.40	-65.502	0.827
8	Boiler 1 Inlet	175.70	132.00	-18.703	0.905
8	Bubble Point	214.95	132.00	2.852	0.939

Table 2 also gives the final thermodynamic cycle state points for this mixture for the high and low pressure cycle, by following the procedure outlined in steps 7 thru 9 and discussed in section on pure fluids. Thus steps 10 thru 12 can now be carried out if so desired.

APPENDIX D

```
**********************************
*  THERMAL ENERGY CONVERSION     *
*       SIMULATOR GEO-4          *
*          DEVELOPED BY          *
*        KHAN ZAFAR IQBAL        *
*          LARRY W. FISH         *
*       KENNETH E. STARLING      *
*      UNIVERSITY OF OKLAHOMA    *
*      NORMAN, OKLAHOMA 73019    *
*          JANUARY 1977          *
**********************************
```

TCW9	TCW10	THW11	THW12	PCW9	PCW10	PHW11	PHW12
80.0000	100.0000	300.0000	193.0900	60.0000	37.6629	100.0000	68.5455

EFFT	EFFC	EFFHWP	EFFCWP	VELHW	VELCW
0.8600	0.8500	0.8500	0.8500	7.0000	7.0000

DPWF12	DPWF35	DPWF56	DPWF78	DPWF81
0.0	2.0683	0.0	0.0	12.7313

DPLIQS	DPLIQT	DP2TUB	DP2S	DPC4	DPCW4
2.2321	16.3092	0.0694	10.4010	0.6544	20.1055

DTWF12	DTWF56	DTWF78	DTHWI	DTHWO	DTCWI	DTCWO
0.0	0.0	0.0	65.0000	13.0000	17.0000	19.0000

DT81	DTEV2	DTS2	DT41	DT51	DTC5
10.0000	5.0000	8.0000	5.0000	5.0000	7.0000

DISEV	DISCND	FRAC	FRACND	DMWF
0.0	0.0	0.1250	0.2500	200.0000

CBRINE	COSTU	DPCTP	DPFC	DPFE	WLFACT	RF
1.0000	3.3300	25.0000	0.2000	0.2000	1.0000	1.0000

PWF2	PWF4	DELTAP	STRESS	COR	PIPLCW	PIPLHW	VMIN
200.0000	43.0000	0.500013500.0000		0.0	1000.0000	5000.0000	0.9000

DITUBE	DOTUBE	FATUBE	TPITCH	ASURF	BSPACE	SPACEB	CONDTW
0.0695	0.0833	0.0038	1.4063	0.2183	20.0000	22.0000	93.0000

NTPASS	NEXHAS	NSTAGE	ND	NID	MIW	NTUBEC	NTUBEV	NWPROD	NWREIN	GC
1	1	0	10	5	4	0	3	0.0	0.0	0.41700D 09

FOULEV	FOULC	FOULHW	FOULCW	FWP	SSPEED
0.0001	0.0001	0.0020	0.0010	0.2400	80.0000

DEQF(I), I=1,ND

0.5000 0.1500 0.7500 0.1000 0.1500 0.0500 0.0500 0.1000 0.0500 0.1000

DIEQF(I), I=1,NID

0.1500 0.1000 0.1500 0.1000 0.1500

DIWEL(I), I=1,MIW

0.1900 0.1400 0.1000 0.1300

MHW	FPWELL	IHWP
0.80963D 07	138.88	1

DTPHI	DTPHO	AREAE	AREAC
0.0	0.0	0.0	0.0

NOPT	IOBJ	ITPARM	IOOPT(1)	IOOPT(2)	IOOP(3)	IOOPT(4)	IOOPT(5)	IOOPT(6)
0	1	10	0	1	0	1	0	1

DPAR(I), I=1,6

5.0000 2.0000 2.0000 2.0000 0.0 2.0000

```
      WBASE     FIXCHG      OPCHG      FLOAD      PRMAX      EPSW      EPSDPW     EPSDPP
      25.00       0.18       0.01       0.85       0.92  0.10D-03   0.50D-01   0.50D-01

 IPROC  IRESRS
    1      1

     EPSD             EPSV             FUGERR           EPSS          STEP          DMAX
  0.10000D-06      0.20000D-06      0.20000D-06      0.10000D-05      1.0000        3.0000

   NC NPHASE     ITNM        ITMAX       IPRNT      NPRINT       NCOS       IDPRNT
   2     4         30          30           0          0           1          0

COMP               IDCOM  CMW        TC           ACF       CD       PC        TBP
ISOBUTANE           2    58.1200  274.9600     0.1830     0.2373  529.1000   11.0300
CI     13.2865       0.3663700-01   0.3496310-03   0.5361000-08  -0.2981110-10   0.5385620-14   0.609350
ISOPENTANE          3    72.1460  369.0000     0.2260     0.2027  490.4000   82.4000
CI     27.6234      -0.3150400-01   0.4698840-03  -0.9828300-07   0.1029850-10  -0.2949500-15   0.871908

   NCFLAG  IFTYPE
       0     1
CKIJ     0.0008

    Z(ISOBUTANE       ) =     0.500000

    Z(ISOPENTANE      ) =     0.500000
```

****SUMMARY OF GEO-4 INPUT****

TEMPERATURE (DEG F)		
INLET COOLING WATER	TCW9	80.0000
OUTLET COOLING WATER	TCW10	100.000
INLET BRINE	THW11	300.000
OUTLET BRINE	THW12	193.090
PRESSURES (PSIA)		
INLET COOLING WATER	PCW9	60.0000
OUTLET COOLING WATER	PCW10	37.6629
INLET BRINE	PHW11	100.000
OUTLET BRINE	PHW12	68.5455
WORKING FLUID AT BHE OUTLET	PWF2	200.000
WORKING FLUID AT CONDENSER INLET	PWF4	43.0000
TEMPERATURE DIFFERENCES (DEG F)		
WORKING FLUID (WF)		
BHE OUTLET AND TURBINE INLET	DTWF12	0.0
COND OUTLET AND CYC PUMP INLET	DTWF56	0.0
CYC PUMP OUTLET AND BHE INLET	DTWF78	0.0
BRINE HEAT EXCHANGER (BHE)		
BRINE INLET MIN APPROCH	DTHWI	65.0000
INTERNAL PINCH POINT	DTHWO	13.0000
SECTION 1&3-EACH SUBSECTION	DT81	10.0000
SECTION 2-EACH SUBSECTION	DTEV2	5.00000
SECTION 2-BRINE AND WF	DTS2	8.00000
PRE-HEATER		
PRE-HEATR INLET MIN APPROACH	DTPHI	0.0
PRE-HEATR OUTLET MIN APPROACH	DTPHO	0.0
CONDENSER (COND)		
COOL. WAT INLET MIN APPROACH	DTCWI	17.0000
COOL. WAT OUTLET MIN APPROACH	DTCWO	19.0000
SECTION 1-EACH SUBSECTION	DT41	5.00000
SECTION 2-EACH SUBSECTION	DT51	5.00000
SECTION 2-WF AND WALL	DTC5	7.00000
PRESSURE DIFFERENCES (PSIA)		
WORKING FLUID (WF)		
BHE OUTLET AND TURBINE INLET	DPWF12	0.0
CONDENSER (TOTAL)	DPWF35	2.06830
COND OUTLET AND CYC PUMP INLET	DPWF56	0.0
CYC PUMP OUTLET AND BHE INLET	DPWF78	0.0
BHE (TOTAL)	DPWF81	12.7313
BHE WF INLET AND BUBBLE POINT INSIDE BHE	DPLIQS	2.23210
DEW POINT AND BUBBLE POINT INSIDE BHE	DP2S	10.4010
COND INLET AND DEW POINT INSIDE COND	DPC4	0.654400
BHE BRINE INLET AND WF BUBBLE POINT	DPLIQT	16.3092

BHE BRINE INLET AND WF DEW POINT	DP2TUB	0.6940000-01
COOLING WATER AT COND INLET AND COOLING WATER AT WORKING FLUID DEW POINT	DPCW4	20.1055
INCREMENT FOR UP-DATING TURBINE OUTLET PRESSURE	DELTAP	0.500000
PRESSURE DROP IN COOLING TOWER	DPCTP	25.0900

EQUIPMENT SPECIFICATIONS

TURBINE		
EFFICIENCY	EFFT	0.860000
NO OF EXHAUSTS	NEXHAS	1
NO OF STAGES	NSTAGE	0
WHEEL SPECIFIC SPEED	SSPEED	80.0900
MIN OUTLET VAPOR MOLE FRAC	VMIN	0.900000
PUMPS		
CYCLE-EFFICIENCY	EFFC	0.850000
BRINE-EFFICIENCY	EFFHWP	0.850000
COOLING WATER-EFFICENCY	EFFCWP	0.850000
BRINE HEAT EXCHANGER (BHE)		
BHE AREA (SQ.FT.)	AREAE	0.0
SHELL INSIDE DIAMETER (FT)	DISEV	0.0
ONE-HALF OF (SHELL ID - TUBE BUNDLE OD) (FT)	FRAC	0.125000
BAFFLE SPACING (FT)	BSPACE	20.0000
NO OF TUBES	NTUBEV	0
WORKING FLUID FOULING FACTOR (HR SQFT DEG F/BTU)	FOULEV	0.1000000-03
BRINE FOULING FACTOR (HR SQFT DEG F/BTU)	FOULHW	0.2000000-02
BRINE VEL IN TUBES (FT/SEC)	VELHW	7.00000
PRESSURE DROP FACTOR	DPFE	0.200000
CONDENSER (COND)		
CONDENSER AREA (SQ.FT.)	AREAC	0.0
SHELL INSIDE DIA., FT.	DISCND	0.0
ONE-HALF OF (SHELL ID - TUBE BUNDLE OD) (FT)	FRACND	0.250000
BAFFLE SPACING (FT)	SPACEB	22.0000
NO OF TUBES	NTUBEC	0
WORKING FLUID FOULING FACTOR (HR SQFT DEG F/BTU)	FOULC	0.1000000-03
COOLING WATER FOULING FACTOR (HR SQFT DEG F/BTU)	FOULCW	0.1000000-02
COOLING WATER VELOCITY IN TUBES (FT/SEC)	VELCW	7.00000
PRESSURE DROP FACTOR	DPFC	0.200000
WELLS		
TOTAL BRINE FLOW RATE(LB/HR)	MHW	0.8096300 07
BRINE FLOW RATE/WELL(LB/SEC)	FPWELL	138.880
NO OF PRODUCTION	NWPROD	0.0
NO OF REINJECTION	NWREIN	0.0
WELL FACTOR	WLFACT	1.00000
TUBES		
INSIDE FLOW AREA(SQFT)	FATUBE	0.3794000-02
PITCH (IN)	TPITCH	1.40625
INSIDE SURFACE AREA(SQFT)	ASURF	0.218340

```
   MATERIAL THERMAL CONDUCTIVITY
     (BTU FT/HR SQFT DEG. F)          CONDTW      93.0000
   NO OF PASSES                       NTPASS            1
   INSIDE DIAMETER (FT)               DITUBE    0.695000D-01
   OUTSIDE DIAMETER (FT)              DUTUBE    0.833333D-01
CORROSION ALLOWANCE (IN)              COR       0.0
MAX ALLOWABLE STRESS (PSI)            STRESS     13500.0
COOLING WATER PIPING LENGTH (FT)      PIPLCW     1000.00
BRINE PIPING LENGTH (FT)              PIPLHW     5000.00
REQUIRED PLANT NET POWER (MW)         WBASE      25.0000

PROGRAM CONTROL
---------------
CONVERGENCE CRITERION
   DENSITIES                          EPSD      0.100000D-05
   FLASH                              EPSV      0.200000D-06
   FUGACITY                           FUGERR    0.200000D-06
   SERCH                              EPSS      0.100000D-05
   WF PRESSURE DROP                   EPSDPW    0.500000D-01
   PLANT POWER                        EPSW      0.100000D-03
   COOLING WATER AND BRINE
     PRESSURE DROP                    EPSDPP    0.500000D-01
ITERATION
   MINIMUM NO FOR PHASE               NPHASE            4
   MAXIMUM NO FOR THERMODYNAMIC
     SUBROUTINES                      ITNM             30
   MAXIMUM NO FOR TURBINE AND
     BRINE FLOW RATE                  ITMAX            30
PRINT CONTROLS
   IPRNT  .NE. 0-HSGC DETAILS         IPRNT             0
   NPRINT .NE. 0-HSGC SUMMARY TAB     NPRINT            0
   NCOS   .NE. 0-HXR PROPERTIES       NCOS              1
   IDPRNT .NE. 0-HXR PROPERTIES
     EACH CYCLE CALCULATION           IDPRNT            0
OPTIMIZATION CONTROL
   NOPT .LT. 0-BRINE FLOW AND
             PRESSURE DROPS
        .EQ. 0-ONCE THRU CALC
        .GT. 0-OPTIMIZATION           NOPT              0
   OBJECTIVE FUNTION TYPE             IOBJ              1
     1 = $/KW    2 = CENTS/KWHR
     3 = -BTU/LB HW    4 = -BTU
     5 = -BTU/AVAILABILITY
   MAX NO OF PARAMETER INCREMENTS     ITPARM           10
   PARAMETER FLAG                     IOOPT
     (NO OPTIMIZATION=0)
     DTHWI- 0    DTCWO- 1
     DTHWO- 1    PWF2- 0
     DTCWI- 0    TCW10- 1
   PARAMETER INCREMENTS               DPAR
     DPAR(1)=  5.00000        DPAR(4)=  2.00000
     DPAR(2)=  2.00000        DPAR54)= 0.0
     DPAR(3)=  2.00000        DPAR(6)=  2.00000
MAX MOLAR DENSITY (LB-MOLE/CUFT)      DMAX       3.00000
INTITIAL FALSE POSITION STEP SIZE     STEP       1.00000
WF FLOW RATE DECREMENT (LB/HR)        DMWF       200.000
BHE TYPE(1=SHELL-TUBE,2=DIR CON)      IPROC             1
RESOURCE TYPE ( 1=BRINE.
```

2= ANY OTHER TYPE)	IRFSRS		1
BRINE PUMP REQUIREMENT (0=NO)	IHWP		1
MAX PSEUDO-REDUCED PRESSURE	PRMAX	0.920000	
INCREMENT FOR WORKING FLUID	DMWF	200.000	
TYPE OF FLUID			
1 =PARAFFINS; 2 =HALOCARBONS	IFTYPE		1
COMP PARAMETER FLAG			
NCFLAG.NE.0, READ PURE			
COMP PARAMETERS, A(I,J)	NCFLAG		0

COST DATA

NO OF MAJ EQ DIR COST FACTORS	ND		10
NO OF MAJ EQ INDIR COST FACTURS	NID		5
NO OF WELL INDIRECT COST FACTORS	MIW		4
GATHERING SYSTEMS FACTOR	FWP	0.240000	
DIRECT COST FACTORS FOR MAJ EQ	DEQFI		
INSTALLATION		0.500000	
INSTRUMENT/CONTROL		0.150000	
PIPING/INSULATION		0.750000	
ELECTRICAL		0.100000D 00	
BLDGS/STUCTURES/CONCRETE		0.150000	
FIRE CONTROL		0.500000D-01	
ENVIRONMENTAL		0.500000D-01	
LAND/IMPROVEMENTS		0.100000D 00	
START-UP		0.500000D-01	
AUXILIARIES		0.100000D 00	
INDIRECT COST FACTORS FOR MAJ EQ	DIEQF		
ENGINEERING/LEGAL		0.150000	
CONTINGENCY		0.100000D 00	
WORKING CAPITAL		0.150000	
ENVIRONMENTAL/SAFETY		0.100000D 00	
OVERHEAD/ESCALATION		0.150000	
INDIRECT COST FACTORS FOR WELLS	DIWEL		
LAND ACQUISITION		0.190000	
EXPLORATORY DRILLING		0.140000	
SURFACE EXPLORATION		0.100000D 00	
CONTINGENCY		0.130000	
FIXED CHARGE FACTOR	FIXCHG	0.180000	
OPERATING AND MAINTENANCE FACTOR	OPCHG	0.100000D-01	
OPERATING TIME FACTOR	FLOAD	0.850000	
UNIT COST OF BRINE	CBRINE	1.00000	
UNIT COST OF COOLING TOWER	COSTU	3.33000	
RATING FACTOR FOR COOLING TOWER	RF	1.00000	

COMPONENT DATA

NO OF COMPONENTS	NC		2
COMPONENT 1			
NAME-ISOBUTANE	COMP		
MOLECULAR WEIGHT	CMW	58.1200	
CRITICAL TEMPERATURE (DEG. R)	TC	734.650	
ACENTRIC FACTOR	ACF	0.183000	
CRITICAL DENSITY(LB-MOLE/CUFT)	CD	0.237300	
CRITICAL PRESSURE(PSIA)	PC	529.100	
NORMAL BOILING POINT (DEG. R)	TBP	470.720	
MOLE FRACTION	Z	0.500000	
IDEAL GAS POLYNOMIAL	CI		

```
     CI(1,1)=  13.2866        CI(1,2)= 0.366370D-01
     CI(1,3)= 0.349631D-03    CI(1,4)= 0.536100D-08
     CI(1,5)=-0.298111D-10    CI(1,6)= 0.538662D-14
     CI(1,7)= 0.609350
COMPONENT 2
   NAME-ISOPENTANE                    COMP
   MOLECULAR WEIGHT                   CMW          72.1460
   CRITICAL TEMPERATURE (DEG. R)      TC           828.690
   ACENTRIC FACTOR                    ACF         0.226000
   CRITICAL DENSITY(LB-MOLE/CUFT)     CD          0.202700
   CRITICAL PRESSURE(PSIA)            PC           490.400
   NORMAL BOILING POINT (DEG. R)      TBP          542.090
   MOLE FRACTION                      Z           0.500000
   IDEAL GAS POLYNOMIAL               CI
     CI(2,1)=  27.6234        CI(2,2)=-0.315040D-01
     CI(2,3)= 0.469884D-03    CI(2,4)=-0.982830D-07
     CI(2,5)= 0.102985D-10    CI(2,6)=-0.294850D-15
     CI(2,7)= 0.871908
INTERACTION PARAMETERS                CKIJ
     CKIJ(1,2)= 0.800000D-03


*****NO OPTIMIZATION TO BE DONE



   HOT WATER PIPE FRICTION FACTOR =     0.10270D-01
```

***** SUMMARY OF GEO-4 SIMULATOR RESULTS *****

WORKING FLUID

COMPONENT	MOLE FRACTION
ISOBUTANE	0.5000
ISOPENTANE	0.5000

STATE POINT	LOCATION	TEMPERATURE (DEG.F)	PRESSURE (PSIA)	ENTHALPY (BTU/LB)	ENTROPY (BTU/LB-R)	VAPOR (MOLE FR.)	DENSITY (LB/FT3)
1	EVAPORATOR OUTLET	235.00	200.00	184.13	1.2075	1.0000	2.3470
2	TURBINE INLET	235.00	200.00	184.13	1.2075	1.0000	2.3470
3	TURBINE OUTLET	159.12	44.401	162.23	1.2133	1.0000	0.46870
3	DEW POINT	120.28	44.401	144.44	1.1836		
3	CONDENSER INLET	159.12	44.401	162.23	1.2133	1.0000	0.46870
4	DEW POINT	119.35	43.747	144.11	1.1834		
5	CONDENSER OUTLET	97.000	42.333	-6.0925	0.91952	0.0	35.632
5	BUBBLE POINT	97.200	42.333	-5.9802	0.91972		
6	CYCLE PUMP INLET	97.000	42.333	-6.0925	0.91952	0.0	35.632
7	CYCLE PUMP OUTLET	98.188	212.73	-5.0527	0.91980	0.0	35.707
8	EVAPORATOR INLET	98.188	212.73	-5.0527	0.91980	0.0	35.707
8	BUBBLE POINT	224.10	210.50	72.912	1.0454		

***** SUMMARY OF GEO-4 SIMULATOR RESULTS *****

BASIS = 1 HOUR AT 0.809630 07 LB/HR BRINE

GROSS TURBINE WORK, MW-HR	=	29.785	NET THERMODYNAMIC EFFICIENCY, %	=	11.025
CYCLE PUMP WORK, MW-HR	=	1.4143	RESOURCE ENERGY EXTRACTION EFFICIENCY,%	=	48.594
COOLING WATER PUMP WORK, MW-HR	=	2.1123	NET THERMO. CYCLE RESOURCE UTIL. EFF.,%	=	5.3576
BRINE PUMP WORK, MW-HR	=	0.52395	PARASITIC POWER EFFICIENCY, %	=	88.129
COOLING TOWER FAN WORK, MW-HR	=	0.73152	NET WORK/AVAILABILITY, BTU/BTU	=	0.29324
NET THERMODYNAMIC CYCLE WORK, MW-HR	=	28.371	COOLING WATER FLOW RATE, LB/HR	=	0.390390 08
NET PLANT WORK, MW-HR	=	25.003	WORKING FLUID FLOW RATE, LB/HR	=	0.464240 07
HEAT INPUT TO EVAPORATOR, BTU	=	0.878260 09	RATIO OF COOLING WATER TO BRINE	=	4.8219
HEAT REJECTED BY CONDENSER, BTU	=	0.781430 09	RATIO OF WORKING FLUID TO BRINE	=	0.57340
TURBINE EFFICIENCY, %	=	86.000	COOLING WATER PUMP EFFICIENCY, %	=	85.000
CYCLE PUMP EFFICIENCY, %	=	85.000	BRINE PUMP EFFICIENCY, %	=	85.000
TURBINE DIAMETER, FT.	=	5.7010	COOLING WATER PIPE DIAMETER, FT.	=	1.4001
TURBINE WHEEL TIP SPEED, FT/SEC.	=	753.73	BRINE CARRYING PIPE DIAMETER, FT.	=	0.65495
TURBINE RPM	=	2546.7	LENGTH OF COOLING WATER PIPE, FT.	=	1000.0
SPECIFIC SPEED OF TURBINE	=	80.000	LENGTH OF BRINE PIPE, FT.	=	5000.0
SPECIFIC DIAMETER OF TURBINE	=	1.2894	CYCLE PUMP DISCHARGE PIPE DIAMETER, FT.	=	3.0048
LIQUID AT TURBINE OUTLET, WEIGHT %	=	0.0	BRINE INLET TEMPERATURE, DEG. F	=	300.00
LIQUID AT TURBINE OUTLET, VOLUME %	=	0.0	BRINE OUTLET TEMPERATURE, DEG. F	=	193.09

***** SUMMARY OF GEO-4 SIMULATOR RESULTS *****

NET 25.00 MW HORIZONTAL TUBE BRINE HEAT EXCHANGER SPECIFICATIONS

TUBE SIDE

TUBE OUTSIDE DIAMETER, IN.	=	1.0000
TUBE INSIDE DIAMETER, IN.	=	0.83400
TUBE PITCH (TRIANGULAR), IN.	=	1.4063
NUMBER OF TUBE PASSES	=	1
NUMBER OF TUBES	=	1438
FLOW AREA, SQ.FT.	=	5.4558
VELOCITY THROUGH TUBES, FT/SEC.	=	7.0024

SHELL SIDE

SHELL INSIDE DIAMETER, FT.	=	4.6664
SHELL OUTSIDE DIAMETER, FT.	=	4.7839
EQUIVALENT DIA. FOR HEAT TRANSFER, FT.	=	0.98379D-01
EQUIVALENT DIA. FOR PRESSURE DROP, FT.	=	0.94692D-01
FLOW AREA, SQ.FT.	=	9.2591

		SECTION 1	SECTION 2	SECTION 3
WEIGHTED AVERAGE TUBE SIDE HEAT TRANSFER COEFFICIENT,	BTU/HR-FT2-F =	2219.1	2475.2	2695.9
WEIGHTED AVERAGE SHELL SIDE HEAT TRANSFER COEFFICIENT,	BTU/HR-FT2-F =	313.01	894.15	381.98
WEIGHTED AVERAGE OVERALL HEAT TRANSFER COEFFICIENT,	BTU/HR-FT2-F =	169.56	262.20	190.93
WEIGHTED AVERAGE LOG MEAN TEMPERATURE DIFFERENCE,	DEG.F =	39.307	32.828	65.379
TOTAL HEAT TRANSFER SURFACE AREA,	SQ.FT. =	54306.	59611.	258.38
LENGTH OF HEAT EXCHANGER TUBES,	FT. =	172.96	189.86	0.82295
TOTAL TUBE SIDE PRESSURE DROP,	PSIA =	15.070	16.152	0.69018D-01
TOTAL SHELL SIDE PRESSURE DROP,	PSIA =	2.2206	10.342	0.97747D-01

OVERALL WEIGHTED HEAT EXCHANGER LOG MEAN TEMPERATURE DIFFERENCE, DEGREES F = 35.290

OVERALL WEIGHTED HEAT EXCHANGER HEAT TRANSFER COEFFICIENT, BTU/HR-FT2-F = 217.97

***** SUMMARY OF GEO-4 SIMULATOR RESULTS *****

NET 25.00 MW HORIZONTAL TUBE CONDENSER SPECIFICATIONS

TUBE SIDE

TUBE OUTSIDE DIAMETER, IN.	=	1.0000
TUBE INSIDE DIAMETER, IN.	=	0.83400
TUBE PITCH (TRIANGULAR), IN.	=	1.4063
NUMBER OF TUBE PASSES	=	1
NUMBER OF TUBES	=	6571
FLOW AREA, SQ.FT.	=	24.930
VELOCITY THROUGH TUBES, FT/SEC.	=	7.0001

SHELL SIDE

SHELL INSIDE DIAMETER, FT.	=	9.9751
SHELL OUTSIDE DIAMETER, FT.	=	10.034
EQUIVALENT DIA. FOR HEAT TRANSFER, FT.	=	0.98379D-01
EQUIVALENT DIA. FOR PRESSURE DROP, FT.	=	0.96619D-01
FLOW AREA, SQ.FT.	=	42.310

		SECTION 1	SECTION 2
WEIGHTED AVERAGE TUBE SIDE HEAT TRANSFER COEFFICIENT, BTU/HR-FT2-F	=	1571.8	1490.0
WEIGHTED AVERAGE SHELL SIDE HEAT TRANSFER COEFFICIENT, BTU/HR-FT2-F	=	89.685	199.21
WEIGHTED AVERAGE OVERALL HEAT TRANSFER COEFFICIENT, BTU/HR-FT2-F	=	76.711	144.06
WEIGHTED AVERAGE LOG MEAN TEMPERATURE DIFFERENCE, DEG.F	=	38.009	19.650
TOTAL HEAT TRANSFER SURFACE AREA, SQ.FT.	=	28138.	0.24706D 06
LENGTH OF HEAT EXCHANGER TUBES, FT.	=	19.612	172.20
TOTAL TUBE SIDE PRESSURE DROP, PSIA	=	2.2284	20.066
TOTAL SHELL SIDE PRESSURE DROP, PSIA	=	0.65347	1.4110

OVERALL WEIGHTED CONDENSER LOG MEAN TEMPERATURE DIFFERENCE, DEGREES F = 20.700

OVERALL WEIGHTED CONDENSER HEAT TRANSFER COEFFICIENT, BTU/HR-FT2-F = 137.18

***** SUMMARY OF GEO-4 SIMULATOR RESULTS *****

ESTIMATED CAPITAL COST BREAKDOWN OF MAJOR COMPONENTS
FOR A 25.00 MW GEOTHERMAL POWER PLANT MODULE

MAJOR EQUIPMENT	MM$ DIRECT	MM$ INSTALLED	PERCENT OF EQUIP CAP INV	PERCENT OF TOTAL CAP INV	$ PER KW TOTAL
TURBINE	0.4668	0.7002	2.41	1.33	18.67
GENERATOR	0.4273	0.6410	2.20	1.22	17.09
CYCLE PUMPS	0.0813	0.1219	0.42	0.23	3.25
EVAPORATOR ($10.15 PER SQ. FT.)	1.1594	1.7392	5.98	3.30	46.37
CONDENSER ($ 5.11 PER SQ. FT.)	1.4061	2.1092	7.25	4.00	56.24
COOLING WATER PUMPS	0.1154	0.1731	0.60	0.33	4.62
COOLING TOWER	0.2613	0.3920	1.35	0.74	10.45
MAJOR EQUIPMENT COST	3.9177	5.8765	20.20	11.16	156.69
SUPPORTING EQUIPMENT					
INSTALLATION	1.9588		10.10	5.58	78.34
INSTRUMENT/CONTROL	0.5877		3.03	1.67	23.50
PIPING/INSULATION	2.9383		15.15	8.37	117.52
ELECTRICAL	0.3918		2.02	1.12	15.67
BUILDING/STRUCTURES/CONCRETE	0.5877		3.03	1.67	23.50
FIRE CONTROL	0.1959		1.01	0.56	7.83
ENVIRONMENTAL	0.1959		1.01	0.56	7.83
LAND/IMPROVEMENT	0.3918		2.02	1.12	15.67
STARTUP	0.1959		1.01	0.56	7.83
AUXILIARIES	0.3918		2.02	1.12	15.67
SUPPORTING EQUIPMENT COST	7.8354		40.40	22.31	313.38
TOTAL DIRECT COST	11.7531		60.61	33.47	470.06
INDIRECT COST					
ENGINEERING/LEGAL	1.7630		9.09	5.02	70.51
CONTINGENCY	1.1753		6.06	3.35	47.01
WORKING CAPITAL	1.7630		9.09	5.02	70.51
ENVIRONMENTAL/SAFETY	1.1753		6.06	3.35	47.01
OVERHEAD/ESCALATION	1.7630		9.09	5.02	70.51
INDIRECT COST	7.6395		39.39	21.75	305.54
EQUIPMENT CAPITAL INVESTMENT	19.3926		100.00	55.22	775.61

WELLS			
DRILLING/CASING (32.39WELLS)	8.0963	23.05	323.81
BRINE PUMPS	0.0341	0.10	1.36
GATHERING SYSTEM	1.9513	5.56	78.04
TOTAL DIRECT COST	10.0817	28.71	403.22
INDIRECT COST			
LAND ACQUISITION	1.9155	5.45	76.61
EXPLORATORY DRILLING	1.4114	4.02	56.45
SURFACE EXPLORATION	1.0082	2.87	40.32
CONTINGENCY	1.3106	3.73	52.42
INDIRECT COST	5.6457	16.08	225.80
WELL CAPITAL INVESTMENT	15.7274	44.78	629.02
TOTAL CAPITAL INVESTMENT	35.1200	100.00	1404.62

OPERATING AND MAINTENANCE COST(CENTS/KWHR) 3.58

BASIS:
- OPER. + MAINT. RATE = 0.01
- FIXED CHARGE RATE = 0.18
- LOAD FACTOR = 0.85

-NET PLANT WORK (BTU/LB BRINE)	-10.540
-NET PLANT WORK (BTU)	-0.85336D 08
-NET PLANT WORK/AVAILABILITY (BTU/BTU)	-0.29324